ΠΑΝΕΠΙΣΤΗΜΙΟ ΚΡΗΤΗΣ
ΣΧΟΛΗ ΕΠΙΣΤΗΜΩΝ ΥΓΕΙΑΣ
ΤΜΗΜΑ ΙΑΤΡΙΚΗΣ
ΤΟΜΕΑΣ ΒΑΣΙΚΩΝ ΕΠΙΣΤΗΜΩΝ

Διδακτορική Διατριβή

Νέες μοριακές προσεγγίσεις για την αύξηση των επίπεδων της λιποπρωτεΐνης υψηλής πυκνότητας (HDL) στο ήπαρ και την θεραπεία της στεφανιαίας νόσου

Μαρία Κανάκη

Επιβλέπων Καθηγητής: Δ. Καρδάσης

Απρίλιος 2017

UNIVERSITY OF CRETE
SCHOOL OF HEALTH SCIENCES
FACULTY OF MEDICINE
DIVISION OF BASIC SCIENCES

Ph.D. Thesis

New molecular approaches for the increase of High Density Lipoprotein (HDL) levels in the liver and the treatment of Coronary Artery Disease

Maria Kanaki

Supervisor: Prof. Dimitris Kardassis

April 2017

Table of Contents

ABSTRACT

The aim of the present PhD thesis was to investigate the molecular mechanisms that control the expression of genes that are involved in lipoprotein metabolism and to identify new molecular approaches that increase HDL levels in plasma.

Lipoprotein metabolism involves the transport of lipids, particularly cholesterol and triglycerides, from intestine and liver to peripheral tissues and from periphery back to the liver (reverse cholesterol transport) and is facilitated by numerous proteins including apolipoproteins, membrane transporters, plasma enzymes and lipoprotein receptors. Lipoprotein lipase (LPL) plays a critical role in lipoprotein remodeling by catalyzing the hydrolysis of triglycerides (TGs) present in TG-rich lipoprotein particles such as very low density lipoprotein (VLDL) and chylomicrons (CMs) to free fatty acids for the subsequent storage in adipose tissue or utilizations for the production of energy by various tissues. LPL is expressed primarily in the adipose tissue but it is also expressed at lower levels in other tissues including the liver. The role of LPL in the adult liver has been controversial due its low levels of expression but recent studies in mouse models of liver LPL overexpression or deficiency have revealed important new roles of the enzyme in glucose and lipid metabolism.

In **Part I** we characterized the mechanism that controls the expression of human LPL in hepatic cells at the level of transcription. First, we cloned the human LPL promoter and performed a deletion analysis using transactivation assays in human hepatoblastoma HepG2 cells. We revealed that the proximal region -109/-28 is important for basal hepatic LPL promoter activity. An in silico analysis of this region showed that it harbors a putative binding site, at position -47/-40, for the hepatic transcription factor forkhead box A2 (FOXA2) or Hepatocyte Nuclear factor 3β (HNF-3β), shown previously to play important roles in lipid and glucose homeostasis. Silencing of endogenous FOXA2 expression in HepG2 cells (using a specific siRNA) reduced the LPL mRNA and protein levels. Direct binding of FOXA2 to the novel binding site was established using chromatin immunoprecipitation assays, ex vivo and DNA affinity precipitation assays in vitro. This element was further characterized by site directed mutagenesis and it was found that five nucleotide substitutions in the FOXA2 site abolished the binding of FOXA2 and reduced the basal activity of the LPL promoter and the FOXA2-mediated transactivation. Next, we studied the effect

of insulin on the hepatic regulation of the LPL gene in HepG2 cells and we showed that insulin induces the phosphorylation of AKT and the nuclear export of FOXA2 causing a reduction in the LPL mRNA levels and promoter activity. Based on these findings, we proposed a novel role of FOXA2 in the regulation of the human LPL gene in hepatic cells by insulin.

In **Part II** we elucidated the mechanism of regulation of the human LPL gene by Liver X Receptors (LXR) in hepatic cells. Previous studies in mice had shown that the expression of LPL gene in the liver is strongly induced by high fat diets and synthetic agonists that activate the nuclear receptors LXR and RXR (Retinoid X Receptor). In agreement with these findings, we showed that treatment of HepG2 cells or primary mouse hepatocytes with the LXR synthetic agonist T0901317 upregulated the expression of LPL gene in mRNA and protein levels. Moreover, the nuclear receptors LXRα and RXRα transactivated strongly the human LPL promoter in response to their ligands in HepG2 cells and deletion analysis of the human LPL promoter established that the minimal region required for LXR/RXR transactivation was the -109/-28, which involves the FOXA2 binding site. Interestingly, we demonstrated very weak binding of nuclear receptors LXRα and RXRα to the proximal human LPL promoter, using chromatin immunoprecipitation assays, suggesting that additional factors are required for LXR action. Silencing of the endogenous FOXA2 gene using a specific siRNA in HepG2 cells and in mouse primary hepatocytes caused an inhibition of the oxysterol-inducible expression of LPL gene at both the mRNA and protein levels. Importantly, insulin, which inactivates FOXA2 via its nuclear exclusion, reduced the oxysterol-inducible expression of LPL gene, indicating the importance of FOXA2 in the lipid homeostasis in the liver. Next, we found that FOXA2 and ligand-activated LXRα/RXRα transactivated the human LPL promoter in a synergistic fashion. The mutations in the FOXA2 binding site (-47/-40) inhibited the synergistic transactivation of the LPL promoter by FOXA2 and LXRα/RXRα. Finally, we performed co-immunoprecipitation and GST pull down assays and established physical interactions between FOXA2, LXRα and RXRα in vitro and in vivo. An extended DNA binding domain (DBD) of LXRα is required for physical interactions with the at least one of the two transactivation domains of FOXA2. In conclusion, the findings of Part I and II suggest that the newly identified FOXA2 binding site in the LPL promoter serves as a novel LXRE that facilitates the induction of the LPL gene by oxysterols via FOXA2. Through an insulin-AKT-FOXA2-LPL signaling pathway

the overexpression of LPL is prevented in the liver under conditions of cholesterol overload protecting this tissue from the toxic effects of LPL.

In **Part III** we focused on the regulation of genes that are involved in HDL biogenesis and the remodeling by transcription factor FOXA2 and LXRs in hepatic cells. Previous studies had shown that mice heterozygous for FOXA2 have reduced levels of HDL in the plasma. Using in silico analysis, we identified putative binding sites for the FOXA2 factor in proximity with characterized LXR responsive elements (LXREs) in the promoters of various human HDL genes encoding the lipid transporters ABCG1, the hepatic lipase (LIPC) and the cholesteryl ester transfer protein (CETP). In agreement with previous studies, we showed that treatment of HepG2 cells and primary mouse hepatocytes with the synthetic LXR ligand, T0901317, caused a strong induction of mRNA levels of ABCG1, ABCG5, ABCG8 and CETP genes. Inactivation of the FOXA2 factor by siRNA silencing or insulin in primary mouse hepatocytes and HepG2 cells reduced the basal mRNA levels and also the induction of ABCG5 and ABCG8 genes, by T0901317, indicating that FOXA2 is critical for the upregulation of these lipid transporters by the LXR ligands. With transactivation assays, we established that FOXA2 or LXRα/RXRα overexpression in the presence of their ligands in HepG2 cells increased the activity of the promoters of the ABCG5 and ABCG8 genes. In agreement with these findings, silencing the expression of LXRα or LXRβ in HepG2 cells, via lentivirus expressing shRNAs specific for each LXR isoform, reduced the mRNA levels of ABCG8 and ABCG5 genes. Furthermore, FOXA2 and ligand-activated LXRα/RXRα transactivated in a synergistic manner the promoter of ABCG8 gene, but not the ABCG5 promoter. Unexpectedly, FOXA2 inhibited the induction of the ABCG5 promoter by LXRs and oxysterols in HepG2 cells, suggesting that more distal transcription factor binding sites far from the coding regions of the genes may be involved and via DNA looping regulate coordinately the expression of ABCG5 and ABCG8 genes. These findings are in line with the synergistic transactivation of LPL promoter by nuclear receptors LXRα/RXRα and the transcription factor FOXA2, as described above.

Understanding in depth the mechanisms by which lipid and glucose metabolic pathways are interconnected in the liver by factors such as FOXA2 may open the way to novel therapeutic strategies to increase HDL levels and protect patients with metabolic diseases such as coronary heart disease, dyslipidemia, diabetes and the metabolic syndrome.

ΠΕΡΙΛΗΨΗ

Οι κύριοι ερευνητικοί στόχοι της παρούσας διδακτορικής διατριβής ήταν να απαντηθούν ερωτήματα που αφορούν στη διερεύνηση των μοριακών μηχανισμών που ρυθμίζουν την έκφραση γονιδίων που συμμετέχουν στο μεταβολισμό των λιποπρωτεϊνών στο ήπαρ και να τακτοποιηθούν νέες μοριακές στρατηγικές για την αύξηση των επιπέδων της HDL στο πλάσμα.

Ο μεταβολισμός των λιποπρωτεϊνών περιλαμβάνει τη μεταφορά λιπιδίων, ιδιαίτερα χοληστερόλης και τριγλυκεριδίων, από το έντερο και το ήπαρ προς τους περιφερικούς ιστούς και αντίστροφα από τη περιφέρεια πίσω στο ήπαρ (αντίστροφη μεταφορά χοληστερόλης). Στα μονοπάτια αυτά εμπλέκονται πολλές πρωτεΐνες, συμπεριλαμβανομένων των απολιποπρωτεϊνών, μεμβρανικοί μεταφορείς, ένζυμα του πλάσματος και υποδοχείς λιποπρωτεϊνών. Η λιποπρωτεινική λιπάση (LPL) παίζει σημαντικό ρόλο στο μεταβολισμό των λιποπρωτεϊνών καθώς καταλύει την υδρόλυση των τριγλυκεριδίων που βρίσκονται στα λιποπρωτεϊνικά σωματίδια πλούσια σε τριγλυκερίδια, όπως είναι τα χυλομικρά και η VLDL (very low density lipoprotein). Τα λιπαρά οξέα που ελευθερώνονται στους ιστούς αποθηκεύονται στο λιπώδη ιστό ή χρησιμοποιούνται για παραγωγή ενέργειας από διάφορους ιστούς. Η LPL εκφράζεται σε υψηλά επίπεδα κυρίως στο λιπώδη ιστό και τους μύες, αλλά ανιχνεύεται σε χαμηλά επίπεδα σε άλλους ιστούς, συμπεριλαμβανομένου και του ήπατος. Ο ρόλος της LPL στο ενήλικο ήπαρ είναι αμφιλεγόμενος εξαιτίας των χαμηλών επιπέδων έκφρασης της σ αυτόν τον ιστό. Παρ' όλα αυτά, πρόσφατες μελέτες σε μοντέλα ποντικών στα οποία υπερκεράζεται ή απαλείφεται η LPL στο ήπαρ, έχουν αναδείξει τη σημαντικότητα αυτού του ενζύμου στο μεταβολισμό των λιπιδίων και της γλυκόζης.

Στην **Ενότητα Ι**, χαρακτηρίσαμε το μηχανισμό που ρυθμίζει την έκφραση του γονιδίου LPL του ανθρώπου στα ηπατικά κύτταρα σε μεταγραφικό επίπεδο. Αρχικά κλωνοποιήσαμε τον υποκινητή της ανθρώπινης LPL και πραγματοποιήσαμε ανάλυση των απαλοιφών του υποκινητή της LPL με πειράματα παροδικής διαμόλυνσης κυττάρων HepG2. Παρατηρήσαμε ότι η κοντινή περιοχή -109/-28 του υποκινητή είναι σημαντική για τη βασική ηπατική ενεργότητα του υποκινητή του γονιδίου LPL. Με βιοπληροφορική ανάλυση αυτής της περιοχής εντοπίστηκε μια πιθανή θέση πρόσδεσης (-47/-40) για τον παράγοντα FOXA2 (HNF3β), ο οποίος παίζει σημαντικό ρόλο στην ομοιόσταση των λιπιδίων και της γλυκόζης. Αποσιώπηση της έκφρασης

της ενδογενούς πρωτεΐνης FOXA2 στα κύτταρα HepG2 (χρησιμοποιώντας ένα ειδικό siRNA), οδήγησε σε μείωση των επιπέδων πρωτεΐνης και mRNA του γονιδίου LPL. Πειράματα ανοσοκατακρήμνισης χρωματίνης και αλληλεπίδρασης DNA-πρωτεϊνών έδειξαν ότι ο μεταγραφικός παράγοντας FOXA2 προσδένεται στην κοντινή περιοχή -141/-10 του υποκινητή της LPL. Αυτό το ρυθμιστικό στοιχείο χαρακτηρίστηκε περαιτέρω με μεταλλαξιγένεση. Μεταλλάξεις πέντε βάσεων στη θέσης πρόσδεσης του FOXA2 (-47/-40) κατάργησαν την πρόσδεση του FOXA2 στη θέση αυτή και μείωσαν σημαντικά τόσο τη βασική ενεργότητα του υποκινητή της LPL όσο και την ενεργοποίηση του υποκινητή από τον παράγοντα FOXA2. Στη συνέχεια, μελετήσαμε την επίδραση της ινσουλίνης στην ηπατική ρύθμιση του γονιδίου LPL στα κύτταρα HepG2. Παρατηρήσαμε ότι η ινσουλίνη αύξησε τα επίπεδα φωσφορυλίωσης της AKT και οδήγησε σε αποκλεισμό του FOXA2 από τον πυρήνα, το οποίο στη συνέχεια προκάλεσε μείωση των επιπέδων mRNA του γονιδίου LPL και της ενεργότητας του υποκινητή. Με βάση αυτά τα ευρήματα, προτείνουμε ένα νέο ρόλο του παράγοντα FOXA2 στη ρύθμιση του γονιδίου LPL του ανθρώπου από την ινσουλίνη, στα ηπατικά κύτταρα.

Στην **Ενότητα ΙΙ**, διερευνήσαμε το μηχανισμό ρύθμισης του γονιδίου LPL του ανθρώπου από τους πυρηνικούς υποδοχείς LXR (Liver X Receptors) στα ηπατικά κύτταρα. Προηγούμενες μελέτες σε μοντέλα ποντικών είχαν δείξει ότι η έκφρασή του γονιδίου LPL στο ήπαρ επάγεται ισχυρά από δίαιτες υψηλές σε χοληστερόλη ή από συνθετικούς LXR αγωνιστές που ενεργοποιούν τους πυρηνικούς υποδοχείς LXR και RXR (Retinoid X Receptor). Σε συμφωνία με αυτά τα ευρήματα, δείξαμε ότι επώαση κυττάρων HepG2 ή πρωτογενών ηπατοκυττάρων ποντικού με τον συνθετικό LXR αγωνιστή T0901317 αύξησαν την έκφραση του γονιδίου της LPL τόσο σε επίπεδό RNA όσο και πρωτεϊνών. Επίσης η υπερέκφραση του ετεροδιμερούς LXRα/RXRα σε κύτταρα HepG2 παρουσία των συνδετών τους, ενεργοποίησε ισχυρά τον υποκινητή -883/+39 της ανθρώπινης LPL. ανάλυση των απαλοιφών του υποκινητή της LPL έδειξαν ότι η ελάχιστη περιοχή που απαιτείται για την ενεργοποίηση από τα ετεροδιμερή LXRα/RXRα ήταν η -109/-28, η οποία περιλαμβάνει τη θέση πρόσδεσης του FOXA2. Ενδιαφέρον παρουσιάζει, το γεγονός ότι οι υποδοχείς LXRα και RXRα προσδένονται πολύ ασθενικά στον υποκινητή του γονιδίου LPL, όπως διαπιστώθηκε με πειράματα ανοσοκατακρήμνισης χρωματίνης, υποδεικνύοντας ότι επιπλέον παράγοντες απαιτούνται για την δράση των LXR. Αποσιώπηση της έκφρασης της ενδογενούς πρωτεΐνης FOXA2 στα κύτταρα HepG2 και σε πρωτογενή ηπατοκύτταρα

ποντικού, χρησιμοποιώντας ένα ειδικό siRNA, προκάλεσε δραματική μείωση της επαγωγής της έκφρασης του γονιδίου LPL από τον συνδέτη του LXR, T0901317, σε επίπεδο πρωτεΐνης και mRNA. Αξιοσημείωτη είναι η διαπίστωση ότι η ινσουλίνη, η οποία απενεργοποιεί τον παράγοντα FOXA2 μέσω πυρηνικού του αποκλεισμού, μείωσε την επαγωγή της έκφρασης του γονιδίου LPL από τις οξυστερόλες, υποδεικνύοντας της σημαντικότητα του παράγοντα FOXA2 στην ομοιόσταση των λιπιδίων στο ήπαρ. Έπειτα, παρατηρήσαμε ότι η ταυτόχρονη υπερέκφραση της πρωτεΐνης FOXA2 και των LXRα/RXRα, παρουσία των συνδετών τους, ενεργοποίησε τον υποκινητή της LPL κατά έναν συνεργατικό τρόπο. Καταστρέφοντας τη θέση πρόσδεσης του παράγοντα FOXA2 (με τις μεταλλάξεις που αναφέρθηκαν παραπάνω), αναστάλθηκε σημαντικά η συνεργατική ενεργοποίηση του υποκινητή της LPL από τους πυρηνικούς υποδοχείς LXRα/RXRα και τον παράγοντα FOXA2.Τέλος, πραγματοποιήσαμε πειράματα συν-ανοσοκατακρήμνισης και δοκιμασίες GST pull down και δείξαμε ότι οι μεταγραφικοί παράγοντες FOXA2 και LXR/RXR αλληλεπιδρούν φυσικά in vivo και in vitro. Μια εκτεταμένη DBD (DNA binding domain) περιοχή του υποδοχέα LXRα απαιτείται για τη τις φυσικές αλληλεπιδράσεις με τουλάχιστον μία από τις δύο περιοχές ενεργοποίησης (transactivation domains) του FOXA2. Συνοψίζοντας, τα ευρήματα των Ενοτήτων I και II υποδεικνύουν ότι ή νέα θέση πρόσδεσης του παράγοντα FOXA2 στον υποκινητή της LPL λειτουργεί σαν ένα νέο ρυθμιστικό στοιχείο LXRE, το οποίο διευκολύνει την επαγωγή του γονιδίου LPL από τις οξυστερόλες μέσω του παράγοντα FOXA2. Μέσω ενός σηματοδοτικού μονοπατιού ινσουλίνης- AKT-FOXA2-LPL η υπερέκφραση της LPL στο ήπαρ εμποδίζεται σε συνθήκες περίσσειας χοληστερόλης, προστατεύοντας τον ιστό αυτό από τις τοξικές δράσεις της LPL.

Στην **Ενότητα III**, εστιαστήκαμε στην ρύθμιση γονιδίων που συμμετέχουν στη βιογένεση και αναδιαμόρφωση της HDL από τους μεταγραφικούς παράγοντες FOXA2 και LXRs στα ηπατικά κύτταρα. Προηγούμενες μελέτες έχουν δείξει ότι σε ποντίκια ετερόζυγα για τον παράγοντα FOXA2, τα επίπεδα της HDL στο πλάσμα είναι μειωμένα. Με βιοπληροφορική ανάλυση, εντοπίστηκαν πιθανές θέσεις πρόσδεσης για τον παράγοντα FOXA2 που βρίσκονται κοντά σε χαρακτηρισμένα ρυθμιστικά στοιχεία LXRE, στους υποκινητές των γονιδίων ABCG1, LIPC και CETP. Σε συμφωνία με προηγούμενες μελέτες, παρατηρήσαμε ότι η επώαση κυττάρων HepG2 και πρωτογενών ηπατοκυττάρων ποντικού με τον συνθετικό LXR αγωνιστή , T0901317, προκάλεσε ισχυρή επαγωγή της έκφρασης των γονιδίων

ABCG1, ABCG5, ABCG8 και CETP, σε επίπεδο mRNA. Απενεργοποίηση του παράγοντα FOXA2, μέσω siRNA αποσιώπησης είτε μέσω επίδρασης με ινσουλίνη σε πρωτογενή ηπατοκύτταρα ποντικού ή σε κύτταρα HepG2, μείωσε τα βασικά επίπεδα mRNA αλλά και την επαγωγή των ABCG5 και ABCG8 γονιδίων, από τον αγωνιστή T0901317, υποδεικνύοντας ότι ο FOXA2 έχει σημαντικό ρόλο στην ενεργοποίηση αυτών των μεταφορέων λιπιδίων από τους συνδέτες των πυρηνικούς υποδοχείς LXR. Πραγματοποιώντας πειράματα παροδικής διαμόλυνσης σε κύτταρα HepG2 παρατηρήσαμε ότι η υπερέκφραση της πρωτεΐνης FOXA2 ή των υποδοχέων LXRα/RXRα οδήγησε σε αύξηση της ενεργότητας των υποκινητών των γονιδίων ABCG5 και ABCG8. Σε συμφωνία με αυτά τα αποτελέσματα, αποσιώπηση της έκφρασης της ενδογενούς πρωτεΐνης LXRα ή LXRβ στα κύτταρα HepG2, μέσω λεντιϊών που εκφράζουν ειδικά shRNAs για κάθε ισομορφή των LXR, μείωσε τα επιπέδων mRNA των γονιδίων ABCG5 και ABCG8. Επιπλέον, η ταυτόχρονη υπερέκφραση των πρωτεϊνών FOXA2 και LXRα/RXRα, παρουσία των συνδετών τους ενεργοποίησε κατά έναν συνεργατικό τρόπο τον υποκινητή του γονιδίου ABCG8, αλλά όχι τον υποκινητή του γονιδίου ABCG5. Αντίθετα, ο FOXA2 ανέστειλε την επαγωγή του υποκινητή του γονιδίου ABCG5 από τους LXRs και τις οξυστερόλες στα κύτταρα HepG2, υποδεικνύοντας την ύπαρξη απομακρυσμένων ρυθμιστικών στοιχείων και μεταγραφικών παραγόντων, τα οποία ίσως συνδέονται με λούπες του DNA και με αυτόν τον τρόπο ρυθμίζουν την έκφραση των γονιδίων ABCG5 και ABCG8. Τα ευρήματα αυτά έρχονται σε συμφωνία με την συνεργατική ενεργοποίηση του υποκινητή της LPL από τους πυρηνικούς υποδοχείς LXRα/RXRα και τον παράγοντα FOXA2, όπως περιγράφηκε παραπάνω.

Η κατανόηση σε βάθος των μηχανισμών, με τους οποίους συνδέονται τα μεταβολικά μονοπάτια λιπιδίων και γλυκόζης στο ήπαρ από παράγοντες όπως ο FOXA2 είναι ιδιαίτερα σημαντική για την ανάπτυξη νέων θεραπευτικών στρατηγικών για την αύξηση των επιπέδων της HDL και την προστασία ασθενών με μεταβολικές ασθένειες, όπως η καρδιαγγειακή νόσος, ο διαβήτης, οι δυσλιπιδαιμίες και το μεταβολικό σύνδρομο.

1. INTRODUCTION

LIPOPROTEINS

Lipids are a heterogeneous group of biomolecules and play various roles in homeostasis. Fatty acids in triglycerides are energy sources, while phospholipids, glycolipids and cholesterol are membrane components.

Lipids are too hydrophobic to be transported in the circulation and thus are packaged into water soluble complexes, termed lipoprotein particles, in order to transport cholesterol and triglycerides in the blood. Lipoproteins are either spherical particles or discoidal particles. The spherical particles contain a hydrophobic lipid core of cholesteryl esters and triglycerides, surrounded by a monolayer of phospholipids, un-esterified cholesterol and apolipoproteins (Apo) (Figure 1.1 A). The discoidal particles consist of mostly polar lipids and proteins in a bilayer conformation. Apolipoproteins serve as lipid acceptors, but also as cofactors of remodeling enzymes, or ligands for lipoprotein receptor-mediated cellular uptake. For instance ApoB100 exclusively binds LDL receptor (LDLR) and ApoE is a ligand for LDLR and LDLR-related protein (LRP). ApoCII is an essential co-factor for Lipoprotein lipase (LPL) and ApoAI activates lecithin:cholesterol acylt transferase (LCAT).

Lipoprotein particles can be separated and classified according to their density or electrophoretic mobility (Table 1.1) and grouped into five major classes: the chylomicrons, the very low density lipoproteins (VLDL), the intermediate density lipoproteins (IDL), the low density lipoproteins (LDL) and the high density lipoproteins (HDL) (Figure 1.1 B). The biggest triglyceride-rich lipoprotein particles are chylomicrons, which are secreted by the intestine and transport dietary fat to the liver and other tissues. Lipids, taken up or synthesized by the liver are redistributed to other organs by VLDL, IDL and LDL. LDL results from the intravascular catabolism of VLDL and contains relatively more cholesterol and fewer triglycerides than VLDL or chylomicrons. CM and VLDL are also called triglyceride-rich lipoproteins (TRL). Finally, the excess of cholesterol is collected from peripheral tissues and directed to the liver for bile excretion by HDL (1, 2).

Table 1.1 Features of Plasma Lipoprotein particles (3).

Lipoprotein Class	Size (nm)	Density (g/ml)	TG (% wt)	PL (% wt)	Cholesterol (% wt)		Protein (% wt)	Primary Apolipoprotein(s)
					Free	Esterified		
CM	75–1,200	.94	80–95	3–6	1–3	2–4	1–2	A-I, A-IV, B-48, C-I, C-III, E
VLDL	30–70	.94–1.006	45–65	15–20	4–8	16–22	6–10	B-100, E, C-I, C-II, C-III
LDL	18–30	1.019–1.063	4–8	18–24	6–8	45–50	18–22	B-100
HDL	5–12	1.063–1.21	2–7	26–32	3–5	15–20	45–55	A-I, A-II, E

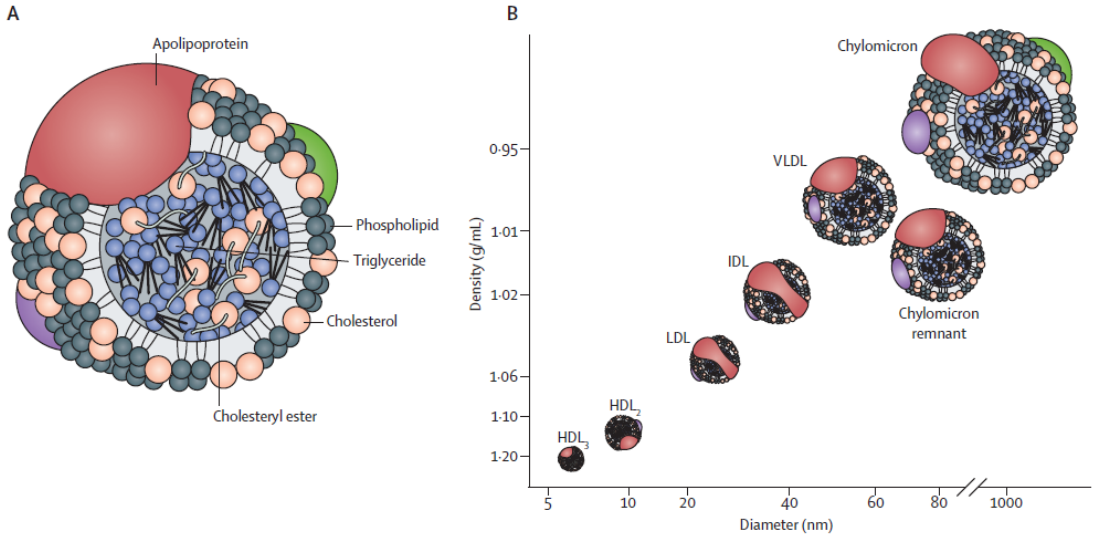

Figure 1.1 The structural components of lipoproteins (A) and their relation to diameter and density (B) (4).

Pathways of Lipoprotein metabolism

Lipoprotein metabolism involves the transport of lipids, particularly cholesterol and triglycerides, in the blood. It is divided into two pathways: a) the pathway of the transport of cholesterol and triglycerides from intestine and liver to peripheral tissues for energy supply or storage (1, 5, 6); and b) the reverse cholesterol transport pathway which is responsible for the removal of cholesterol excess from periphery back to the liver for excretion (1, 7-10).

In the first pathway, dietary lipids such as free faty acids (FFA), cholesterol and monoglycerides are absorbed by the intestinal enterocytes where they are packaged along with apolipoprotein apoB-48 into large chylomicron lipoproteins (exogenous pathway). These particles then are secreted via the lymphatic vessels into the circulation. Chylomicrons are responsible for the transport of dietary lipids from the enterocytes into to peripheral tissues through the blood. In the adipose and muscle

tissue the majority of the triglycerides in the chylomicrons are hydrolyzed by the enzyme lipoprotein lipase (LPL) which is located on the surface of vascular endothelial cells. For LPL catalytic activity apoC-II is required as a cofactor. Fatty acids are released and taken up by tissues for oxidation and energy production in muscles or for re-esterification into triglycerides and storage in adipose tissue. The hydrolysis of triglycerides results in the formation of smaller, denser, cholesterol-enriched particles known as chylomicron remnants, which travel back to the liver to be cleared from the body. Hepatic uptake is mediated mainly by the LDL receptor (LDLR) with apoE, LPL, and hepatic lipase (HL) as ligand proteins (11-13).

The liver plays a key role in the delivery of dietary lipids to peripheral tissues. Endogenous cholesterol and triglycerides are packaged with apolipoprotein apoB-100 to synthesize very low density lipoprotein (VLDL) particles, a process catalyzed by microsomal triglyceride transfer protein (MTP) (endogenous pathway) (14). Hepatocytes secrete these particles into the bloodstream and similar to chylomicrons, LPL rapidly hydrolyses VLDL's triglycerides. This reaction produces fatty acids that are used by the tissues and cholesterol-enriched intermediate density lipoproteins (IDL). The IDL particles are either taken up by the liver via specific receptors such as LDLR, LRP and VLDL receptors or further catabolized by the action of hepatic lipase (HL) to LDL (15). Finally, most of LDL is taken up by the liver and the rest by other peripheral tissues via interaction with ubiquitously expressed LDL receptors (Figure 1.2).

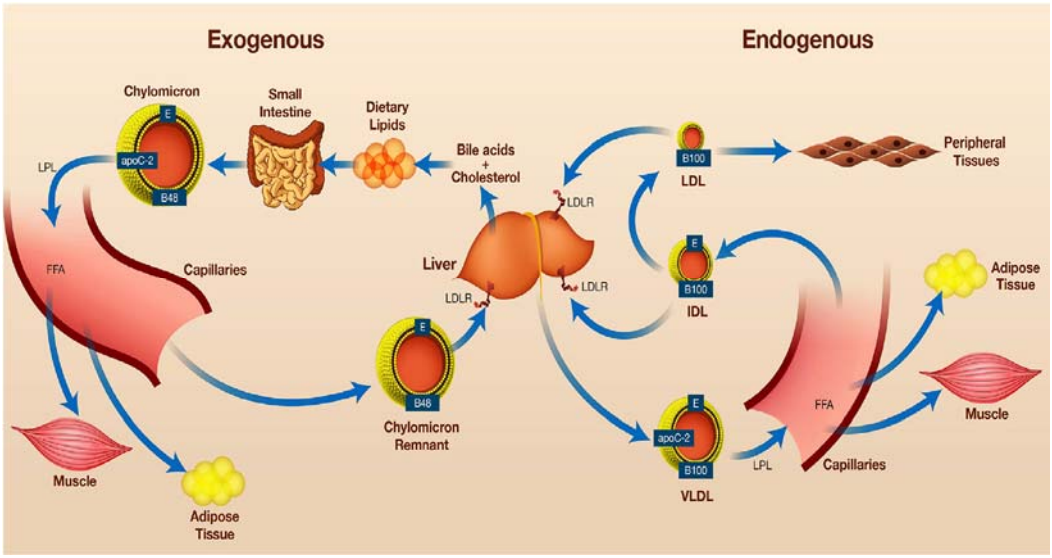

Figure 1.2 Exogenous and endogenous pathways of triglyceride-rich lipoprotein metabolism (see text for details) (16).

The pathway of HDL metabolism has been termed Reverse Cholesterol Transport due to the ability of HDL particles to transfer excess cholesterol in the opposite way i.e. from peripheral cells, such as macrophages of the arterial wall, to the liver for excretion (Figure 1.3). This pathway starts with the synthesis and secretion of apolipoprotein apoA-I mainly by the liver and intestine. Lipid-free apolipoprotein A-I (apoA-I) interacts with the ATP Binding Cassette Transporter A1 (ABCA1) membrane transporter, which transfers cholesterol and phospholipids from cells to apoA-I, forming lipid-poor apoA-I (7, 17, 18). These lipid-poor apoA-I particles are lipidated further with phospholipids and cholesterol from peripheral cells via ABCA1 and converted to discoidal particles, termed preβ-HDL (nascent HDL) (19). Preβ-HDL particles are converted into mature spherical α-HDL by the enzyme lecithin:cholesterol acyl transferase (LCAT), which forms cholesterol esters in HDL (7, 18, 20). The spherical a-HDL interact with macrophages, to facilitate the efflux of excess cholesterol, a process facilitated by the transporter ABCG1 (21). The process just described is called HDL biogenesis. In circulation, HDL particles are modified by enzymes and lipid transfer proteins. Remodeling of HDL particles is facilitated by two lipid transfer proteins, the phospholipid transfer protein (PLTP) and the cholesterol ester transfer protein (CETP). PLTP is responsible for the exchange of phospholipids between HDL particles and apoB-containing lipoproteins (VLDL, LDL), while CETP exchanges cholesterol esters in HDL particles with triglycerides in the LDL VLDL and LDL particles (22, 23). HDL triglycerides can be also hydrolyzed by lipases such as the hepatic lipase (LIPC) and the endothelial lipase (LIPG). Hepatic lipase hydrolyzes both triglycerides and phospholipids of all lipoproteins, while endothelial lipase exhibits manly a high phospholipase activity and primarily hydrolyzes HDL lipids (24-26). Finally, cholesterol esters of α-HDL particles are removed by the liver via the Scavenger Receptor class B type I (SR-BI), which is a receptor for HDL by a process called selective cholesterol ester uptake that does require the internalization of the lipoprotein particle (27). This cholesterol is partly recycled by the liver in newly synthesized plasma VLDL and partly excreted from the body either as bile acid or as free cholesterol in the bile via the lipid transporters ABCG5/ABCG8 (28, 29). SR-BI is expressed also in adrenal cells, where it facilitates the uptake of HDL cholesterol ester for the synthesis of steroid hormones (30). Recently, cholesterol from HDL has been shown to be transported also back to the intestine via a process called TICE (Trans Intestinal Cholesterol Excretion) (31).

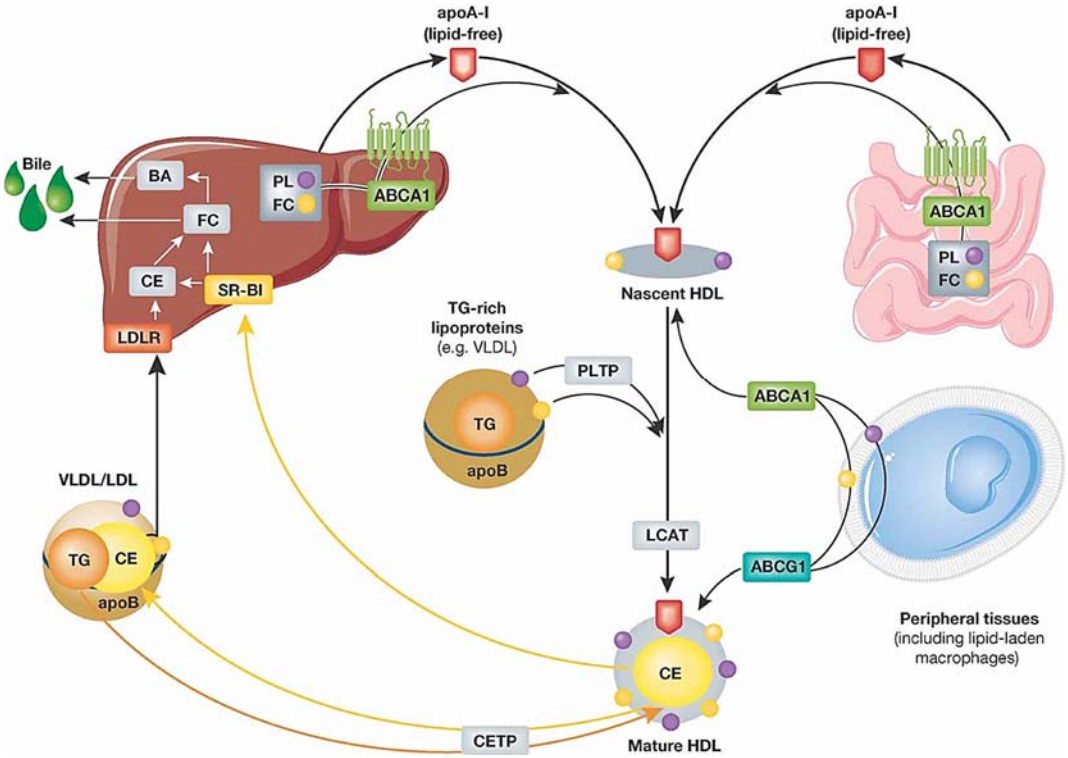

Figure 1.3 HDL biogenesis, metabolism and functions (see text for details)(32).

ATHEROSCLEROSIS AND HDL

Cholesterol is an essential component of cellular membranes and a precursor for bile acids and steroids synthesis. However, cholesterol levels must be tightly regulated both intracellularly and in plasma because excess cholesterol is toxic and can promote the development of coronary artery disease (CAD) and its underlying cause, atherosclerosis. Coronary artery disease is a complex and polygenic disorder since it is the result of interactions between genetic and environmental factors. It is the leading cause of mortality in developed countries, and accounts for nearly 50% of deaths. Smoking, obesity, blood pressure, diabetes, dietary factors, lack of exercise and most importantly excess cholesterol consist the major risk factors that contribute to the development of CAD (33).

Atherosclerosis is the primary cause of coronary artery disease and is characterized by the accumulation of lipid-rich plaques within the arterial walls. During atherosclerosis, the arterial wall gradually thickens to form an atherosclerotic

plaque, due to the gradual accumulation of cholesterol. That results in the narrowing of the lumen of the artery and consequently in the reduction in the amount of blood supplied to various organs incuding the heart and the brain. When plaques rupture, a blood clot is released and frequently causes myocardial infarction (heart attack) or stroke or peripheral vascular disease (34, 35).

Various epidemiological and clinical studies have identified high levels of LDL-C as a major contributor in developing atherosclerosis. In contrast, HDL cholesterol levels in plasma are reversely related to the risk for atherosclerosis in humans. A decrease in plasma HDL-C concentration by 1mg/ dL is associated with a 2-3% increased risk of CAD while an increase by 1mg/dL is associated with a 6 % lower risk of coronary death, independently of LDL-C level (36-39). Furthermore, both reduced plasma levels of HDL-C and elevated triglycerides are associated with CAD, potentially through the increased TRL remnants (40, 41). LDL-C lowering in plasma remains the first priority for prevention from thrombotic events and for reduction of CAD risk. However, these studies suggested that by increasing the levels of HDL cholesterol could reduce cardiovascular disease. Emerging evidence from studies in animals and humans indicate that high levels of HDL are not sufficient to confer atheroprotection but that the functionality of the HDL particles is more important. Patients with CAD or diabetes are frequently characterized by dyslipidemia including high LDL and triglycerides and low HDL, as well as dysfunctional HDL (42). Despite these obstacles, HDL raising is still a promising strategy for the treatment of atherosclerosis and reduction of CAD risk.

The atheroprotective properties of the HDL particles

The plasma HDL is produced mainly (~80%) by the liver and to a lesser extent (~20%) by the intestine (43). The population of HDL particles in plasma is very heterogeneous in terms of size, shape and protein/lipid content. As mentioned above, during the initial steps of HDL biogenesis, discoidal HDL particles are initially formed which then undergo extensive remodeling to form mature spherical HDL particles (44). HDL can be separated by two dimensional gel electrophoresis into sub-populations, pre-β1, pre-β2, α4, α3, α2 and α1. The larger α1, α2 particles may be

associated with protection from cardiovascular disease. HDL is the smallest lipoprotein particle and contains approximately 50% apolipoprotein and 50% lipid moieties. Apolipoprotein AI is the major structural component of all HDL particles. Additionally apoA-II, apoE, apoA-IV, apoM and apoCIII are found in certain HDL sub-populations (7). Proteomic studies identified more than 50 different non-structural proteins that are associated with HDL particles, some of which are proteins that are implicated in the anti-inflammatory functions of HDL (45, 46).

Although the atheroprotective effects of HDL involve multiple mechanisms, the importance of HDL in reverse cholesterol transport and maintenance of normal cholesterol homeostasis is thought to be the major contributor. Several lines of evidence indicate that reverse cholesterol transport is important for removing cholesterol from the actual site of atherogenesis in the vasculature. In addition to its effects on cholesterol homeostasis, HDL displays a wide spectrum of biological atheroprotective properties. These include anti-oxidative, anti-inflammatory, anti-infective, anti-thrombotic and anti-apoptotic properties as well as effects on endothelial cell function (Figure 1.4) (47, 48). The anti-oxidative activity of HDL protects LDL from oxidation in the intima, which is an early event in the formation of atherosclerotic lesions and promotes inflammation in the artery wall (49, 50). The anti-inflammatory function of HDL includes the inhibition of the expression of cytokines, adhesion molecules and monocyte chemoattractant proteins (e.g. MCP1) thus reducing the infiltration of monocytes into the artery wall (51). Through its antithrombotic properties, it promotes blood flow by increasing NO production and vasodilation, inhibits generation of thrombin and prevents platelet aggregation and alterations of the surface of the endothelial cells that could lead to the formation of thrombus (52, 53). HDL also protects endothelial cells from apoptosis, stimulates endothelial cell proliferation and migration, repairing damaged endothelium. Moreover, it protects the integrity of the endothelial cells by promoting the production of nitric oxide (NO), via induction of the enzyme endothelial nitric oxide synthase (eNOs) (52, 54-57). All of these actions may potentially attenuate steps of atherosclerotic plaque formation.

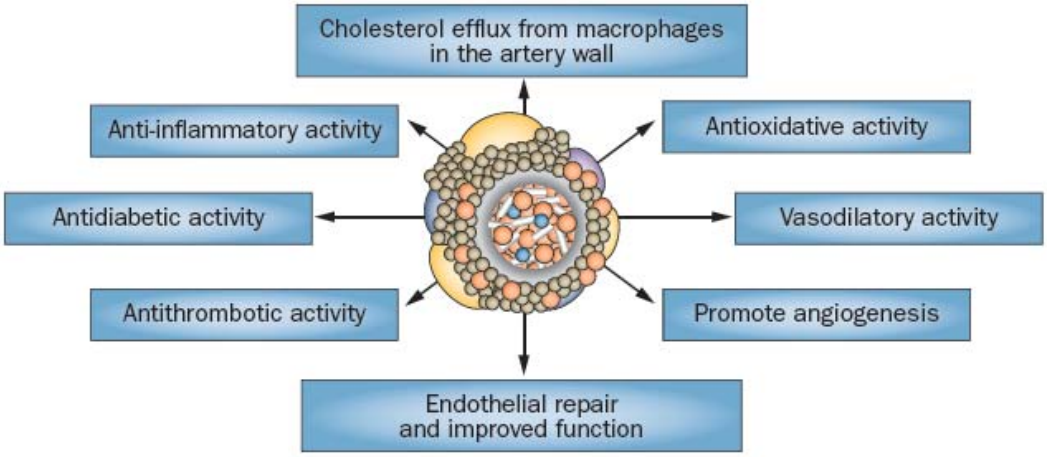

Figure 1.4 Anti-atherogenic properties of HDL (58).

HDL as therapeutic target

HDL is an attractive target for the development of therapies for CAD due to its multiple atheroprotective functions. HDL metabolism as described above can be regulated pharmacologically (59, 60). However, current therapeutic interventions have not been designed to specifically act on HDL and therefore have moderate effects on plasma HDL-cholesterol levels (2–30 %). Fibrates such as clofibrate and gemfibrozil have been used pharmacologically for decades but their beneficial effects on mortality is controversial. On average, fibrates increase HDL-C by 4.5% (61-63). Their effects are mediated by the Peroxisome Proliferator Activated Receptors (PPARs) which regulate the transcription of various genes including apoA-I. A dual PPAR α/γ agonist (aleglitazar) has been developed recently, with initial encouraging results. However, phase III clinical trial failed due to adverse effects on heart failure (64). Results from clinical trials of novel PPAR agonists show obvious clinical benefits and no side effects, thus these PPAR agonists appear as promising drugs for the reduction of cardiovascular risk associated with metabolic syndrome and type 2 diabetes (65). Niacin is the most potent drug in increasing HDL-cholesterol levels (up to 30 %), however its use is limited by side effects such as hepatotoxicity, glycaemia and flushing (66-68). Statins typically increase HDL-C levels by approximately 5% to 15% (69) and reduce cardiovascular disease events by only 25%, thus being

inadequate as monotherapy for increasing HDL-C (70-72). Statins were also shown to increase apoA-I gene transcription by inhibiting the activity of the small GTPase RhoA and by activating PPARa (73). The concept that CETP inhibition could be a promising HDL-C raising therapy was based on the observation that gene mutations in CETP were shown to increase HDL-C and apoA-I in humans with no evidence for premature atherosclerosis (74). Inhibition of CETP activity prevents the transfer of cholesteryl esters from HDL to VLDL/LDL particles and of triglycerides from VLDL/LDL to HDL causing a disturbance in HDL remodeling. Clinical trials in phase III of the CETP inhibitor torcetrapib showed a marked increase in HDL-cholesterol and a moderate decrease in LDL-cholesterol (75). However, an increased risk of cardiovascular events and an excess of mortality was observed that was independent of CETP inhibition. Two other CETP inhibitors, anacetrapib and dalcetrapib, were shown to cause a drastic increase in HDL-C levels in recent large clinical trials but failed to demonstrate a beneficial effect on cardiovascular disease (76).

Due to the recent disappointing clinical trials aiming to prevent CAD events by HDL-raising strategies and the failure of genetics to correlate HDL levels with CAD events (77), the development of additional therapeutic agents for the prevention and treatment of atherosclerosis is needed. The challenges now are to develop novel strategies that would increase HDL levels and improve also HDL functionality. As apoA-I is the major functional component of HDL, new therapies are being designed to mimic this apolipoprotein. ApoA-I mimetic peptides were designed based on the apoA-I sequence in a way that they maintain the fundamental properties of apoA-I. Administration of apoA-I mimetic peptides to mouse models showed increase in macrophage RCT, reduction in atherosclerosis and enhancement of the anti-inflammatory functions of HDL (78-80). In a similar context, the beneficial effects of apoA-I-based infusion therapies on atherosclerosis have been examined and shown inhibition of atherosclerotic plaque formation (81-83). Furthermore, infusion of rHDL compounds, consisting of native apoA-I and phospholipids, has resulted in an increase in both apoA-I and pre-β HDL levels, which was accompanied by enhanced ABCA1-mediated cholesterol efflux and reduced atherosclerotic plaque size (84). However, the actual clinical benefit from apoA-I-based therapies needs to be addressed by well-designed clinical trials in patients. Current interest and research is also directed at the genes and proteins that regulate HDL biosynthesis and metabolism. Drugs that could

specifically increase the expression of apoA-I, ABCA1 and may other HDL genes (such as LCAT and LPL) are anticipated to be of great clinical benefit because they will increase the rate of HDL biogenesis and RCT. In order to develop such drugs, which do not exist yet, we need to understand in depth the molecular mechanisms (regulatory elements and transcription factors) that control the expression of these genes in hepatic cells. Among these, PPAR- or LXR-targeting drugs could be of great value. Regarding LXR-based therapies, the current synthetic agonists greatly enhance RCT in vitro and in vivo in animal models but have not yet been tested in clinical trials due to their severe lipogenic effects in the liver (hepatic lipogenesis, hypertriglyceridemia and hepatosteatosis) (85, 86). Thus the development of novel isoform-specific and maybe tissue-specific drugs are anticipated.

LIPOPROTEIN LIPASE

Gene and structure of LPL

The gene of the human LPL is located on chromosome 8p22, spans about 30 kb and is divided into 10 exons. The first exon encodes the 5' untranslated region, a signal peptide and the first two amino acids of the protein, while the tenth exon encodes the 3' untranslated region (Figure 1.5). The cDNA for LPL codes for a protein of 448 amino acids resulting in a calculated molecular weight of 55 kDa (87-90). LPL belongs to the triglyceride lipase gene family that includes also hepatic lipase, pancreatic lipase and endothelial lipase (91, 92).

Despite the lack of an X-ray crystal structure, the structural homology between members of the lipase family has enabled the prediction of molecular models of the protein structure and functional domains. The protein is thought to be organized into two structurally distinct domains: a larger N-terminal and a smaller C-terminal domain, that are connected by a flexible peptide linker (93). The N-terminal domain contains the binding site for the cofactor apolipoprotein C-II (94) and the highly conserved catalytic active site of the enzyme (Ser132, Asp156, His241) responsible for the lipolytic function. The C-terminal region has been shown to be important for specificity and binding of substrate lipoproteins (93, 95, 96).

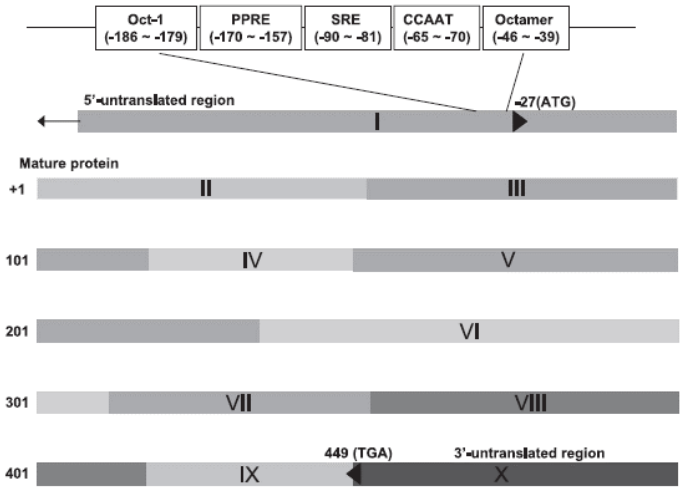

Figure1.5 Lipoprotein lipase gene structure and proximal promoter elements. The 10 exons of the LPL gene are schematically diagrammed with notations of the start codon, stop codon, 5'-untranslated region containing most of the transcriptional regulatory elements, and 3'-untranslated region that also contains some translational regulatory elements (97).

Both the N-and C-terminal domains contain heparin binding sites distal to the lipid binding sites (98, 99). Therefore LPL serves as a bridge between the cell surface and lipoproteins. LPL monomers dimerize to form an active noncovalent homodimer. In the head to tail orientation, the catalytic site of the N-terminal region of one monomer is in close juxtaposition to the C-terminal region of the other monomer. This dimerization and the head to tail orientation are key for the activity of the enzyme because the monomers have been shown to be inactive (93, 100, 101). The active site of the LPL is covered by a lid region (residues 216-239), which is postulated to have an impact on the substrate specificity of the lipase gene family. In the most well accepted model of LPL activity, once LPL is activated by apoC-II and triglyceride-rich lipoproteins, the C-terminal region of the dimer presents the substrate to the lid region, causing a conformational change to the lid and providing access to the active site (96, 102, 103).

Synthesis, maturation and transportation of LPL

LPL is expressed predominantly in the parenchymal cells of adipose tissue, heart and skeletal muscles. High expression levels can be detected also in lactating

mammary glands that originate from adipocytes and lower levels of LPL are produced by macrophages, brain, lung, adrenals, testes, spleen and kidney (97, 104-106). LPL is also synthesized transiently by the Kupffer cells of liver during fetal and early postnatal life (107).

In brief, following synthesis LPL is secreted as a glycosylated homodimer and , is subsequently translocated through the extracellular matrix and across endothelial cells to reach its site of physiological actions i.e. the capillary lumen in the blood vessels of the respective organs (97, 108-110). Inactive monomeric lipase needs to be processed by post-translational conformational changes and to assemble into homodimers in order to be catalytically active and translocated. Lipase maturation factor 1 (LMF-1) is a lipase-specific endoplasmatic reticulum (ER) chaperone which is crucial for the proper folding and assembly of LPL monomers as well as for maintaining the stability of LPL dimer in the ER (111, 112). An additional ER factor, Sel-1 suppressor of lin-12-like protein (Sel1L), has been shown recently to be required for the folding and secretion of LPL. It stabilizes the complex between LPL and LMF1 and mediates the release of active LPL from the ER. Indeed, absence of LMF1 or Sel1L leads to accumulation and retention of LPL in the ER in the form of high molecular weight protein aggregates, indicating that these ER proteins are needed to create an ER environment in which LPL folds into its active form (113, 114). The active LPL is then delivered to the Golgi for further modification, sorting and packaging. Thus, a part of active LPL is degraded prior to being secreted, via binding to the sortilin-related receptor with A-type repeats (SorLA) (115).

The remaining active LPL is secreted in interstitial space. There it binds initially to heparan sulfate proteoglycans (HSPGs) surrounding the parenchymal cells. However, it is transferred quickly to the endothelial cell surface where it binds to glycosylphosphatidyl-inositol anchored high-density lipoprotein binding protein 1 (GPIHBP1) (109, 116). Heparanase secreted from endothelial cells, support this transport of LPL from cardiomyocytes to the endothelium in the heart, as it splits the oligosaccharide chains on HSPG and LPL is released for interaction with GPIHBP1 in the endothelial surface (117, 118). Sub-endothelial extracellular matrix consisting of collagens, fibronectin, laminin and glycosaminoglycans, such as HSPG, is able to bind, sequester and stabilize the secreted LPL (119). It was believed that HSPGs played an important role in LPL binding in the sub-endothelial space, its trans-endothelial transport and its anchoring on the surface of the capillary lumen, but this

traditionally accepted model has been challenged by the recent discovery of the novel protein GPIHBP1, a member of the lymphocyte antigen 6 (Ly6) family. GPIHBP1 glycoprotein binds to the LPL and they move in vesicles across capillary endothelial cells, from the basolateral to the apical side, anchoring LPL in luminal surface of endothelial cells (120). LPL found in the circulating blood is mostly inactive, so the TG-rich lipoproteins must come into close proximity with LPL at the endothelium to be hydrolyzed, a process called margination. The LPL–GPIHBP1 complex is responsible for this margination, since GPIHBP1 provides a ‘‘platform for lipolysis’’ on capillaries (121, 122). Furthermore, the conformation of the catalytic domain of LPL is markedly stabilized by interaction with the acidic domain of GPIHBP1 (Figure 1.6) (123).

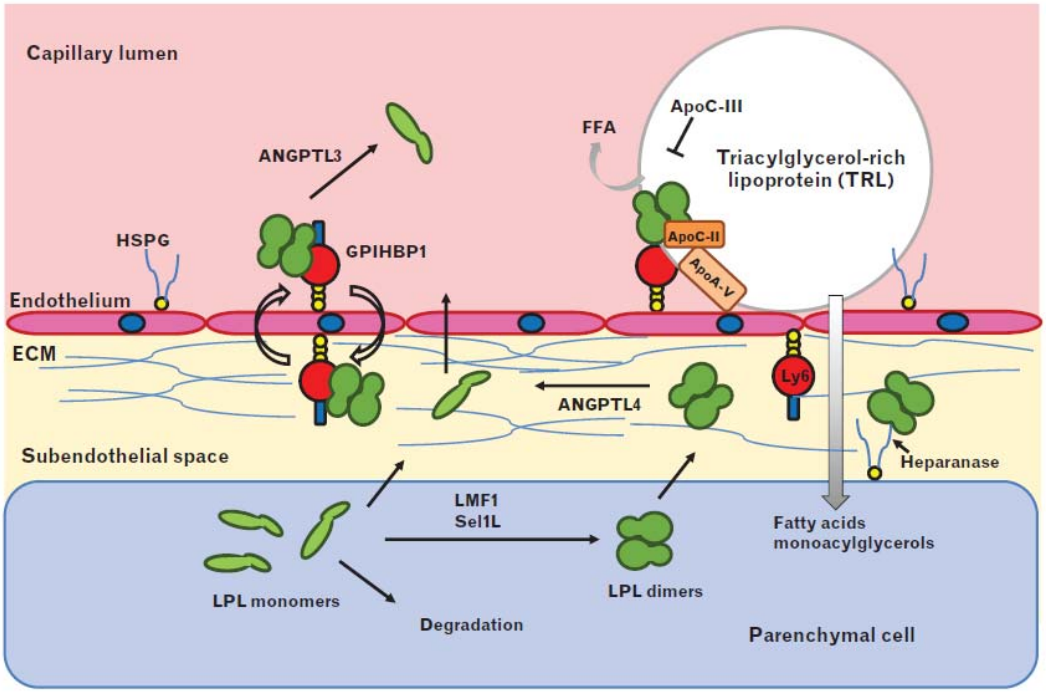

Figure1.6 Schematic view of LPL in action at endothelial binding-lipolysis sites (see text for details) (124).

Natural mutations and metabolic disease

The main function of LPL enzyme in lipid metabolism is to break down the triglyceride core of the plasma triglyceride-rich lipoproteins such as chylomicrons and very-low-density lipoproteins (VLDLs), at the luminal side of the endothelium. The

reaction that it catalyzes is the hydrolytic cleavage of the ester bonds of the triacylglycerols to form glycerol and free fatty acids which are used in a tissue-specific manner. In heart and muscle, FFAs are used as a source of energy, whereas in the adipose tissue are used for storage as fat depots (108, 110, 125-127). Active homodimeric lipoprotein lipase requires the presence of the cofactor apolipoprotein CII to catalyze the hydrolysis of the TG. The apoCII is a component of the surface of the triglyceride-rich lipoproteins and increases the Vmax of the reaction (108, 128-130). In addition to its well-known lipolytic function, a non-enzymatic bridging function of the LPL has been described. LPL binds simultaneously to both lipoproteins and cell surface receptors, including HSPG, LDL receptor, and apoE receptor 2. So, it facilitates the uptake of chylomicron remnants, free fatty acids, cholesterol-rich lipoproteins and lipophilic vitamins into tissues by accumulating them to the vessel wall and by serving as a ligand for the lipoprotein receptors (99, 108, 131-137).

Lipid abnormalities are a consequence of metabolic dysregulation resulting in mild to severe hypertriglyceridemia (elevated levels of triglycerides in the bloodstream) due to enhanced VLDL production, a delayed hepatic remnant clearance and mild disturbances in peripheral lipolysis.

More than 220 naturally occurring mutations in the LpL gene have been reported in humans, the majority of which are missense and are spread over the exons 4, 5 and 6 (138). Most of these mutations are rare and if they are present in homozygote or compound heterozygote state they lead to a complete loss of LPL activity and LPL deficiency in humans. LPL deficiency is a rare recessive genetic disorder causing profound hypertriglyceridemia (TG>2000 mg/dL), due to lack of plasma triglyceride hydrolysis and massive increases in chylomicrons. Creamy blood, marked hypercholesterolemia (300 to 1000 mg/dL) and extremely low HDL-cholesterol are also often present, secondary to the hyperchylomicronemia. The disorder usually presents early in the first year of life and is associated with the usual clinical findings of familial chylomicronemia, eruptive xanthomas, lipemia retinalis, hepatosplenomegaly, recurrent abdominal pain, pancreatitis, memory loss and/or dyspnea. LPL deficiency in the heterozygous state clearly leads to moderate increases in plasma triglyceride levels that tend to increase later in life, as a result of a decrease in the LPL activity. The heterozygotes more often have decreased HDL-cholesterol

levels and high risk of developing chylomicronemia and pancreatitis with stresses such as diabetes, pregnancy and high alcohol intake (138-146).

Moreover, various mutations in the apoC-II, GPIHBP1 or LMF1 genes result in decreased or absent LPL activity, defective lipoprotein catabolism that leads to severe massive hypertriglyceridemia and familial chylomicronaemia.(111, 112, 147). Dysfunction of the LPL system increases also the risk for metabolic disease connected to obesity, diabetes and premature atherosclerosis (141).

The role of LPL in the development of atherosclerosis and the risk of cardiovascular disease is not very clear, because LPL confers pro-atherogenic or anti-atherogenic effects depending on its locations. In the general population, elevated triglyceride levels have been associated with cardiovascular risk. The enzyme expressed by adipose tissue and muscle protects from atherosclerosis by facilitating the clearance of circulating triglyceride-rich lipoprotein particles. In this line, it drives the lipoprotein profile in a non-atherogenic direction with low levels of atherogenic lipoproteins and high atheroprotective HDL levels (148-152). Indeed, a variant of LPL that is associated with increased activity, decreased TG and higher HDL levels has been shown to confer protection against coronary heart disease (153). Furthermore, several commercially available hypolipidemic and antidiabetic drugs and mouse models of LPL overexpression have been associated with an LPL stimulatory activity that probably contributes to global lowering of plasma lipids and improvement of cardiovascular outcome (154-156). Contrary, LPL deficiency in human studies has been shown to correlate with worsened atherosclerotic outcomes (141, 157).

However, macrophage-derived LPL has been ascribed a pro-atherogenic role with its catalytic activity and non-catalytic bridging action contributing to this effect. LPL-mediated accumulation of lipids or oxidized LDL in vessel wall, cellular uptake of lipoproteins remnants and FA (that can be re-esterified) are associated with the formation of foam cells and subsequent progression to atherosclerotic plaques (108, 150-152, 158-160). Uptake of lipids by LPL in THP-1 macrophages or addition of FFA were shown to decrease the transcription of ABC transporters and scavenger receptor BI (SR-BI) and resulted in reduced cholesterol efflux from the cells (161, 162). Furthermore, downregulation of LPL in macrophages caused prevention of atherosclerosis in apoE–/– mice (163). However, the relative contribution of macrophage LPL to overall physiological effects of LPL is unclear. In spite of the

pro-atherogenic role of macrophage LPL, a large body of evidence suggests that LPL is an attractive target in treating dyslipidemias and associated complications.

Studies in mice

Several loss-of-function and gain-of-function studies have provided insight into the key role of LPL in metabolic homeostasis. Mouse models lacking LPL expression in the whole body have shown a severe hypertriglyceridemic phenotype (~20.000 mg/dl). The homozygote knockouts are born with threefold higher triglyceride levels, sevenfold higher VLDL cholesterol levels, decreased HDL cholesterol levels, depleted tissue storage of TG and developed spontaneous atherosclerosis. When permitted to suckle, the LPL knockout mice became pale, then cyanotic, were unable to metabolize milk lipids and finally died 18–24 hours after birth from severe hypoglycemia (164, 165). LPL heterozygote mice on standard mouse chow survived to adulthood but they suffered from mild hypertriglyceridemia, impaired VLDL clearance, and somewhat lower levels of fasting plasma glucose. This was connected to increased body weight and ectopic lipid storage resulting in β-cell dysfunction, insulin resistance and impaired glucose tolerance (165-167).

On the contrary, adenovirus-mediated expression of LPL can rescue LPL knockout pups, but they are still hypertriglyceridemic with plasma TG levels ~3.000 mg/dl on a chow diet (168). Transgenic mice overexpressing LPL throughout the body showed higher LPL activity, markedly lower plasma TG, resistance to diet-induced hypertriglyceridemia and hypercholesterolemia and decreased development of atherosclerosis due to the reduction of lipoprotein remnants (148, 149, 169). Interestingly, overexpression of a catalytically inactive LPL in mice also improved the high-fat diet-induced insulin resistance and hypertriglyceridemia (170). Moreover, inactive LPL overexpressed in LPL heterozygous mice can act in vivo to mediate VLDL removal from plasma and uptake into tissues in which it is expressed (131).

It is interesting to note that mice with selective overexpression of LPL in the liver develop insulin resistance and are characterized by increased liver triglycerides, glucose and large amounts of intracellular lipid droplets in their livers (171). In another study, expression of LPL exclusively in the liver (in LPL knockout

background) rescued mice from neonatal death but developed severe cachexia during high fat suckling and had elevated TG and glucose and excessive hepatic steatosis. Adult mice showed slower turnover of VLDL, increased production of liver VLDL TG, and three to fourfold increased plasma ketones bodies (172). On the other hand, the selective deletion of LPL in hepatocytes leads to impaired postprandial triglyceride clearance and elevated levels of plasma triglycerides and cholesterol due to decreased plasma LPL content and activity. These studies indicate the importance of the hepatic LPL in plasma lipid homeostasis despite its relatively low expression in the adult liver.

Transcriptional regulation of LPL

The expression and activity of LPL gene can be regulated by several factors at the level of transcription, translation and post-translation in a tissue-specific manner. A large number of specific cis-acting elements are located at the 5' regulatory region of LPL gene that extends ~4 kb from the transcription start site (Figure 1.5). LPL transcription has been shown to be controlled in a tissue specific manner by the peroxisome proliferator-activated receptors (PPARs) and their heterodimer retinoid X receptor (RXR), through binding to the PPRE element in the LPL promoter (at region -169/-157) in response to fibrates, fatty acids or other PPAR agonists (173, 174). The transcription factor PPARγ mainly influences adipocyte differentiation and lipid storage by stimulating transcription of the LPL gene. Fasting reduces expression of PPARγ in adipose tissue, providing a potential explanation for the reduction in LPL expression during fasting (175-177). On the other hand, many natural ligands of PPARα and PPARδ are associated with increased LPL mRNA expression and lipid accumulation in hepatocytes and macrophages (174, 178, 179).

Previous studies in mice have shown that the transcription of LPL gene in the liver is induced by high fat diets and synthetic agonists that activate the nuclear receptors LXR (Liver X Receptor) and RXR (Retinoid X Receptor) (180-182). Especially, Zhang et al. demonstrated that LXRα promotes the expression of LPL gene in response to diet rich in cholesterol or to synthetic LXR agonist selectively in the liver and to a lesser extent in macrophages, but not in other tissues expressing LPL

in high levels, including adipose, muscle and heart. This response is mediated by an LXR responsible element in the first intron of mouse LPL gene that binds LXR/RXR receptors (181). In addition to these findings, LPL gene has been shown to be induced also by natural LXR and RXR ligands or synthetic LXR agonists in human endothelial cells and macrophages (183, 184). In the liver a single dose of TNFa can induce LPL mRNA levels (185) and treatment with fibrates, which activate PPARs, stimulate also LPL activity (186).

In the 3T3-L1 adipocyte cell line, a proximal octamer motif at region -45/-38 of mouse LPL promoter was shown to interact with the factor Oct-1. This factor plays a positive role in LPL gene transcription as it can interact with the transcription factor TFIIB at this site and make it function as a TATA box. Indeed, a natural mutation, a T to C substitution at nucleotide -39, was identified in a patient with familial combined hyperlipidemia and low LPL activity. This substitution, which is localized within the binding site for the transcription factor Oct-1, was shown to be associated with a 85% reduction in LPL promoter activity in human macrophages (187-189).

A CCAAT box just upstream of the octamer sequence (at position –65) binds nuclear factor Y (NF-Y) and plays an important role in basal promoter activity in the 3T3-L1 adipocyte cell line (190). The nuclear factor Y complex possesses histone acetyltransferase activity, providing a potential mechanism to regulate the tissue-specific transcription of the LPL gene by remodeling of chromatin (137). Tumor necrosis factor α (TNF-α) and interferon–γ (INF-γ) can inhibit LPL gene transcription by blocking the binding of NF-Y to the LPL promoter, in the 3T3-L1 adipocyte cell line or mouse macrophages (191, 192).

In the human LPL promoter an evolutionarily conserved CT element (from –91 to –83) was identified which is important for the basal activity of LPL gene and interacts with Sp1 and Sp3 factors. A naturally occurring T to G mutation was identified at position –93 of the promoter which is associated with a reduction in promoter activity and the Sp1/Sp3 binding (193). In addition, interferon-γ cytokine mediates suppression of macrophage LPL gene transcription possibly via PI3K pathway that leads to decreased binding of Sp1 and Sp3 to the LPL gene (192, 194). Interestingly, the –90 to –81 region of LPL promoter also interacts with sterol regulatory element binding protein, which mediates the induction of LPL gene transcription in adipocytes, in response to decreased cellular cholesterol levels (195).

Another DNA binding factor that has been implicated in the regulation of LPL gene transcription is the cAMP response element binding protein (CREB) that activates LPL promoter in response to cAMP-elevating agents via a cAMP-responsive element located at the first 230 base pairs of the proximal LPL promoter (196). It has been shown that an Activator Protein-1-like motif located at -1856/-1850 of LPL promoter is responsible for the suppression of the LPL gene transcription by estrogen (197). Inhibition of the transcription of LPL is mediated also by the transforming growth factor-β (TGF-β) cytokine via a TGF- responsive element in macrophages (198). Furthermore, silencing elements are also located in the human promoter at positions –225 to –81 reducing promoter activity, but the protein that is responsible for the suppression of transcription is unknown (199).

Post-translation regulation of LPL

LPL regulatory proteins

Physiological variation in LPL activity in various tissues is achieved via post-translational mechanisms involving a number of extracellular regulatory proteins. These "LPL regulatory proteins" can be divided into two main groups, the apolipoproteins (APOs) and the angiopoietin-like proteins (ANGPTLs) (Figure 1.7).

ApoC-II and apoA-V have been described to have LPL-stimulatory properties. apoC-II, the cofactor of LPL, is required for maximal rates of TG-rich lipoprotein lipolysis guiding the lipoproteins to the active site of LPL (128, 200-202). Human genetic and in vitro studies have supported the plasma TG-lowering effect of apoC-II via stimulation of LPL activity. Indeed, apoC-II deficiency is associated with marked elevation of plasma TG, VLDL and chylomicron levels and decreased LPL activity, LDL and HDL levels (144). Paradoxically, overexpression of apoC-II gene in mice leads to marked hypertriglyceridemia via impaired plasma TG clearance, suggesting that at high concentrations apoC-II may inhibit LPL (200, 203). Apolipoprotein A-V (apoA-V) is inversely correlated with plasma TG. Like LPL, apoA-V can also bind to vascular cell surface HSPG, thus promoting lipoprotein interaction with LPL and facilitating LPL-catalyzed TG lipolysis in these lipoproteins (204). Interestingly, apoA-V also binds to GPIHBP1, the major binding site for luminal LPL and the

platform for lipolysis and promotes LPL-mediated lipolysis through enhancing attachment of lipoproteins to endothelial cell surface GPIHBP1 (202, 205). ApoA-V knockout mice display severe hypertriglyceridemia (206, 207) and loss of function mutations in the apoA-V gene cause hyperchylomicronemia in humans (208, 209).

As opposed to apoC-II and apoA-V, apoC-I, apoC-III and apoE inhibit LPL activity and thus TG clearance, as shown by mice overexpressing or lacking these apolipoproteins (210-212). Furthermore, human heterozygous carriers of null mutation in the APOC3 gene exhibit lower plasma TG levels confirming its LPL inhibitory activity (213). It has been proposed that apoC-I and apoC-III inhibit LPL activity by displacement of the enzyme from TG-rich particles. Further, apoC-III also inhibits receptor-mediated uptake of lipoprotein remnants and LDL (214). ApoE elevates circulating levels of TG-rich lipoproteins, partly by reducing the LPL-mediated plasma TG lipolysis rate, and partly by stimulating hepatic VLDL-TG production (215, 216).

Other LPL inhibitory proteins include several members of the family of angiopoietin-like proteins, specifically ANGPTL3, ANGPTL4 and ANGPTL8. These proteins inhibit LPL lining the capillary endothelium in many tissues that results in elevated TGs in the bloodstream (217, 218). Studies using various animal models of ANGPTL3, ANGPTL4 and ANGPTL8 overexpression or deletion have confirmed the stimulatory effect of these proteins on plasma TG levels, which is achieved by impairing plasma TG clearance and inhibiting LPL activity (217, 219-222). ANGPTL4 inhibits LPL activity by converting the catalytically active LPL dimers into inactive monomers (223, 224). Alternatively, it has also been proposed that ANGPTL4 forms a reversible complex with LPL and functions as a conventional noncompetitive inhibitor preventing the hydrolysis of the substrate (225). However, according to another study, ANGPTL4 acts intracellularly to promote LPL degradation, probably after its processing in the ER (226). The biochemical mechanism for LPL inhibition by ANGPTL3 seems to be stoichiometrically distinct from ANGPTL4. ANGPTL3 may cooperate with the related protein ANGPTL8, which inhibits LPL activity directly or indirectly, by promoting cleavage and coordinating the trafficking of TGs to tissues in response to food intake (227-230).

Other proteins that regulate LPL stability and activity are LMF1, HSPGs and GPIHBP1 which have already discussed above (Figure 1.7).

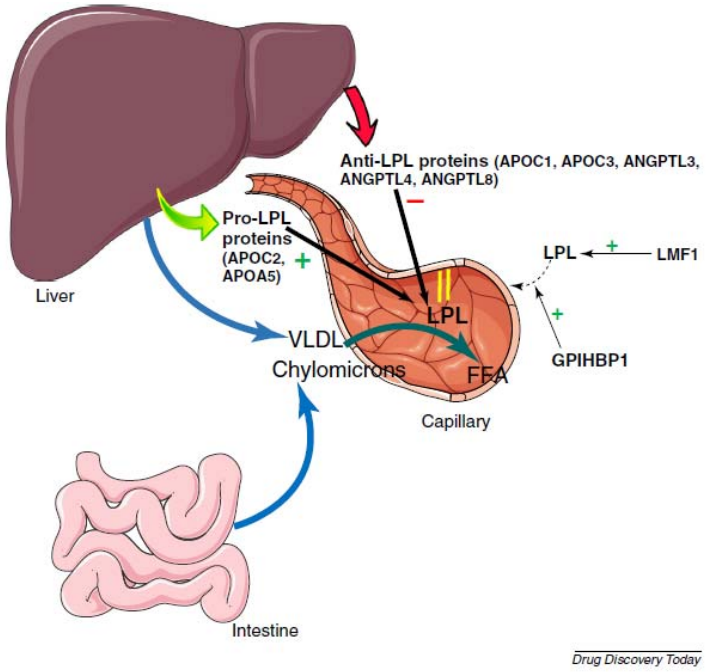

Figure 1.7 Regulation of LPL activity at post-transcriptional level by 'regulatory proteins' (see text for details)(231).

Regulation by physiological conditions

LPL activity is known to change rapidly in a tissue-specific manner in response to changes in the physiological state, for example, feeding/fasting, exercise and cold exposure (Figure 1.8)(232) LPL activity and thus clearance of TG-rich lipoproteins in white adipose tissue is markedly elevated in the fed state while fasting is associated with a pronounced decrease in LPL activity, which is likely partly mediated by the presence or absence of insulin (233). Insulin has been shown to play a central role in the postprandial response of adipose LPL activity and expression (234, 235). Indeed, ANGPTL4 has been suggested to represent the factor that governs regulation of LPL activity during fasting and feeding in fat tissue. It was found that insulin suppresses ANGPTL4 expression in adipocytes and increases adipose LPL activity (236, 237).

In contrast to LPL in adipose tissue, most studies indicate that fasting and starvation raise total LPL activity in skeletal muscle, while insulin decreases skeletal muscle LPL activity (238-240) . Similar to the situation in adipose tissue, expression of the LPL inhibitor ANGPTL4 is markedly increased during fasting in mouse and human skeletal muscle (241, 242). LPL in adipose tissue is also affected by physical activity. Numerous studies in humans and rodents have demonstrated that a single bout of physical exercise leads to a marked increase in LPL activity in the exercising

muscle, in order to increase the supply of fatty acids to the cell for subsequent oxidation and ATP generation (243-246).

Similar to the muscle, LPL activity in the heart is increased in response to fasting (247, 248) and insulin decreases cardiac heparin-releasable LPL activity (249). Feeding is also associated with increased expression of the LPL inhibitor ANGPTL4, which reduces cardiac heparin-releasable LPL activity (250). Moreover, cold exposure, which increases energetic demands in the heart, was found to stimulate total and heparin-releasable LPL activity in the rat heart (251). Similarly, cold markedly stimulates plasma and brown adipose tissue LPL activity causing reduction in plasma TG (252, 253). Fatty acids that produced are used by this highly oxidative tissue to generate heat and maintain body temperature as part of cold-adaptive thermogenesis (254).

In macrophage, fatty acids released upon hydrolysis of TG by LPL are an important fuel during periods of intense metabolic activity, such as phagocytosis and proliferation (255, 256). Furthermore, lipopolysaccharide (LPS) and numerous cytokines released in response to LPS, including TNF-α, interferon γ and IL-1β, inhibit secreted LPL activity, which is likely mediated at the level of LPL gene transcription (257-259) (Figure 1.8).

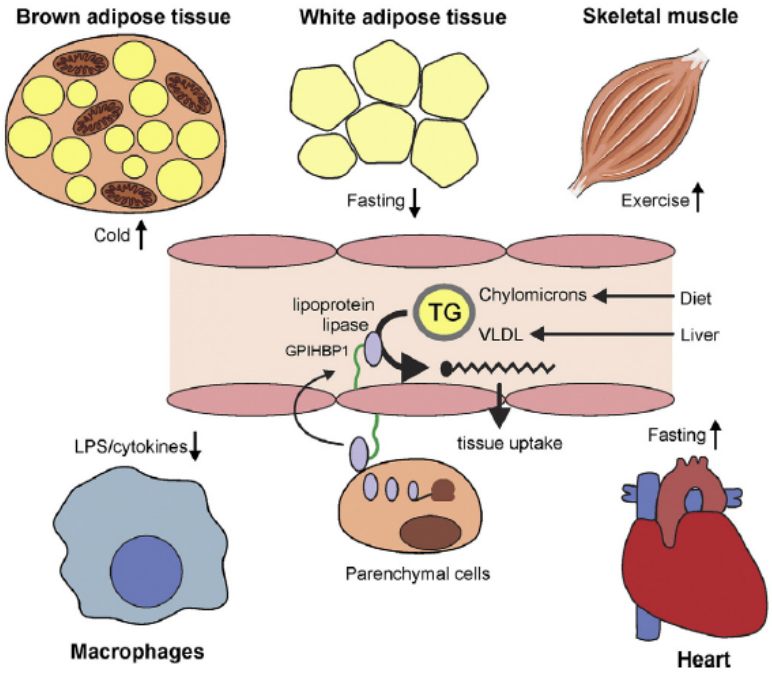

Figure 1.8 Summary of the main physiological stimuli regulating LPL activity in various tissues (see text for details) (232).

FOX family and FOXA subfamily

The Forkhead box (FOX) family represents a large family of transcription factors that share a highly conserved 110 amino acid 'winged helix' DNA binding domain (DBD), known as a 'forkhead box' domain (260). The name of this family came from the first gene containing this domain in Drosophila melanogaster, the forkhead (fkh) gene. Mutations in this gene result in a characteristic 'forkedhead' appearance resulting from the transformation of the foregut into ectopic spike-formed head structures (261-263). More than 170 members of this family have been identified in organisms ranging from yeast to humans, but not in plants (264, 265). In mammals, more than 40 FOX transcription factors are categorized into 19 subfamilies (from FOXA to FOXS) based on sequence similarity (266-269). Outside of the winged helix domain in many of these genes of forkhead family, there is very little sequence similarity (263, 265). Many FOX proteins serve as pioneer factors due to their unique ability to open up compacted chromatin and initiate regulatory control of transcription, facilitating the loading of subsequent transcription factors (270). Other FOX members function as classic transcription factors facilitating the recruitment of chromatin remodeling factors such as acetyltransferases, histone deacetylases and ATP-dependent chromatin remodeling complex.

The FOXA subfamily includes three genes, FOXA1, FOXA2, and FOXA3. They were identified in rat liver cells to bind to specific sequences in the transthyretin (TTR) and alpha1-antitrypsin (α1-AT) promoters and activate their transcription and therefore named hepatocyte nuclear factor (HNF) 3α, 3β, and 3γ respectively (262, 263, 271). FOXA proteins have critical roles in early development, organogenesis, growth, stem cell differentiation and metabolism in worms, flies and mammals (272-275).

Structure of FOXA factors

FOXA proteins contain three well-defined functional domains including the highly conserved forkhead DBD and two flanking transactivation domains. FOXAs interact with the target DNA as monomers through their forkhead DBD. DNA

response elements usually span 15–17 bp with a conserved 7 bp core recognition site 5'- T(G/A)TTT(A/G)(C/T)T-3' (276-278). The three-dimensional structure of FOXA3 DBD was first resolved by X-ray crystallography (279). Subsequently, the sequence conservation in the DBD of the forkhead family members indicated that all members share this structural domain. Particularly, the three FOXA proteins display 95% sequence homology in their DBDs. Outside of this region, FOXA1 and FOXA2 are only 39% identical, with FOXA3 being even more distinct (263). The Forkhead box of the FOXA proteins contains three N-terminal α-helices (H1-3), three β-strands and two loops or wings (W1-2) towards the C-terminal region, typically organized into an α1-β1-α2-α3-β2-W1-β3-W2 order and folded into a helix–turn–helix (HTH) motif flanked by loops on either side forming wings (W1 and W2)(280). This folding resembles the shape of butterflies and thus resulted in the label 'winged-helix domain' (279, 281).

At the amino (N)- and the carboxy (C) -terminal regions of the proteins two transactivation domains (TA) can be found. The C-terminal TA domain contains two stretches of amino acids which are unique to FOXAs and bind to core histones H3 and H4. The N-terminal TA domain requires the C-terminal TA domain for transcriptional activation (282-284). FOXA proteins have also two nuclear localization sequences (NLS) that are located at both N-terminal (α1) and C-terminal (W2) ends of the forkhead domain (280, 282, 285). Furthermore, FOXA2 is the only member of the FOXA family that contains an AKT2/PKB phosphorylation site (T156) at the N-terminus end of the forkhead domain (Figure 1.9)(286, 287).

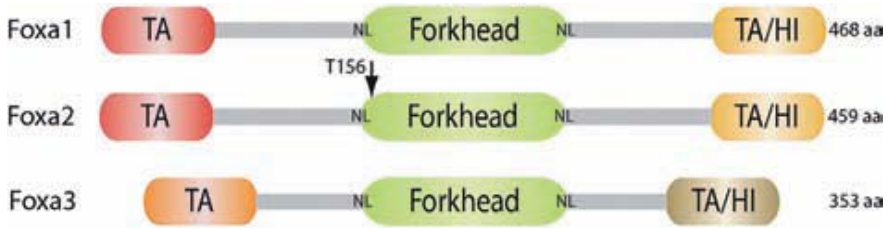

Figure 1.9 Schematic representation of functional domains present in mouse FOXA1–3. T156, AKT2 phosphorylation site; TA, transactivation domain; HI, histone interaction domain; NL, nuclear localization (286).

Expression of FOXA factors during development

FOXA transcription factors are expressed in early development and play crucial roles in the fetal development and homeostasis of various cells and tissues. They exhibit overlapping but distinct expression patterns in a variety of developing and mature tissues (263, 286, 288).

FOXA2 is the first gene of the FOXA family to be expressed in the progress of embryogenesis (289). At embryonic day (E) 6.5, the expression of the FOXA2 gene can be detected in the primitive streak, node, notochord and neural plate (290, 291). The expression of FOXA2 is also detected in definitive endoderm and endoderm-derived tissues such as liver, pancreas, intestine, thyroid, prostate and lung, where is then maintained through development to adulthood (289, 290, 292-295) FOXA2 is also observed in dopaminergic neurons in ventral midbrain, at late embryonic stage (288, 296). In collaboration with FOXA1, FOXA2 is essential for liver organogenesis in mouse, as embryos deficient for both genes in the foregut endoderm do not develop liver bud and the expression of the hepatoblast marker alpha-fetoprotein (Afp) is lost (297). Thus, FOXA2 has an essential role in the development of axial mesoderm, foregut endoderm and the onset of hepatogenesis in the mouse.

The earlier expression of FOXA2 compared with the other FOXA factors is reflected in the severity of phenotype in mice lacking this factor. Mice homozygous for a FOXA2 null mutation die in early embryogenesis shortly after gastrulation, show defects in node development and lack a notochord which leads to secondary defects in neural tube and foregut morphogenesis (298, 299). Heterozygotes for FOXA2 are viable but display a Parkinson's-like phenotype following aging (300).

During early embryogenesis, the expression of FOXA1 appears with a short delay compared with FOXA2 expression. At E7.0 expression of FOXA1 gene can first be detected in the primitive streak, and then later in the notochord, neural plate and neural tube (289). Although FOXA1 is initially highly expressed in the developing pancreas, its expression falls in the adult pancreas (301). In addition, FOXA1 is more widely expressed in several adult tissues, including the respiratory system, brain, gastrointestinal tract, male reproductive organs, the ureter and bladder (286). Contrary to FOXA2 null mice, those lacking FOXA1 survive until after birth, but develop neonatal hypoglycemia, hormonal insufficiencies, pancreatic and kidney

dysfunction and defects in prostate morphogenesis. Finally they die between postnatal days 2 and 12 (267, 302-304).

The expression of FOXA3 can first be detected at E8.5 in the foregut endoderm and then is maintained strongly in the liver and also in the pancreas and intestine through development to adulthood (289). Due to its restricted expression pattern, FOXA3-deficient mice are viable and develop normally. However, they display hypoglycemia after a prolonged fast because of defects in hepatic glucose production (298, 299, 305, 306).

Role of FOXA proteins as pioneer factors

Classic transcription factors depend on the recruitment of chromatin modifying enzymes to open up the chromatin. However, the key cellular function of FOXA proteins is to interact with specific DNA sequences within compacted chromatin and promote nucleosome decompaction without ATP-dependent enzymes. Thereby, they initiate transcriptional regulation by making the genomic region more accessible to other regulatory transcription factors. For this reason, FOXA family members have been characterized as 'pioneer' transcription factors (Figure 1.10) (284, 286, 307, 308).

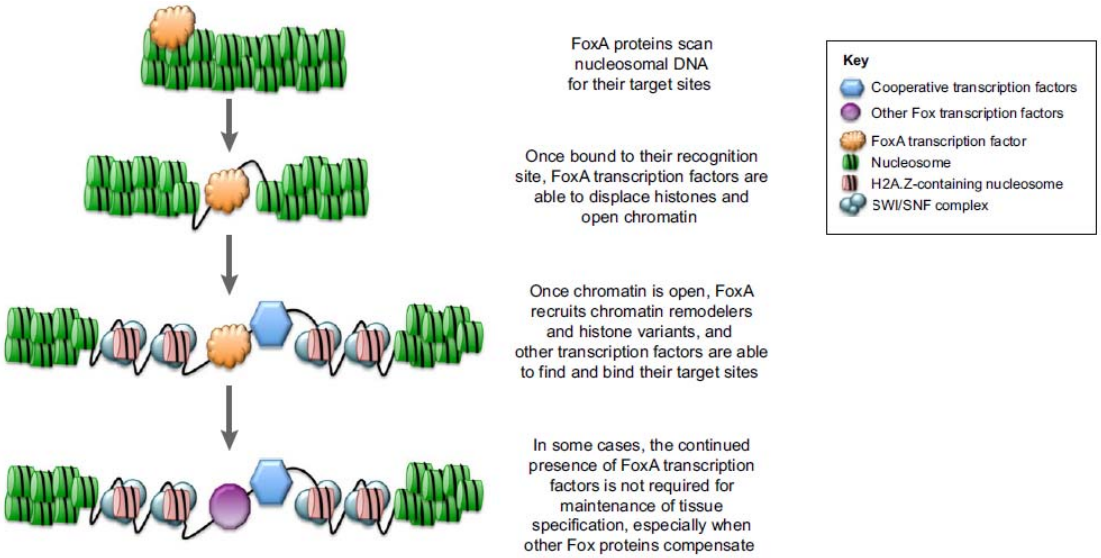

Figure 1.10 FOXA proteins function as pioneer factors. The schematic depicts how FOXA transcription factors are able to function as pioneer factors that control gene expression via their interaction with chromatin (309).

This pioneering function of FOXA is mediated by its ability to bind DNA sites and core histones H3 and H4 simultaneously. Structural comparisons showed that the winged-helix structure of FOXA forkhead box is highly similar to that of linker histones H1 and H5 (279, 284, 310). This feature in combination with C terminal regions mediating interaction with histones H3 and H4 allow FOXA transcription factors to access closed chromatin, replacing linker histones and relieving chromatin compaction at target enhancer and/or promoter sites. This creates an open chromatin configuration, allowing the recruitment of alternative histones and other transcription factors to induce target gene expression. FOXA proteins, which are associated with transcriptionally active chromatin, lack critical amino acids required for DNA compaction by linker histones and therefore are distinguished by linker histones that repress gene expression (284, 311).

Because of their actions as pioneer factors, FOXA proteins facilitate the binding of nuclear hormone receptors to the promoters of their targets in multiple organ systems in the adult. Genome-wide mapping of forkhead DNA binding elements showed that they are frequently located in close proximity to hormone response elements (HREs). Specifically, it has been shown that binding of the glucocorticoid receptor (GR) to its targets is dependent in part on FOXA2, during the fasting response (312). Similarly, estrogen-response elements and androgen response elements were found in close proximity to binding sites for FOXA1 in several target genes of nuclear receptors. Binding of FOXA1 precedes that of the androgen receptor and inhibition of FOXA1 expression reduces activation of estrogen-responsive gene (313-315)

Role of FOXA2 in metabolism

Liver and pancreas play essential roles in glucose and lipid homeostasis by protecting organisms from hypoglycemia. In response to feeding, insulin secreted from pancreatic beta cells induces the uptake of glucose and inhibits endogenous glucose production. Conversely, in fasting states insulin levels are low and hepatic programs of gluconeogenesis and fatty acid oxidation are induced, thus maintaining glucose homeostasis (316, 317). In addition to its critical role in embryonic

development, FOXA2 has been also implicated in the regulation of these metabolic processes in the adult (318-321).

Since FOXA2 knockout mice are embryonic lethal, the generation of mice with conditional deletions of FOXA2 was necessitated. In $FOXA2^{loxP/loxP}$; FOXA3-Cre mouse, FOXA2 is not expressed throughout the regions of FOXA3 expression, including the endoderm at the foregut/midgut border that gives rise to the liver bud. Their liver morphology is normal and the initial steps of pancreatic bud formation occur normally. However, the α-cell lineage fails to reach its final differentiated state that results in mild hypoglycemia, hypoglucagonemia and death between P0 and P5 (320). More focused deletion of FOXA2 specifically in pancreatic β-cells also leads to severe hypoglycemia and relative hyperinsulinemia and usually death between P9 and P12. Islets isolated from $FOXA2^{loxP/loxP}$;Ins.Cre mice are disorganized and do not secrete insulin in response to elevated glucose concentrations, but inappropriately in response to amino acids. This is explained by the decreased expression of the FOXA2 target genes Kir6.2 (Kcnj11) and Sur1 (Abcc8), which are expressed in pancreatic α- and β-cells and play important role in the secretion of insulin and glucagon, comprising the KATP glucose-sensing channel (321, 322). In addition, hadhsc gene expression is reduced in $FOXA2^{loxP/loxP}$;Ins.Cre islets. This gene encodes a short chain fatty acid dehydrogenase, a mitochondrial matrix protein important for fatty acid oxidation (321).

A mouse model that explains the role of FOXA2 in hepatic glucose homeostasis is $FOXA2^{loxP/loxP}$;Alfp.Cre mice. The expression of FOXA2 in these mice is deleted specifically in hepatocytes. They are euglycemic, but they fail to fully activate gluconeogenic enzymes during fasting, such as Pepck (phosphoenolpyruvate carboxykinase), IGFBP-1 (insulin groth factor binding protein 1) and Tat (tyrosine aminotransferase) (312). Furthermore, another study with FOXA2 liver-deficient mice, showed that FOXA2 plays an important role in bile acid homeostasis, regulating multiple genes involved in bile acid metabolism including those encoding lipid and bile acid transporters of hepatocytes. $FOXA2^{loxP/loxP}$;Alfp.Cre mice develop mild hepatic cholestasis, which is worsened after a cholic acid rich diet. These mice show also intrahepatic cholestasis, a significant increase in serum bile acids ER stress and liver injury (323). Additional mouse genetic studies have also revealed that FOXA2 activity in the adult liver mediates fasting responses, including fatty acid oxidation, ketogenesis and increased secretion of VLDL and HDL by activating gene expression

of key enzymes of these pathways (312, 324-326). All these phenotypes show the requirement of FOXA2 for the normal regulation of the gluconeogenic program, in both the liver and pancreas.

Heterozygous FOXA2+/– mouse indicated the role of FOXA2 in promoting energy utilization in adipose tissue in excess of caloric intake. FOXA2+/– mice have normal glucose levels, but in response to high-fat diet they have increased adiposity and decreased energy expenditure, adipocyte glucose uptake, glycolysis and lipolysis. Expression of genes involved in these processes were down-regulated in primary adipocytes from FOXA2+/– mice fed a high-fat diet and the adipocytes showed decreased insulin sensitivity(327).

FOXA2 has been implicated also in the regulation of plasma HDL levels in mice. Haploinsufficient FOXA2+/- or hyperinsulinemic mice (caused by genetic mutations in leptin signaling or high fat diet-induced obese mice that exhibit dyslipidemia, hyperglycemia and insulin resistance) exhibited and plasma pre-β HDL levels. This has been correlated with the inactivation of FOXA2 that results to decreased expression of the apolipoprotein M (apoM) gene which is a target of FOXA2 (325, 328). FOXA2 is recruited to a conserved binding site on the human apoM promoter located between nucleotides -398 and -388. Furthermore, leptin treatment of ob/ob (leptin deficient) and db/db (leptin receptor deficient) mice restored apoM expression through relocation of FOXA2 to the nucleus.

FOXA2 plays a wider role in HDL metabolism by regulating in a positive or a negative manner, the expression of several genes in hepatic cells. Although FOXA2 is a nuclear factor that activates gene transcription when bound to DNA due to the presence of two transactivation domains, FOXA2 may also inhibit gene expression. In a previous study from our group we showed that FOXA2 binds to three sites on the proximal promoter of the human cholesterol and phospholipid transporter ATP binding cassette transporter 1 (ABCA1) gene. One of these sites is the TATA box and FOXA2 binding to this site inhibits the up-regulation of ABCA1 gene expression by oxysterol-activated LXRs in hepatic cells under conditions of cholesterol loading (329).

Regulation of FOXA2 by insulin

FOXA2, but not FOXA1 or FOXA3, is negatively regulated by nutrient metabolism and specific by insulin in the liver. In fasting states, FOXA2 is located consistently in the nucleus. However, in response to insulin signaling in vitro and in vivo in perfused mouse liver, FOXA2 transcriptional activity is blocked by a mechanism that involves phosphorylation at threonine 156 by AKT2/PKB kinase and nuclear exclusion. Only a single point mutation of T156 to alanine (T156A) that results to a constitutively active variant abolishes insulin-induced nuclear exclusion. Direct phosphorylation of FOXA2 by AKT was further supported by co-immunoprecipitation experiments, in which wildtype FOXA2, but not FOXA2 T156A, can be immunoprecipitated and phosphorylated by AKT (287, 324).

These findings have been extended in vivo by demonstrating nuclear exclusion of FOXA2 in fed mice, hyperinsulinemic ob/ob mice, and mice maintained on a high-fat diet. In these mice, FOXA2 is permanently excluded from the nucleus and its inactivation results to hepatic steatosis and insulin resistance. Furthermore, expression of the constitutively nuclear FOXA2 variant (T156A) in these diabetic mice leads to improvements in glucose levels, reduced hepatic TG content and increased fatty acid oxidation, VLDL secretion and insulin sensitivity (324).

According to this molecular model that has been proposed, FOXA2 is nuclear only in the starved state to activate multiple genes involved in hepatic glucose utilization, fatty acid oxidation, and ketogenesis and this gluconeogenic activity of FOXA2 is blocked via feeding-induced insulin secretion (Figure 1.11). However, other studies cannot confirm this model of nuclear exclusion of FOXA2 by insulin, but have found FOXA2 protein to be nuclear regardless of metabolic state (312, 330). So, more experiments are needed to address this controversy.

Genome wide studies in hepatic FOXA2

FOXA2 plays a pioneering role in establishing liver transcriptional program. Several groups have used genome wide analysis such as ChIP-on-chip (chromatin immunoprecipitation followed by microarrays) and ChIP-Seq (chromatin immunoprecipitation followed by sequencing) to investigate the in vivo binding sites of FOXA2 in the adult mouse liver or liver-derived cells (HepG2).

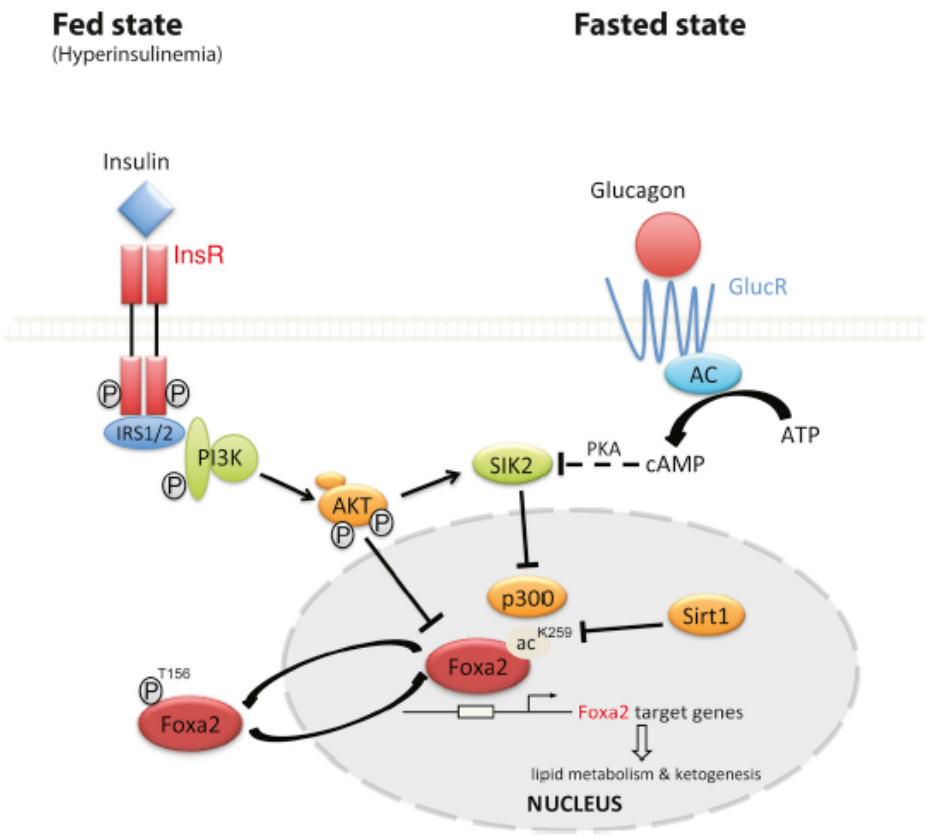

Figure 1.11 Model for regulation of FOXA2 activity by insulin and glucagon signaling in fed and fasted states, respectively. Schematic representation illustrating the regulation of FOXA2 and its target genes in hepatic lipid metabolism and ketogenesis. After feeding, insulin signaling leads to the inactivation of FOXA2 through phosphorylation of Thr156 and nuclear exclusion, thereby resulting in inhibition of FOXA2 target gene expression and reduced hepatic lipid metabolism and gluconeogenesis. During fasting, plasma insulin levels decrease and glucagon levels rise. Glucagon signaling activates the adenylate cyclase (AC), leading to inhibition of SIK2, a negative regulator of p300 activity. Acetylation of FOXA2 Lys259 by p300 increases its transcriptional activity. Sirt1 can inactivate FOXA2 by deacetylation and can thereby fine-tune the activity of FOXA2 (319).

Wolfrum et al., generated gene chip expression profiles from livers of wild type mice that had been infected with adenoviruses expressing either GFP or a constitutively active form of FOXA2 that cannot be phosphorylated by AKT (FOXA2-T156A) and they observed robust increases in the expression of genes involved in HDL metabolism (SR-BI, HNF-4α), triglyceride degradation (LPL, LIPC), β-oxidation, ketogenesis and glycolysis (324). In another ChIP-Seq analysis, approximately 11,000 FOXA2 binding sites were identified in the adult mouse liver. The majority of these binding sites were localized within 10 kb upstream of the

transcription start sites of genes and within the first introns. It was also found that 43.5% of genes expressed in the liver were also associated with at least one FOXA2 binding site, including genes of HDL metabolism (apoA-I, apoB, HNF-4α, LPL), with the greatest enrichment of 30-fold for apoA-II (331).

Studies by the group of K. Kaestner have used ChIP-Seq and Chip on chip analysis in samples of livers of wild type and hepatocyte specific FOXA2 *knockout* mice ($FOXA2_{loxP/loxP}$Alfp-Cre) (323, 332, 333). They identified 574 enhancer and promoter regions, corresponding to 484 unique genes, occupied by FOXA2 and clustered in categories of genes involved in lipid and steroid metabolism such as ABCA1, ABCC2, ApoA-I, ApoE, LIPC, LDLR (323). Furthermore, in FOXA2-deficient mice fed with cholic acid (CA) diet, the expression of genes involved in lipid metabolism/transport (ABCG8, LCAT, LIPC, LPL, PLTP) was significantly reduced and the expression of apoB gene was increased (332).

ChIP-Seq studies in HepG2 cells identified binding sites for FOXA2 in genes associated with HDL metabolism such as apoA-I , apoA-II, apoA-IV, hepatic lipase (LIPC), LDL receptor (LDLR), phospholipid transfer protein (PLTP) and nuclear receptors HNF1α, HNF1β, HNF4α and RXRα thus confirming the role of FOXA2 in HDL metabolism(277, 334).

LIVER X RECEPTORS (LXRs)

Liver X receptors (LXRs) belong to the nuclear receptor superfamily of transcription factors which bind to specific DNA sequences of target genes known as hormone response elements (HREs) and, upon ligand binding, they stimulate their transcription (335, 336). Retinoid X receptor (RXR) is a common partner for several nuclear receptors, including peroxisome proliferator-activated receptor (PPAR), vitamin D receptor (VDR), thyroid hormone receptor (TR) and farnesoid X receptor (FXR). Many of them regulate genes involved in essential metabolic and developmental processes (337-339).

LXRs were initially isolated from a human liver cDNA library as orphan nuclear receptors since their natural ligands were unknown (340). Later, oxidized cholesterol derivatives or oxysterols were identified as specific natural ligands of

LXRs, which are therefore also named “oxysterol receptors”. LXRs are implicated in various metabolic pathways such as cholesterol homeostasis, fatty acid homeostasis, glucose homeostasis, inflammation and immunity (341-345). The LXR subfamily consists of two isoforms, LXRα (NR1H3) and LXRβ (NR1H2). Whereas the two LXRs share sequence homology and appear to respond to the same ligands, their tissue distribution differs. In adults, LXRα is highly expressed in metabolically active tissues including liver, intestine, macrophages, and adipose tissue whereas LXRβ is more widely expressed in the immune system, glial cells in in the central nervous system, the gall bladder, islets of pancreas, skeletal muscle and prostate epithelium(346-348). During mouse development at embryonic day 11.5, both LXRα and LXRβ mRNA are detected in the liver. Hepatic LXRα maintains high expression throughout life while LXRβ decreases during later embryonic development (346, 349).

Structure of LXRs

LXR α and β share also the canonical nuclear receptor structure (Figure 1.12). The LXR molecule consists of five functional domains, an A/B region (N-terminal activation function-1 domain, AF-1), a C region (DNA-binding domain, DBD), a D region (hinge region), an E region (hydrophobic ligand-binding domain, LBD) and a C-terminal ligand-dependent transactivation domain (F region). The A/B ligand-independent domain contains the activation function 1 (AF-1) which may stimulate transcription in the absence of a ligand(350). This domain is also implicated in recruitment of ligand-independent co-activators. The DNA-binding domain (DBD) is highly conserved and contains two zinc fingers that bind to specific sequences of DNA called LXR responsive elements (LXRE). DBD and LBD are connected with a flexible domain, the hinge region, which appears to allow for conformational changes in the protein structure following ligand binding and also binds co-repressors in the absence of ligand. The Ligand binding domain (LBD) contains a-helices organized around a hydrophobic binding pocket. It determines the selectivity for the ligand and mediates transcriptional activation in a ligand-dependent fashion. In addition, it binds co-activator and co-repressor proteins and along with the DBD, contributes to the receptor dimerization. The C-terminal ligand-dependent domain (F region)

contains the activation function 2 (AF-2) which stimulates transcription in response to ligand binding (340, 350-352). Both isoforms of LXRs share ~78% identity of their amino acid sequences in both DNA- and ligand- binding domains (353).

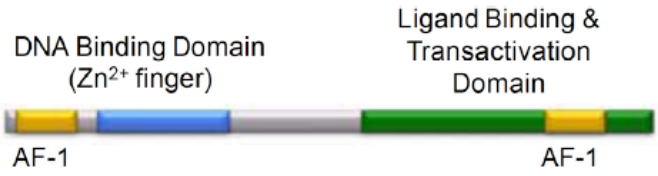

Figure 1.12 Domain structure of a typical hormone nuclear receptor. The structure is modular and consists of a N-terminal ligand-independent Activation Function 1 (AF-1) domain, a DNA binding domain of the zinc finger type, a composite domain consisting of the ligand binding, the dimerization and the Activation Function 2 (AF-2) domain (10) .

Ligands

It is widely accepted that endogenous LXR agonists are oxidized cholesterol derivatives referred to as oxysterols. Oxysterols in the animal body are synthesized from endogenous production in enzymatic reactions, endogenous production through the non-enzymatic reactive oxygen species (ROS)-dependent oxidation of cholesterol and delivery from alimentary sources. In general, oxysterols produced in enzymatic reactions are potent LXR agonists, whereas non-enzymatically generated ones have weak or no agonistic activity.

The most potent enzymatically generated oxysterols are 22(R)-hydroxycholesterol and 20(S)-hydroxycholesterol, 24(S)-hydroxycholesterol and 24(S),25-epoxycholesterol which were shown to bind to and stimulate transcriptional activity of LXRs at physiological concentrations (354-357). 22(R)-hydroxycholesterol and 20(S)-hydroxycholesterol are intermediates in the synthesis of steroid hormones from cholesterol while 24(S)-hydroxycholesterol is produced in the brain and represents the major oxysterol of human plasma. 24-(S),25-Epoxycholesterol is intermediate of the cholesterol biosynthetic pathway and particularly abundant in the liver, where both cholesterol metabolism and LXR expression are high (354). In human macrophages sterol 27-hydroxylase (CYP27) abundantly generates 27-hydroxycholesterol, representing the putative endogenous LXR ligand in these cells (358). Most endogenous oxysterols have similar affinity toward LXRα and LXRβ.

However, 5,6,24(S),25-dieopoxycholesterol and 6a-hydroxyl bile acids are somewhat selective for LXRα (356, 359) and N-aryl-3,3,3-trifluoro-2-hydroxy-2-methylpropionamides and cinnolines/quinolines derivatives exhibit LXRβ specificity (360, 361).

Glucose and glucose-6-phosphate are endogenous agonists for LXRα and LXRβ with efficacy comparable to that of oxysterols, suggesting that LXR may function not only as cholesterol, but also as a glucose sensor (362). However, glucose and its metabolites are unable to influence the interaction of cofactors with either LXRα or LXRβ (363). Some exogenous phytosterols or their derivatives may be physiologically important LXR ligands, Plant sterols (such as sitosterol, stigmasterol, campesterol, brasicasterol, and ergosterol) have similar chemical structure with cholesterol, but are poorly absorbed from the intestine and inhibit cholesterol absorption by displacing it from bile micelles. Supplementation of plant sterols may reduce plasma cholesterol level and is considered a potential anti-atherosclerotic therapy(364). Indeed, "oxyphytosterols", certain oxidized derivatives of phytosterols, are more effective LXR activators than 24(S),25-epoxycholesterol(365).

The involvement of LXR in various metabolic, inflammatory and proliferative diseases makes them highly attractive pharmaceutical targets for novel therapies. Two non-steroid synthetic LXR agonists, T0901317 and GW3965, are most commonly used in experimental studies (347, 366-368). It should be noted that T0901317 is not completely specific for LXR since it activates also the pregnane X receptor (PXR) and farnesoid X receptor (369, 370). T0901317 activates both LXRα and LXRβ (366), but GW3965 has a greater affinity toward LXRβ. However, the difference is too small to be useful in differentiating the two isoforms. However, neither of these two compounds was characterized clinically due to undesirable side effects of elevated plasma triglyceride levels and hepatic steatosis observed in preclinical animal studies due to activation of hepatic lipogenic enzymes (366, 371). In order to circumvent these off-target effects, novel high-potency LXR agonists have been developed that do not stimulate hepatic steatosis and hypertriglyceridemia. Many of them, including ATI-111, DMHCA, ATI-829, AZ876, MHEC and WAY-252623, drive promising anti-atherosclerotic effects in animal models (372). The WAY-252623 (LXR-623) agonist, which progressed recently towards phase I clinical trials, has anti-atherogenic activity and activates LXR without causing hepatic lipogenesis in humans. However additional trials were halted due to the neurological side effects (373-375).

In contrast to oxidized cholesterol metabolites that enhance transcriptional activity of LXRs, geranylgeranylpyrophosphate (GGPP), an intermediate of cholesterol biosynthesis, inhibits the transcriptional activity of LXRα and LXRβ by antagonizing their interaction with co-activators (376, 377). Moreover, polyunsaturated fatty acids (PUFAs) such as arachidonic acid, eicosapentaenoic acid, docosahexaenoic acid, and linoleic acid, are competitive antagonists of the interaction between LXRs and their ligands (378, 379). Transcriptional activity of LXRs was also shown to be inhibited by endogenous 5a,6a-epoxycholesterol and 7-cetocholesterol-3-sulfate which interfere with the agonistic action of LXR ligands (380, 381). In addition, ursodeoxycholic acid, one of the secondary bile acids, inhibits LXRα-induced lipogenic gene expression by increasing the expression of the LXRα co-repressor, SMILE (small heterodimer partner interacting leucine zipper protein) (382). Thus, endogenous LXR antagonists could counteract LXR agonist action in cholesterol homeostasis and atherogenesis.

Mechanism of LXR action

LXRs regulate gene transcription through two different mechanisms of action: direct activation and trans-repression. In the first mechanism, LXR forms obligate heterodimer with the RXR (337, 352) and LXR/RXR heterodimers bind directly to LXR-responsive elements (LXRE) in the promoter region of target genes. The LXRE sequence contains two direct repeats of the hexameric sequence 5'-AGGTCA-3' separated by four nucleotides (DR4 element) (Figure 1.13) (354, 383-385).

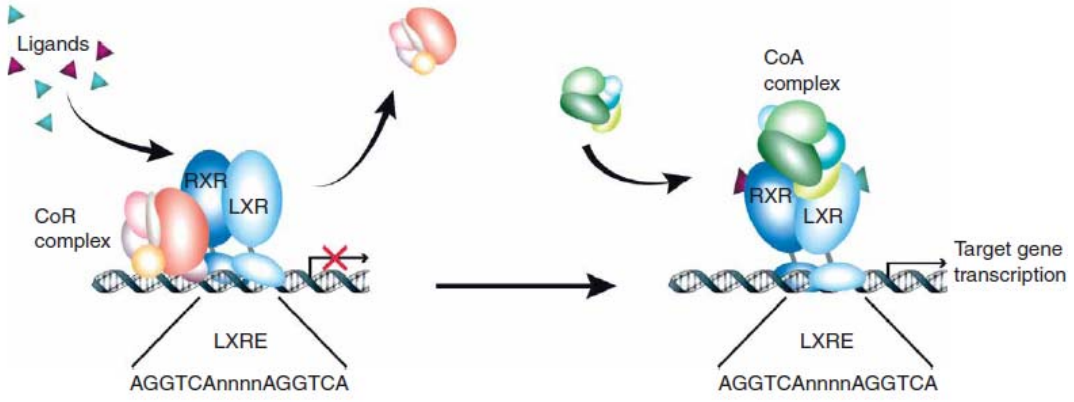

Figure 1.13 Model of classical transactivation pathway of LXR (see text for details). CoA, Co-activators; CoR, Co-repressor; LXRE, LXR response element (386).

In the absence of ligands, the LXR/RXR heterodimers remain bound to the promoter region of their target genes in a non-active state. They form complexes with co-repressors such as the Nuclear Receptor Corepressor (NCoR) or the Silencing Mediator of Retinoic Acid and Thyroid Hormone Receptor (SMRT) and thus actively inhibit gene activation (387-389). Indeed, deletion of LXRs in some cell types has been associated with elevated expression (de-repression) of target genes such as ABCA1 (390). Ligand binding first induces a conformational change of the LXR–RXR complex that enables the displacement of corepressors, and the recruitment of coactivators such as Peroxisome Proliferator Activated Receptor-g (PPARg) coativator-1a (PGC-1a), Steroid Receptor Coactivator-1 (SRC-1), Activating Signal Cointegrator-2 (ASC-2) and E1A-associated protein p300 (EP300) (391-393). These events lead to the direct activation of gene transcription (Figure 1.13).

In the second mechanism of action, transrepression, LXRs actively repress the expression of genes that lack an LXRE, particularly NF-kB-regulated pro-inflammatory genes (394, 395). Upon ligand binding, LXR undergoes SUMOylation by SUMO-2/3 and interacts with GPS2, a subunit of the N-CoR complex. In this setting the N-CoR complex cannot dissociate from NF-kB and thus the transcription of pro-inflammatory genes is inhibited (Figure 1.14) (394, 396).

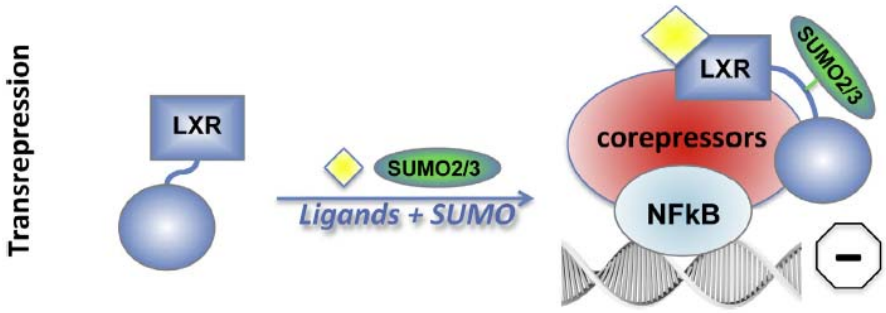

Figure 1.14 Molecular mechanism of LXR transrepression. LXRs influence gene expression by transrepressing NF-kB regulated genes after SUMOylation and interaction with corepressors (see text for details) (397).

Role of LXRs in lipid metabolism

Cholesterol metabolism

LXRs function as cholesterol sensors and trigger various adaptive mechanisms, protecting the cells from cholesterol overload. Activation of LXRs results in stimulation of cholesterol efflux from cells to HDL (reverse cholesterol transport), biliary cholesterol excretion, inhibition of intestinal absorption of dietary cholesterol and suppression of cholesterol synthesis de novo. The effects of LXRs on reverse cholesterol transport and excretion into bile as well as on intestinal cholesterol absorption are the major mechanisms, whereas those on cholesterol synthesis are weak and play a minor role (Figure 1.15).

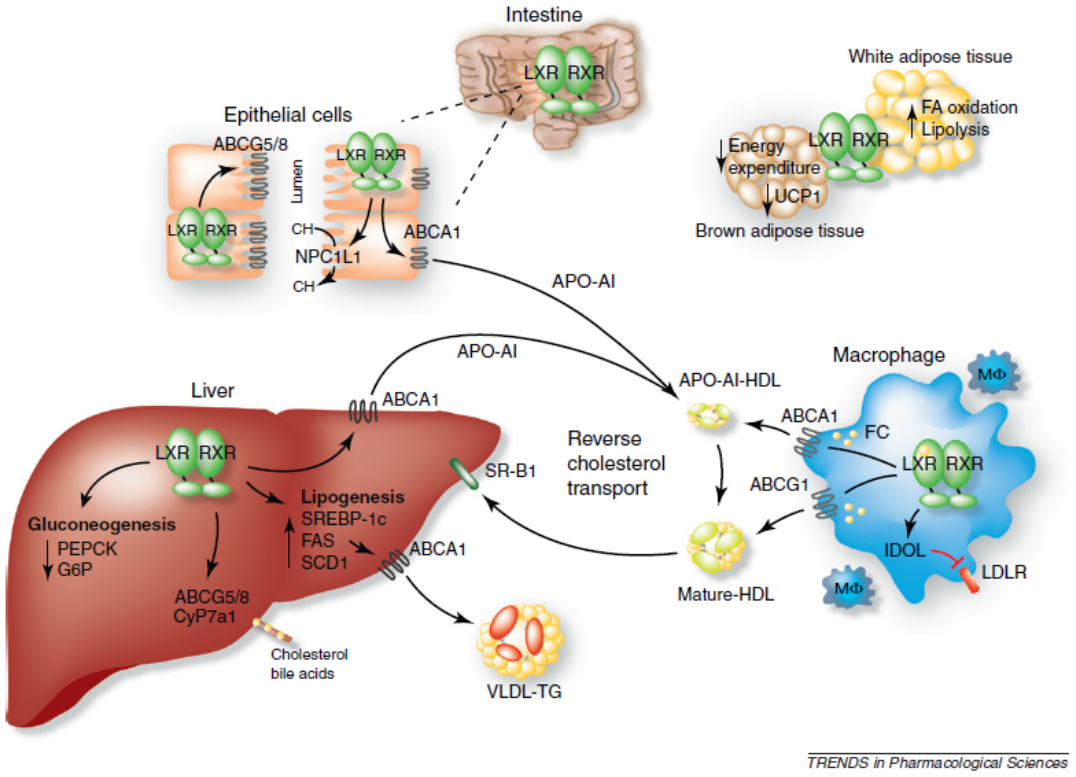

Figure 1.15 The role of LXRs in lipid metabolism in discrete cell types (see text for details) (398).

Reverse cholesterol transport

Elimination of cholesterol from the organism occurs almost exclusively in the liver. Therefore, excess cholesterol from peripheral tissues must be transported via HDL particles to the liver where it is excreted in the bile as cholesterol or after conversion to bile acids, a process known as reverse cholesterol transport (RCT). Almost every step of this process is stimulated by LXRs.

Cholesterol efflux from the peripheral cells is the first step in RCT that is stimulated by LXRs. As discussed above, ABCA1 and ABCG1 are expressed in macrophages where they prevent foam cell formation, but they are also found in many other cell types, including hepatocytes, enterocytes, and adipocytes. ABCA1 transfers both cholesterol and phospholipids to lipid-free apolipoprotein A-I and ABCG1 transfer cholesterol to HDL(399). Upon LXR activation, the expression of these transporters is increased via functional LXREs found in their genes and as a consequence the cholesterol efflux is stimulated from various cell types and the plasma HDL levels are elevated (Figure 1.16) (400-408). Moreover, Engel et al.(409) demonstrated that LXR agonist increases the expression of ABCG4, a half-transporter homologous to ABCG1, in human macrophages. Before efflux, cholesterol has to be transported from the endosomal compartment to the plasma membrane by the proteins Niemann-Pick C1 (NPC1) and C2 (NPC2). LXRs are also involved in the regulation of this process since LXR agonists upregulate expression of NPC1 and NPC2 in primary human macrophages and thus stimulate the redistribution of cholesterol from intracellular pools to the plasma membrane, where it becomes available for efflux to extracellular acceptors (410). As macrophages or other peripheral cell types become overloaded with lipids, LXRs activate a negative feedback mechanism to limit the uptake of more cholesterol, by inhibiting LDL uptake. LXR agonists induce the expression of the E3 ubiquitin ligase Idol (inducible degrader of LDL receptor), which targets LDL receptor family (LDLR, VLDL receptor and ApoE receptor 2) for ubiquitination and subsequent degradation (411-413). SR-B1, the specific HDL receptor expressed in the liver, is essential for the delivery of cholesterol esters from HDLs to hepatocytes. LXR ligand increases the expression of this receptor in human hepatoma HepG2 cells, by the binding of the LXR/RXR dimer to the LXRE of SR-B1 promoter (Figure 1.16) (414).

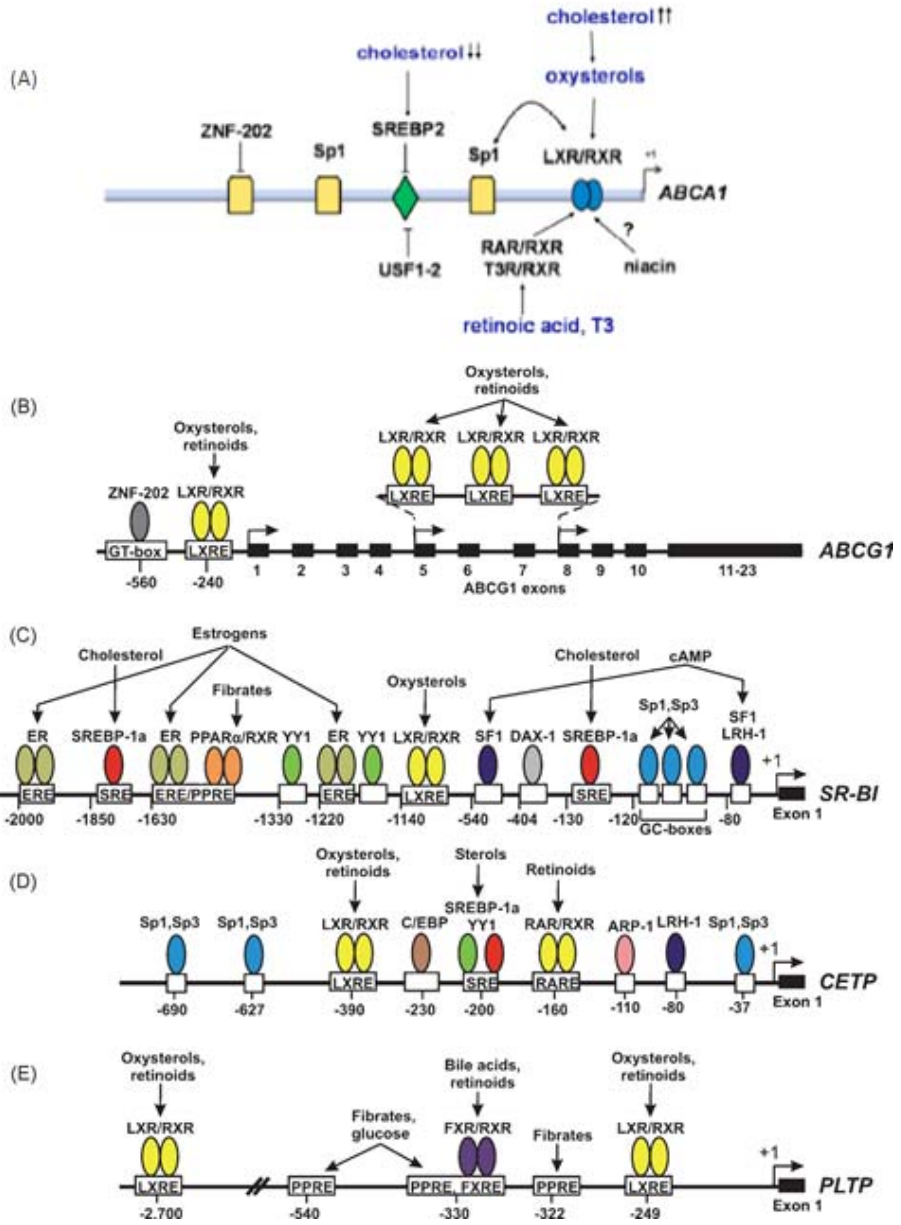

Figure 1.16 Regulatory elements and factors, including LXR/RXR heterodimers, governing the expression of ABCA1, ABCG1, SR-BI, CETP, and PLTP genes. Modified from (10, 415).

Apart from cholesterol transporters and receptor, LXR agonists stimulate the synthesis of alternative extracellular cholesterol acceptors such as apolipoproteins E, A-IV, C-I, C-II and C-IV(416, 417). ApoE is a component of VLDL and chylomicron remnants and is required for their hepatic uptake. In addition, it serves as extracellular acceptor for cholesterol effluxed via ABCA1, promoting reverse cholesterol transport (418). Laffitte et al. (417) showed that LXR agonists stimulate the expression of

apolipoprotein-E selectively in macrophages and in adipose tissue but not in the liver, through interaction with the LXREs. Furthermore, remodeling enzymes of lipoproteins are targets of LXRs. LXR agonists increase the synthesis of hepatic CETP, which transfers cholesterol esters from HDLs to VLDLs in the exchange for triglycerides and PLTP that transfers phospholipids from VLDL and chylomicron remnants to HDL, increasing HDL levels in plasma (Figure 1.16) (419-421). The expression of LPL gene, which hydrolyzes triglyceride rich lipoproteins, is induced also by LXRs in the liver and macrophages, via an LXRE within the first intron of the gene (181).

Cholesterol metabolism to bile acids and excretion into bile

A rate-limiting enzyme of hepatic bile acid synthesis is cholesterol 7a-hydroxylase (CYP7A1). LXR agonists upregulate the expression of mouse and rat CYP7A1 genes through the LXREs in their promoters and in consequence stimulate bile acid synthesis (354, 422). In contrast to rodents, human Cyp7a1 gene promoter, which does not contain an LXRE, is not induced by LXRα which may be responsible for greater susceptibility of humans to diet-induced hypercholesterolemia (423, 424). ABCG5 and ABCG8 transporters are abundantly expressed in the canalicular membrane of hepatocytes, and are responsible for the cholesterol transport to the bile(425). In addition to stimulation of bile acid synthesis, LXR agonists stimulate also biliary cholesterol excretion by inducing the expression of the hepatic ABCG5 and ABCG8 genes (426, 427).

Intestinal cholesterol absorption

Dietary cholesterol is absorbed in the small intestine through the apical Niemann-Pick C1-like 1 protein (NPC1L1). Most of it is subsequently esterified inside the enterocyte by ACAT-2, and cholesteryl esters are incorporated into chylomicrons. Some intracellular cholesterol is back-extruded to the intestinal lumen through the apical ABCG5/ABCG8 transporters and the minority of cholesterol is exported through the basolateral ABCA1 transporter to locally generated apoA-I-forming HDL particles (428).

Upon LXR activation, the expression of NPC1L1 protein is decreased and the expression of both ABCG5 and ABCG8 is increased in mouse intestine and in human enterocyte cell culture. In consequence LXR agonists reduce intestinal cholesterol

absorption in mice (399, 405, 427, 429). This effect was initially associated with increased ABCA1 expression in enterocytes (405), but subsequent studies with mice lacking either ABCA1 or ABCG5 and ABCG8 transporters revealed that only ABCG5 and ABCG8 are involved in the LXR-induced inhibition of dietary cholesterol absorption (426, 430).

De novo cholesterol synthesis

Several key enzymes in the cholesterol biosynthesis pathway, including 3-hydroxy-3-methylglutarylcoenzyme A (HMG-CoA) reductase and squalene synthase, are stimulated by the sterol regulatory element binding protein-2 (SREBP-2), a transcription factor that is proteolytically cleaved in order to be activated (431). Synthetic LXR agonist reduces hepatic expression of squalene synthase and hydroxymethyl glutaryl coenzymeA synthase in wild-type mice (366). Concordantly, LXRα or LXRβ deficient mice exhibit higher hepatic expression of SREBP-2 and several of its target genes including hydroxymethyl glutaryl-coenzyme A synthase and reductase, farnesyl diphosphate synthase and squalene synthase (376, 432). Interestingly, Peet et al. (432) reported that elevated expression of cholesterogenic enzymes in the liver of LXRα-deficient mice does not result in the predicted increase in hepatic cholesterol synthesis. Although it is suggested that LXRs inhibit cholesterol biosynthesis, their role in the regulation of this pathway is unclear and requires further investigation.

Fatty acid metabolism

In addition to cholesterol metabolism LXRs have also been shown to regulate hepatic fatty acid biosynthesis (lipogenesis) (Figure 1.15). In 2000, Schultz et al. (366) first demonstrated that treatment with T0901317 markedly increased hepatic triglyceride content and plasma triglyceride concentration in mice and hamsters. The regulation of fatty acid biosynthesis by LXRs is governed initially by the lipogenic transcription factor, sterol regulatory element binding protein-1c (SREBP-1c) that induces the transcription of genes involved in fatty acid biosynthesis pathway, including acetyl-CoA carboxylase (ACC), fatty acid synthase (FAS) and stearoyl-CoA desaturase (SCD). LXR agonists markedly induce the expression of SREBP-1c through a functional LXRE in the promoter region of the SREBPF1 gene.

Subsequently, SREBP-1c binds to the sterol response element (SRE) within the promoter region of the lipogenic genes and stimulates fatty acid synthesis in hepatocytes (433-435). T0901317-induced activation of lipogenesis leads to massive hepatic accumulation of triglycerides, liver steatosis and hypertriglyceridemia in mice, rats and hamsters (366, 436, 437). Subsequent studies revealed that these three lipogenic genes (ACC, FAS and SCD-1) contain functional LXREs and therefore are directly regulated by LXRs in a SREBP-1c independent manner (436-439). Grefhorst et al. (440) reported that hypertriglyceridemia induced by LXR agonists results from increased secretion of VLDL particles from the liver. Although the number of VLDL particles formed does not change, their diameter increases due to the higher amount of triglycerides per particle.

It should be noted that effects of synthetic and physiologic LXR activation differ markedly. In physiological states of cholesterol excess, oxysterols inhibit SREBP-1c activation through inhibition of its proteolytic cleavage (431). Furthermore, cholesterol-rich diet has very modest effect on hepatic lipogenesis and triglyceride content (432). In contrast, synthetic LXR agonists cannot suppress SREBP-1c activation, but induce SREBP-1c expression which results in dramatic increase in fatty acid biosynthesis.

Some groups reported that only LXRα is responsible for the liver accumulation of TG (432). As LXRα is most strongly expressed in the liver, the predominant strategy for avoiding the hepatic lipogenic effects is the development of LXR ligands that selectively activate LXRβ. However, recent studies have shown that both LXRα and LXRβ may be responsible for liver lipogenesis (441, 442). In LXRα knockout mice, lipogenesis in liver is less than in WT mice, but when treated with GW3965 agonist, both SREBP1c expression and hepatic TG increased, implying that LXRβ contributes to this lipogenic side effect (441). However, various synthetic LXR agonists seem to differ in their potency to stimulate lipogenesis as discussed above.

Hepatic gluconeogenesis metabolism

LXR agonist treatment decreased expression of PGC-1α, a key regulator of hepatic glucose production, in murine liver resulting in decreased expression of gluconeogenic enzymes such as phosphenolpyruvate carboxykinase (PEPCK) (343,

443, 444). In addition to reduced expression of PEPCK, reduced expression of G6Pase, an enzyme which controls the flux of glucose-6-phosphate (G6P) towards glucolysis, might also be suppressed upon LXR activation. However, although these enzymes are inhibited by LXR activation, gluconeogenesis and flux through G6Pase were not affected in mice (445). In addition, the insulin-sensitive glucose transporter GLUT4 was shown to be a direct LXR target gene, through an LXRE in the promoter of the gene and upon LXR synthetic agonists the expression of GLUT4 is increased in adipocytes.(341, 343). Notably, LXR agonists enhance insulin secretion by pancreatic β-cells, by stimulating the expression of GLUT2 and glucokinase, suggesting a role of LXR in lowering blood glucose in diabetes (446-448). Interestingly, the LXR agonists T0901317 and GW3965 were shown also to reduce hepatic glucose output and improve insulin sensitivity in insulin resistant zucker (fa/fa) rats and diet-induced obese mice (343, 444, 449). However, in diabetic mice LXR agonists only slightly improve insulin sensitivity despite considerable reduction in blood glucose concentrations, indicating that other mechanisms could underlie their anti-diabetic action (445).

2. MATERIALS AND METHODS

Dulbecco's modified Eagle's medium (DMEM), Opti-MEM I Reduced Serum Medium, Newborn Calf Serum (NBCS), penicillin/streptomycin, trypsin/EDTA, puromycin for cell culture, Hank's Balanced Salt Solution (HBSS), Liver Digest Medium for hepatocyte isolation, Lipofectamine RNAiMAX Transfection Reagent and Lipofeactamine 2000 were purchased from Invitrogen/Life Technologies (Carlsbad, CA). Fetal bovine serum (FBS) was purchased from BioChrom Labs (Terre Haute, IN). Charcoal-stripped serum (CSS) was prepared after treatment of FBS with charcoal and dextran. Restriction enzymes and T4 DNA ligase were purchased from Minotech (Heraklion, Greece) or New England Biolabs (Beverly, MA). Go Taq DNA polymerase, dNTPs, the luciferase assay system, Cell culture lysis 5x reagent and the Wizard SV gel and PCR cleanup system were purchased from Promega (Madison, WI). Sodium pyruvate, dexamethasone (D2915), insulin (I0516), isobutylmethylxanthine (IBMX-I5879) for culture of 3T3-L1 cells, Percoll, BSA fraction V for hepatocyte isolation, 9-cis retinoic acid (9-cis RA), 22(R)-hydroxycholesterol, poly (dI/dC), ONPG (o-nitrophenyl β-D-galactopyranoside), PMSF (phenylmethylsulfonyl fluoride), aprotinin and benzamidine and streptavidin agarose beads were purchased from Sigma-Aldrich (St.Louis, MI). T0901317 was purchased from Cayman Chemicals (Ann Arbor, MI) and IPTG (isopropyl β-D-thiogalactoside) was purchased from Anatrace (Maumee, OH). Collagen rat, shrimp alkaline phosphatase and Complete Protease inhibitor cocktail tablets were purchased from Roche (Mannheim, Germany). Glutathione-Sepharose 4B, protein G Sepharose and nitrocellulose membrane were purchased from GE healthcare Life-sciences (Freiburg, Germany). QuickChange Site-Directed Mutagenesis Kit was purchased from Stratagene (La Jolla, CA). Trizol reagent for RNA extraction, SuperScript II, M-MLV reverse transcriptases, random hexamers, BenchMark Prestained Protein Ladder, Dynabeads M-280 streptavidin and Dynabeads protein G were purchased from Invitrogen/Life Technologies (Carlsbad, CA). KAPA SYBR FAST qPCR Master Mix for quantitative PCR was purchased from Kapa Biosystems (Wilmington, MA). The Super Signal West Pico chemiluminescent substrate and stripping buffer restore western blot were purchased from Pierce-Thermo Scientific (Waltham, MA). MG132 proteasome inhibitor and Coomassie Brilliant Blue R-250 were purchased from Merck Millipore (Darmstadt, Germany). Biotinylated oligonucleotides were

synthesized at VBC Biotech (Vienna, Austria). FOXA2 si-RNA and scrambled si-RNA were synthesized at Eurofins MWG Operon (Ebersberg, Germany). All other oligonucleotides were synthesized at the microchemical facility of the Institute of Molecular Biology and Biotechnology (IMBB, Heraklion, Greece) or Eurofins Genomics (Ebersberg, Germany).

Antibodies

Primary antibodies, anti-HNF-3β/FOXA2 (M-20), anti-RXR (D-20), anti-LXR (H-144), a-Gal4 DBD and anti-LPL (H-53) were purchased from Santa Cruz Biotechnology (Santa Cruz, CA). Anti-LXRα (ab41902) ChIP Grade antibody was purchased from Abcam (Cambridge, MA). Anti-pAKT (Ser473) was purchased from Cell Signaling (Danvers, MA) and anti-actin (MAB1501R) was purchased from Merck Millipore (Darmstadt, Germany). Anti c-myc (9E-10) and anti-Flag M2 (F-3165) antibodies were purchased from Sigma-Aldrich (St.Louis, MO, USA). Anti-goat, anti-rabbit and anti-mouse peroxidase-conjugated secondary antibodies were purchased from Jackson ImmunoResearch Laboratories (West Grove, PA). Anti-rabbit peroxidase-conjugated antibody was also purchased from Merck Millipore and anti-goat was also purchased from Sigma-Aldrich (St.Louis, MI).

Table 2.1. Antibodies used for analysis of protein expression by western blot.

Antibody	Dilution - WB	Co-IP	ChIP
anti-HNF-3β	1:200 or 1:500 in 5% w/v milk in TBS-T 0.1%, 0.02% $NαN_3$	2ug/IP	5ug/IP
anti-RXRα	1:500 in 5% w/v milk in TBS-T 0.1%, 0.02% NαN3		5ug/IP
anti-LXRα (H-144)	1:2000 in 5% w/v milk in TBS-T 0.1%, 0.02% $NαN_3$		12ug/IP (HEK cells)
anti-LXRα (ab41902)			7ug/IP (HepG2 cells)
anti-LPL	1:200 or 1:300 in 5% w/v milk in TBS-T 0.1%, 0.02% $NαN_3$		
anti-actin	1:5000 in TBS-T 0,1%, 0,02% $NαN_3$		
anti-pAKT	1:1000 in 5% BSA in TBS-T 0.1%, 0.02% $NαN_3$		
anti-myc	1:1000 in 5% w/v milk in TBS-T 0.1%, 0.02% $NαN_3$		
anti-flag	1:1000 in 5% w/v milk in TBS-T 0.1%, 0.02% $NαN_3$	4μl/IP	
anti-Gal4 DBD	1:500 in 5% w/v milk in TBS-T 0.1%, 0.02% $NαN_3$	2ug/IP	

Molecular Cloning Protocols

Molecular enzyme reactions

The promoter or cDNA sequences of the human and mouse genes were amplified by PCR using the primers shown in Tables 2.4 and 2.6 and subsequently cloned into appropriate vectors. Generally, plasmids and PCR products were digested with the appropriate restriction enzymes. The digestions were performed in the proper reaction conditions as recommended by the manufacturer (Minotech or New England Biolabs). Small amounts of DNA (~1 μg of DNA) were digested at 37 °C (or 25°C) for 1 hour, while in large-scale digests 5-15 μg of DNA were incubated at 37 °C (or 25°C) for 3-6 hours. In cases a single enzyme is used for vector digestion, shrimp alkaline phosphatase (SAP) (Roche) was used for the dephosphorylation of digested DNA fragments to catalyze the dephosphorylation of 5' phosphates from DNA and prevent recircularization. The reaction assay was performed by adding 1 μl of SAP in the

digestion, followed by incubation at 37 °C for 1 hour and heat inactivation of the enzyme at 65 °C for 20 minutes.

Agarose gel electrophoresis

Agarose gels were performed in 1x TAE (Table 2.2) containing 1-3% agarose, depending on the estimated size of the expected DNA fragments. The solution was boiled in a microwave oven for 2-3 minutes and cooled down. 4 μL of ethidium bromide (10 mg/ml) or midori green advance (Nippon Genetics) were added per 100 ml of agarose solution. λDNA digested with BstEII or 100 bp DNA ladder (Invitrogen) was used as a DNA size marker. DNA samples were mixed with 6x gel loading dye (Table 2.2) and run in tanks under the appropriate electrical field. The bands were visualized using the TFX-35M UV transilluminator.

Table 2.2. Buffers used for agarose gel electrophoresis

50x TAE		6x gel loading dye	
Tris	121 g	bromophenol blue	0.25%
EDTA	18.6 g	xylene cyanol FF	0.25%
acetic acid glacial	28.55 ml	glycerol	30%
Volume	500 ml		

DNA isolation and purification from agarose gel

PCR products digested DNA fragments and reaction mixtures, run on agarose gels, were purified with the use of Wizard SV Gel and PCR Clean-Up System by Promega according to the manufacturer's instructions. The concentration of the purified DNA fragments was determined either by gel quantitation or by spectrophotometry.

Ligation reaction

For ligation of digested DNA fragments, T4 DNA Ligase was used and the reactions were performed in a final volume of 15 μl containing 1x T4 DNA ligation buffer supplemented with ATP and 1μl T4 DNA ligase. The molar ratio of insert to vector was 3:1 to 5:1 molecules by using 50-100 ng of the vector DNA. The final mixture was incubated at 4 °C overnight.

Transformation of E.coli competent cells

The ligation reaction and expression plasmids were used for transformation of chemically competent Escherichia coli DH10β cells. 100 µl of frozen competent cells were thawed on ice and the appropriate amount of DNA (15 µl ligation reaction or 100-500 ng of plasmid) was added to the cells. The cells were incubated for 30 minutes on ice, heat-shocked at 42 °C for 45 seconds and immediately cooled on ice for 2 minutes. 900µl growth medium LB (Table 2.3) was added to the cells and they were incubated at 37 °C for 1 hour. If the DNA derived from a ligation reaction, the cells were centrifuged at 2.000rpm for 5 minutes, resuspended in 100-150 µl LB and all cells were spread on LB agar plate with the appropriate antibiotic. If plasmid DNA was used for transformation, ~100 µL of cells were spread on the agar plate. The plates were incubated at 37 °C for 16 hours.

Table 2.3 Composition of LB medium

LB (Luria-Bertani)	
NaCl	10 g
yeast extract	5 g
tryptone	10 g
Volume	1 L
autoclave	

Cultivation of bacteria

E.coli bacteria were grown in LB medium shaking cultures or on LB agar plates. Depending on the resistance cassette on the transformed plasmids, appropriate antibiotics were used to a final concentration of 100 µg/mL for ampicillin and 50 µg/mL for kanamycin. E.coli cultures were incubated at 37 °C for 16 hours.

Purification of plasmid DNA by alkaline lysis (mini-preparation)

A single bacterial colony was picked from a selective plate, inoculated 2-3 ml LB medium containing the appropriate selective antibiotic and incubated at 37°C for 16 hours with vigorous shaking. The mini cultures were transferred in eppendorf tubes and the cells were harvested by centrifugation at 13.000 rpm for 1 minute. Plasmid extraction and purification was performed using either the QIAGEN Plasmid Mini Kit

according to the manufacturer's instructions. Briefly, the LB supernatant was removed and the bacterial pellet was resuspended in 150 μl P1 buffer supplemented with RNase A (100 μg/ml). The cells were lysed by adding 150 μl P2 buffer in the solution, mixed gently by inverting 4-6 times. 150μl of chilled buffer P3 also added in the solution, mixed 4-6 times and centrifuged at 13.000 rpm for 10 minutes to pellet cell debris. The supernatant containing plasmid DNA was collected and plasmid DNA was precipitated by adding 400 μl RT isopropanol, mixed and centrifuged at 13.000 rpm for 10 minutes. The DNA pellet was washed with 500 μl RT 70% ethanol centrifuge at 13.000 rpm for 10 minutes, air-dried and resuspended in 30-40 μl sterile dH_2O.

Glycerol Stocks and Purification of plasmid DNA (midi/maxi-preparation)

A single bacterial colony was picked from a selective plate, inoculated 2-4 ml LB medium containing the appropriate selective antibiotic and incubated at 37 °C for 2-4 hours with vigorous shaking. The mini cultures were transferred in 150-200ml LB medium containing the appropriate selective antibiotic and incubated at 37^{oC} for 16 hours with vigorous shaking. For preparation of glycerol stocks, 500μl sterile glycerol were mixed by vortex with 500 μl saturated bacterial culture and stored at -80 o C. Large-scale preparations (up to 500 μg) of plasmids DNA were performed, using the QIAGEN-tips-100 or -500 according to the protocols provided by QIAGEN (QIAGEN Plasmid Midi and Maxi Protocol) or NucleoBond PC 100 by Macherey-Nagel.

Quantification of nucleic acid concentration

The concentration of the purified nucleic acids (DNA or RNA) was determined by spectrophotometry, using the Jenway 6405 UV/VIS Spectrophotometer. 1 ml of dH2O was added in the cuvette and used to calibrate the instrument. The samples were diluted 1:200 in dH2O (5 μl nucleic acid sample + 995 μL dH2O) and the absorbance was measured at wavelengths of 260 nm and 280 nm. Pure preparations of nucleic acids had OD260/OD280 =1.8 - 2.0. The concentration of each sample was calculated from the below equations. For double-stranded DNA: Concentration=OD260 x 50 ng/μl x dilution factor. For single-stranded DNA: OD260 x 35 ng/μl x dilution factor. For RNA: OD260 x 40 ng/μl x dilution factor.

Alternatively, the concentration and purity of the nucleic acids was determined by the TECAN Infinite 200 PRO instrument.

Site-directed mutagenesis

The mutated promoter constructs (-883/+39 LPL-luc mut and -883/+39 LPL-luc -39T/C) were generated by site-directed mutagenesis using the QuickChange II Site-Directed Mutagenesis Kit from Stratagene according to the manufacturer's instructions. Briefly, a PCR reaction was performed using 5 μl 10x buffer for Pfu Ultra HF DNA polymerase, 10 ng ds DNA template, 125 ng primer #1, 125 ng primer #2, 2,5 μl dNTPs 10mM, 1 μl Pfu Ultra HF DNA polymerase (2.5 U/μl) and dH20 up to 50 μl. The cycling parameters were: 95°C 30 seconds, 95°C 30 seconds, 55°C 1 minute, 68°C 6 minutes for 18 cycles. When PCR reaction was completed, 1 μl of the DpnI restriction enzyme (20U/ml) was added in the reaction and incubated at 37°C for 1.5 hours. 1 μl, 5 μl, 10 μl were used for the transformation of DH10β competent cells, which were spread on the LB agar plates, as discussed above. Colonies were selected for plasmid DNA purification. DNA sequencing reactions were performed by Macrogen Corporation (Amsterdam, The Netherlands), to verify the presence of the desired mutation in the selected clones. The sequence of the primers utilized for the site-directed mutagenesis is shown in Table 2.5.

Plasmid constructions

Promoter constructs

The human LPL promoter plasmids (-883/+39) LPL-Luc, (-669/+39) LPL-Luc, (-466/+39) LPL-Luc, (-262/+39) LPL-Luc, (-109/+39) LPL-Luc and (-28/+39) LPL-luc were generated by PCR amplification of the corresponding fragments of LPL promoter using human genomic DNA as template and cloned at the XhoI-HindIII sites of pBluescript vector bearing the luciferase gene (pBS-luc). The promoter constructs (-883/+39) mut LPL-luc, which bear mutations in the FOXA2 binding site of the LPL promoter and (-883/+39) -39T/C LPL-luc, a T to C substitution at nucleotide -39, were generated by site-directed mutagenesis using the QuickChange

Site-Directed Mutagenesis Kit and the primers shown in Table 2.5 according to the manufacturer's instructions (described above). The LPL promoter construct (-109/+39) mut LPL-luc, bearing mutations in the FOXA2 binding site, were generated by PCR amplification of the -109/+39 fragment of LPL promoter using the (-883/+39) mut LPL-luc as template and subsequent cloning into the XhoI-HindIII sites of the pBluescript vector bearing the luciferase gene. The sequence of all oligonucleotides used as primers in PCR amplification or in mutagenesis is shown in Table 2.4 and 2.5.

The human ABCG5 and ABCG8 promoter constructs, (−972/+72) ABCG5-luc and (−939/+12) ABCG8-luc, were available in the lab.

Table 2.4. Oligonucleotides used for cloning LPL promoter fragments [α]

Name	Sequence
LPL -883 Fw	5' - CCGCTCGAGCAGAGTTGTGCAGCATCAGCAT -3'
LPL -669 Fw	5' - CCGCTCGAGACGGCTTTAGATTATTTGACCTCG - 3'
LPL -466 Fw	5' - CCGCTCGAGACGCAATGTGTGTCCCTCTAT -3'
LPL -262 Fw	5' - CCGCTCGAGACCTGTGTTTGGTGCTTAGACA - 3'
LPL -109 Fw	5' - CCGCTCGAGTAGAAGTGAATTTAGGTCCCTC - 3'
LPL -28 Fw	5' - CCGCTCGAGACATAAGCAGCCTTGGCGTGAAAA - 3'
LPL +39 Rev	5' - CCCAAGCTTTTCCCTTGAGGAGGAGGAAGAG - 3'

[α] XhoI (CTCGAG) and HindIII (AAGCTT) sites are underlined.

Table 2.5. Oligonucleotides used for site-directed mutagenesis [α]

Name	Sequence
LPL-FOXA2-Mut-Fw	5' - ATAGGTGATGAGGTT***CCCGG***GCATATTTCCAGTCA - 3'
LPL-FOXA2-Mut-Rev	5' - TGACTGGAAATATGC***CCGGG***AACCTCATCACCTAT - 3'
LPL-39T/C-Fw	5' - GGTGATGAGGTTTATTTGCA***C***ATTTCCAGTCACATAAGCAG - 3'
LPL-39T/C-Rev	5' - CTGCTTATGTGACTGGAAAT***G***TGCAAATAAACCTCATCACC - 3'

[α] Nucleotide substitutions in the primers used for site-directed mutagenesis are in bold and italic.

Expression vectors

The vectors expressing the truncated forms of rat FOXA2 1-94, 144-279 and 361-458, were constructed by PCR amplification of the corresponding fragments of rat FOXA2 cDNA and subsequent cloning at the EcoRI-NotI sites of vector pGEX-4T1 (Amersham Biosciences). Then the above fragments were sub-cloned into the

pCDNA3-6myc expression vector at the same restriction sites, in frame with a 6myc epitope tag. For the construction of plasmids pCDNA3-6myc-FOXA2 and its truncated forms 280-360, 1-360, 95-458, 1-279, 95-360, the corresponding fragments of rat FOXA2 cDNA were amplified by PCR amplification and cloned at the EcoRI-NotI sites of pCDNA3-6myc vector. To generate the expression plasmids GAL4-DBD FOXA2 1-94 and 95-458, the truncated forms of FOXA2 1-94 and 95-458 were excised from pCDNA3-6myc vector by EcoRI and XbaI and then sub-cloned into the corresponding sites of the pBXG1 vector in frame with the DNA binding domain (DBD) of GAL4. The expression vector Bio-FOXA2 was constructed by PCR amplification of the rat FOXA2 cDNA and cloning at the EcoRI-NotI sites of pCDNA3-Bio vector in frame with a biotinylation peptide tag (450). The GST-FOXA2 plasmid was constructed by sub-cloning the FOXA2 cDNA into the pGEX-4T1 expression vector at the EcoRI-NotI sites. The bacterial vector expressing LXRα fused with GST was constructed by PCR amplification of the human LXRα cDNA and cloning into the expression vector pGEX-4T1 at the BamHI and NotI sites. The sequence of all oligonucleotides used as primers in PCR amplification or in mutagenesis is shown in Table 2.6.

The expression vectors Flag-FOXO1, CMV-rFOXA2, pCMX-LXRα, pCDNA3-BirA, pCDNA3-6myc-RXRα, pCDNA3-6myc-LXRα and its truncated forms (1-163, 164-447, 1-97, 98-163, 1-127, 30-127, 30-163) and were available in the lab. The expression plasmids Flag-LXRβ and GST-mFOXO1 were kind gifts from Dr. Blobe G. (Departments of Medicine and Pharmacology and Cancer Biology, Durham, North Carolina) and Dr. Negishi M. (National Institute of Environmental Health Sciences, Research Triangle Park, North Carolina), respectively.

Table 2.6. Oligonucleotides used in PCR amplifications for cloning of rat (r) FOXA2 or human (h) LXRα cDNAs into appropriate vectors [α]

Name	Sequence
rFOXA2 1 Fw	5' - CCGGAATTCATGCTGGGAGCCGTGAAGATGGAAGG - 3'
rFOXA2 95 Fw	5' - GGAATTCGGGGCGGCCGGCGTGGCGGGCAT - 3'
rFOXA2 144 Fw	5' - CCGGAATTCGCTCGGGACCCCAAGACGTAC - 3'
rFOXA2 280 Fw	5' - CCGGAATTCACACAGGCTTCTCAGGTTCAGCTCGG - 3'
rFOXA2 361 Fw	5' - CCGGAATTCGAGGCCCACCTGAAGCCCGA' - 3'
rFOXA2 94 Rev	5' - TTTGCGGCCGCTTAAGCTGAGCCGCTCATGCCC - 3'
rFOXA2 279 Rev	5' - TTTGCGGCCGCTTACCCAGGAGCGGTCTTCT - 3'
rFOXA2 360 Rev	5' - TTGCGGCCGCTTATGGTGGCAGGCCAGGATGGT - 3'
rFOXA2 458 Rev	5' - TTTGCGGCCGCTTAGGACGAGTTCATAATAGGCCTGG - 3'
hLXRα Fw	5' - CGCGGATCCATGTCCTTGTGGCTGGGGGC - 3'
hLXRα Rev	5' - TTGCGGCCGCTCATTCGTGCACATCCCAGAT - 3'

[α] EcoRI (GAATTC), NotI (GCGGCCGC) and BamHI (GGATCC) are underlined.

shRNA producing vectors

The LXRα shRNA, LXRβ shRNA and control shRNA producing vectors were generated by ligation of double-stranded oligonucleotides that contained the siRNA-expressing sequence targeting LXRα, LXRβ or a scrambled sequence respectively, into the BglII-HindIII sites of the pSuper.retro.GFP/neo vector (Oligoengine, Seattle). In order to generate lentiviruses expressing the shRNAs for LXRα, LXRβ and control, the double-stranded oligonucleotides that contained the siRNA-expressing sequences inserted also into pLKO.1 TRC-cloning vector between Age1 and EcoR1 sites, according to the pLKO.1 protocol instructions (addgene) . All oligonucleotides used for shRNA producing vectors are shown in Table 2.7.

The pLKO.1 vector, scrambled shRNA pLKO.1 vector and the packaging expression vectors Δ8.2 and VSV-G, which were used for lentivirus production, were kindly provided by Dr. Sourvinos G. (Medical School of University of Crete, Heraklion,Greece).

Table 2.7. Oligonucleotides used for sh-RNA cloning into appropriate vectors [α]

Name	Sequence	Purpose
shRNA LXRα sense	5'- GATCCCC*GAACAGATCCGCCTGAAGA*TTCAAGAGA*TCTTCAGGCGGATCTGTTC*TTTTTA-3'	Cloning of shRNA for human LXRα into pSuper.retro.neo.gfp vector
shRNA LXRα antisense	5'- AGCTTAAAAA*GAACAGATCCGCCTGAAGA*TCTCTTGAA*TCTTCAGGCGGATCTGTTC*GGG-3'	
shRNA LXRβ sense	5'- GATCCCC*GAACAGATCCGGAAGAAGA*TTCAAGAGA*TCTTCTTCCGGATCTGTTC*TTTTTA-3'	Cloning of shRNA for human LXRβ into pSuper.retro.neo.gfp vector
shRNA LXRβ antisense	5'- AGCTTAAAAA*GAACAGATCCGGAAGAAGA*TCTCTTGAA*TCTTCTTCCGGATCTGTTC*GGG-3'	
shRNA control sense	5'- GATCCCC*TTCTCCGAACGTGTCACGT*TTCAAGAGA*ACGTGACACGTTCGGAGAA*TTTTTA-3'	Cloning of shRNA control into pSuper.retro.neo.gfp vector
shRNA control antisense	5'- AGCTTAAAAA*TTCTCCGAACGTGTCACGT*TCTCTTGAA*ACGTGACACGTTCGGAGAA*GGG-3'	
shRNA LXRα sense	5'- CCGG*GAACAGATCCGCCTGAAGA*CTCGAG*TCTTCAGGCGGATCTGTTC*TTTTTG-3'	Cloning of shRNA for human LXRα into pLKO.1 vector
shRNA LXRα antisense	5'- AATTCAAAAA*GAACAGATCCGCCTGAAGA*CTCGAG*TCTTCAGGCGGATCTGTTC* -3'	
shRNA LXRβ sense	5'- CCGG*GAACAGATCCGGAAGAAGA*CTCGAG*TCTTCTTCCGGATCTGTTC*TTTTTG-3'	Cloning of shRNA for human LXRβ into pLKO.1 vector
shRNA LXRβ antisense	5'- AATTCAAAAA*GAACAGATCCGGAAGAAGA*CTCGAG*TCTTCTTCCGGATCTGTTC* -3'	

[α] si-RNA sequence targeting LXRα, LXRβ or si-control (scrambled) sequence is italic and underlined

Cell culture and treatments

The cell lines used in the present study were HepG2 (human hepatocellular liver carcinoma cells), HEK293T (human embryonic kidney 293T cells), and 3T3-L1 (mouse embryonic fibroblasts-like preadipocytes). HepG2 cells and HEK293T cells were cultured in Dulbecco's modified Eagle's medium (DMEM high glucose) supplemented with 10% fetal bovine serum (FBS), L-glutamine, and penicillin/streptomycin at 37 °C in a 5% CO_2 atmosphere. The medium was renewed every 48 h. As soon as a confluent monolayer had been formed in the flask, the cells were subcultured to an appropriate concentration using trypsin-EDTA.

For the treatment of cells with 22(R)-hydroxycholesterol, 9-cis-retinoic acid and T0901317, 10% FBS was replaced by 5% charcoal-stripped serum (CSS) and the ligands were added for 24 hours at a final concentration of 1 μM. For the treatment of HepG2 cells with insulin, cells were plated in DMEM low glucose +Glutamax supplemented with 10% fetal bovine serum, and penicillin/streptomycin, serum-starved for 18 hours with DMEM low glucose +Glutamax supplemented with penicillin/streptomycin and stimulated with insulin for 24 hours at a final concentration of 500nM. For the treatment of HepG2 cells with insulin and T0901317, cells were serum-starved for 18 hours and stimulated with insulin or/and T0901317 for 24 hours at a final concentration of 500nM and 1μM, respectively.

Mouse 3T3-L1 pre-adipocytes were grown in DMEM (high glucose) supplemented with 10% newborn calf serum (NBCS), L-glutamine, 1% sodium pyruvate and penicillin/streptomycin (Normal Growth Medium) at 37°C in a 5% CO2 atmosphere. For adipocyte differentiation, 3T3-L1 cells were maintained for 1 day in normal growth medium and then switched for 2 days to differentiation medium, a mixture of DMEM supplemented with 10% fetal bovine serum, 1% sodium pyruvate, penicillin/streptomycin, 0.17μM insulin, 0.25μM dexamethasone and 0.5mM isobutylmethylxanthine (IBMX). After this time cells were cultivated in differentiation medium without the inducers dexamethasone and IBMX for 2-3 days. About 2 days after removal of dexamethasone and IBMX, adipocyte colonies began to be visible as regions containing rounded cells with numerous intracellular lipid droplets. Then the medium of cells was switched again to the differentiation medium

supplemented with the inducers (dexamethasone and IBMX) for 2 more days. The cells were maintained for 1 day in differentiation medium without the inducers and the next day cells were harvested. Mature adipocyte differentiation and lipid accumulation in the cells was observed by phase contrast microscopy at days 1 and 8.

Charcoal Stripped Serum (CSS)

When very low concentration of hormones is needed, CSS was used instead of FBS. This procedure removes lipophilic material such as cholesterol and hormones. 50ml FBS were mixed with 0.125 gr charcoal and 0.0125 gr dextran, incubated at 56 °C for 30 minutes and centrifuged at 3.000 rpm for 15 minutes. The supernatant was transferred to a new falcon, mixed again with 0.125 gr charcoal and 0.0125 gr dextran, incubated at $^{37\ °C}$ for 30 minutes and centrifuged at 3.000 rpm for 15 minutes. The supernatant was transferred to a new falcon, filtered using a 0.20μm filter and stored at -20°C.

Transient transfections and siRNA silencing

Transient transfections of HepG2 and HEK293T cells were performed using the calcium phosphate [$Ca_3(PO_4)_2$] co-precipitation method. One day before the transfection experiment, the appropriate number of cells (Table 2.8) was plated such that they will be 60% confluent at the time of transfection. To transfect cells, the proper amount of DNA, 2M CaCl2 and H2O were added in an eppendorf tube. Salmon Sperm DNA Solution was used either as control or to equilibrate the DNA amount in all samples. The DNA-CaCl2 mix was added dropwise while vortexing to a tube containing an equal amount of 2x HBS (Table 2.9). The mixture was incubated at RT for 15 minutes and added to the cells dropwise. Cells were mixed gently by rocking the plate back and forth, incubated at 37 °C and the medium was replaced with fresh medium 17-18 hours post-transfection. Cells were incubated at 37 °C for another 24 h and then harvested.

Lipofectamine 2000 reagent was used in HepG2 cells that were transfected with FOXA2 expression vector for protein and RNA extraction, according to the manufacturer's instructions. Transient transfections in 3T3-L1 cells and insulin treated HepG2 cells were performed also using Lipofectamine 2000. HepG2 and HEK293T cells were transfected with scrambled siRNA or siRNA against FOXA2

(Table 2.10) for 40 hours using Lipofectamine RNAiMAX according to the manufacturer's instructions. The silencing efficiency of FOXA2 was confirmed by western blotting or/and quantitative PCR.

Table 2.8. Setup for transfection assays using the $CaPO_4$ method.

Culture plate	Number of cells		Volume of medium	DNA (µg)	CaCl2 2M (µl)	H2O (µl)	2x HBS (µl)
	HepG2	HEK293T					
6-well	500.000	250.000	1-2	6	15.5	up to 125	125
p60	10^6	500.000	3	15	31	up to 250	250
p100	$2x10^6$	$1\text{-}1.2x10^6$	5	30	31	up to 250	250

Table 2.9. Composition of 2x HBS

2x HBS	
NaCl	274mM
KCl	10mM
$Na_2HPO_4{\cdot}H_2O$	1,5mM
Dextrose	12mM
Hepes	42mM
pH 7 ± 0.1	

Table 2.10. Oligonucleotides used for human FOXA2 siRNA-mediated silencing

Name	Sequence
FOXA2 siRNA	5'- CAGCAGAGCCCCAACAAGA -3'
non-specific scrambled siRNA	5'- CAGTCGCGTTTGCGACTGG -3'

Isolation of primary mouse hepatocytes and treatments

Primary mouse hepatocytes were isolated by perfusion of whole liver and percoll gradient purification. Eight-week-old to 12-wk-old male mice were euthanized immediately before the procedure. The liver was perfused with warm Hank's buffered saline supplemented with 0.4 g/L KCl, 1.0 g/L glucose, 2.1 g/L $NaHCO_3$, and 0.2 g/L EDTA (pH 7.4, 42°C) via the inferior vena cava. The portal vein was severed to allow drainage. Perfusion was continued with warm Liver Digest Medium (pH 7.4, 42°C). Dissected liver was manually disrupted in DMEM supplemented with 10% FBS, 4.5 g/L glucose, 2 mM sodium pyruvate, 1 µM dexamethasone, 0.1 µM insulin, and

penicillin/streptomycin (plating medium). The cell suspension was filtered (70 μM) and viable hepatocytes were isolated after resuspension of pelleted cells in plating medium:PBS-buffered Percoll (1:1) and centrifugation at 1000 rpm for 5 minutes. The cell pellet was washed two times with plating medium before seeding (30000 cells/cm^2) in collagen-coated plates. Three hours after seeding, the medium was changed to DMEM supplemented with 0.2% BSA, 4.5 g/L glucose, 2 mM sodium pyruvate, 0.1 μM dexamethasone and 1 nM insulin (maintenance medium). Next day, the cells were transfected with siRNAs (Table 2.10) using Lipofectamine 2000 reagent according to the manufacturer's instructions. Six hours after transfection, cells were incubated overnight with media lacking dexamethasone and insulin (starvation media) and then treated with T0901317 ligand (1μM) for 24 hours before isolating RNA and proteins.

Luciferase assays

For Luciferase assays, cells were plated in 6-well plates and were subsequently transfected with the calcium phosphate method. For the collection of whole cell protein extracts, cells were washed with ice-cold PBS, lysed in cell culture lysis 1x reagent (Promega) and incubated for 5 minutes at RT in a shaking platform. Cells were scraped, collected and after a cycle of freeze-thaw at 37 °C for 2 minutes, the lysates were purified by centrifugation at 13.000rpm for 1 minute at RT. The supernatant was collected as total cell lysate and used for measurement of luciferase and β-galactosidase activity. Luciferase assays were performed 40 hours post transfections using the luciferase assay kit from Promega Corp. according to the manufacturer' instructions. Normalization for transfection efficiency was performed by β-galactosidase assays

Measurement of luciferase activity

60 μl of cell extract were mixed with 60 μl luciferase substrate (Promega) and the relative light units (RLU) were measured in the luminometer.

Measurement of β-galactosidase activity

5-20 µl of cell extract were mixed with 456 µl sodium phosphate buffer (P buffer), 132 µl ONPG (8 mg/ml), 6 µl Mg^{2+} buffer (Table 2.11) and incubated at 37 °C until the samples are colored yellow. 5 µl of 1X Lysis buffer were used as blank. The reaction was stopped with the addition of 200 µl NaCO3 1M and the β-galactosidase activity was measured from the absorbance at 410 nm by Jenway 6405 UV/VIS Spectrophotometer. Alternatively, 5µl of cell extract were mixed with 149 µl sodium phosphate buffer, 44 µl ONPG, 2 µl Mg^{2+} buffer and incubated at 37 °C using the TECAN Infinite 200 PRO instrument. B-galactosidase activity was measured from the absorbance at 410 nm by TECAN Infinite 200 PRO at different time points until the samples are colored yellow.

Sodium phosphate buffer (P puffer):

Adjust the pH of Na_2HPO_4 0.1M to 7.3 with NaH_2PO_4 0.1M

ONPG:

Resuspend the appropriate amount of O-nitrophenyl-galactopyranoside (ONPG) in P buffer to a final concentration 8 mg/ml

Table 2.11. Composition of Mg2+ buffer

Mg^{2+} buffer	
KCl	1 M
$MgCl_2$	0,1 M
β-mercaptoethanol	352 mM

RNA isolation, reverse transcription,

Total RNA was prepared from HepG2, primary mouse hepatocytes, HEK293T, 3T3-L1 cells or tissues using Trizol or RNAiso Plus (Takara) reagents according to the manufacturer's instructions. RNA was diluted in Nuclease Free Water and its concentration and purity was calculated from the absorbance at 260nm by Jenway 6405 UV/VIS Spectrophotometer (as discussed above) or TECAN Infinite 200 PRO instrument. For each sample, one μg isolated RNA was reverse transcribed using random hexamers by the enzymes SuperScript II Reverse Transcriptase or M-MLV Reverse Transcriptase according to the manufacturer's instructions.

PCR and quantitative PCR (qPCR)

The cDNAs produced by 3T3-L1 cells, HepG2 cells, primary mouse hepatocytes or tissues were used for standard PCR amplification with primers specific for human or mouse genes (Table 2.12). For the normalization of the samples, the cDNA of the housekeeping GAPDH (glyceraldehyde 3-phosphate dehydrogenase) gene was also amplified by PCR.

The cDNAs produced by HepG2, HEK293T cells or primary mouse hepatocytes, were used for quantitative PCR (qPCR) that performed on a Step-OnePlus Real-Time PCR system (Applied Biosystems) using KAPA SYBR FAST qPCR Master Mix. The expression of the target genes was normalized to the expression of the housekeeping gene GUSB (Glucuronidase beta) or Hprt (Hypoxanthine phosphoribosyltransferase 1) and the normalized Ct (threshold cycle) values were calibrated against the control condition for each sample. The relative gene expression levels were determined using the comparative ΔΔCt method as described in Applied Biosystems Guide. All oligonucleotide sequences used as primers for qPCR or PCR experiments are shown in Table 2.12 and 2.13.

Table 2.12. Primers used in standard PCR analysis

Name	Sequence	Specificity
mLPL Fw	5' - TACAGCCTTGGAGCCCATGCT - 3'	mouse
mLPL Rev	5' - GAAGAGATGAATGGAGCGCTCGT- 3'	
mFOXA2 Fw	5' - CGTGAAGATGGAAGGGCACGAGC - 3'	mouse
mFOXA2 Rev	5' - TTCATGTTGGCGTAGGGGGCAAG - 3'	
mGAPDH Fw	5' - ACCACAGTCCATGCCATCAC - 3'	human/ mouse
mGAPDH Rev	5' - TCCACCACCCTGTTGCTGTA - 3'	
h/mABCG1 Fw	5' - AACTACTGGTACAGCCTGAA - 3'	human/ mouse
h/mABCG1 Rev	5' - TGACATAGGAGATGTAGGACA - 3'	
h/mABCG5 Fw	5' - GTCAGCGACCAGGAGAGTCA - 3'	human/ mouse
h/mABCG5 Rev	5' - GCACCTGGGCAGGTTTTCTC - 3'	
h/mABCG8 Fw	5' - CCTTGGTTTGAGCAGCTGGCTCA - 3'	human/ mouse
h/mABCG8 Rev	5' - TTTGTCACGCTGGGCCTGGGA - 3'	
h/mLIPC Fw	5' - CCTAATTGGGTACAGCCTGG - 3'	human/ mouse
h/mLIPC Rev	5' - GATGAACTGGATCTTGAACTGGT - 3'	
h/mPLTP Fw	5' - AGGGCCACCTACTTTGGGAGCA - 3'	human/ mouse
h/mPLTP Rev	5' - GATCTGCACCCCACGCCAGGT - 3'	
hCETP Fw	5' - AGATCAGCCACTTGTCCATCGCCA - 3'	human
hCETP Rev	5' - CCTTGTCTGGACAAAATCGGCCAT - 3'	

Table 2.13. Primers used in Quantitative PCR

Name	Sequence	Specificity
hLPL Fw	5' - AGCATTACCCAGTGTCCGC - 3'	human
hLPL Rev	5' - GGGCTCCAAGGCTGTATCC - 3'	
hGUSB Fw	5' - CACAAGAGTGGTGCTGAGGA - 3'	human
hGUSB Rev	5' - ACCAGGTTGCTGATGTCGG - 3'	
hFOXA2 Fw	5' - CTGGGAGCGGTGAAGATGG - 3'	human
hFOXA2 Rev	5' - CATGTTGCTCACGGAGGAGT - 3'	
hHPRT Fw	5' - CCCTGGCGTCGTGATTAGTG - 3'	human
hHPRT Rev	5' - TCGAGCAAGACGTTCAGTCC - 3'	
hLXRα Fw	5' - CTGCGATCGAGGTGATGCTT - 3'	human
hLXRα Rev	5' - GGGGTTGATGAATTCCACTTGC - 3'	
hLXRβ Fw	5' - CCAGCCCAAAGTCACGCC - 3'	human
hLXRβ Rev	5' - GCCCAGCTGCAGGAAACC - 3'	
mLPL Fw	5' - TGAGGATGGCAAGCAACACAA - 3'	mouse
mLPL Rev	5' - ATGAGCAGTTCTCCGATGTCC - 3'	
mHPRT Fw	5' - CGAAGTGTTGGATACAGGCC - 3'	mouse
mHPRT Rev	5' - GGCAACATCAACAGGACTCC - 3'	

Protein Isolation from Cells

Protein extracts for western blot experiments were obtained from cells using different lysis protocols. Whole cell extracts were isolated from primary mouse hepatocytes, HepG2 and HEK293T cells that had been transfected and nuclear extracts and cytoplasmic extracts were isolated from HepG2 and 3T3-L1 cells.

Purification of whole cell protein extracts

For the collection of whole cell protein extracts, cells were washed with ice-cold PBS, scraped, collected by centrifugation at 5000rpm for 5 minutes at 4°C and lysed on ice in cell culture lysis 5x reagent. After a cycle of freeze (at -80°C)-thaw (on ice), the lysates were purified by centrifugation at 13.000rpm for 5 minutes at 4°C. The supernatant was collected as total cell lysate.

Purification of nuclear and cytoplasmic extracts

For the purification of nuclear and cytoplasmic extracts, cells were washed twice with ice-cold PBS, scraped, and collected in buffer A, supplemented with complete Protease Inhibitor Cocktail (Table 2.14). Cell lysates were rotated on a platform for 10 minutes, and the cytosolic fraction was purified by centrifugation at 13000 rpm at 4°C for 4 minutes. The pellet of nuclei was resuspended in buffer B, supplemented with complete Protease Inhibitor Cocktail (Table 2.14), and extracts were incubated on ice for 30 minutes. The nuclear fraction was purified by centrifugation at 13,000 rpm at 4°C for 6 minutes.

Table 2.14. Buffers used for purification nuclear and cytoplasmic extracts

Buffer A		Buffer B	
Hepes pH 7.9	10 mM	Hepes pH 7.9	20 mM
EDTA pH 8.0	0,1 mM	EDTA pH 8.0	0,1 mM
KCl	10 mM	NaCl	400 mM
NP-40	0.4%	Glycerol	0,1%

Calculation of protein concentration (Lowry)

In all protocols protein concentration in protein extracts was determined from the absorbance at 750nm by Jenway 6405 UV/VIS Spectrophotometer (as discussed above) or TECAN Infinite 200 PRO instrument, using the DC Protein Assay kit (Bio-Rad Hercules, CA) according to the manufacturer's instructions

SDS-PAGE analysis

After protein concentration measurement, equal amounts of protein lysates were mixed with 4x Sample buffer (Table 2.15), denatured by boiling at 100 °C for 10 minutes and loaded on 8.5, 10.5 or 12.5% SDS polyacrylamide gel (Table 2.16). The BenchMark Prestained Protein Ladder was used as a size marker. Electrophoresis was performed in 1x TGS solution (Table 2.15) using Mini-PROTEAN Tetra Cell System (Bio-Rad). For visualization of the protein bands, gels were either stained with Coomassie Brilliant Blue or used for immunoblotting as described below.

Table 2.15. Buffers used for SDS-PAGE

4x Sample buffer		10x TGS	
Tris-Cl 1M pH 6.8	5 ml	Tris	30.3 g
β-mercaptoethanol	1.6 ml	Glycine	144.2 g
glycerol	4 ml	SDS	10 g
SDS	1.6 g	Volume	1 L
bromophenol blue	8 mg		
Volume	20 ml		

Table 2.16. Buffers used for the preparation of SDS polyacrylamide gels.

Separating buffer			Stacking buffer		
Tris	18.165 g	1.5 M	Tris	6.05 g	0.5 M
SDS	0.4 g	0.4 %	SDS	0.4 g	0.4 %
Volume	100 ml		Volume	100 ml	
pH (with HCl)	8.8		pH (with HCl)	6.8	

Stacking gel		Separating gel			
			8.5%	10.5%	12.5%
ddH_2O	2.4 ml	ddH_2O	4.6 ml	3.9 ml	3.2 ml
30% acrylamide	600 µl	30% acrylamide	2.8 ml	3.5 ml	4.2 ml
stacking buffer	1 ml	Separating buffer	2.5 ml	2.5 ml	2.5 ml
10% APS	40 µl	10% APS	160 µl	160 µl	160 µl
TEMED	4 µl	TEMED	8 µl	8 µl	8 µl
Volume	4 ml	Volume	10 ml	10 ml	10 ml

Coomassie Brilliant Blue staining

For visualization of the protein bands, polyacrylamide gels were stained with Coomassie Brilliant Blue R-250 (2.5 g Coomassie Brilliant Blue R in 45 % methanol and 10% acetic acid) for 20-30 minutes on a shaking platform, at RT. Then gels were destained in fast destaining solution for 1 hour on a shaking platform, at RT and in slow destaining solution (Table 2.17) overnight on a shaking platform, at RT. The gels were rehydrated in dH_2O overnight and dried in a Hoefer SE 1160 gel dryer under vacuum at 80 °C for 1 hour.

Table 2.17. Buffers used for gel destaining

Fast destaining		Slow destaining	
ddH_2O	400 ml	ddH_2O	875 ml
Methanol	500 ml	Methanol	75 ml
Acetic acid	100 ml	Acetic acid	50 ml
Volume	1 L	Volume	1 L

Western blot analysis

Following SDS-PAGE, proteins were transferred onto nitrocellulose membranes in transfer buffer (Table 2.18), using Mini-PROTEAN Tetra Cell System (Bio-Rad). Membranes were then washed with TBS-0.1% Tween 20 (TBS-T) solution (Table 2.18) and nonspecific sites were blocked in 5% nonfat milk TBS-T for 1 hour. Membranes were probed with appropriate primary antibodies overnight at 4°C, as shown in Table 2.1. After extensive washes with TBS-T solution, the membranes incubated with horseradish-peroxidase-conjugated secondary antibodies diluted 1:10,000 or 1:20,000 (for anti-rabbit, Merck Millipore) in 5% non-fat milk in TBS-T for 1 hour at RT, followed by washes with TBS-T solution. Signals were detected by enhanced chemiluminescence and proteins were visualized on a Chemi-Doc XRS+ Imaging System (Bio-Rad, Hercules, CA). Band intensities were quantified using the Image Lab Software (Bio-Rad). Alternatively, membranes were exposed on film (Fujifilm). To normalize the variations for proteins amounts, membranes were stripped with stripping buffer (restore western blot, Thermo), according to the manufacturer's instructions) or blocked with 0.02% NaN3 in TBS-T and reprobed with an antibody to β-actin.

Table 2.18. Buffers used for Western Blot

Transfer Buffer		10x TBS	
10 x TGS	100 ml	NaCl	180 g
Methanol	200 ml	Tris	121.14 g
ddH_2O	700 ml	pH (with HCl)	7.3
Volume	1 L	Volume	1 L

DNA-Protein Interactions

Chromatin Immunoprecipitation (ChIP) Assays

Chromatin preparation from cell lines

HepG2 were grown for 2-3 days and HEK293T cells that had been transfected with expression vectors for FOXA2, LXRα, RXRα and their ligands were cultured in 100 mm dishes. Cells were washed with DMEM, cross-linked for 10 minutes at 37 °C

with 1% formaldehyde and cross-linking was stopped by adding glycine to a final concentration of 137.5 mM. The cells were then rinsed three times with ice-cold PBS and 0.5 mM PMSF, scraped in ice-cold PBS containing 0.5% NP-40 and 0.5 mM PMSF, and centrifuged at 1000 rpm for 5 minutes at 4 °C. The pellets were resuspended in swelling buffer, supplemented with complete Protease Inhibitor Cocktail (Table 2.19) and left on ice for 10 minutes. Subsequently, the cells were homogenized using a Dounce homogenizer, the nuclei were checked in microscope by mixing 5μl with equal volume of 0.4%Trypan Blue and centrifuged at 2000 rpm for 5 minutes at 4 °C. The nuclei were resuspended in sonication buffer, supplemented with complete Protease Inhibitor Cocktail (Table 2.19) and sonicated 10-13 times for 30 seconds at 50% amplitude on ice, leading to the generation of chromatin fragments. The samples were cleared by centrifugation at 13000 rpm for 15 minutes at 4 °C and stored -80oC.

Table 2.19. Buffers used for chromatin purification

Swelling Buffer		Sonication Buffer	
Hepes pH 7.9	25 mM	Hepes pH 7.9	50 mM
$MgCl_2$	1.5 mM	NaCl	140 mM
KCl	10 mM	EDTA pH 8.0	1 mM
NP-40	0.5%	Triton X-100	1%
DTT	1 mM	Na-deoxycholic acid	0.1%
Aprotinin	2 μg/ml	SDS	0.1%
PMSF	0.5 mM	Aprotinin	2 μg/ml
		PMSF	0.5 mM

Chromatin preparation from tissues

Fresh liver (~300mg) from C57BL/6 male mice was used for 4 ChIP assays. Small pieces of the tissue were homogenized in ice-cold PBS and 0.5 mM PMSF AND the cells were cross-linked for 15 minutes at 37 °C with 1% formaldehyde. Cross-linking was stopped by adding glycine to a final concentration of 137.5 mM. The tissue cells were then centrifuged at 1200rpm for 20 minutes at 4°C and washed three times with ice-cold PBS, 0.5 mM PMSF and once with ice-cold PBS containing 0.5% NP-40 and 0.5 mM PMSF. The cell pellet was resuspended in swelling buffer supplemented with

protease inhibitors and left on ice for 10 minutes. Subsequently, the cells were homogenized using a Dounce homogenizer, the nuclei were checked in microscope by mixing 5µl with equal volume of 0.4% Trypan Blue and centrifuged at 2000 rpm for 5 minutes at 4 °C. The nuclei were resuspended in sonication buffer supplemented with protease inhibitors and sonicated 60 times for 30 seconds at 70% amplitude on ice using Q Sonica Q800R, leading to the generation of chromatin fragments. The samples were cleared by centrifugation at 13000 rpm for 15 minutes at 4 °C and stored -80oC.

Sonication check

50µl aliquot of chromatin was used for sonication check. Chromatin was mixed with 150 µl H2O and 10.5 µl NaCl (4M stock), incubated overnight at 65°C. Then was mixed with 2µl RNAse A (10 mg/ml stock) and incubated for 1 hour at 37°C. 2 µl EDTA (0.5M stock) and equal volume of phenol/chloroform/isoamylalcohol was added to the mix. Chromatin was centrifuged at 13000 rpm for 5 minutes, equal volume of chloroform and 4 µl glycogen (5 µg/µl stock) were added to the upper phase and after mixing, was centrifuged again at 13000 rpm for 5 minutes. To the upper phase was added 1/10 volume Na-acetate (3M stock), 2.5 volumes 100% ethanol and incubated to -80oC for 30 minutes. Chromatin pellet was centrifuged at 13000 rpm for 10 minutes, washed with 75% ethanol, and resuspended in H20. The quality of the fragmented chromatin was checked on an agarose gel (fragment size should be less than 1000nt).

Equilibration and blocking of beads

For each sample 160 µl Protein-G Sepharose beads or 100 µl Protein-G dynabeads were used. The Beads were washed 3 times with sonication buffer (rotation for 10 minutes at 4°C and removal of supernatant by centrifugation at 2000rpm for 3 minutes at 4°C or by magnetic rack). Then, the beads were blocked with 494 µl sonication buffer, 5µl BSA (100 mg/ml stock), and 1 µl sonicated λ DNA (0.5 µg/µl stock) and rotated for 2 hours at 4°C.

Preclearing of chromatin and immunoprecipitation

The chromatin (1.5ml) was precleared by rotation at 4 °C for 2 hours with equilibrated protein G Sepharose or Dynabeads and 15µl BSA (100 mg/ml stock) and 3 µl sonicated λ DNA (0.5µg/µl stock). After removal of beads (by centrifugation at 2000rpm for 3 minutes at 4°C or by magnetic rack), one-tenth of the volume of supernatant was used as input, and the remaining volume was immunoprecipitated with a-FOXA2 (M-20) or a-LXRα (ab41902) or a-RXR (D-20) overnight at 4 °C.

Washes of beads and De-crosslinking

The immunoprecipitated chromatin was mixed with equilibrated Protein-G Sepharose or dynabeads and rotated for 2 hours at 4°C. The samples were washed twice with buffer A, buffer B, buffer C and TE (Table 2.20). DNA was eluted in 300 µl of elution buffer (Table 2.20), mixed with 100 µl H2O and 21µl NaCl (4M stock) and the cross-links were reversed by overnight incubation at 65 °C.

Table 2.20. Buffers used for ChIP assays

Wash Buffer A		Wash Buffer B		Wash Buffer C	
Hepes pH 7.9	50 mM	Hepes pH 7.9	50 mM	Tris-Cl	20 mM
NaCl	140 mM	NaCl	500 mM	EDTA pH 8.0	1 mM
EDTA pH 8.0	1 mM	EDTA pH 8.0	1 mM	LiCl	250 mM
Triton X-100	1%	Triton X-100	1%	NP-40	0.5%
Na-deoxycholic acid	0.1%	Na-deoxycholic acid	0.1%	Na-deoxycholic acid	0.5%
SDS	0.1%	SDS	0.1%	Aprotinin	2 µg/ml
Aprotinin	2 µg/ml	Aprotinin	2 µg/ml	PMSF	0.5 mM
PMSF	0.5 mM	PMSF	0.5 mM		

TE		Elution Buffer	
Tris-Cl pH 8.0	10 mM	Tris-Cl pH 8.0	50 mM
EDTA pH 8.0	1 mM	EDTA pH 8.0	1 mM
Aprotinin	2 µg/ml	SDS	1%
PMSF	0.5 mM	$NaHC0_3$	50 mM

DNA Purification and PCR amplification

The samples were subjected to RNAse A treatment for 1 hour at 37 °C and to digestion of proteins by 2 µl proteinase K (10 mg/ml stock) for 2 hours at 42 °C. DNA was purified by phenol-chloroform extraction and ethanol precipitation. 200µl H2O, 1/10 volume Na-acetate (3M stock) and equal volume phenol/chloroform/isoamylalcohol were added to the samples. After vortexing, chromatin was centrifuged at 13000 rpm for 5 minutes and equal volume of chloroform was added to the upper phase. The samples were centrifuged again at 13000 rpm for 5 minutes and 4 µl glycogen (5 µg/µl stock) and 2.5 volumes 100% Ethanol were added to the upper phase and incubated overnight to -20oC. Precipitated chromatin was centrifuged at 13000 rpm for 30 minutes at 4 °C , washed with 75% EtOH, centrifuged at 13000 rpm for 10 minutes and resuspended in 10 mM Tris-Cl, pH 7.5. Immunoprecipitation eluates and 1% chromatin input were used for PCR amplification or analyzed by SYBR-Green quantitative PCR (KAPA SYBR® FAST qPCR Kit) using the StepOnePlus™ Real-Time PCR System (Applied Biosystems). The Ct values of the ChIP signals detected by qPCR were converted to the percentage of the input DNA using the "percent input method" as recommended by the manufacturer. The oligonucleotides used as primers in these assays are shown in Table 2.21.

Table 2.21. Oligonucleotides used in chromatin immunoprecipitation (ChIP) assays [a]

Name	Sequence	Purpose
hLPL -141 ChIP Fw	5' - GGTTGATCCTCATTACTGTTTGCT- 3'	ChIP analysis of the human LPL promoter, starting at position -141
hLPL -10 ChIP Rev	5' - ACGCCAAGGCTGCTTATGT - 3'	ChIP analysis of the humanLPL promoter, ending at position -10
hLPL intron2 ChIP Fw	5' - GACGGTGCCACTTCCTATCA - 3'	ChIP analysis of the distal region of the 2nd intron of human LPL
hLPL intron2 ChIP Rev	5' - TGCACAGACCCAACTCAGTC - 3'	ChIP analysis of the distal region of the 2nd intron of human LPL
hLPL intron1 ChIP Fw	5' - CGCGCTATCCCTTCCACTCT - 3'	ChIP analysis of the distal region of the 1st intron of human LPL
hLPL intron1 ChIP Rev	5' - CCAACCAAGGCGAGGTCAC - 3'	ChIP analysis of the distal region of the 1st intron of human LPL
hABCA1 -139 ChIP Fw	5' - ACGTGCTTTCTGCTGAGTGA - 3'	ChIP analysis of the human ABCA1 promoter, starting at position -139
hABCA1 -41 ChIP Rev	5' - GCGCAGAGGTTACTATCGGT- 3'	ChIP analysis of the human ABCA1 promoter, ending at position -41
mLPL -143 ChIP Fw	5' - ACCGTTGAGCCTCGTTACC- 3'	ChIP analysis of the mouse LPL promoter, starting at position -143
mLPL +1 ChIP Rev	5' - CACTGTTTCCACTGCACAGC- 3'	ChIP analysis of the mouse LPL promoter, ending at position +1
mLPL intron9 ChIP Fw	5' - GCTGACCTTCATCCCAGACA- 3'	ChIP analysis of the distal region of the 9th intron of mouse LPL
mLPL intron9 ChIP Rev	5' - GAGGCTCACAACCACCCATA- 3'	ChIP analysis of the distal region of the 9th intron of mouse LPL

DNA affinity precipitation (DNAP) assays

For DNA affinity precipitation assays were used whole cell extracts from HEK293T cells that had been transfected with CMV-rFOXA2 or 6myc LXRα, RXRα expression vectors or nuclear extracts from HepG2 cells (as described above). In all protocols protein concentration was determined by DC Protein Assay (Bio-Rad).

Purification of whole cell extracts

For the collection of whole cell protein extracts, HEK293T cells were washed with ice-cold PBS, scraped, collected by centrifugation at 5000 rpm at 4 °C for 5 minutes and resuspended in Co-IP lysis buffer (Table 2.22). Lysates were rotated on a rotating platform for 30 minutes at 4°C and purified by centrifugation at 13000 rpm for 5 minutes at 4°C.

Table 2.22. Composition of Co-IP lysis buffer

Co-IP lysis buffer	
Tris-HCl pH 7.5	20 mM
NaCl	150 mM
Triton X-100	1%
glycerol	10%
PMSF	1 mM
benzamydine	0.5 mM

Preparation of biotinylated PCR fragments

For the generation of biotinylated PCR fragments, PCR products were amplified with the use of a biotinylated and a non-biotinylated primer and isolated by gel extraction. The amount used in the reaction was calculated based on the fact that for a 600bp fragment, 2 μg of the PCR product is required. Biotinylated PCR fragments corresponding to the regions -466/+39, -262/+39, -109/+39 (wt or mutant) and -28/+39 of the human LPL and -535/-39 of the human ABCA1 gene were utilized. The sequence of the primers utilized for the isolation of the biotinylated PCR promoter fragments are shown in Table 2.23.

Table 2.23. Oligonucleotides used in DNA affinity precipitation (DNAP) assays [a]

Name	Sequence	Purpose
LPL -466 Fw	5' - CCGCTCGAGACGCAATGTGTGTCCCTCTAT -3'	DNAP, non-biotinylated
LPL -262 Fw	5' - CCGCTCGAGACCTGTGTTTGGTGCTTAGACA - 3'	DNAP, non-biotinylated
LPL -109 Fw	5' - CCGCTCGAGTAGAAGTGAATTTAGGTCCCTC - 3'	DNAP, non-biotinylated
LPL -28 Fw	5' - CCGCTCGAGACATAAGCAGCCTTGGCGTGAAAA - 3'	DNAP, non-biotinylated
LPL +39 Rev-Bio	5'-Bio- TTCCCTTGAGGAGGAGGAAGAGGGGGAAT-3'	DNAP, 5' biotinylated
ABCA1 -535 Fw-Bio	5'- Bio- AGGCCTTTGAAAGGAAACAAAAGACAAGACAAA -3'	DNAP, 5' biotinylated
ABCA1 -39 Rev	5'-TCGAGGAATTCGAGCGCAGAGGTTACTATCGGTCAAAGCCTGTGGTAC-3'	DNAP

[α] XhoI (CTCGAG) and HindIII (AAGCTT) sites are underlined.

Beads preparation

For each sample 5µl (50µg) Dynabeads M-280 Streptavidin were used. For protein-DNA interactions, Streptavidin Dynabeads were washed with 1x B&W buffer (Table 2.24), mixed with 7 µl 2x B&W buffer and 7 µl biotinylated PCR products and incubated at room temperature for 15 minutes, with occasional shaking. The DNA-coupled beads were washed twice with 1x B&W buffer and once with BBRC buffer (Table 2.24).

Table 2.24. Buffers used for DNAP assays

2x B&W		BBRC	
Tris-HCl pH 7.5	10 mM	Tris-HCl pH 7.5	10 mM
EDTA	1 mM	KCl	50 mM
NaCl	2 mM	MgCl2	4 mM
		EDTA	0,2 mM
		glycerol	10%

Protein – DNA binding interactions

Each reaction mixture included 150 µg of whole cell extracts or nuclear protein extracts, 7.5 µg of competitor poly (deoxyinosine/deoxycytosine) and the biotinylated DNA-coupled Dynabeads or uncoupled Dynabeads as controls, in a total reaction volume of 500µl BBRC buffer (supplemented with 1 mM PMSF and 0.5 mM benzamidine). The protein-DNA binding reactions were allowed to proceed for 2.5 hours on a rotator at 4 °C and then the protein-DNA-coupled beads were washed three times with BBRC buffer, supplemented with 1 mM PMSF and 0.5 mM benzamidine, and resuspended in 4x SDS loading buffer. Nuclear receptors (LXRα/ RXRα) or FOXA2 bound to the biotinylated fragments were detected by SDS-PAGE and immunoblotting using the corresponding antibodies.

Co-immunoprecipitation assays

For co-immunoprecipitation experiments, HEK293T cells that had been transfected with 6myc LXRα, FOXA2 or Flag FOXO1 expression vectors were lysed in Co-IP lysis buffer supplemented with complete Protease Inhibitor Cocktail, as described above, and protein concentration was determined by DC Protein Assay (Bio-Rad).

Equilibration of beads

For each sample 40 μl Protein-G Sepharose beads were used. The beads were equilibrated with 10 volumes of PBS, centrifuged at 2000rpm for 5 minutes at 4°C. The supernatant was removed and the beads were resuspended in equal volume of PBS.

Protein – protein binding interactions

The protein lysates were precleared by incubation with 40μl of pre-equilibrated Protein G-Sepharose beads on a rotating platform for 30 minutes at 4°C, and collection of the supernatant. Supernatants were incubated with a proper dilution of the antibody anti-FOXA2 or anti-flag on a rotating platform overnight at 4°C, followed by incubation with 40μl of pre-equilibrated Protein G–Sepharose beads for 1 hour at 4°C. The beads were washed three times with Co-IP lysis buffer supplemented with complete Protease Inhibitor Cocktail, rotated for 10 minutes at 4°C, followed by 5 minutes of centrifugation at 2000 rpm and resuspended in 4x SDS loading buffer. Immunoprecipitated proteins were analyzed by SDS-PAGE and immunoblotting using the corresponding antibodies.

Protein–protein interaction assays based on biotinylation in vivo

For the in vivo biotinylation assay, HEK293T cells were co-transfected with the Bio-FOXA2 expression vector along with the expression vectors for 6myc-LXRα and 6myc-RXRα, in the presence or in the absence of a vector expressing the bacterial biotin ligase BirA. The cells were lysed in Co-IP lysis buffer supplemented with

complete Protease Inhibitor Cocktail, as described above, and protein concentration was determined by DC Protein Assay (Bio-Rad).

Equilibration of beads

For each sample 50 µl Streptavidin-agarose beads were used. The beads were equilibrated with 10 volumes of Co-IP lysis buffer and centrifuged at 2000rpm for 5 minutes at 4°C. The supernatant was removed and the beads were resuspended in equal volume of Co-IP lysis buffer.

Protein – protein binding interactions

The protein lysates were allowed to interact with pre-equilibrated beads on a rotating platform for 3-4 hours at 4ºC. The beads were washed three times with Co-IP lysis buffer and re-suspended in 4x SDS loading buffer. Bound proteins were subjected to SDS-PAGE followed by immunoblotting using anti-myc or streptavidin-HRP.

Bacterial expression and purification of GST-fusion proteins

The GST-fusion proteins were expressed in *E. coli* strains BL21. Bacteria were grown in LB/ampicillin overnight at 37◦C, diluted 1:20 and, after reaching a A600 of 0.7, were stimulated with 1 mM IPTG (isopropyl *β*-D-thiogalactoside) for 4-5 h at 37◦C. Bacteria were then harvested by centrifugation at 3500 rpm for 30 minutes at 4°C, resuspended in 1/10 of the original culture volume of PBS, and sonicated 10 times for 30 seconds in PBS on ice. Then, they were lysed by the addition of Triton X-100 to a final concentration of 1% and rotation at 4°C for 30 minutes. Lysates were subsequently cleared by centrifugation at 10000 rpm for 10 minutes at 4°C and the first supernatant was collected. The pellets were re-dissolved in 300 µl of solubilization buffer (Table 2.25) for 10 minutes at 4°C, with rotation. Triton X-100 to a final concentration of 2% and $CaCl_2$ to a final concentration of 1 mM were added, the lysates were cleared by centrifugation at 10000 rpm, at 4 °C, for 10 minutes and the second supernatant was collected. The two supernatants of the expressed proteins were monitored by SDS-PAGE and Coomassie Blue staining.

Table 2.25. Composition of Solubilization buffer

Solubilization solution	
Triethanolamine	25 mM
N-laurylsarcosine	1.5%
EDTA	1 mM

Equilibration of beads and protein purification with beads

Glutathione–Sepharose beads were equilibrated with 10 volumes of PBS, mixed and centrifuged at 1000rpm for 5 minutes. The supernatant was removed and the beads were resuspended in equal volume of PBS. The bacterially expressed GST-fusion protein supernatants were allowed to interact with 250 µl pre-equilibrated beads on a rotating platform overnight at 4◦C. The beads were washed four times with 10 volumes of PBS containing 1% Triton X-100 (rotation for 10 minutes at 4 ºC and centrifugation at 2000 rpm for 5 minutes at 4ºC) and then resuspended in equal volume of PBS. Coupling efficiency was monitored by SDS-PAGE and Coomassie Blue staining.

GST pull-down assays

For the GST pull-down assays, HEK293T cells were transfected with expression vectors for: 6myc LXRα (1-447) or its truncated forms 1-163, 164-447, 1-97, 98-163, 1-127, 30-127 and 30-163; 6myc-RXRα; 6myc FOXA2 (1-458) or its truncated forms 1-360, 95-458, 1-279, 95-360, 1-94, 144-279, 280-360, 361-458. After transfection with the truncated forms of FOXA2 1-94, 144-279, 280-360 and 361-458, cells were treated with proteasome inhibitor MG132 (10µM) for 6 hours. The cells were washed with ice-cold PBS, pelleted by centrifugation at 5000 rpm for 5 minutes at 4°C and resuspended in WCE lysis buffer, supplemented with complete Protease Inhibitor Cocktail (Table 2.26). After three cycles of freeze (at -80°C)-thaw (on ice), lysates were collected by centrifugation at 13000rpm for 4 minutes at 4°C.

Table 2.26. Composition of WCE Buffer

WCE Buffer	
Tris-HCl pH 7.4	20mM
KCl	400mM
Glycerol	10%
DTT	2mM

Protein – protein binding interactions

For the binding reaction, an appropriate amount of a 50% slurry GST–Sepharose beads were equilibrated with 1ml 2x interaction buffer (Table 2.27), mixed and the supernatant was removed by centrifugation at 2000 rpm for 5 minutes at 4°C. The beads were resuspended in 200 µl 2x interaction buffer supplemented with complete Protease Inhibitor Cocktail, combined with the lysates from HEK293T cells, in a final volume of 400 µl and incubated overnight on a rotary shaker at 4°C. Then the beads were then washed once with washing buffer-100 mM KCl, supplemented with complete Protease Inhibitor Cocktail, and twice with washing buffer-250 mM KCl, supplemented with complete Protease Inhibitor Cocktail (Table 2.27). The bound proteins were eluted by boiling in 4x SDS loading buffer, subjected to SDS-PAGE and immunoblotting using the corresponding antibodies.

Table 2.27. Buffers used for GST-pull down assays

2x Interaction Buffer		Washing Buffer	
Hepes pH 7.9	40 mM	KCl	100mM/250mM
$MgCl_2$	10 mM	Hepes pH 7.9	20mM
NP40	0.4%	$MgCl_2$	5mM
BSA	0.4%	NP40	0.2%
Glycerol	15%		

The lentiviruses expressing the shRNAs for LXRα, LXRβ and scrambled were produced in HEK293T cells and then they were collected and used for infection of HepG2 cells.

Packaging and Amplification of lentiviruses

For shRNA lentiviruses Production, HEK293T cells were transfected using 18 µl Lipofectamine 2000 reagent, with 3µg of either shLXRα, shLXRβ or shcontrol pLKO.1 vectors, 2 µg of Δ8.2 (Delta 8.2) and 1 µg of VSV-G packaging plasmids, according to the manufacturer's protocol. The shRNA control was used as a control lentiviral vector. The transfected cells were maintained at 37 °C in a 5% CO2 incubator for 18 hours. The medium was replaced by fresh medium and the whole transfection was repeated onto the same cells. 48 hours after the first transfection, the supernatant (1st supernatant) containing lentiviral particles was harvested, centrifuged at 1200rpm for 5 minutes at 4°C to pellet any HEK cells, filtered using 0.45um filters to remove any cells and stored at -80°C for long term storage. The medium was replaced by fresh medium to the cells and 24 hours later the supernatant (2nd supernatant) was harvested, centrifuged at 1200rpm for 5 minutes at 4°C, filtered using 0.45um filters and stored at -80°C for long term storage.

Lentiviruses infection of HepG2 cells

For viral infections, HepG2 cells were infected by adding virus supernatants directly to the cell culture medium. HepG2 cells were plated in 6-well plates in ~50% confluency and incubated for 20-24 hours. The medium was replaced by 1ml DMEM and the cells were infected with 1ml from the 1st supernatant containing 5µg/ml polybrene. After incubation for 24 hours at 37°C, the inoculum was removed and the cells were re-infected with the 2nd viral supernatant (1ml) and 1ml DMEM containing 5µg/ml polybrene. Next day, the inoculum was removed and fresh medium containing puromycin at final concentration 1.5 µg/ml was added to the cells. Transduced cells were selected and maintained in the presence of this antibiotic for 5 days. The cells were collected for mRNA extraction using the Trizol protocol as described above, to confirm the silencing of LXRα or LXRβ and the impact on their target genes.

3. RESULTS AND DISCUSSION

<u>PART I</u>:

Regulation of the human lipoprotein lipase gene by the forkhead box transcription factor FOXA2/HNF-3β in hepatic cells

Functional analysis of the human LPL promoter in hepatic cells reveals a putative FOXA2 binding site in the proximal region.

In order to identify and characterize regulatory elements that are critical for the expression of the human LPL gene, we amplified by polymerase chain reaction from human genomic DNA the human LPL promoter -883/+39 and generated a series of 5' deletions: -669/+39, -466/+39, -262/+39, -109/+39 and -28/+39 (Figure 3.1A). These LPL promoter fragments were cloned upstream of the luciferase gene and their relative transcriptional activity was determined by luciferase assays in human hepatoma HepG2 cells that express FOXA2 endogenously. As shown in Figure 3.1B, serial deletions of the LPL promoter from position -883 to position -262 were associated with a step-wise increase in the activity of the promoter suggesting the presence of inhibitory regulatory region(s) in the area defined by nucleotides -883 and -262. Further deletion to -109 caused a small reduction in promoter activity. Importantly, deletion of the LPL promoter from -109 to -28 abolished the activity of the LPL promoter suggesting the presence of positive regulatory elements within the -109/-28 region (Figure 3.1B).

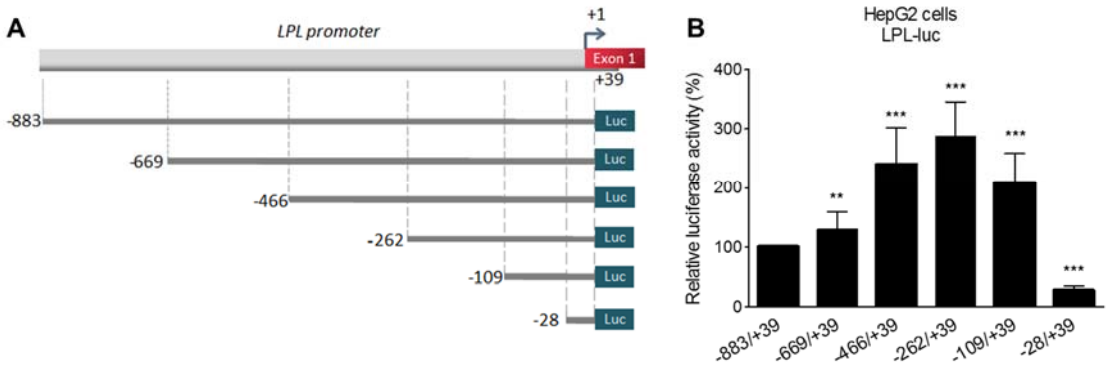

Figure 3.1. The region -109/-28 of the human LPL promoter may contain important regulatory elements. (A) Schematic representation of the 5'-deletion fragments of the (-883/+39) human LPL promoter that were cloned upstream of the luciferase reporter gene (Luc) and used in the transactivation experiments of panel B. (B) HepG2 cells were transiently transfected with the indicated LPL-luc reporter plasmids (1μg) along with a β-galactosidase expression plasmid (1μg) which was included in each sample for normalization of transfection variability. Luciferase activity was normalized to β-galactosidase activity and presented with histographs. Each value represents the average (±SD) from eight independent experiments performed in duplicate. **, $p<0.01$; ***, $p < 0.001$

A database search for putative transcription factor binding sites (www.genomatix.de) revealed that the proximal -122/+28 region of the human LPL promoter contains one putative binding site for the hepatocyte-specific transcription factor forkhead box A2 (FOXA2) also known as hepatocyte nuclear factor 3β (HNF-3β) at position -47/-40 having homology (7/8 nucleotides) with the consensus FOXA2 recognition sequence 5'-T(G/A)TTT(A/G)(C/T)T-3' (Figure 3.2A)(277). To examine the role of the putative FOXA2 binding site in LPL gene regulation, we transfected HepG2 cells with a plasmid vector expressing FOXA2.

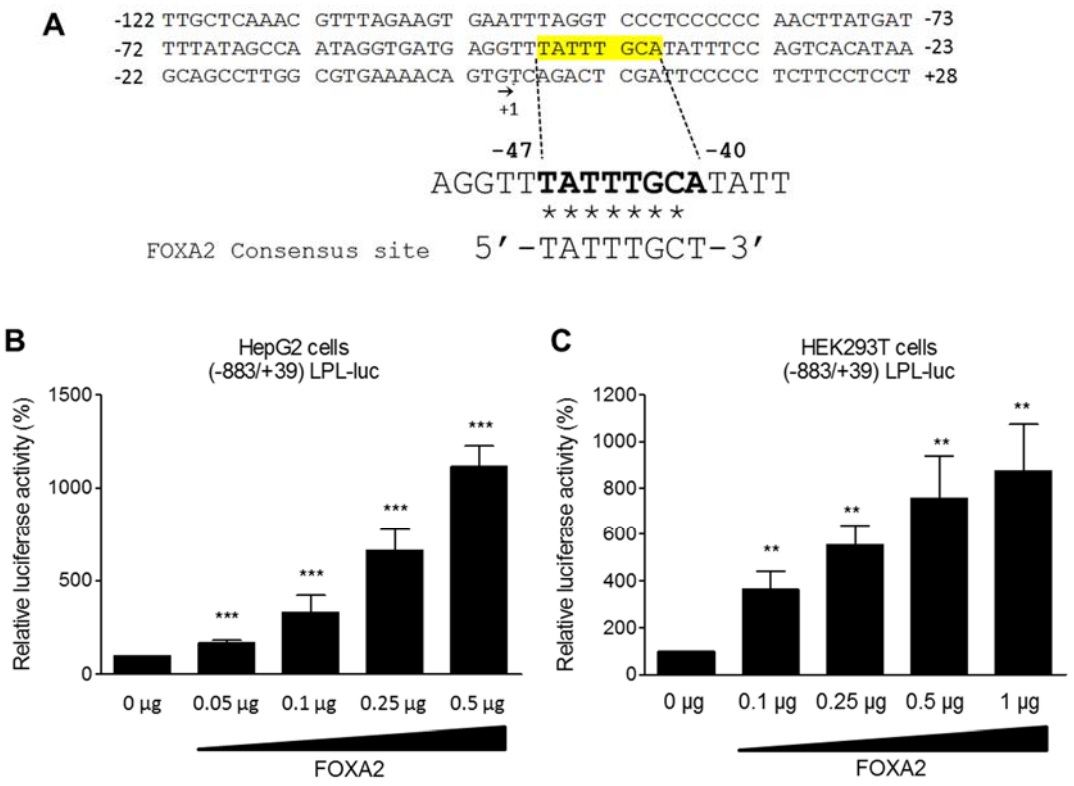

Figure 3.2. The human LPL promoter contains a putative FOXA2 binding element. (A) Sequence of the proximal human LPL promoter region -122/+28. The putative FOXA2 binding site in the -47/-40 region is in bold letters. Homology of the putative FOXA2 binding site of the LPL promoter with the FOXA2 consensus site is indicated with the asterisks. (B) HepG2 cells were transiently transfected with the (−883/+39) LPL-luc reporter plasmid (1µg) along with increasing concentrations (0.05–0.5µg) of a FOXA2 expression vector and a β-galactosidase expression plasmid (1µg). The normalized relative luciferase activity is presented with histographs. Each value represents the average (±SD) from at least three independent experiments performed in duplicate. (C) HEK293T cells were transiently transfected with the (−883/+39) LPL-luc reporter plasmid (1µg) along with increasing concentrations (0.1–1µg) of the FOXA2 expression vector and a β-galactosidase expression plasmid (1µg). The normalized relative luciferase activity is presented with histograph. Each value represents the average (±SD) from two independent experiments performed in duplicate. **, $p<0.01$; ***, $p < 0.001$

Using luciferase activity assays we showed that FOXA2 increased the activity of the -883/+39 LPL promoter in a dose-dependent manner (Figure 3.2B). Similar dose-dependent transactivation of the -883/+39 LPL promoter was observed in HEK293T cells (that do not express endogenous FOXA2) when FOXA2 was exogenously overexpressed (Figure 3.2C).

Collectively, the data of Figures 3.1 and 3.2 showed that the forkhead box transcription factor FOXA2 has the ability to transactivate the human LPL promoter in hepatic cells and this transactivation may be facilitated via a putative FOXA2 responsive element present in the proximal LPL promoter.

FOXA2 is important for LPL gene expression in hepatic cells.

To investigate the role of FOXA2 in LPL gene expression in hepatic cells, we performed siRNA-mediated gene silencing experiments. For this purpose, HepG2 cells were transfected with a FOXA2-specific siRNA or a non-specific siRNA (scrambled) and the mRNA and protein levels of FOXA2 and LPL were determined by reverse transcription quantitative PCR (qPCR) and Western blotting respectively. Figure 3.3A and B shows that the siRNA specific for FOXA2 abolished the expression of the endogenous FOXA2 gene in HepG2 cells, at mRNA and protein level. This silencing was associated with a 65% decrease in LPL mRNA (Figure 3.3A) and 75% decrease in LPL protein levels (Figure 3.3B and C). Furthermore, silencing of endogenous FOXA2 in HepG2 cells caused a 50% decrease in the activity of the -883/+39 LPL promoter relative to the same concentration of a control (scrambled) siRNA (Figure 3.3D). Similar, protein levels of LPL were reduced by 60% in HEK293T cells that had been co-transfected with the FOXA2 expression vector and the siRNA for FOXA2 (Figure 3.3E and F).

In line with the data of Figure 3.3, overexpression of FOXA2 in HepG2 cells was associated with a ~4 fold increase in the protein levels of LPL both the intracellular (Figure 3.4A and B) and the secreted forms (Figure 3.4A and C). Moreover, transfection of FOXA2 expression vector in HepG2 and HEK293T cells caused 1.4-fold and 1.9-fold increase in the LPL mRNA levels, respectively (Figure 3.4 D and E).

In summary, the findings of Figures 3.3 and 3.4 indicated that the hepatocyte-specific transcription factor FOXA2 plays a positive role in LPL gene expression in hepatic cells.

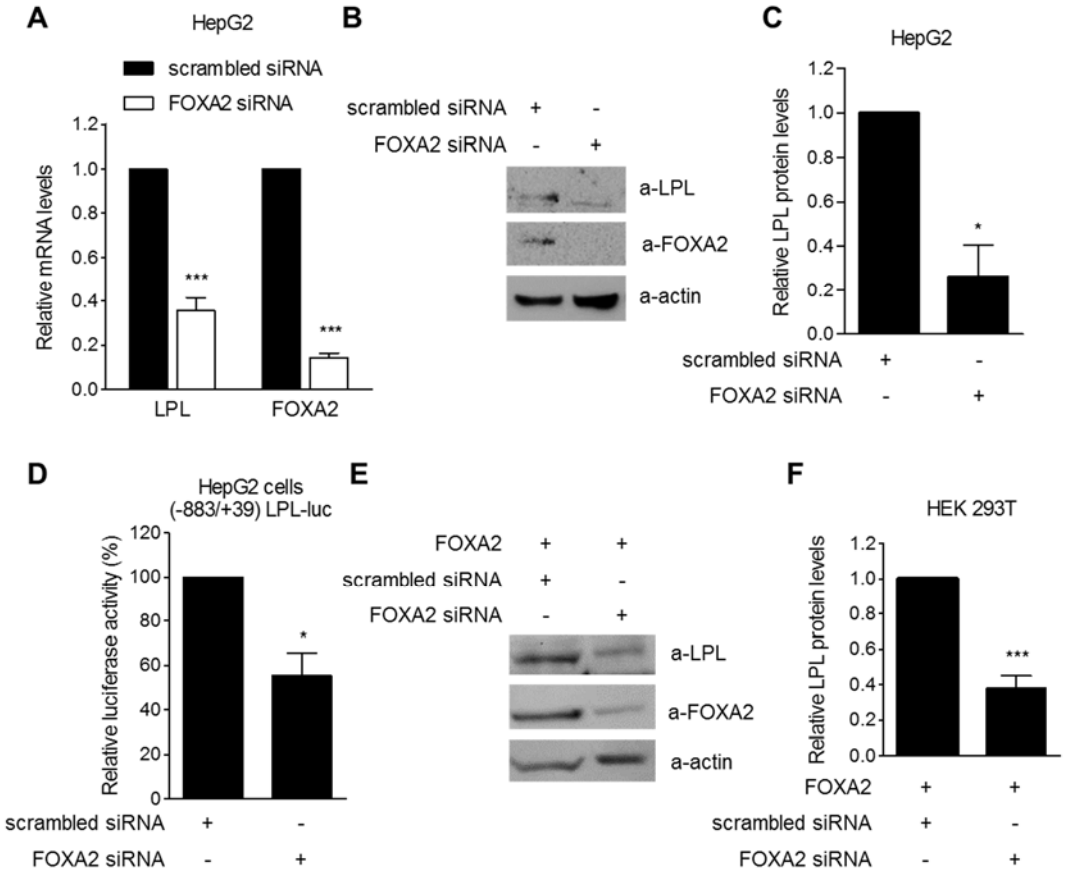

Figure 3.3. FOXA2 is a positive regulator of LPL gene expression in HepG2 and HEK293T cells. (A) HepG2 cells were transfected with 50nM of scrambled si-RNA or FOXA2 specific si-RNA, total RNA was extracted and LPL and FOXA2 mRNA levels were determined by reverse transcription quantitative PCR. LPL and FOXA2 mRNA levels were normalized relative to the GUSB mRNA levels. Results are expressed as mean (±SD) from at least three independent experiments and shown as a histograph. (B) HepG2 cells were transfected with 50nM of scrambled si-RNA or FOXA2 si-RNA and the protein levels of LPL, FOXA2 and actin (loading control) were determined by immunoblotting using the corresponding antibodies. The experiment was performed three times and representative images are presented. (C) Levels of LPL and actin were quantified by densitometry and the normalized relative protein levels are shown as a histograph. Results are expressed as mean (±SD) from at least three independent experiments. (D) HepG2 cells were transiently transfected with the (−883/+39) LPL-luc reporter plasmid (0.8µg) in the presence of 200nM of scrambled si-RNA or FOXA2 si-RNA. Each value of luciferase activity represents the average (±SD) from three independent experiments performed in duplicate. (E) HEK293T cells were co-transfected with a FOXA2 expression vector (0.5µg) and 50nM of scrambled si-RNA or FOXA2 si-RNA. The protein levels of LPL, FOXA2 and actin (loading control) were determined by immunoblotting using the corresponding antibodies. The experiment was performed four times and representative images are presented. (F) Levels of LPL and actin were quantified by densitometry and the normalized relative protein levels are shown as a histograph. Results are expressed as mean (±SD) from four independent experiments. *, $p<0.05$; ***, $p< 0.001$.

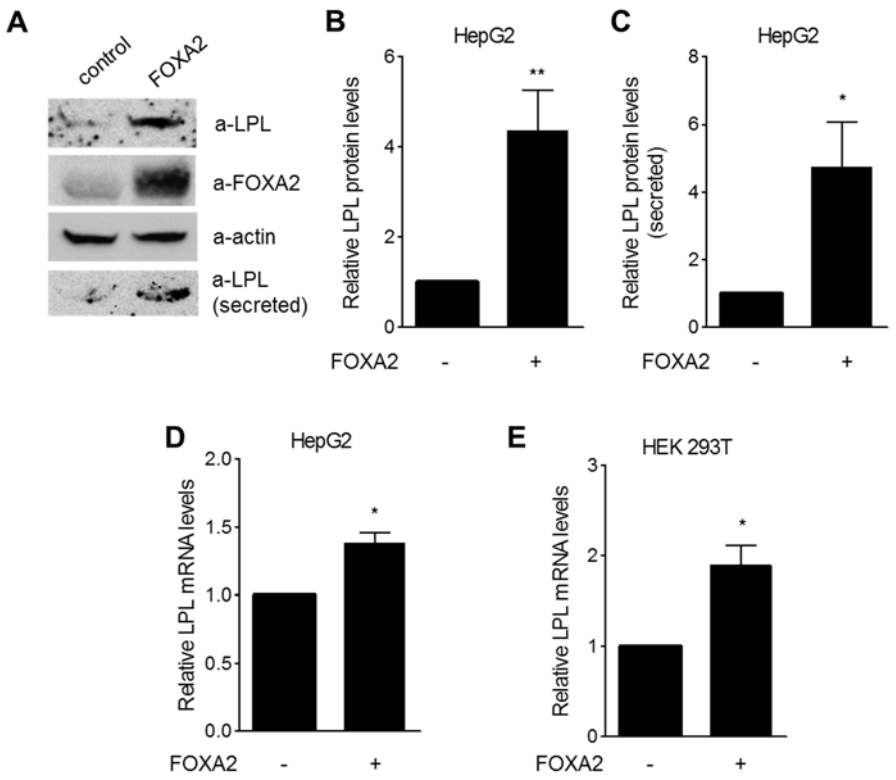

Figure 3.4. FOXA2 is a positive regulator of LPL gene expression in HepG2 and HEK293T cells. (A) HepG2 cells were transiently transfected with a FOXA2 expression vector (8μg) and the intracellular protein levels of LPL, FOXA2 and actin (loading control) as well as of the secreted LPL were determined by immunoblotting using the corresponding antibodies. The experiment was performed at least three times and representative images are presented. (B and C) Levels of intracellular LPL and actin were quantified by densitometry and the normalized relative protein levels or the secreted LPL protein levels are shown. (D) HepG2 cells were transiently transfected with a FOXA2 expression vector (6μg) and RNA was extracted. LPL mRNA levels were determined by reverse transcription quantitative PCR, normalized relative to the mRNA levels of the GUSB gene and are shown as a histograph. (B, C and D) Results are expressed as mean (±SD) from at least three independent experiments. (E) HEK293T cells were transiently transfected with a FOXA2 expression vector (0.6μg). Total RNA was extracted, and LPL mRNA levels were determined by reverse transcription quantitative PCR. The mRNA levels of the GUSB gene were determined for normalization purposes. The relative mRNA levels of the LPL gene are shown as a histograph. Results are expressed as mean (±SD) from three independent experiments. *, $p<0.05$; **, $p<0.01$.

FOXA2 binds to the proximal -47/-40 region of the LPL promoter in vitro and in vivo.

To identify regulatory regions in the LPL promoter that could serve as binding sites for FOXA2 and could facilitate the transactivation of the LPL promoter by FOXA2, we used the LPL promoter constructs shown in Figure 3.5A in transient transfections in HepG2 cells along with an expression vector for wild type FOXA2 or

an empty vector as a control and their transcriptional activity was analyzed. As shown in Figure 3.5B, ectopically overexpressed FOXA2 transactivated the -883/+39, -669/+39, -466/+39, -262/+39 and -109/+39 LPL promoter fragments in HepG2 cells. The proximal LPL promoter between nucleotides -109/+39, that contains the putative -47/-40 FOXA2 element (Figure 3.5 A), was the shortest LPL promoter fragment that was responsive to FOXA2 overexpression because further deletion to -28 abolished the transactivation by FOXA2 (the transactivation of the -28/+39 LPL promoter by FOXA2, although statistically significant, was comparable to the transactivation of the empty luciferase vector pBS-Luc) (Figure 3.5 B).

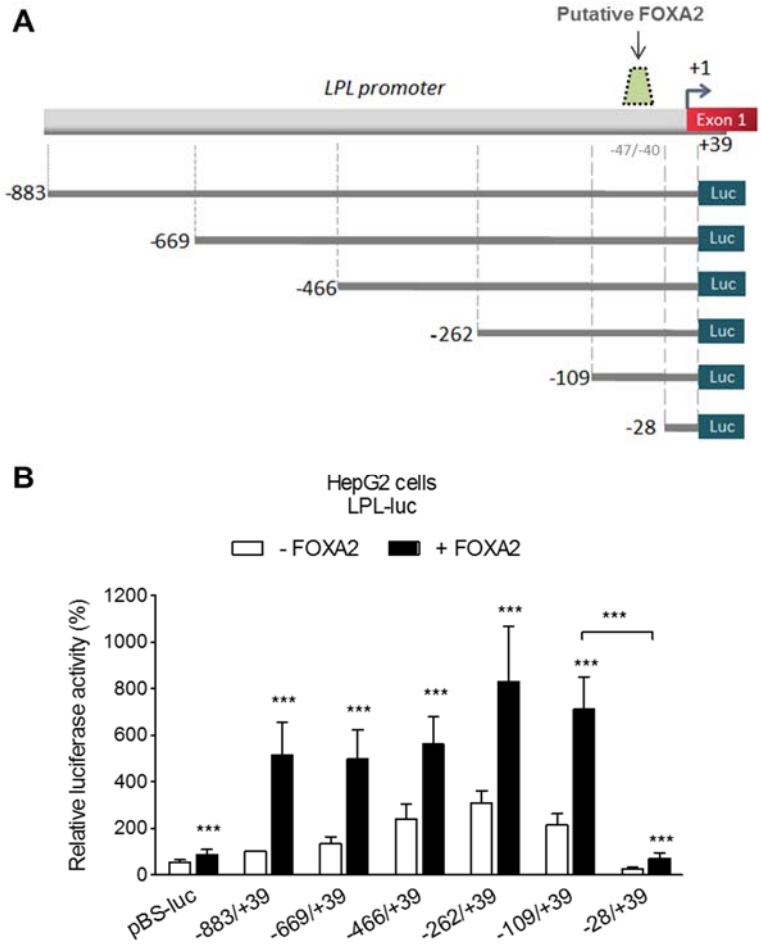

Figure 3.5. Transactivation of the human LPL promoter by FOXA2 requires the proximal -109/-28 region which contains the putative FOXA2 binding site. (A) Schematic representation of the 5'-deletion fragments of the (-883/+39) human LPL promoter that were used in the transactivation experiments of panel B. The putative FOXA2 binding site in the -47/-40 region is indicated. (B) HepG2 cells were transiently transfected with the hLPL-luc reporter plasmids (1μg) shown in Figure 1A, along with a FOXA2 expression vector (0.25μg). Each value of luciferase activity represents the average (±SD) from at least four independent experiments performed in duplicate. ***p< 0.001.

Next, we performed a series of protein-DNA binding assays in order to confirm the interaction of FOXA2 with the LPL promoter. First, we monitored the recruitment of endogenous FOXA2 to the LPL promoter in vivo using the chromatin immunoprecipitation assay. This experiment was performed with immunoprecipitated chromatin-bound FOXA2 from fixed and sonicated HepG2 cell extracts. For the PCR assays we used primers that recognize either the proximal -141/-10 region of the human LPL promoter bearing the putative FOXA2 site or a non-related distal region in the 2nd intron of this gene (Figure 3.6A). As shown in Figure 3.6B, endogenous FOXA2 in HepG2 cells was found to be recruited to the proximal human LPL promoter but not to the unrelated region in the 2nd intron. Similar results were obtained in immunoprecipitated chromatin-bound FOXA2 from fixed and sonicated liver extracts isolated from C57BL/6 mice. As shown in Figure 3.6C, the FOXA2 antibody immunoprecipitated the proximal -143/+1 region of the mouse LPL promoter more efficiently than the distal region in the 9th intron of the mouse LPL gene (Figure 3.6 A).

Direct binding of FOXA2 to the proximal human LPL promoter was confirmed *in vitro* using the DNA affinity precipitation assay (DNAP). For this purpose, biotinylated PCR fragments corresponding to the LPL promoter regions -466/+39, -262/+39, -109/+39 and -28/+39 (Figure 3.7A) were amplified, coupled to streptavidin dynabeads and incubated with extracts from HEK293T cells that had been transfected with an expression vector for FOXA2. FOXA2 binding to the biotinylated oligonucleotides was visualized by immunoblotting using an anti-FOXA2 antibody. As shown in Figure 3.7B and C, FOXA2 bound very strongly to the -466/+39, -262/+39 and -109/+39 LPL promoter fragments but did not bind to the -28/+39 fragment lacking the putative FOXA2 site. In control experiments it was shown that FOXA2 did not bind to the streptavidin dynabeads (2nd lane, no oligo). To confirm that the site at -47/-40 is a true FOXA2 binding element, we substituted five nucleotides in this site thus creating a DNA sequence that differed significantly from the consensus FOXA2 recognition element 5'-T(G/A)TTT(A/G)(C/T)T-3' (277). The mutations that were introduced are shown in Figure 3.7A. As shown in Figure 3.7C, these mutations completely abolished the interaction of FOXA2 with the -109/+39 LPL promoter fragment (compare lanes 4 and 5).

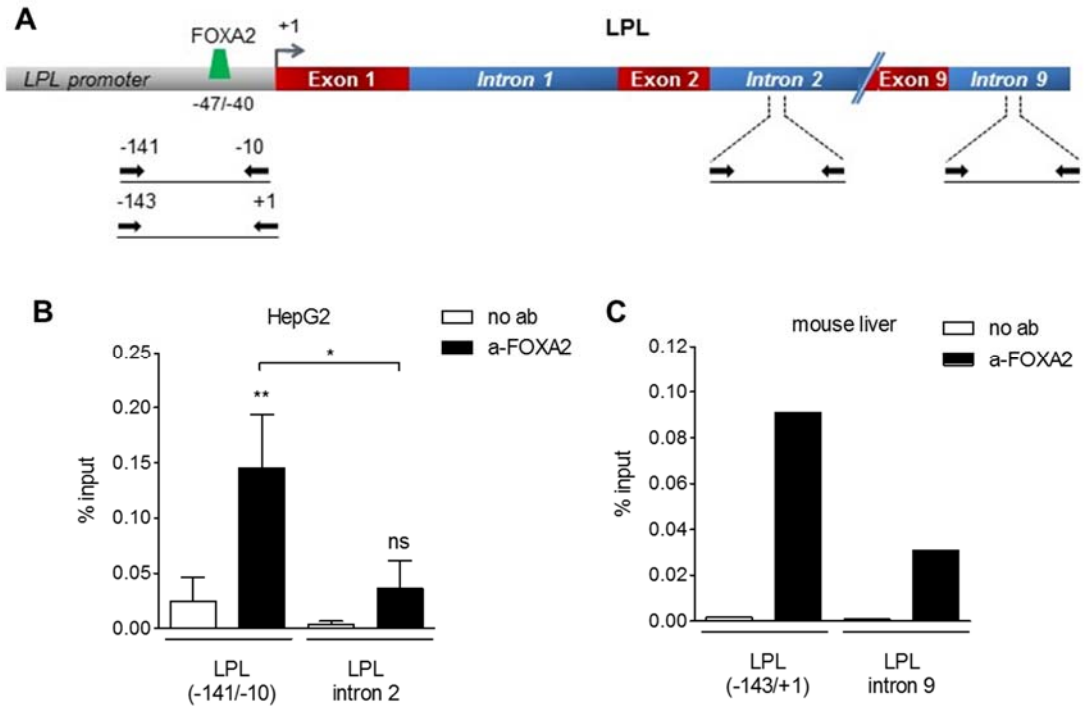

Figure 3.6. FOXA2 binds to the proximal human and mouse LPL promoter in vivo. (A) Schematic representation of the LPL gene, showing by arrows the location of the primer sets (distal regions: introns 2 or 9, proximal promoter regions: -141/-10 or -143/+1) that were utilized in the chromatin immunoprecipitation assays of panels B and C. (B) HepG2 cells were subjected to chromatin immunoprecipitation using an anti-FOXA2 antibody or no antibody as negative control (no ab). The precipitation of the LPL promoter was detected by reverse transcription quantitative PCR using primers that are complementary to the proximal (−141/-10) region of the human LPL promoter or to a distal region in the 2nd intron of the LPL gene. Results from reverse transcription quantitative PCR are expressed as binding relative to the input (%). Each value represents the average (±SD) from four independent experiments. (C) Chromatin immunoprecipitation in liver from C57BL/6 mice using an anti-FOXA2 antibody or no antibody as negative control (no ab). The immunoprecipitated chromatin was detected by quantitative PCR using primer sets corresponding to the proximal region of the mouse LPL promoter (−143/+1) or to a distal region in the 9th intron of the LPL gene. Results from reverse transcription quantitative PCR are expressed as binding relative to the input (%). *, $p<0.05$; **, $p < 0.01$; ns, not significant.

Similar results were obtained when the DNAP assays were performed using endogenous FOXA2 present in nuclear extracts from HepG2 cells (Figure 3.7D). FOXA2 bound to the -466/+39, -262/+39 and -109/+39 LPL promoter fragments more strongly than to the -28/+39 and -109/+39 mut LPL fragments.

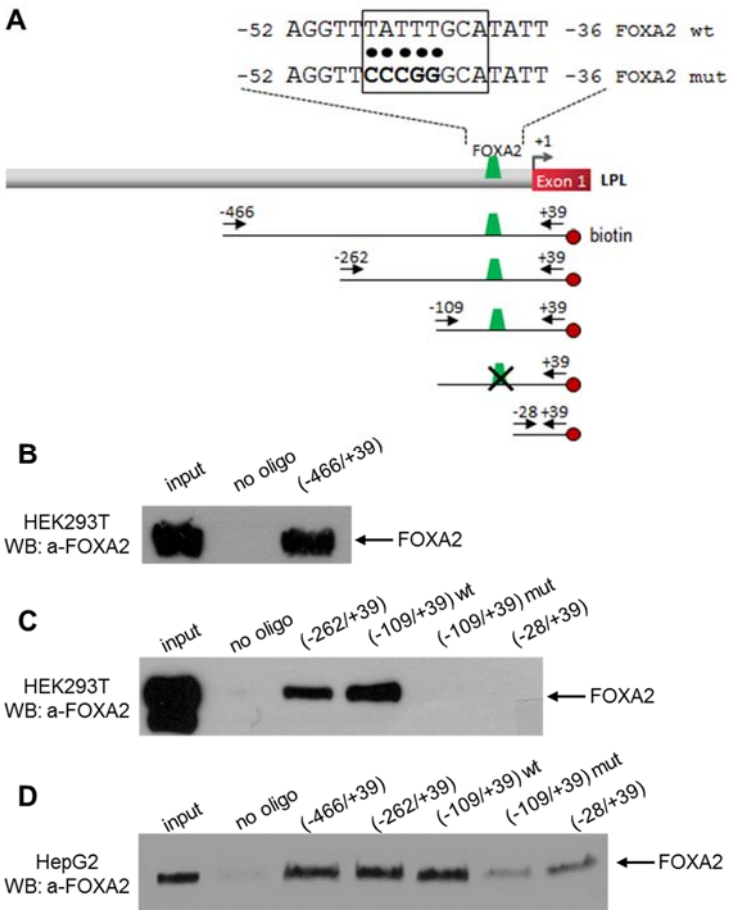

Figure 3.7. FOXA2 binds to the proximal region (-47/-40) of the human LPL promoter in vitro. (A) Schematic representation of the human LPL promoter showing the biotinylated promoter fragments used for the experiments of panels B-D and the primer sets (arrows) used for the amplification of the fragments. Five nucleotide substitutions in the FOXA2 site are indicated with the black dots and in bold. (B and C) DNA-affinity precipitation experiments using whole cell extracts from HEK293T cells expressing FOXA2 and the following biotinylated fragments of the human LPL promoter: -466/+39, -262/+39, -109/+39 (wild type or mutated) and -28/+39. DNA-bound FOXA2 was detected by Western blotting using a specific anti-FOXA2 antibody. (D) DNA-affinity precipitation using nuclear extracts from HepG2 cells and biotinylated PCR fragments corresponding to the -466/+39, -262/+39, -109/+39 (wild type or mutated) and -28/+39 region of the human LPL promoter. DNA-bound FOXA2 was detected by Western blotting using the a-FOXA2 antibody. The experiments in B-D were performed at least two times and representative images are presented.

To investigate the functional importance of the proximal FOXA2 element for the FOXA2-mediated transactivation of the LPL promoter, we introduced the same five mutations into the -883/+39 and -109/+39 LPL promoter constructs, creating the reporter plasmids (-883/+39) LPL-luc mut and (-109/+39) LPL-luc mut, respectively (Figure 3.8A). Mutagenesis of this FOXA2 site decreased the basal activity of the (-883/+39) and (-109/+39) LPL promoters by 60% relative to the wild type promoter

constructs in HepG2 cells (Figure 3.8B and D). Furthermore, the transactivation of the mutated LPL promoters by FOXA2 was compromised (Figure 3.8C and E).

Overall, the combined findings of Figures 3.5, 3.6, 3.7 and 3.8 established the presence a novel FOXA2 binding site in the proximal -47/-40 region of the human LPL promoter that binds FOXA2 with high efficiency and specificity and is critical for the basal and the FOXA2-inducible activity of the LPL promoter in hepatic cells.

The -39T/C mutation in the human LPL promoter reduces basal promoter activity but does not affect FOXA2 binding and transactivation.

In a previous study (188) it was shown that a natural mutation in the proximal human LPL promoter, a T to C substitution at nucleotide -39 (-39T/C), was identified in a patient with familial combined hyperlipidemia and low LPL activity. The -39T/C substitution which is localized within a binding site for the transcription factor Oct-1, was shown to be associated with a 85% reduction in LPL promoter activity in human macrophages but its effect on hepatic LPL expression was unknown (187, 188). The mutation is localized one nucleotide downstream of the novel FOXA2 binding site that was characterized in this study. We hypothesized that this close proximity to the FOXA2 site could affect the binding of FOXA2 and the FOXA2-mediated transactivation of the LPL promoter thus reducing the levels of expression of the LPL gene in hepatic cells.

To address this question, we initially performed DNAP assays using biotinylated fragments corresponding to either the wild type -109/+39 LPL promoter or the promoter bearing the T/C substitution at position -39 (Figure 3.9A). The -39T/C substitution did not affect the binding of FOXA2 expressed endogenously in HepG2 cells (Figure 3.9B, compare lanes 4 and 5 with lane 3) or exogenously in HEK293T cells (Figure 3.9C, compare lanes 4 and 5 with lane 3). To study further the effect of this mutation on LPL promoter activity, we generated this -39T/C substitution in the -883/+39 LPL promoter and we cloned it upstream of the luciferase gene (Figure 3.10A). We performed luciferase activity assays and as shown in Figure 3.10B, the -39T/C mutation reduced the basal activity of the -883/+39 LPL promoter by 60% but did not affect the FOXA2-mediated transactivation of the LPL promoter in HepG2 cells.

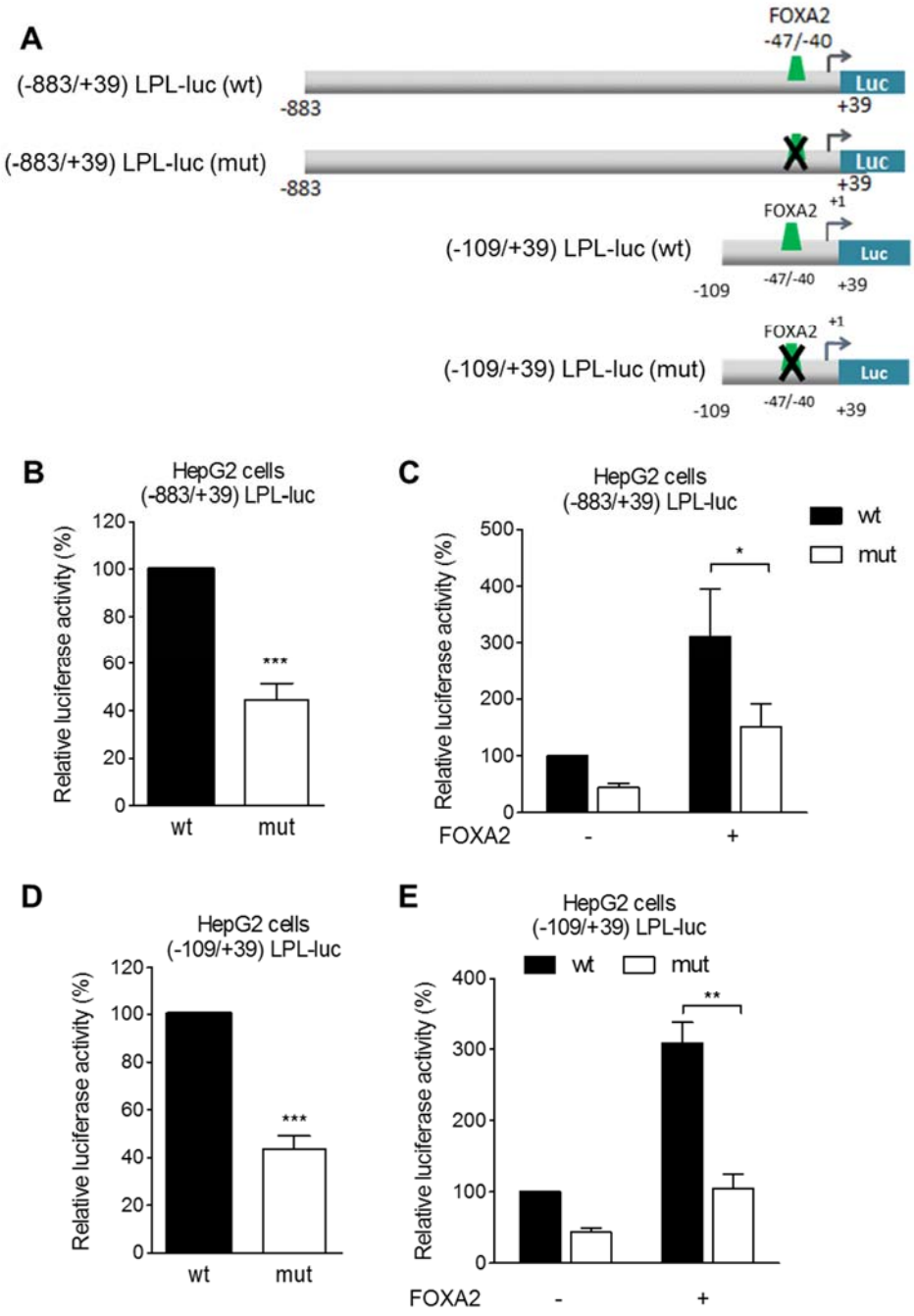

Figure 3.8. Mutations in the FOXA2 binding site reduce basal LPL promoter activity and FOXA2-mediated transactivation. (A) Schematic representation of the wild type LPL promoter constructs (-883/+39) and (-109/+39) LPL-luc and the corresponding constructs bearing the mutations in the FOXA2 site that are shown in Figure 3.7A. (B and D) HepG2 cells were transiently transfected with the (-883/+39) or (-109/+39) LPL-luc (wt) and (-883/+39) or (-109/+39) LPL-luc (mut) reporter plasmids (1μg) along with the β-galactosidase expression vector (1μg). (C and E) HepG2 cells were transiently transfected with the WT or mutated (-883/+39) and (-109/+39) LPL-luc reporter plasmids (1μg) in the presence or in the absence of the expression vector for FOXA2 (0.25μg) and the β-galactosidase expression vector (1μg). (B-E) The normalized, relative luciferase activity (±SD) calculated from at least three independent experiments performed in duplicate is presented with histographs.*, $p<0.05$; **, $p < 0.01$; ***, $p < 0.001$.

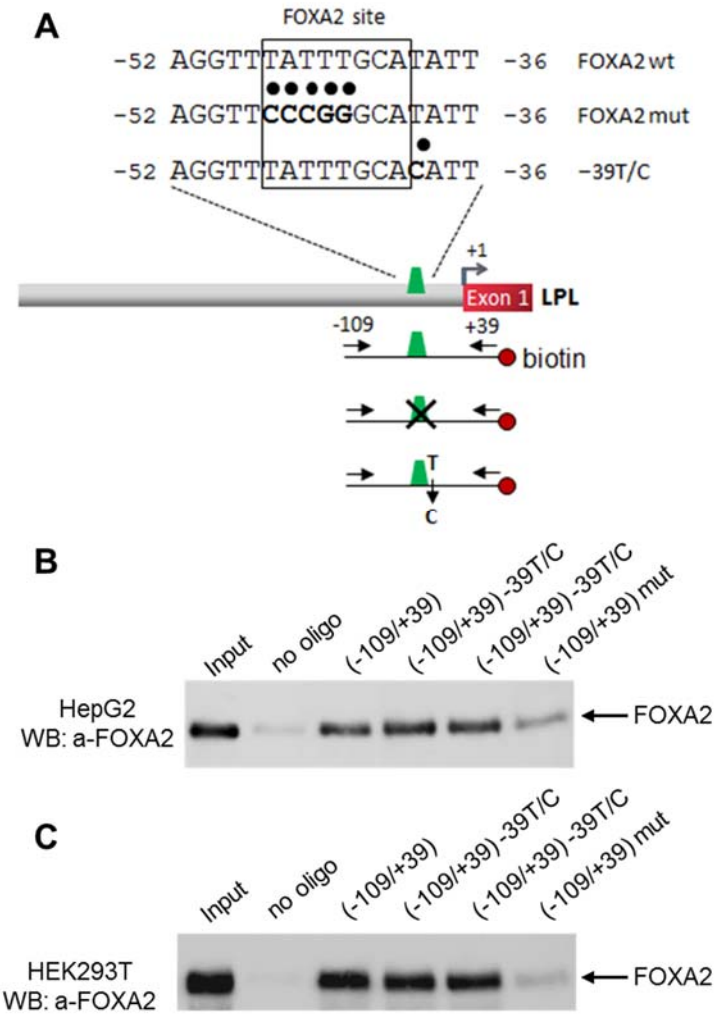

Figure 3.9. A single nucleotide substitution downstream of the FOXA2 site does not affect the binding of FOXA2 to the LPL promoter. (A) Schematic representation of the human LPL promoter showing the biotinylated promoter fragments used for the experiments of panels B and C and the primer sets (arrows) used for the amplification of the fragments. Nucleotide mutations in the sequence of LPL promoter are indicated with black dots and in bold. (B) DNA-affinity precipitation using HepG2 nuclear extracts and biotinylated PCR fragments corresponding to the -109/+39 region (wild type or mutated) of the human LPL promoter. FOXA2 binding to the probes was detected by Western blotting using the anti-FOXA2 antibody. (C) DNA-affinity precipitation using whole cell extracts from HEK293T cells expressing FOXA2 and biotinylated probes corresponding to the region -109/+39 (wild type or mutated) of the human LPL promoter. DNA-bound FOXA2 was detected by Western blotting using the anti-FOXA2 antibody. The experiments in B and C were performed two times and representative images are presented.

The combined data of Figures 3.9 and 3.10 indicate that the -39T/C mutation in the human LPL promoter reduces basal promoter activity but does not affect FOXA2 binding and transactivation, in hepatic cells.

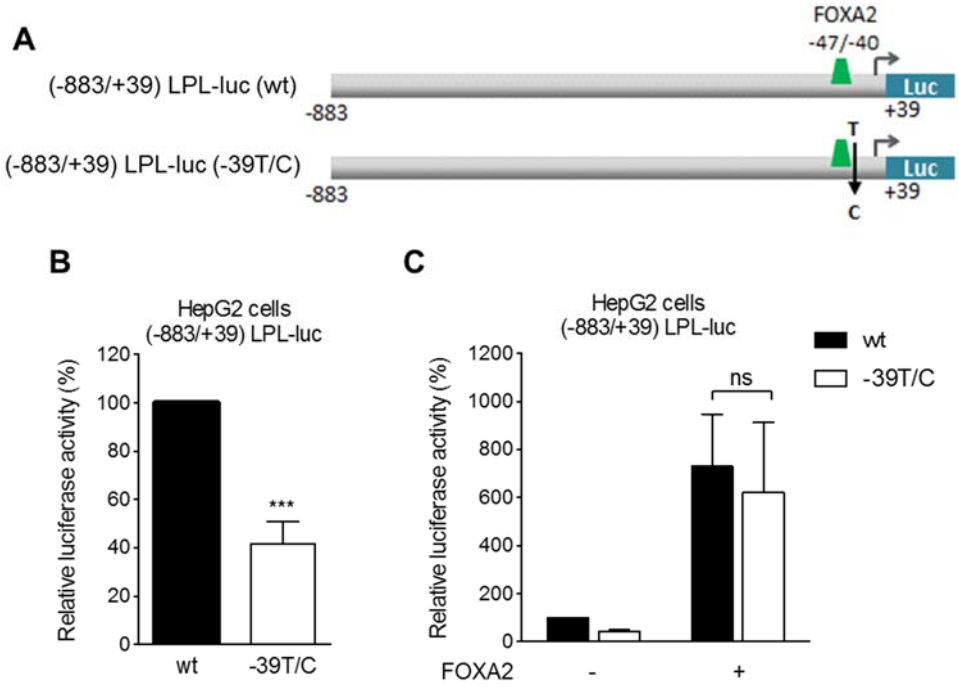

Figure 3.10. A single nucleotide substitution downstream of the FOXA2 site does not affect the FOXA2-mediated transactivation of the LPL promoter. (A) Schematic representation of the wild type -883/+39 LPL promoter construct and the corresponding construct bearing a single T/C substitution (at nucleotide -39) after the FOXA2 site that is shown in Figure 3.9A. (B) HepG2 cells were transiently transfected with the (-883/+39) LPL-luc (wt) or (-883/+39) LPL-luc (-39T/C) reporter plasmids (1μg) along with the β-galactosidase expression vector (1μg). (C) HepG2 cells were transiently transfected with the wt or mutated (-883/+39) LPL-luc reporter plasmids (1μg) in the presence or in the absence of the FOXA2 expression vector (0.25μg) and the β-galactosidase expression vector (1μg). (B and C) The normalized, relative luciferase activity (±SD) calculated from six independent experiments performed in duplicate is presented with histographs. ***, $p < 0.001$; ns, not significant.

Reduction in LPL expression and promoter activity by insulin in HepG2 cells due to an insulin-mediated nuclear export of FOXA2.

It has been shown previously that the activity of FOXA2 is regulated by insulin, via phosphorylation by AKT kinase which causes the export of FOXA2 from the nucleus leading to the inhibition of the expression of FOXA2 target genes (324). To confirm this mechanism in hepatic cells, we treated HepG2 cells with insulin and we measured the intracellular localization of FOXA2. As shown in Figure 3.11A and B, insulin induced the phosphorylation of AKT kinase (4-fold increase). This induction was associated with a 70% decrease in the nuclear localization and a 3,5-fold increase in the cytoplasmic localization of endogenous FOXA2 in HepG2 cells (Figure 3.11A, C and D).

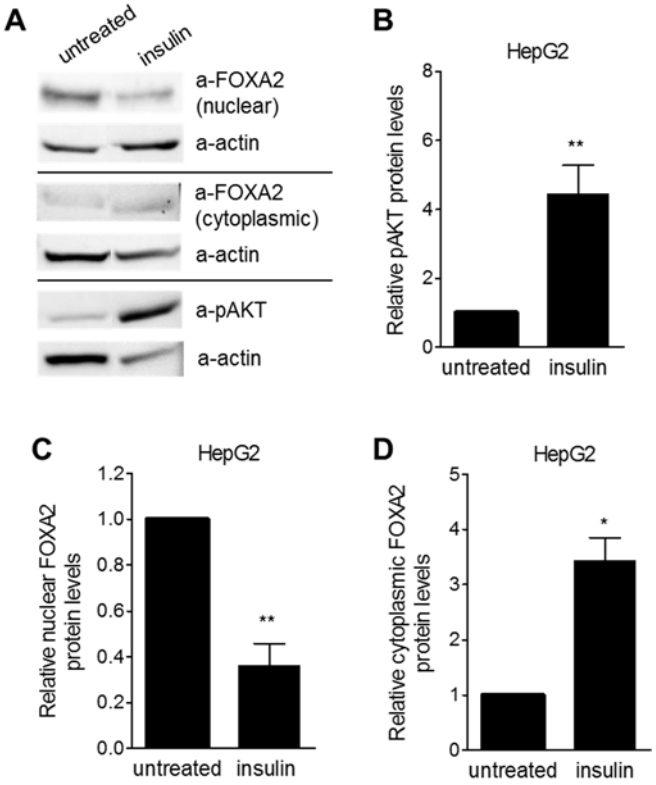

Figure 3.11. Nuclear exclusion of FOXA2 by insulin. (A) HepG2 cells were treated with insulin (500nM) for 24 hours or left untreated. Nuclear and cytoplasmic protein extracts were isolated and subcellular localization of FOXA2 was determined by immunoblotting using the anti-FOXA2 antibody. The protein levels of actin (loading control) and pAKT (positive control) were determined by immunoblotting using the corresponding antibodies. The experiment was performed at least three times and representative images are presented. (B-D) Levels of pAKT (panel B), nuclear FOXA2 (panel C), cytoplasmic FOXA2 (panel D) and actin were quantified by densitometry and the normalized relative protein levels are shown as histographs. Results are expressed as mean (±SD) from at least three independent experiments. *, $p<0.05$; **, $p<0.01$.

Next, we examined whether this insulin-mediated mechanism of FOXA2 nuclear exclusion applies to the hepatic regulation of the LPL gene. To this end, we treated HepG2 cells with insulin and we determined the effect of insulin on the expression of LPL gene. As shown in Figure 3.12A and D, cytoplasmic sequestration of FOXA2 by insulin was associated with a 50% reduction in the mRNA levels of LPL and a 25% inhibition in the activity of the -883/+39 LPL promoter, in HepG2 cells. The mRNA levels of the FOXA2 gene were not affected by the insulin treatment (Figure 3.12B). Furthermore, insulin abolished the expression of the endogenous LPL gene in HepG2 cells at the protein level (Figure 3.12C).

The data of Figures 3.11 and 3.12 suggest that the phosphorylation of FOXA2 by the insulin/PI3K/AKT pathway and its nuclear export inhibits the expression of the LPL gene in HepG2 cells.

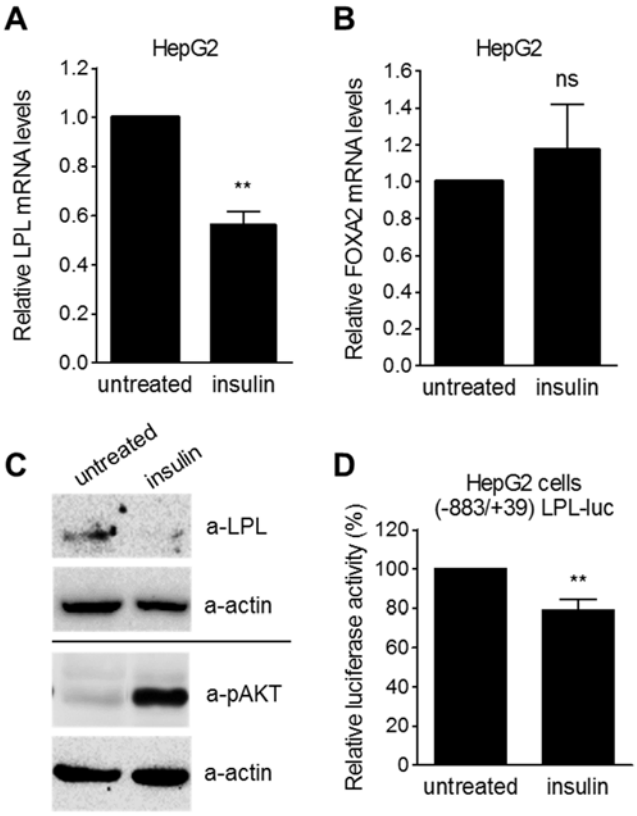

Figure 3.12. Nuclear exclusion of FOXA2 by insulin results in the downregulation of LPL gene expression. (A and B) HepG2 cells were treated with insulin (500nM) for 24 hours or left untreated and total RNA was extracted. LPL (panel A) and FOXA2 (panel B) mRNA levels were determined by quantitative reverse transcription quantitative PCR , normalized relative to the mRNA levels of the GUSB gene and are shown as histographs. Results are expressed as mean (±SD) from three independent experiments. (C) HepG2 cells were treated with insulin (500nM) for 24 hours or left untreated. Protein extracts were isolated and and the intracellular protein levels of LPL, pAKT and actin (loading control) were determined by immunoblotting using the corresponding antibodies. (D) HepG2 cells were transiently transfected with the (-883/+39) LPL-luc reporter plasmid (1μg). Following transfection, the cells were treated with 500nM insulin for 24 hours or left untreated. Normalized relative luciferase activity values are shown. Each value represents the average (±SD) from two independent experiments performed in duplicate. **, $p<0.01$; ns, not significant.

The expression of LPL gene in adipocytes is not regulated by FOXA2.

The regulation of the human LPL gene by FOXA2 could be a general regulatory mechanism that may operate in other tissues that express highly the LPL gene such as the adipocytes. To address this hypothesis, we transfected 3T3-L1 pre-adipocytes with different LPL promoter fragments (-883/+39, -262/+39, -109/+39 and -28/+39), fused with the luciferase report gene (Figure 3.1A) and their activity was determined by luciferase assays. We found that deletions of the LPL promoter from position -883 to -109 did not affect the promoter activity but further deletion to position -28 abolished the activity of the LPL promoter in a similar fashion as in HepG2 cells (Figure 3.13B).

To examine the role of FOXA2 in the LPL promoter activity, we transfected 3T3-L1 pre-adipocytes with increasing concentrations of the plasmid vector expressing FOXA2 and we did not observe any transactivation of the -883/+39 LPL promoter (Figure 3.13A). We also transfected 3T3-L1 cells with wild type or mutated -883/+39, -109/+39 LPL promoter constructs, bearing the mutations in FOXA2 element (Figure 3.13C and D). In agreement with the findings in HepG2 cells, the mutations into the FOXA2 site reduced the basal activity of the -883/+39 and -109/+39 LPL promoters by 50%, indicating the importance of this element for the regulation of LPL in 3T3-L1 cells (Figure 3.13 C and D).

Next, we differentiated 3T3-L1 pre-adipocytes for 9 days following the protocol shown in Figure 3.14A (upper panel) to mature adipocytes containing numerous intracellular lipid droplets (Figure 3.14A lower panel). We determined the expression of FOXA2 in pre- and adipocytes at the mRNA and protein levels. As shown in Figure 3.14C and D, FOXA2 is expressed at low levels in pre-adipocytes. In contrast, FOXA2 is highly expressed in mouse liver and large intestine (Figure 3.14B). However, differentiation of 3T3-L1 pre-adipocytes to adipocytes was associated with a severe reduction in FOXA2 mRNA levels (Figure 3.14C) and nuclear protein levels (Figure 3.14D). Moreover, we determined the mRNA levels of LPL gene (positive control of adipocytes) and we observed a strong induction of LPL gene during adipocyte differentiation (Figure 3.14C).

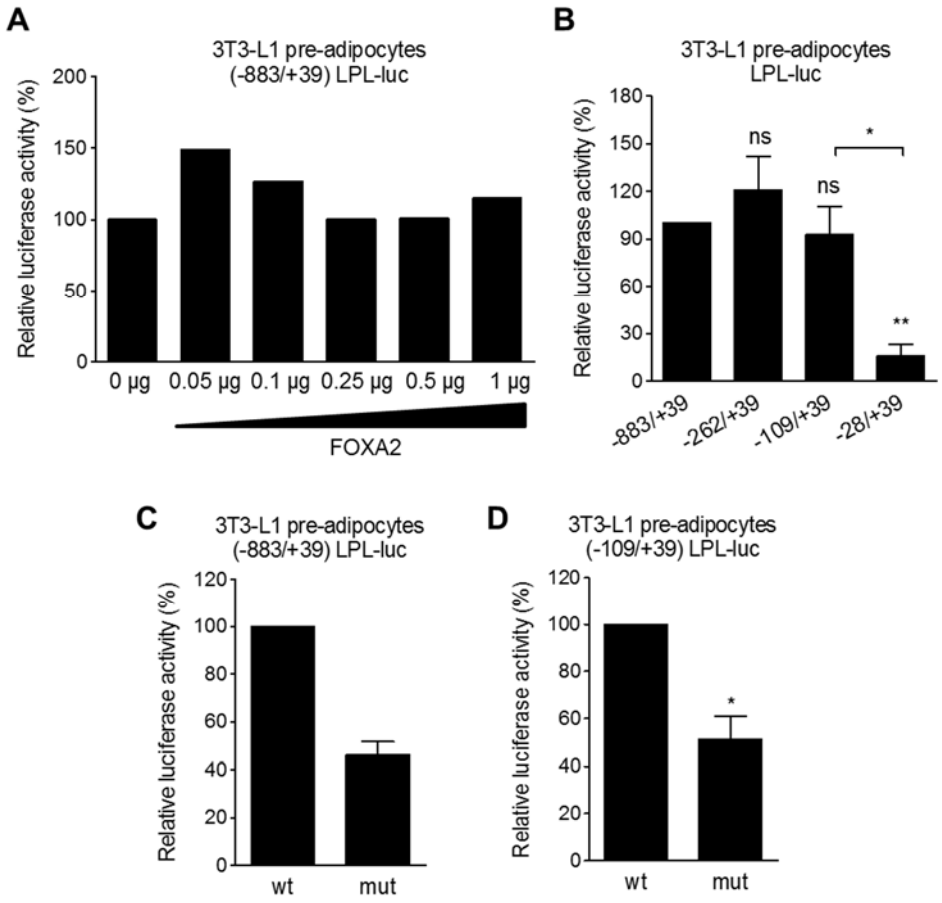

Figure 3.13. The LPL promoter activity is not regulated by FOXA2 in 3T3-L1 pre-adipocytes. (A) 3T3-L1 pre-adipocytes (85.000 cells/6-well) were transiently transfected with the (−883/+39) LPL-luc reporter plasmid (1μg) along with increasing concentrations (0.05–1μg) of a FOXA2 expression vector and a β-galactosidase expression plasmid (1μg). The normalized relative luciferase activity is presented with a histograph. (B) 3T3-L1 cells (85.000 cells/6-well) were transiently transfected with the 5'-deletion fragments of the (-883/+39) LPL promoter (1μg) shown in Figure 1A along with the β-galactosidase expression plasmid (1μg). (C and D) 3T3-L1 cells (85.000 cells/6-well) were transiently transfected with the (-883/+39) or (-109/+39) LPL-luc (wt) reporter plasmids and the corresponding constructs (1μg), bearing five mutations in the FOXA2 site that are shown in Figure 3.7A (mut), along with the β-galactosidase expression vector (1μg). (A-D) Luciferase activity was normalized to β-galactosidase activity and presented with histographs. Each value represents the average (±SD) from three independent experiments (panels B and D) or two independent experiments (panel C). *, $p<0.05$; **, $p<0.01$; ns, not significant.

The combined data of Figures 3.13 and 3.14 indicate that the LPL gene expression is not regulated by FOXA2 in adipocytes. However, the FOXA2 element at -47/-40 of LPL promoter may facilitate the involvement of other adipocyte transcription factors that regulate the LPL gene.

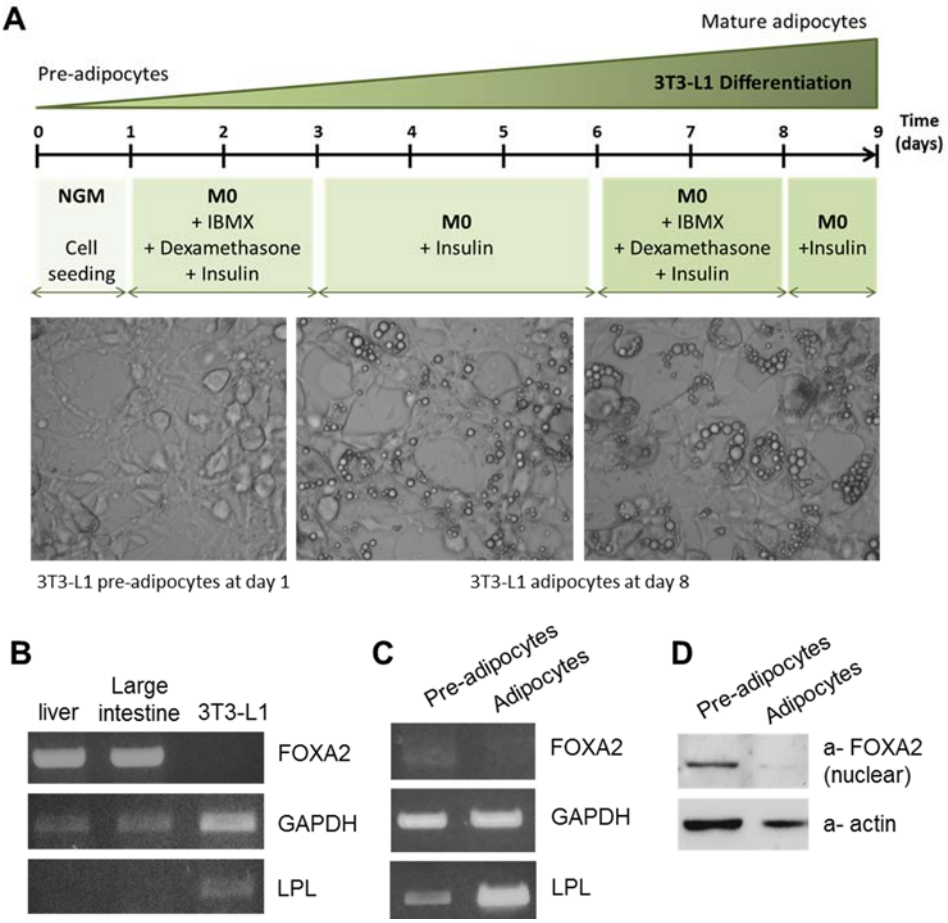

Figure 3.14. The LPL gene expression is not regulated by FOXA2 in 3T3-L1 cells. (A) Upper panel shows the experimental protocol for the differentiation of 3T3-L1 pre-adipocytes to adipocytes. Lower panel shows representative microscopic images of undifferentiated 3T3-L1 pre-adipocytes (at day 1) and 3T3-L1 cells subjected to adipocyte differentiation for 8 days using the protocol presented in the upper panel. (B and C) Total RNA was extracted from mouse liver and large intestine or from 3T3-L1 pre-adipocytes and differentiated adipocytes. The expression of the mouse LPL and FOXA2 genes was analyzed by reverse transcription PCR. The expression levels of GAPDH gene were used for normalization purposes. (D) Nuclear lysates were isolated from 3T3-L1 pre-adipocytes and differentiated adipocytes and protein levels of FOXA2 and actin (loading control) were determined by immunoblotting using the corresponding antibodies.

Lipoprotein Lipase (LPL) is a member of the triglyceride lipase gene family that plays a critical role in lipid metabolism by catalyzing the hydrolysis of triglycerides (TG) in plasma TG-rich lipoproteins such as VLDL and chylomicrons (124). LPL is primarily synthesized by the parenchymal cells in adipose tissue, skeletal muscle and heart but can be found at lower levels in many other tissues, including macrophages, kidney, brain, adrenals, lung and embryonic liver (104-106, 451, 452). In adult mice LPL gene expression in the liver is low compared with other tissues (453) but the physiological role of liver LPL still remains controversial. Previous studies in mouse models of liver LPL overexpression or deficiency have addressed the physiological role of LPL in the liver and revealed important new roles of the enzyme in glucose and lipid metabolism. Merkel et al created a transgenic mouse model that expresses LPL exclusively in the liver (172). These mice had elevated triglycerides, increased plasma ketones and glucose and large amounts of intracellular lipid droplets in their livers. Expression of LPL in the adult liver was associated with slower turnover of VLDL than wild-type mice and increased production of VLDL TG (172). In another study, Kim et al. showed that liver-specific overexpression of LPL in mice leads to an increase in liver TG content and glucose and develop insulin resistance associated with defects in the activation of insulin receptor substrate-2 (IRS2) associated phosphatidylinositol 3-kinase (PI3K) activity by insulin (171). Recently Liu et al. generated a mouse with the LPL gene specifically ablated in hepatocytes (453). The unexpected finding of this study was that deletion of hepatic LPL resulted in a significant decrease in plasma LPL content and activity and as a result, the postprandial TG clearance was markedly impaired and plasma TG and cholesterol levels were significantly elevated. These findings suggested that despite the relatively low levels of expression in the adult liver, hepatic LPL has a physiologically significant role in plasma lipid homeostasis and lipoprotein metabolism that needs to be explored further under pathological or non-pathological conditions.

In the present study we show for the first time that the human lipoprotein lipase gene is a direct target of the forkhead box family transcription factor FOXA2 in hepatic cells. FOXA2 is a positive modulator of the LPL gene. The activation of the LPL gene by FOXA2 is mediated via a novel FOXA2 responsive element that is

localized in the proximal LPL promoter. Mutations in this FOXA2 element abolished binding of FOXA2 and the FOXA2-mediated transactivation of the LPL promoter in hepatic cells whereas silencing of FOXA2 was associated with a reduction in the mRNA and protein levels of LPL. Importantly, we show that insulin inhibits the expression of LPL in HepG2 cells via a mechanism that involves the activation of AKT kinase and the subsequent inactivation of FOXA2 via phosphorylation which causes the translocation of FOXA2 from the nucleus to the cytoplasm (Figure 3.15).

FOXA2 (also called Hepatocyte Nuclear Factor 3β) is a member of the hepatocyte nuclear factor 3/forkhead box family of transcription factors known mainly for its gluconeogenic effects in hepatic cells. FOXA2 is expressed primarily in the liver and also in pancreas, stomach, intestine and lung (295). In the liver, FOXA2 has been shown to stimulate the oxidation of fatty acids, to increase the production of ketone bodies and to increase the secretion of lipoproteins (VLDL, HDL) during fasting by activating the expression of genes involved in these pathways (312, 324). Using adenovirus-mediated gene transfer combined with gene expression profiling it was shown that a constitutively active form of FOXA2 (that cannot be inhibited by AKT) increased the expression of genes involved in HDL metabolism, β-oxidation, ketogenesis, glycolysis and triglyceride degradation including the genes for the lipases LPL and LIPC (324). In another study, it was found that there are approximately 11,000 FOXA2 binding sites in the adult mouse liver and that almost half of the genes expressed in the adult liver including the LPL gene contain at least one FOXA2 binding site (331). Although FOXA2 is a nuclear factor that activates gene transcription when bound to DNA due to the presence of two transactivation domains (295), FOXA2 may also inhibit gene expression. In a previous study we showed that FOXA2 binds to three sites on the proximal promoter of the human ABCA1 gene, one of which is the TATA box and compromises the upregulation of ABCA1 gene expression by oxysterol-activated LXRs under conditions of cholesterol loading (329). In the liver, excess cholesterol is converted to bile acids for excretion through the bile (454-456). Importantly, inactivation of FOXA2 in the liver of mice inhibited the expression of bile acid transporters resulting in intrahepatic cholestasis (323). Furthermore, it was also shown that patients with cholestatic syndromes have lower FOXA2 levels in their livers (323). Thus, FOXA2 emerges as a key regulator of lipid and lipoprotein metabolism in the liver.

The regulation of the human LPL gene by FOXA2 could be a general regulatory mechanism that may operate in tissues other than the liver that express the LPL gene such as the adipocytes. To address this hypothesis, we used 3T3-L1 pre-adipocytes and differentiated mature adipocytes. We found that the region -109/-28 of the LPL promoter is important for the basal activity of LPL in 3T3-L1 pre-adipocytes, but we did not observe any transactivation of the LPL promoter by the FOXA2, in contrast to the data from HepG2 cells. However, the mutations in the FOXA2 element reduced the basal activity of the LPL promoter in pre-adipocytes, in agreement with the findings in HepG2 cells, indicating the importance of this element for the regulation of LPL gene. We showed that FOXA2 is not expressed in adipocytes and this may explain the inability of this factor to participate in LPL regulation in adipose tissue. However, the FOXA2 element at -47/-40 of LPL promoter may facilitate the involvement of other adipocyte transcription factors that regulate the LPL gene.

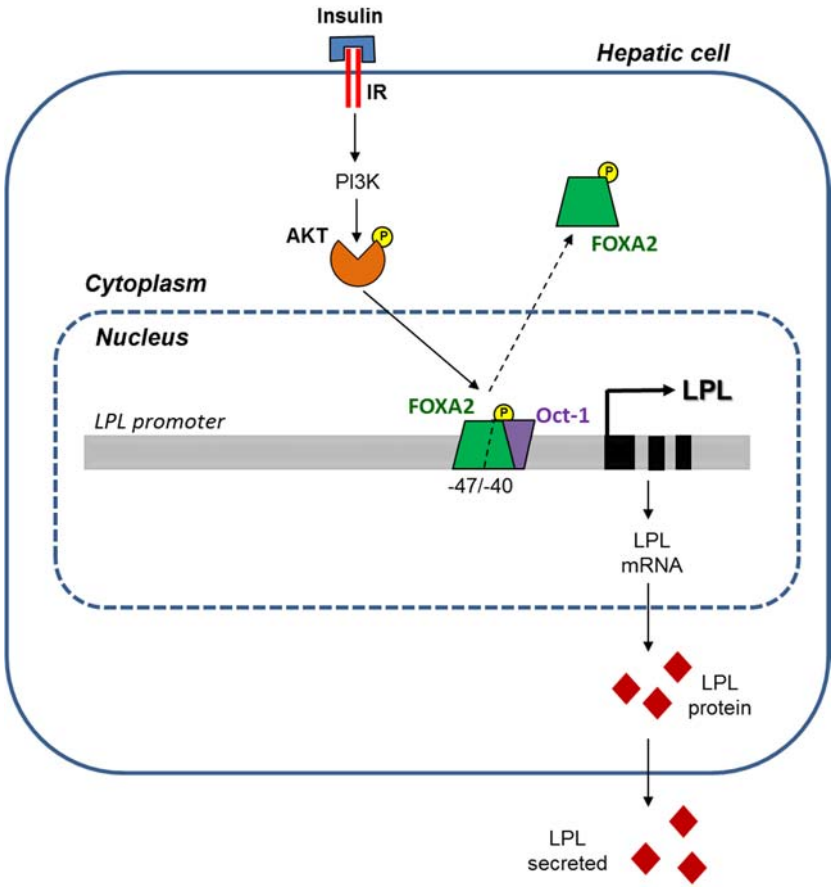

Figure 3.15. Summary of forkhead box transcription factor FOXA2 regulatory element in the LPL promoter and the insulin signaling pathway that participate in the control of human LPL gene expression in hepatic cells. See text for details.

Mutations in the LPL promoter in humans are associated with reduced LPL expression levels and promoter activity (457). In one of these cases, a compound heterozygote [-39T/C; -39T/G] was identified with familial combined hyperlipidemia and reduced post-heparin LPL levels. The -39T/C substitution was shown to be associated with a 85% reduction in LPL promoter activity in human macrophages but its effect on hepatic LPL expression was unknown (188). This substitution is localized within a binding site for the transcription factor Oct-1 and it was shown that Oct-1 binds to the -45/-38 LPL promoter in vitro (187). Oct-1 is a member of the POU domain of transcription factors that bind to a DNA sequence motif known as the octamer motif having the consensus sequence 5' "ATGC(A/T)AAT" 3' (458). Oct-1 is ubiquitously expressed and serves as a sensor for both metabolic and stress signals (458-460). In liver cells, Oct-1 binds to the promoter of the carbohydrate response element binding protein (ChREBP) gene and inhibits its expression (461). Interestingly, insulin increases the activity of the ChREBP promoter in hepatic cells and stimulates ChREBP expression via the octamer motif (461, 462) suggesting that insulin signaling regulates the activity of Oct-1 by an unknown mechanism. The precise role of Oct-1 in LPL gene regulation has not been elucidated but the decrease in the LPL promoter activity caused by the -39T/C substitution which destroys the octamer motif suggests that this factor plays a positive role in LPL gene transcription. The close proximity of the -39T/C substitution to the FOXA2 binding site identified in the present study (-47/-40) prompted us to functionally characterize this substitution in the context of the hepatic LPL regulation. Our data showed that the -39T/C substitution reduced LPL promoter activity by 60% in HepG2 cells but had no effect on the binding of FOXA2 to the LPL promoter *in vitro* as well as on the FOXA2-mediated transactivation of the LPL promoter in HepG2 cells. Importantly, both FOXA2 and Oct-1 factors are inhibited by insulin in hepatic cells (Figure 3.12 and ref (462)). The combined data propose that the -47/-38 region of the human LPL promoter is a novel dual insulin-responsive element that can bind either Oct-1 or FOXA2 in an overlapping manner and could facilitate the inhibition of the human LPL gene expression by insulin and possibly by other factors that regulate the activity of the two nuclear proteins in LPL-expressing cells or in hepatic cells (Figure 3.15).

We had shown previously that FOXA2, in addition to its established role in glucose production, regulates the biogenesis and the remodelling of High Density Lipoproteins (HDL) by inhibiting the expression of ABCA1 gene in the livers (329).

With this study we reveal a new role of this transcription factor in the liver that is not restricted to HDL biogenesis or gluconeogenesis but through an insulin-AKT-FOXA2-LPL signaling cascade may control the catabolism of triglyceride-rich lipoproteins such as VLDL and chylomicrons.

Interestingly, the expression of the LPL gene in the adult mouse liver is also induced strongly by oxysterols, either synthetic or endogenous following a cholesterol-rich diet (181). It was shown previously that LXRs induce LPL gene expression in the liver by acting on a distal LXRE present in the first intron of the LPL gene (181). We hypothesize that inhibition of FOXA2 by insulin, in addition to its role in basal hepatic LPL gene expression, could also control the levels of LPL gene induction in response to intracellular or extracellular signals such as cholesterol overload. This signalling pathway may prevent the accumulation of LPL in the liver under certain conditions, maintaining liver LPL expression at low levels and thus protecting this tissue from the toxic effects of LPL overexpression as demonstrated recently in mouse studies (171). This hypothesis will be discussed in detail in the second part.

In summary, the present study identified FOXA2 as a critical regulator of LPL gene expression in hepatocytes under basal conditions or in response to extracellular signals such as insulin treatment. Understanding the mechanisms by which FOXA2 regulates the expression of the LPL gene in the liver may open the way to novel therapeutic strategies for the correction of plasma lipoprotein levels in humans with lipid disorders.

<u>PART II</u>:

Physical and functional interactions between nuclear receptors LXRα/RXRα and the forkhead box transcription factor FOXA2 regulate the response of the human lipoprotein lipase gene to oxysterols in hepatic cells

Regulation of the human lipoprotein lipase gene expression in hepatic cells by the LXR agonist T0901317.

Liver X receptors are activated by several hydroxylated products of cholesterol metabolism (oxysterols) or, more potently, by artificial compounds such as T0901317 (354, 384, 385). In order to investigate the role of LXRs in the regulation of the LPL gene in hepatocytes, we treated primary mouse hepatocytes, isolated from the livers of C57BL/6J mice, or human hepatoblastoma HepG2 cells, with T0901317 (1μM) for 24 hours and the mRNA and protein levels of LPL were determined. As shown in Figure 3.16A and B, T0901317 treatment caused a 5.5-fold increase in the mRNA levels of the mouse LPL (primary hepatocytes, panel A) or a 1.4-fold increase in the mRNA levels of the human LPL (HepG2, panel B). HepG2 cells were treated also with T0901317 and 9-cis retinoic acid, which is the natural ligand of nuclear receptor RXRα, for 24 hours. We observed that the mRNA levels of LPL were increased more when 9cisRA was added in cells (Figure 3.16 C). Similar LPL upregulation was observed when HepG2 cells were treated with 22(OH)Cholesterol, the natural ligand of nuclear receptor LXRα, and 9cisRA (Figure 3.16D). In agreement with these findings, T0901317 treatment of HepG2 cells caused a 4-fold increase in the intracellular levels and a 2-fold increase in the secreted levels of the human LPL protein (Figure 3.16E-G).

LXRα/RXRα heterodimers transactivate the human LPL promoter.

In order to investigate the LXR isoform (LXRα or LXRβ) that activates the human LPL gene, HepG2 cells were transfected with the reporter plasmid -883/+39 LPL-Luc that is bearing the human LPL promoter -883/+39 upstream of the luciferase gene in the presence or absence of exogenous LXRα/RXRα or LXRβ/RXRα and were treated with 22(OH)C and 9cisRA for 24 hours or left untreated. As shown in Figure 3.17A, overexpression of LXRα and RXRα, but not LXRβ and RXRα, transactivated the human LPL promoter and this transactivation was enhanced further by adding the ligands of the two receptors.

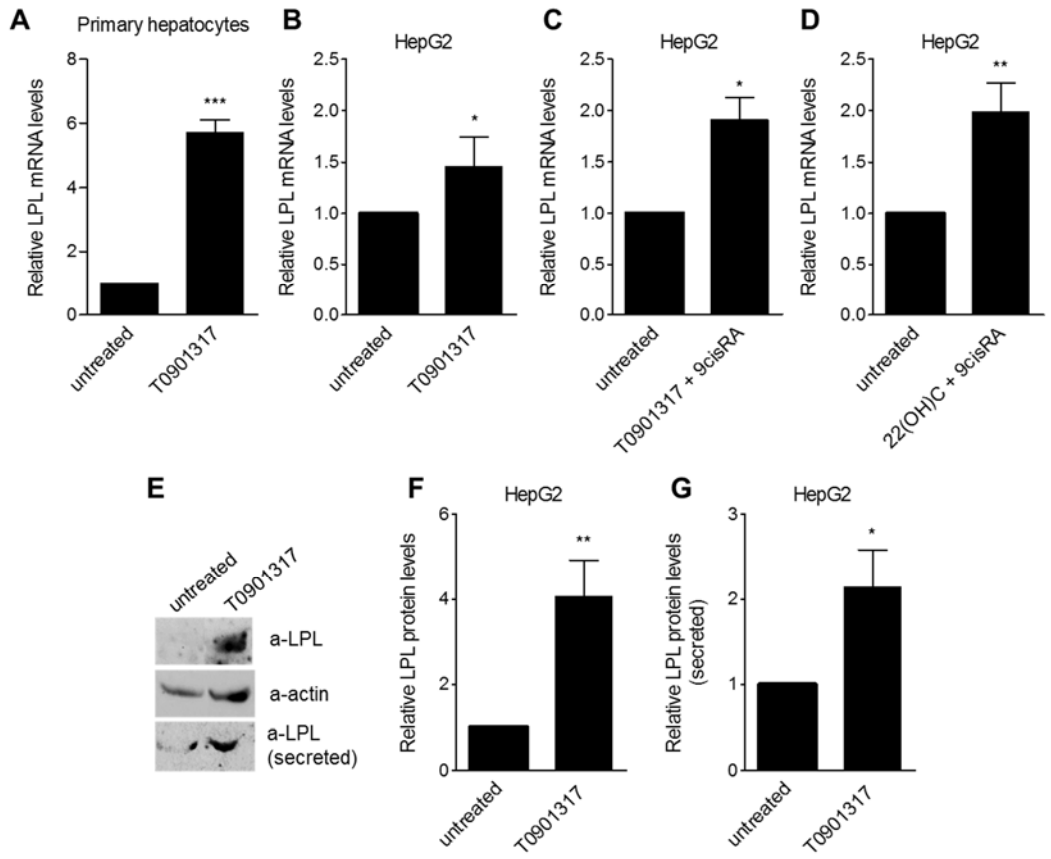

Figure 3.16. The synthetic LXR agonist T0901317 and the LXR/RXR agonists, 22(OH)C and 9cisRA, upregulate the expression of LPL gene in hepatocytes. Primary mouse hepatocytes (panel A) and HepG2 cells (panel B) were treated with the LXR ligand, T0901317 (1μM), for 24 hours or left untreated and total RNA was extracted. (A) LPL mRNA levels were normalized relative to the mRNA levels of the HPRT gene and are shown as a histograph. Results are expressed as mean (±SEM) from seven independent experiments. (B) LPL mRNA levels were determined by reverse transcription quantitative PCR, normalized relative to the mRNA levels of the GUSB gene. Results are expressed as mean (±SD) from six independent experiments and shown as a histograph. (C) HepG2 cells were treated with T0901317 and the RXR agonist 9cisRA (1μM each), for 24 hours or left untreated and total RNA was extracted. LPL mRNA levels were determined by reverse transcription quantitative PCR, normalized relative to the mRNA levels of the GUSB gene. Results are expressed as mean (±SD) from three independent experiments and shown as a histograph. (D) HepG2 cells were treated with the LXR and RXR ligands, 22(OH)C and 9cisRA (1μM each), for 24 hours or left untreated. Total RNA was extracted, LPL mRNA levels were determined by reverse transcription quantitative PCR and normalized relative to the mRNA levels of the GUSB gene. Results are expressed as mean (±SD) from four independent experiments and shown as a histograph. (E) HepG2 cells were treated with the LXR ligand, T0901317 (1μM), for 24hours or left untreated and the intracellular protein levels of LPL and actin (loading control) as well as of the secreted LPL were determined by immunoblotting using the corresponding antibodies. The experiment was performed at least three times and representative images are presented. (F and G) Levels of intracellular LPL and actin were quantified by densitometry and the normalized relative protein levels (F) or the secreted LPL protein levels (G) are shown as histographs. Results are expressed as mean (±SD) from at least three independent experiments. *, $p<0.05$; **, $p<0.01$; ***, $p< 0.001$.

In line with this finding, silencing the expression of endogenous LXRα in HepG2 cells via a LXRα-specific shRNA producing vector (Figure 3.17B) reduced the activity of the LPL promoter by 30% (Figure 3.17C) suggesting that LXRα is a transcriptional activator of the human LPL promoter in hepatic cells.

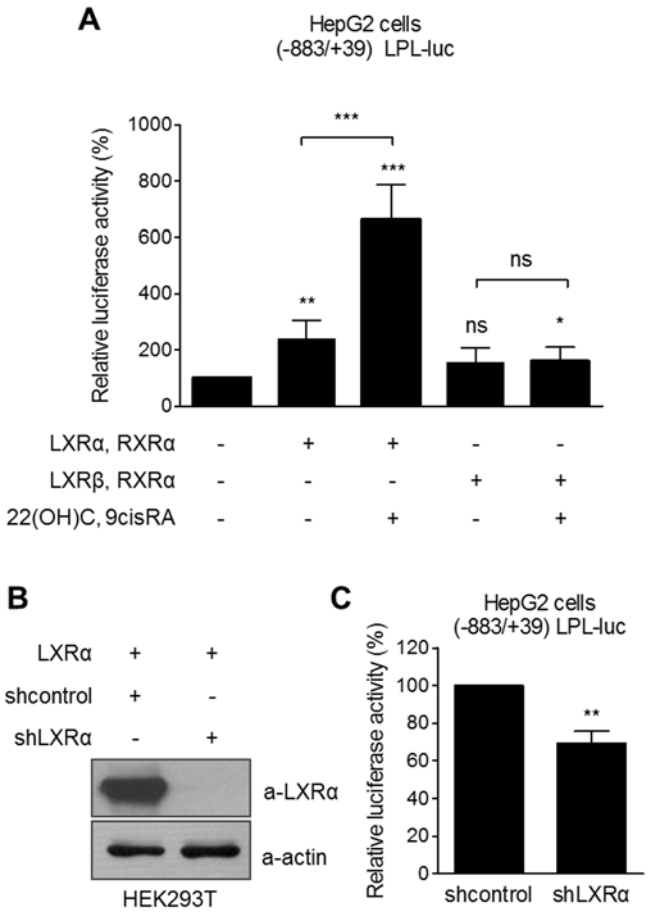

Figure 3.17. LPL promoter activity is regulated by nuclear receptors LXRα/RXRα and their agonists. (A) HepG2 cells were transiently transfected with the (−883/+39) LPL-luc reporter plasmid (1μg) along with plasmids expressing LXRα or LXRβ and RXRα (0.5μg each) and β-galactosidase (1μg). Cells were treated with 22(OH)C and 9cisRA (1μM) for 24 hours or left untreated. The normalized, relative luciferase activity (±SD) calculated form three independent experiments performed in duplicate is presented with histographs. (B) HEK293T cells were transfected with an LXRα expression vector (1μg) along with expression vectors for control shRNA or LXRα shRNA (1μg) and the protein levels of LXRα and actin (loading control) were determined by immunoblotting using the corresponding antibodies. (C) HepG2 cells were transiently transfected with the (−883/+39) LPL-luc reporter plasmid (1μg) along with expression vectors for control shRNA or LXRα shRNA (1μg) and β-galactosidase (1μg). The normalized, relative luciferase activity (±SD) calculated form two independent experiments performed in duplicate is presented with histographs. *, $p<0.05$; **, $p<0.01$; ***, $p< 0.001$; ns, not significant.

A series of 5' deletions of the human -883/+39 LPL promoter (Figure 3.18A) were employed in order to map the region(s) of the promoter that is mediating the transactivation by the LXRα/RXRα heterodimers. As shown in Figure 3.18B, a gradual increase in the basal promoter activity as well as in the LXRα/RXRα-mediated transactivation was observed as the LPL promoter was serially deleted down to nucleotide -262. Further deletion to position -109 did not have a significant effect on this activity. However, deletion to position -109 severely reduced the basal activity of the human LPL promoter but more importantly, the activity of this short proximal LPL promoter fragment remained at very low levels in the presence of overexpressed LXRα/RXRα and their ligands (Figure 3.18B). The findings of Figure 3.18 indicated that the -109/-28 proximal region of the human LPL promoter is critical for its transactivation by ligand-activated LXRα/RXRα heterodimers in HepG2 cells.

Nuclear receptors LXRα and RXRα bind weakly to the proximal region of the LPL promoter in vivo and in vitro.

A chromatin immunoprecipitation experiment in vivo was performed in order to monitor the recruitment of LXRα and RXRα to the human LPL promoter in HEK293T cells that express exogenous LXRα/RXRα in the presence of their ligands, 22(OH)C and 9cisRA. However, we did not observe any binding of LXRα or RXRα to the -141/-10 region of LPL promoter (Figure 3.19B). We performed also a series of chromatin immunoprecipitation assays in HepG2 cells, monitoring the binding of endogenous LXRα/RXRα receptors to the LPL promoter. As shown in Figure 3.19C, LXRα bound specifically to the -141/-10 but not to the intron 1 of the human LPL gene that was used as a negative control. Of note, this binding was significantly weaker compared to the binding to LXRα to the human ABCA1 promoter region -139/-41 that was used as a positive control. Similar results were obtained when the chromatin immunoprecipitation experiment was performed using an antibody specific for RXRα (Figure 3.19D).

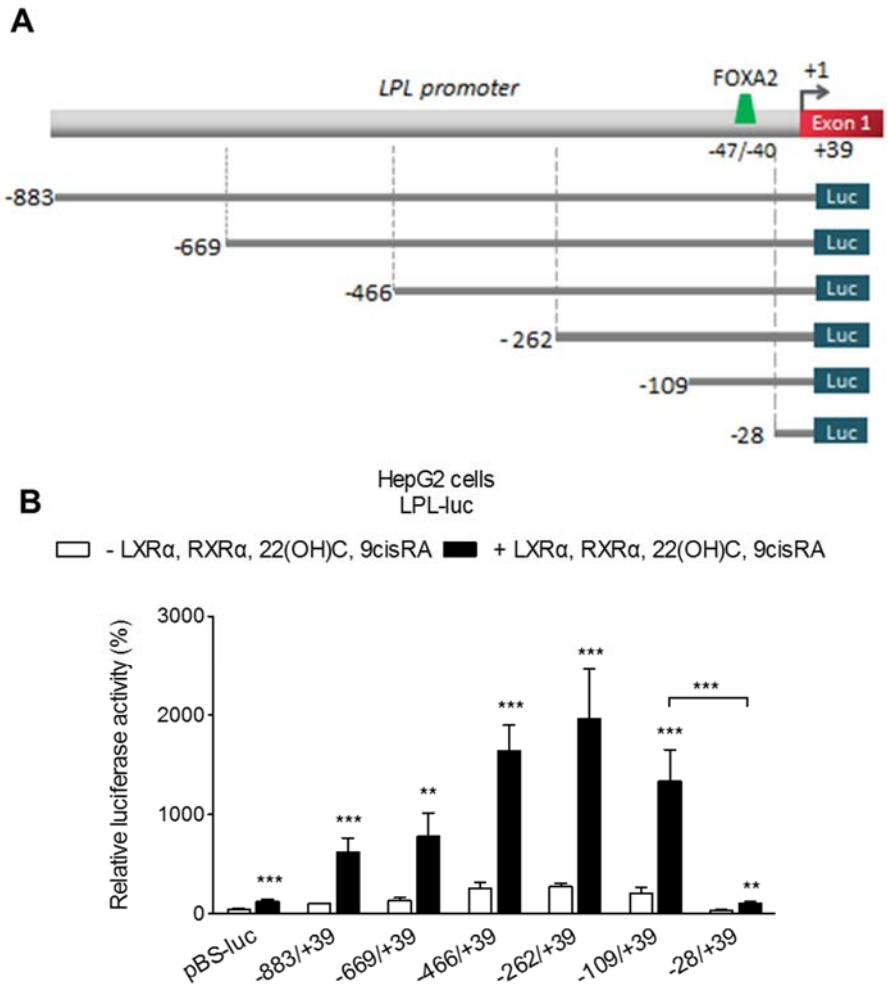

Figure 3.18. Transactivation of the human LPL promoter by LXRα/RXRα heterodimer requires the proximal -109/-28 region. (A) Schematic representation of the 5'-deletion fragments of the (-883/+39) human LPL promoter that were cloned upstream of the luciferase reporter gene (Luc) and used in the transactivation experiments of panel B. The FOXA2 binding site at the region -47/-40 is indicated. (B) HepG2 cells were transiently transfected with the hLPL-luc reporter plasmids (1μg), shown in panel A, along with a β-galactosidase expression plasmid (1μg) in the presence or absence of expression vectors for LXRα, RXRα (0.5μg each) and were treated with the ligands 22(OH)C and 9cisRA (1μM each) for 24 hours or left untreated. The normalized, relative luciferase activity (±SD) calculated form at least three independent experiments performed in duplicate is presented with a histograph. **, $p<0.01$; ***, $p< 0.001$.

Binding of LXRα/RXRα heterodimers to the LPL promoter *in vitro* was established using the DNA-affinity precipitation assays in HEK293T and HepG2 cells. For this purpose, biotinylated PCR fragments corresponding to the LPL promoter regions -466/+39, -262/+39, -109/+39 and -28/+39 (Figure 3.20A) were amplified, coupled to streptavidin dynabeads and incubated with extracts from HEK293T cells

overexpressing the two nuclear receptors LXRα/RXRα. In agreement with the findings of Figure 3.19, very weak binding of LXRα/RXRα heterodimers only to the -109/-39 human LPL promoter was observed in HEK293T cells (Figure 3.20B-D).

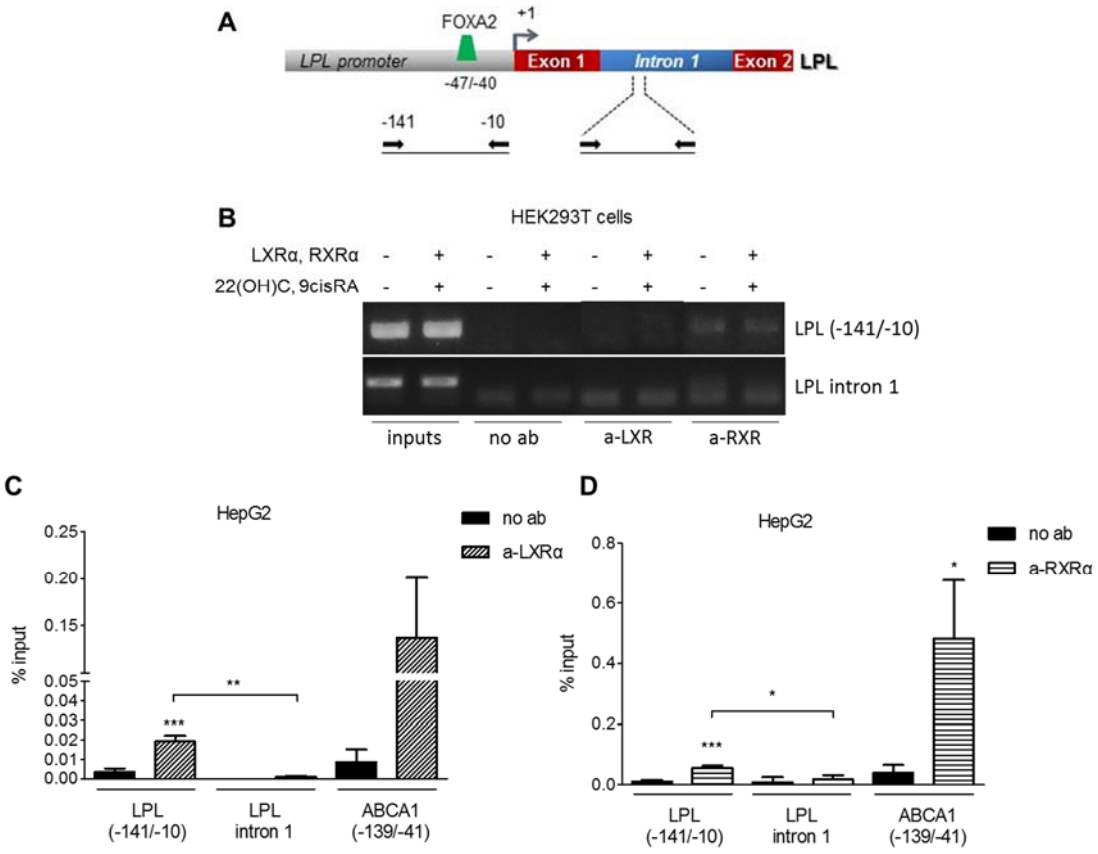

Figure 3.19. Nuclear receptors LXRα and RXRα bind weakly to the proximal human LPL promoter in vivo. (A) Schematic representation of the LPL gene, showing by arrows the location of the primer sets (proximal promoter region -141/-10 and intron 1,) that were utilized in the chromatin immunoprecipitation assays of panels B, C and D. (B) HEK293T cells were transiently transfected with the expression vectors for LXRα, RXRα (10μg each) and were treated with the ligands 22(OH)C and 9cisRA (1μM each) for 24 hours or left untreated. Cells were subjected to chromatin immunoprecipitation using an anti-LXRα antibody or an anti-RXRα antibody or no antibody as negative control (no ab). The immunoprecipitated chromatin was detected by PCR using primers corresponding to the proximal (−141/-10) region of the human LPL promoter or to a distal region in the 1st intron of the LPL gene. (C and D) HepG2 cells were subjected to chromatin immunoprecipitation using an anti-LXRα antibody (panel C) or an anti-RXRα antibody (panel D) or no antibody as negative control (no ab). The immunoprecipitated chromatin was detected by reverse transcription quantitative PCR using primers corresponding to the proximal (−141/-10) region of the human LPL promoter or to a distal region in the 1st intron of the LPL gene or to the proximal (−139/-41) region of the human ABCA1 promoter (positive control). Results from reverse transcription quantitative PCR are expressed as binding relative to the input (%). Each value represents the average (±SD) from four independent experiments. *, $p<0.05$; **, $p < 0.01$; ***, $p< 0.001$.

However, endogenous RXRα present in nuclear extracts from HepG2 cells did not bind to the LPL biotinylated promoter fragments (Figure 3.20E), indicating the weak binding of nuclear receptors to the LPL gene.

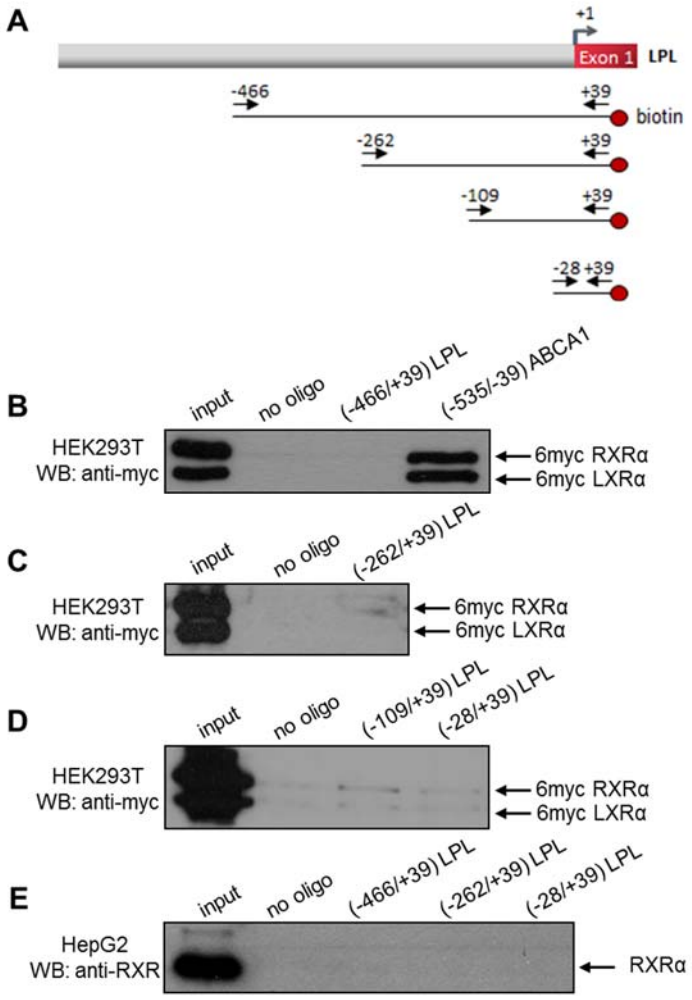

Figure 3.20. Nuclear receptors LXRα and RXRα bind weakly to the LPL promoter in vitro. (A) Schematic representation of the human LPL promoter showing the biotinylated promoter fragments used for the experiments of panels B-D and the primer sets (arrows) used for the amplification of the fragments. (B-D) DNA-affinity precipitation experiments using whole cell extracts from HEK293T cells transiently transfected with expression vectors for 6myc-LXRα (12.5μg) and 6myc-RXRα (10μg) and biotinylated oligonucleotides corresponding to the -466/+39, -262/+39, -109/+39 and -28/+39 regions of the human LPL promoter or the -535/-39 region of the human ABCA1 promoter. Oligonucleotide-bound LXRα/RXRα were detected by Western blotting using the anti-myc antibody. The experiments in B-D were performed three times and representative images are presented. (E) DNA-affinity precipitation using nuclear extracts from HepG2 cells and biotinylated PCR fragments corresponding to the -466/+39, -262/+39 and -28/+39 region of the human LPL promoter. DNA-bound RXRα was detected by Western blotting using the a-RXRα antibody.

FOXA2 is required for the induction of the human and mouse LPL genes by the LXR ligand T0901317.

We hypothesized that LPL promoter induction by LXRα/RXRα is indirect and may require additional transcription factors, because of the weak or absence of binding of LXRα/RXRα to the LPL promoter. FOXA2 forkhead box transcription factor could be a possible mediator, because we showed in the first part that the proximal promoter of the human lipoprotein lipase gene bears a binding site for this factor at position –47 to –40 and that FOXA2 is important for the activity of this promoter in hepatic cells. Indeed, this FOXA2 binding site is located in the region of the human LPL promoter that is required for the induction by LXRα/RXRα (Figure 3.18B).

To investigate the involvement of FOXA2 in the regulation of LPL gene expression by oxysterols, we silenced endogenous FOXA2 expression in HepG2 cells. Cells were treated with the LXR ligand T0901317 in the presence a FOXA2-specific siRNA or a control (scrambled) siRNA and the protein levels of LPL were determined by immunoblotting using actin as an internal control. As shown in Figure 3.21A and B, a FOXA2-specific siRNA abolished both the basal and the T0901317-inducible expression of the LPL gene. We confirmed these findings at the mRNA level, in primary hepatocytes, isolated from the livers of C57BL/6J mice. Silencing of endogenous FOXA2 in primary hepatocytes by the FOXA2-specific siRNA inhibited significantly the induction of LPL gene by T09031317 as determined by reverse transcription quantitative PCR (Figure 3.21C). The findings of Figure 3.21 indicated that FOXA2 is essential for the upregulation of the mouse and human LPL gene by the LXR ligand T0901317. Of note, alignment of the mouse and human LPL promoters showed that the FOXA2 binding site at position -47/-40 is fully conserved in the two species (Figure 3.22B), suggesting a possible common regulatory mechanism of LPL gene regulation by FOXA2 and LXRα/RXRα.

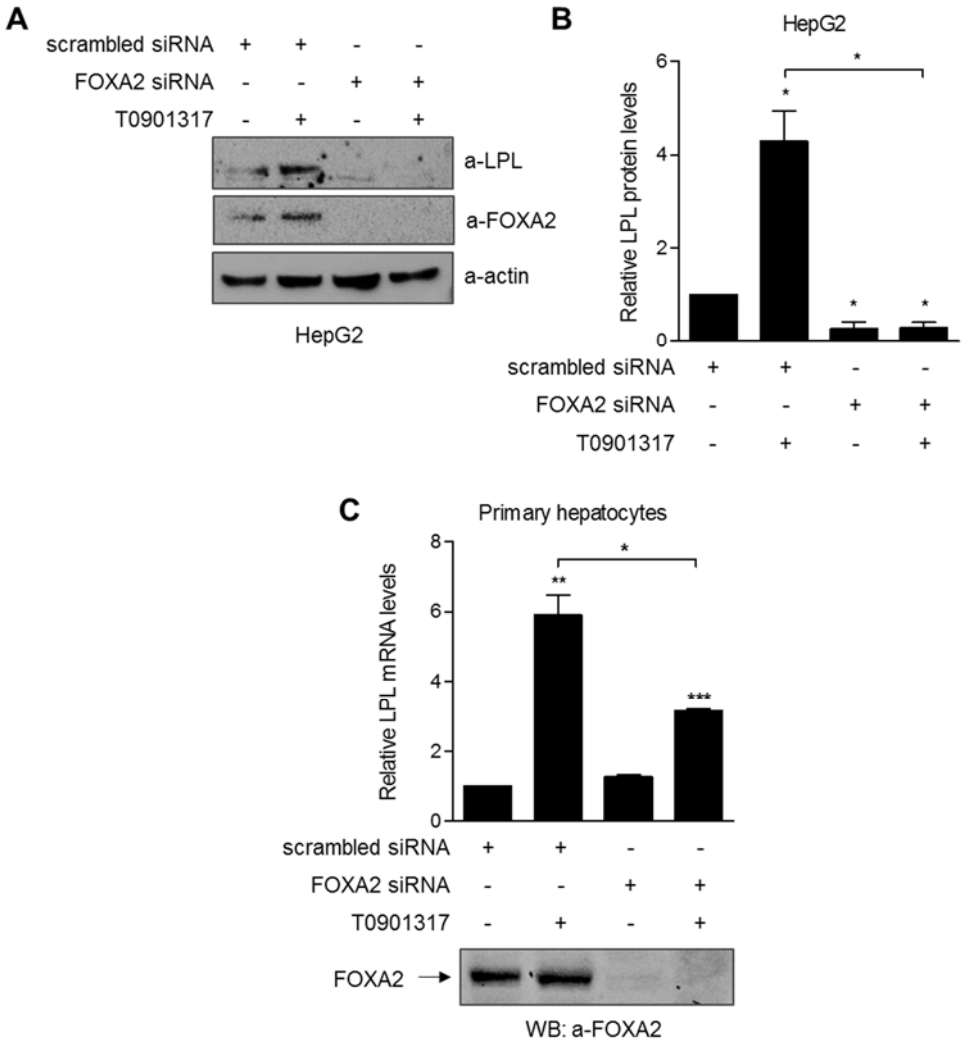

Figure 3.21. Inactivation of the hepatic factor FOXA2 by siRNA silencing inhibits LPL gene induction by T0901317. (A) HepG2 cells were transfected with 50nM of a scrambled siRNA or a FOXA2 specific siRNA and were treated with the synthetic agonist T0901317 (1μM) for 24 hours or left untreated. Protein levels of LPL, FOXA2 and actin (loading control) were determined by immunoblotting using the corresponding antibodies. The experiment was performed three times and representative images are presented. (B) Levels of LPL and actin were quantified by densitometry and the normalized relative protein levels are shown as a histograph. (C) Primary mouse hepatocytes were transfected with 50nM of a scrambled siRNA or a FOXA2 specific siRNA and were treated with the synthetic agonist T0901317 (1μM) for 24 hours or left untreated. Total RNA was extracted and LPL mRNA levels were determined by quantitative reverse transcription PCR and normalized relative to the HPRT mRNA levels. Results are expressed as mean (±SEM) from five independent experiments and shown as a histograph. *, $p<0.05$; **, $p < 0.01$; ***, $p< 0.001$.

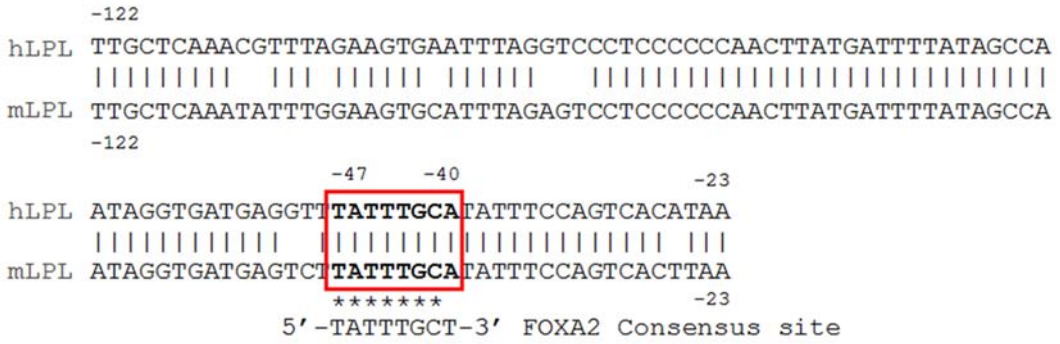

Figure 3.22. Sequence alignment of the mouse and human LPL sequences in the promoter region. The human LPL promoter including the FOXA2 binding site was aligned with the corresponding mouse LPL sequence. Asterisks indicate that the FOXA2 binding site is conserved in the two species. Identical nucleotides are indicated by vertical lines under the sequences. Numbers refer to distance in base pairs from the transcription start site of the human and mouse genes and the red box shows the FOXA2 binding site.

Insulin inhibits the induction of the LPL gene by oxysterols.

In Part I, we showed that treatment of HepG2 cells with insulin leads to the phosphorylation of AKT via the IR/IRS/PI3K/AKT signaling pathway which causes the nuclear export of FOXA2 and the inhibition of the basal LPL gene expression. In order to investigate the effect of insulin in the induction of LPL gene by LXRα and oxysterols, we treated HepG2 cells simultaneously with insulin and T0901317 agonist for 24 hours, and the mRNA and protein levels of LPL were determined. As shown in Figure 3.23A-C, insulin abolished the induction of the LPL gene, both at the mRNA and protein levels, by T0901317 in HepG2 cells. This finding, combined with the data of Figure 3.22 strongly indicate that induction of the LPL gene by oxysterols in hepatic cells requires the presence of FOXA2 in the nucleus.

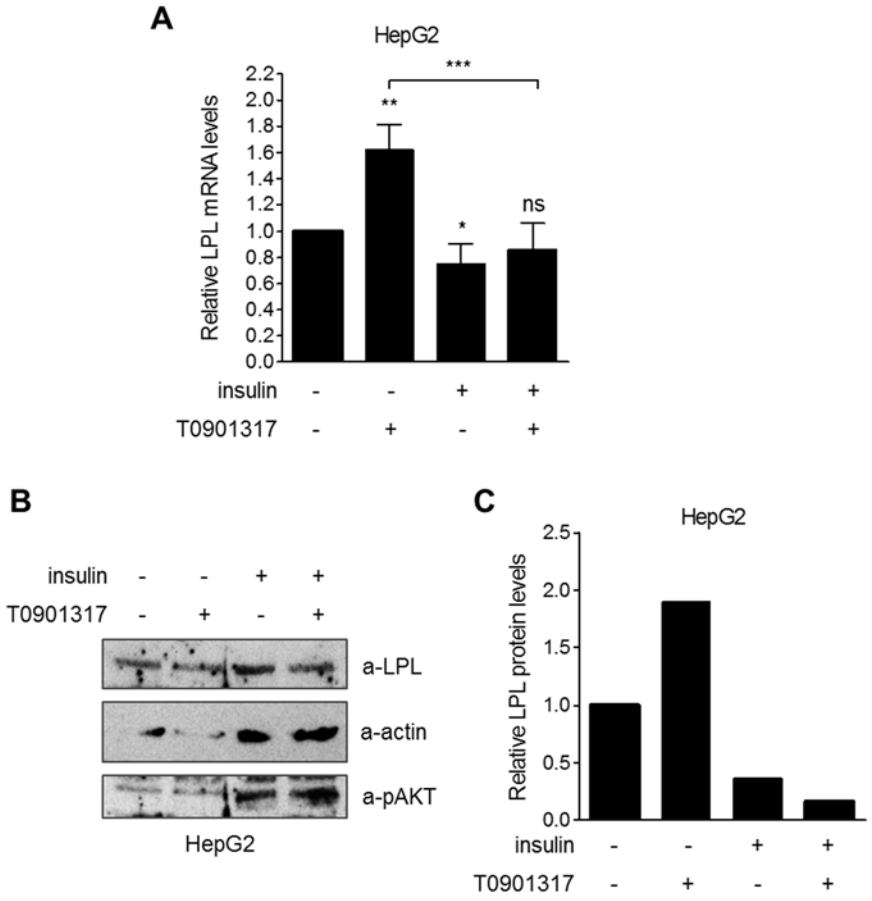

Figure 3.23. Inactivation of the hepatic factor FOXA2 by insulin inhibits LPL gene induction by T0901317. (A) HepG2 cells were treated with insulin (500nM) or/and T0901317 agonist (1μM) for 24 hours or left untreated and total RNA was extracted. LPL mRNA levels were determined by reverse transcription quantitative PCR, normalized relative to the mRNA levels of the GUSB gene and shown as a histograph. Results are expressed as mean (±SD) from three independent experiments. (B) HepG2 cells were treated with insulin (500nM) or/and T0901317 agonist (1μM) for 24 hours or left untreated. Protein levels of LPL, pAKT and actin (loading control) were determined by immunoblotting using the corresponding antibodies. (C) Levels of LPL and actin were quantified by densitometry and the normalized relative protein levels of LPL are shown as a histograph. *, $p<0.05$; **, $p < 0.01$; ***, $p< 0.001$; ns, not significant.

LXRα and RXRα synergistically with FOXA2 transactivate the human LPL promoter, but they do not bind to the LPL promoter, even in the presence of FOXA2.

The requirement of FOXA2 for the upregulation of the LPL gene by oxysterols suggested that FOXA2 and LXRα/RXRα may cooperate and transactivate the human LPL promoter in a synergistic fashion. First, we showed that LXRα/RXRα

heterodimers transactivated the -883/+39 LPL promoter 3 times more strongly in HepG2 cells that express endogenous FOXA2 than in HEK293T cells that do not (Figure 3.24A). Second, ectopically expressed FOXA2 in HEK293T cells restored the transactivation of the LPL promoter by ligand-activated LXRα/RXRα to levels similar to the ones in HepG2 cells (Figure 3.24B). Moreover, simultaneous overexpression of FOXA2, LXRα and RXRα, in the presence of their ligands, in HEK293T cells caused a synergistic transactivation (stronger than the sum of the individual factors) of the LPL promoter (Figure 3.24B). In line with these findings, exogenous FOXA2, LXRα, RXRα and their ligands in HEK293T cells caused a 1.5-fold increase in the protein levels of the secreted LPL (Figure 3.25A and B) and a 3-fold increase in the mRNA levels of the LPL (Figure 3.25C). Similar increase in the mRNA levels of the LPL was observed when these factors (FOXA2, LXRα, RXRα) were overexpessed in HepG2 cells (Figure 3.25D).

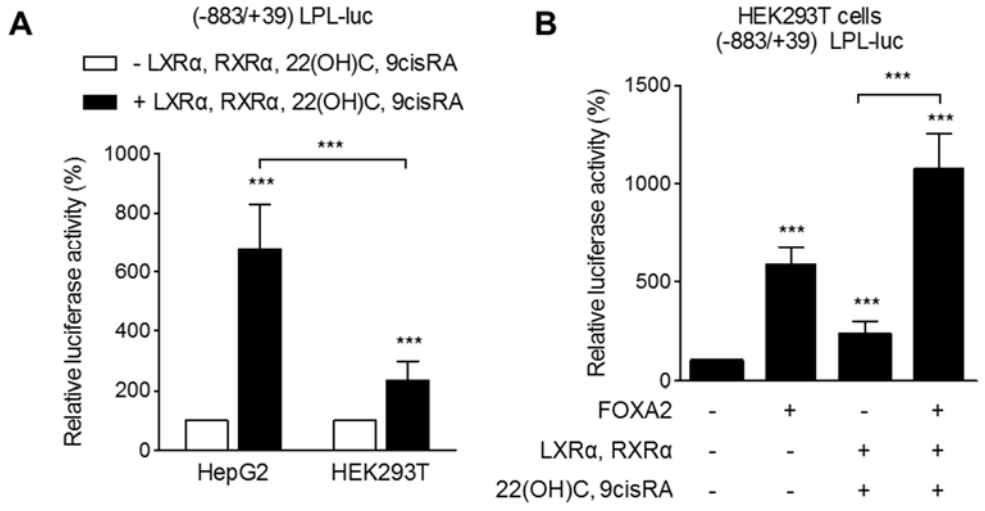

Figure 3.24. FOXA2 and LXRα/RXRα heterodimers transactivate the LPL promoter in a synergistic manner in HEK293T cells. (A) HepG2 and HEK293T cells were transiently transfected with the (−883/+39) LPL-luc reporter plasmid (1μg), along with a β-galactosidase expression plasmid (1μg) in the presence or absence of expression vectors for LXRα, RXRα (0.5μg each) and were treated with the ligands 22(OH)C and 9cisRA (1μM) for 24 hours or left untreated. The normalized, relative luciferase activity (±SD) calculated form at least four independent experiments performed in duplicate is presented with histographs. (B) HEK293T cells were transiently transfected with the (−883/+39) LPL-luc reporter plasmid (1μg), along with a β-galactosidase expression plasmid (1μg) in the presence or absence of expression vectors for FOXA2 (0.25μg), LXRα, RXRα (0.5μg each) and were treated with the ligands 22(OH)C and 9cisRA (1μM) for 24 hours or left untreated. The normalized, relative luciferase activity (±SD) calculated form at least three independent experiments performed in duplicate is presented with histographs. ***, $p< 0.001$.

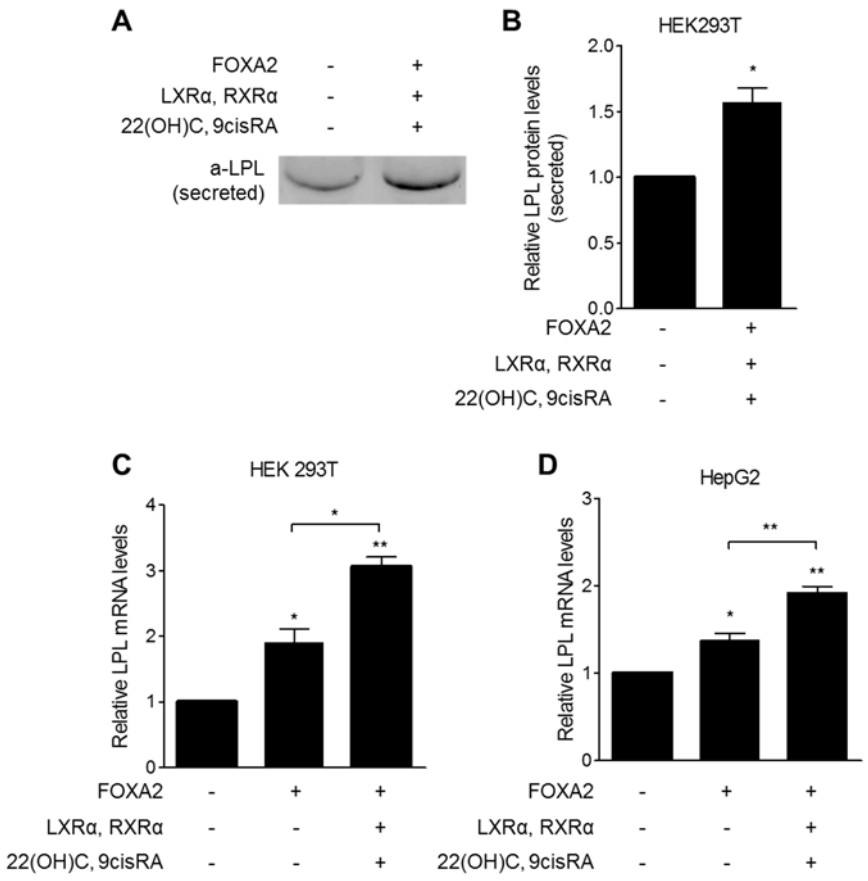

Figure 3.25. FOXA2 and LXRα/RXRα heterodimers induce the expression of LPL gene in HEK293T cells and HepG2 cells. (A) HEK293T cells were transiently transfected with the expression vectors for FOXA2 (1.5μg), LXRα, RXRα (3μg each) and were treated with the ligands 22(OH)C and 9cisRA (1μM) for 24 hours or left untreated. Protein levels of secreted LPL were determined by immunoblotting using the anti-LPL antibody. The experiment was performed three times and representative images are presented. (B) Levels of LPL were quantified by densitometry and the normalized relative protein levels are shown as a histograph. (C and D) HEK293T (panel C) and HepG2 (panel D) cells were transiently transfected with the expression vectors for FOXA2 (1.5μg), LXRα, RXRα (3μg each) and were treated with the ligands 22(OH)C and 9cisRA (1μM) for 24 hours or left untreated. Total RNA was extracted, LPL mRNA levels were determined by reverse transcription quantitative PCR, normalized relative to the mRNA levels of the GUSB gene. Results are expressed as mean (±SD) from at least three independent experiments and shown as histographs. *, $p<0.05$; **, $p < 0.01$

We performed a series of transactivation assays in HepG2 cells using the human -883/+39 LPL promoter or its 5' deletions (Figure 3.26A) along with expression vectors for FOXA2 and LXRα/RXRα individually or in combination. As shown in Figure 3.26B, all three factors and their ligands transactivated synergistically the -883/+39 LPL promoter. Importantly, the synergistic transactivation by FOXA2 and ligand-activated LXRα/RXRα was abolished when the

LPL promoter was deleted to nucleotide -28 suggesting that the FOXA2 binding site at position -47/-40 is critical for this synergistic regulation (Figure 3.26C).

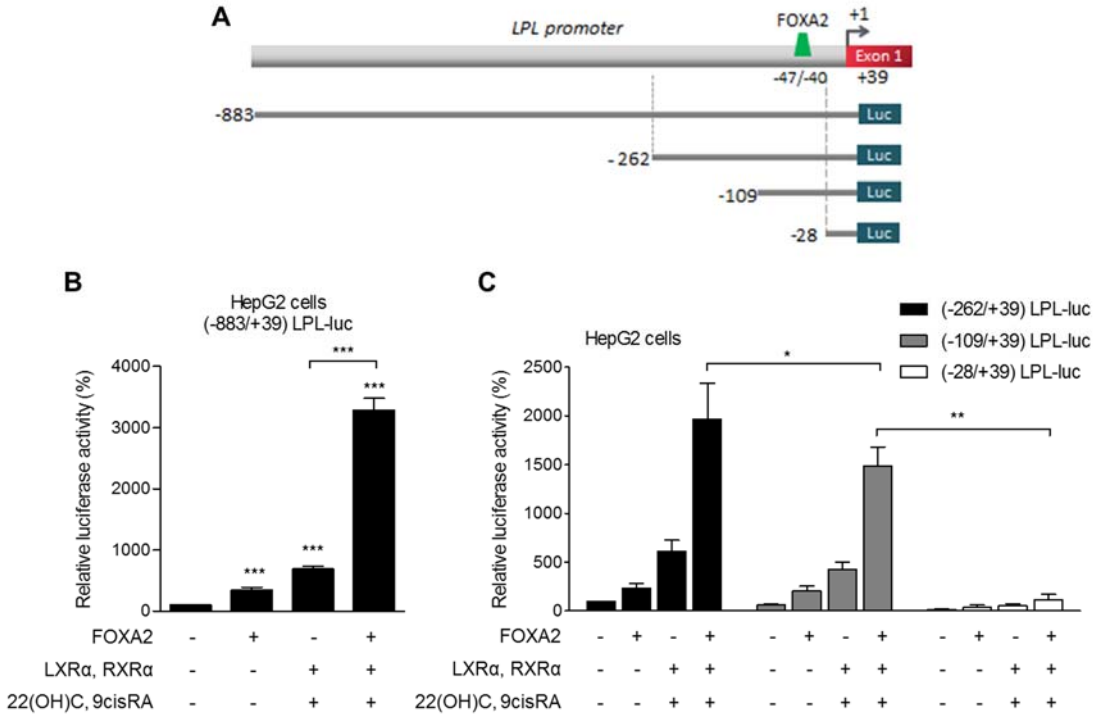

Figure 3.26. FOXA2 element is required for LPL gene induction by LXRα/RXRα in HepG2 cells. (A) Schematic representation of the 5'-deletion fragments of the (-883/+39) human LPL promoter that were used in the transactivation experiments of panels B and C. The FOXA2 binding site at the region -47/-40 is indicated. (B and C) HepG2 cells were transiently transfected with the (−883/+39) hLPL-luc reporter plasmid (panel B), (−262/+39), (−109/+39) and (−28/+39) hLPL-luc (panel C) reporter plasmids (1μg), along with a β-galactosidase expression plasmid (1μg) in the presence or absence of expression vectors for FOXA2 (0.25μg), LXRα or RXRα (0.5μg each) and were treated with the ligands 22(OH)C and 9cisRA (1μM) for 24 hours or left untreated. The normalized, relative luciferase activity (±SD) calculated from at least five (panel B) or two (panel C) independent experiments performed in duplicate is presented with histographs. *, $p<0.05$; **, $p < 0.01$; ***, $p< 0.001$.

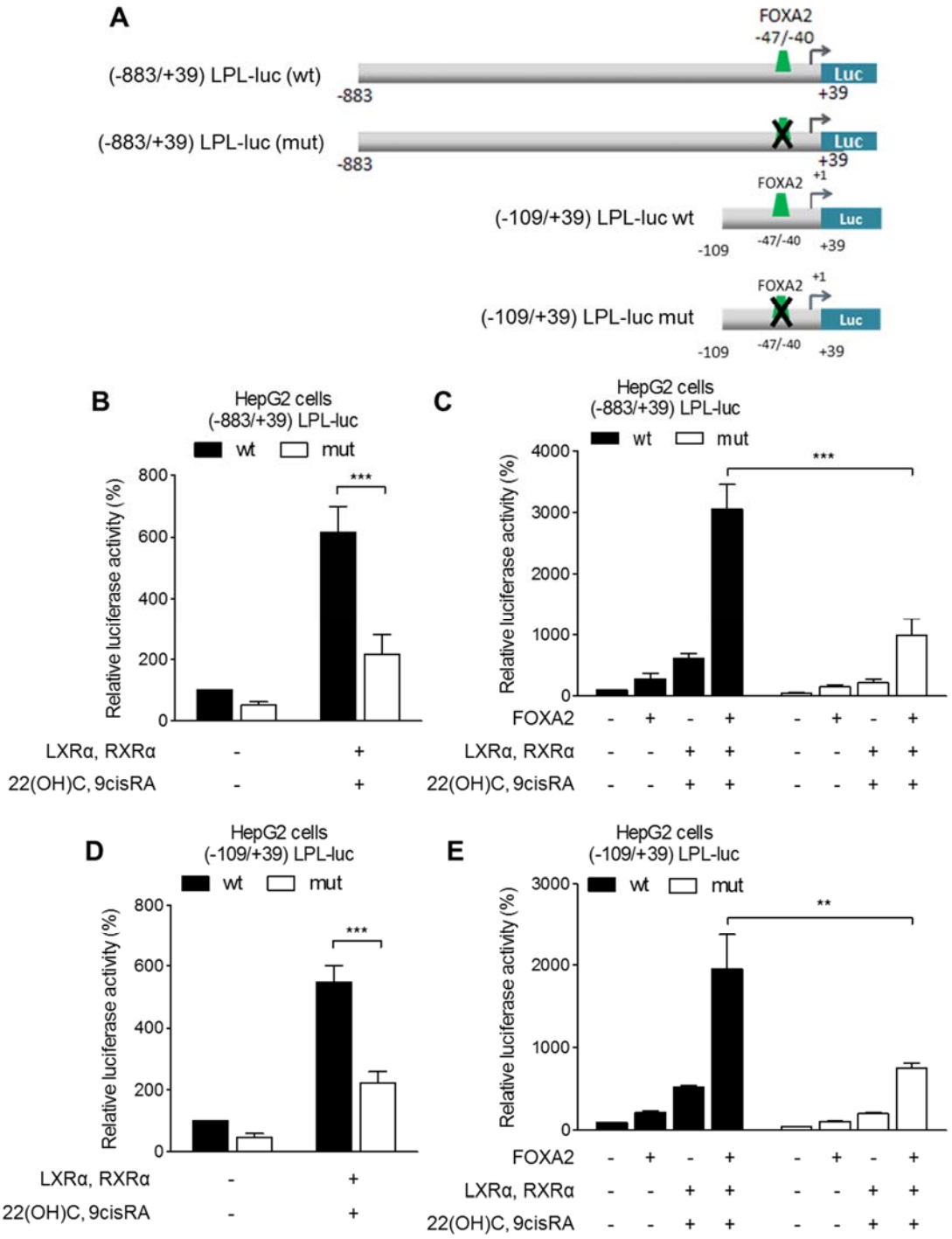

Figure 3.27. Transactivation of LPL promoter by LXRα/RXRα and synergistic induction of LPL promoter by FOXA2 and LXRα/RXRα is dependent on the FOXA2 binding site. (A) Schematic representation of the wild type -883/+39 and -109/+39 LPL promoter constructs and the corresponding construct bearing mutations in the FOXA2 site. (B and D) HepG2 cells were transiently transfected with the WT or mutated (-883/+39) LPL-luc and (-109/+39) LPL-luc reporter plasmids (1μg) along with the β-galactosidase expression vector (1μg), in the presence or in the absence of expression vectors for LXRα and RXRα (0.5μg each) and were treated with the ligands 22(OH)C and 9cisRA (1μM) for 24 hours or left untreated. The normalized, relative luciferase activity (±SD) calculated form four (panel B) or two (panel D) independent experiments performed in duplicate is presented with histographs. (C and E) HepG2 cells were transiently transfected with the WT or mutated (-

883/+39) LPL-luc and (-109/+39) LPL-luc reporter plasmids (1μg) along with the β-galactosidase expression vector (1μg), in the presence or in the absence of expression vectors for FOXA2 (0.25μg), LXRα and RXRα (0.5μg each) and were treated with the ligands 22(OH)C and 9cisRA (1μM) for 24 hours or left untreated. The normalized, relative luciferase activity (±SD) calculated form at least four (panel C) or three (panel E) independent experiments performed in duplicate is presented with histographs. **, $p<0.01$; ***, $p < 0.001$.

This finding was confirmed using two mutant LPL promoter constructs, -883/+39 and -109/+39 (Figure 3.27A), which are bearing nucleotide substitutions within the FOXA2 binding site that abolished the binding of FOXA2 to this site (Figure 3.7). As shown in Figure 3.27B, the mutations in the FOXA2 site strongly inhibited the transactivation of the LPL promoter by ligand-activated LXRα/RXRα and abolished the synergistic transactivation of the LPL promoter by FOXA2 and LXRα/RXRα heterodimers (Figure 3.27C). These transactivation experiments were reproduced using the proximal LPL promoter -109/+38, wt or mutated in the FOXA2 site, with similar results (Figure 3.27D and E), confirming the importance of FOXA2 binding site for the synergistic transactivation of the human LPL promoter by LXRα/RXRα.

Next, we investigated the recruitment of LXRα and RXRα to the LPL promoter in HEK293T cells that express exogenous LXRα/RXRα and also FOXA2 that is required for the synergism with the nuclear receptors. We performed DNA-affinity precipitation assay, using the biotinylated PCR fragments corresponding to the LPL promoter regions -466/+39 and -262/+39 (Figure 3.28A bottom), and as shown in Figure 3.28B, LXRα/RXRα heterodimers did not bind to the promoter, even in the presence of FOXA2. As positive control we used FOXA2 which bound strongly to the -466/+39 and -262/+39 LPL promoter fragments. Similar results were obtained using chromatin immunoprecipitation experiment in HEK293T cells overexpressing LXRα/RXRα in the presence of their ligands, and FOXA2. We did not observe any binding of LXRα or RXRα to the -141/-10 region of LPL promoter, in contrast to FOXA2 that bound very strongly to the -141/-10 promoter region but not to the 1st intron of the LPL gene (Figure 3.28C).

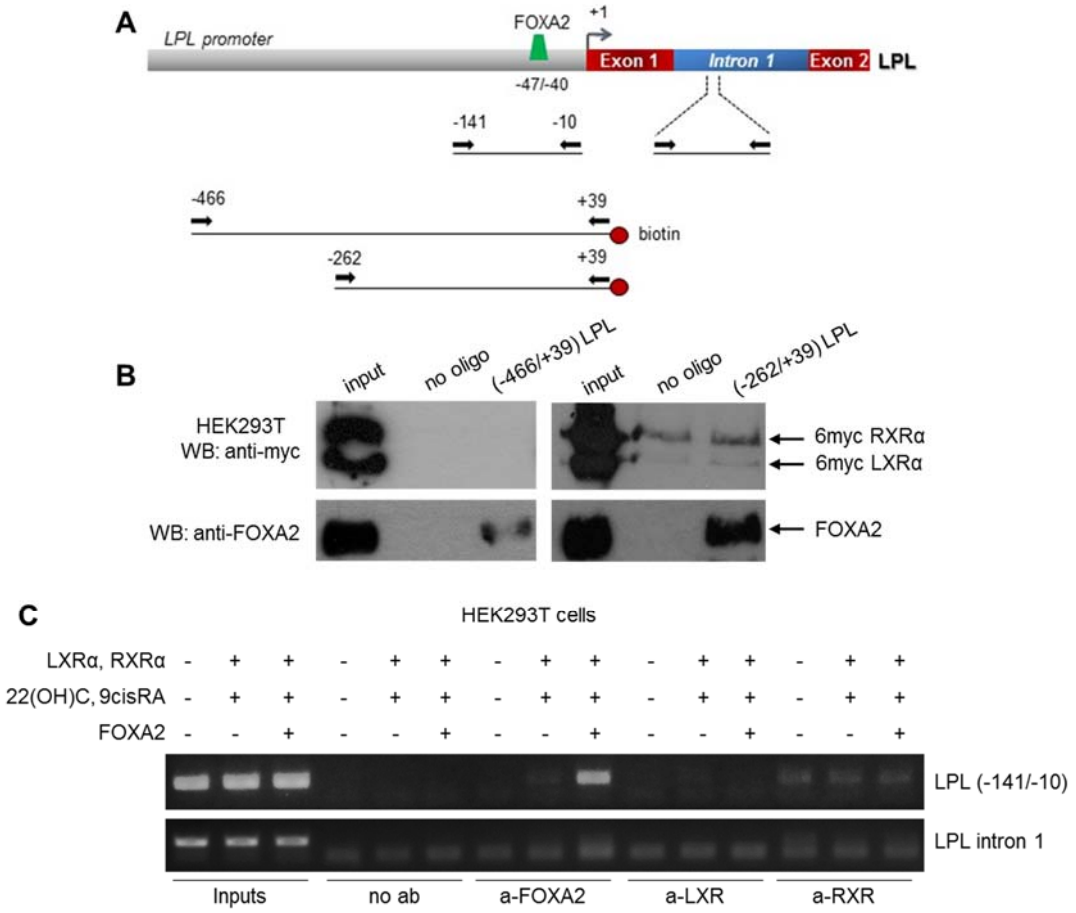

Figure 3.28. Nuclear receptors LXRα and RXRα do not bind to the LPL promoter, even in the presence of FOXA2. (A) Schematic representation of the LPL gene, showing by arrows the location of the primer sets that were utilized in the chromatin immunoprecipitation assays of panel C (distal regions: intron 1, proximal promoter regions: -141/-10) or in the DNA-affinity precipitation assays of panel B for the amplification of the biotinylated fragments (promoter regions: -466/+39 and -262/+39). (B) DNA-affinity precipitation experiments using whole cell extracts from HEK293T cells transiently transfected with expression vectors for 6myc-LXRα (12.5μg) and 6myc-RXRα (10μg), or FOXA2 (13μg) and biotinylated oligonucleotides corresponding to the -466/+39 and -262/+39, region of the human LPL promoter. Oligonucleotide-bound LXRα/RXRα or FOXA2 were detected by Western blotting using the anti-myc or anti-FOXA2 antibody, respectively. (C) HEK293T cells were transiently transfected with the expression vectors for FOXA2, LXRα, RXRα (10μg each) and were treated with the ligands 22(OH)C and 9cisRA (1μM each) for 24 hours or left untreated. Cells were subjected to chromatin immunoprecipitation using an anti-LXRα or an anti-RXRα antibody or no antibody as negative control (no ab) or an anti-FOXA2 as positive control. The immunoprecipitated chromatin was detected by PCR using primers corresponding to the proximal (−141/-10) region of the human LPL promoter or to a distal region in the 1st intron of the LPL gene.

In part I we showed that the -39T/C nucleotide substitution in LPL promoter that is located one nucleotide downstream of the FOXA2 binding site reduced the basal promoter activity but did not affect FOXA2 binding and transactivation (Figure 3.9 and 3.10). We performed luciferase activity assays in HepG2 cells using a mutant -883/+39 LPL promoter that is bearing this mutation (Figure 3.29A) and as shown in Figure 3.29B and C, the -39T/C mutation inhibited strongly (about ~79%) the transactivation of the LPL promoter by ligand-activated LXRα/RXRα (panel B) and reduced about 50% the synergistic transactivation of the LPL promoter by FOXA2 and LXRα/RXRα heterodimers (panel C).

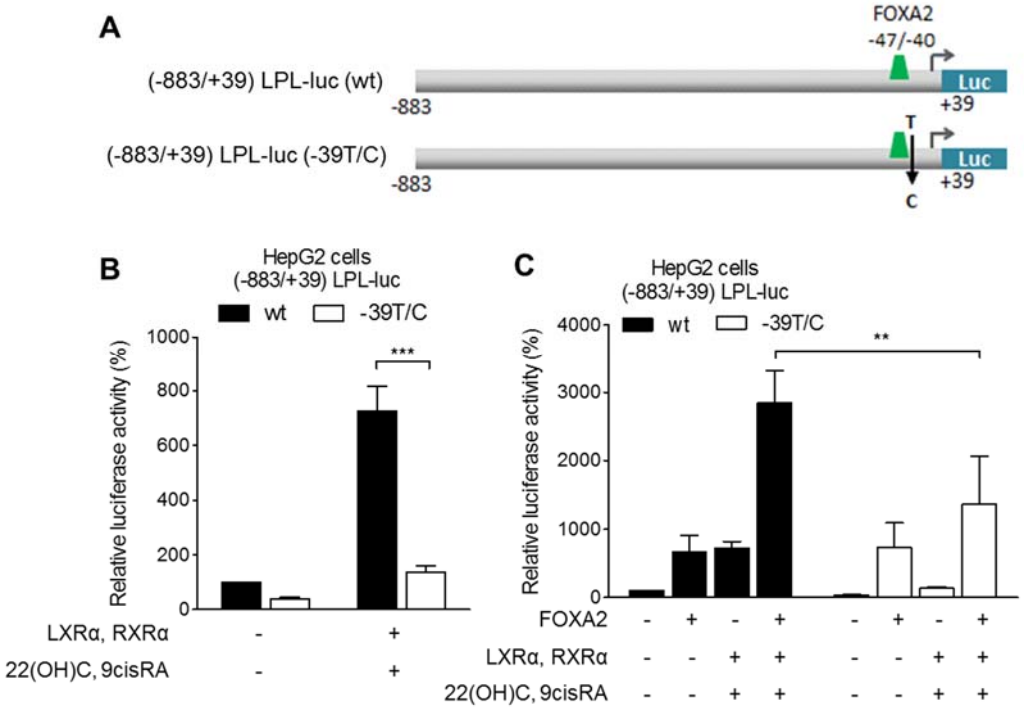

Figure 3.29. A single nucleotide substitution downstream of the FOXA2 binding site reduced the synergistic transactivation of LPL promoter by FOXA2 and LXRα/RXRα. (A) Schematic representation of the wild type LPL promoter construct and the corresponding construct bearing a single T/C substitution (at nucleotide -39) after the FOXA2 site. (B) HepG2 cells were transiently transfected with the (-883/+39) LPL-luc wt or -39T/C reporter plasmids (1μg) along with the β-galactosidase expression vector (1μg), in the presence or in the absence of expression vectors for LXRα, RXRα (0.5μg each) and were treated with the ligands 22(OH)C and 9cisRA (1μM) for 24 hours or left untreated. (C) HepG2 cells were transiently transfected with the wt or mutated (-883/+39) LPL-luc reporter plasmids (1μg) along with the β-galactosidase expression vector (1μg), in the presence or in the absence of expression vectors for FOXA2 (0.25μg), LXRα, RXRα (0.5μg each) and were treated with the ligands 22(OH)C and 9cisRA (1μM) for 24 hours or left untreated. (B and C) The normalized, relative luciferase activity (±SD) calculated form three independent experiments performed in duplicate is presented with histographs. **, $p<0.01$; ***, $p < 0.001$.

The data of Figures 3.9, 3.10 and 3.29 indicate that the -39T/C mutation in the human LPL promoter reduces basal promoter activity and its transativation by LXRα/RXRα or its synergistic transactivation by LXRα/RXRα and FOXA2 but does not affect FOXA2 binding and transactivation, in hepatic cells, suggesting the involvement of additional, yet unknown factor(s) in the regulation of LPL promoter via this region.

Physical interactions between FOXA2 and nuclear receptors LXRα and RXRα.

The functional cooperation between FOXA2 and LXRα/RXRα in the transactivation of the human LPL promoter strongly suggested that these factors physically interact with each other. This hypothesis was validated by several complementary approaches. Physical interactions between FOXA2 and LXRα in vivo were first demonstrated by a co-immunoprecipitation experiment. As shown in Figure 3.30A, LXRα was immunoprecipitated along with FOXA2 in HEK293T cells ectopically expressing both factors by an antibody specific for FOXA2 (top row lane 2) but not by a non-specific antibody (anti-Gal4, top row lane 3) or when FOXA2 was not expressed (top row lane 4). Binding of FOXA2 to LXRα/RXRα heterodimers was also shown by a protein-protein interaction assay which is based on protein biotinylation (463). As shown in Figure 3.30B, both LXRα and RXRα were co-purified with biotinylated FOXA2 using streptavidin agarose beads (top row lane 2) but not with non-biotinylated FOXA2 that was used as a negative control (top row lane 1).

GST pull down assays were employed in order to map the region of LXRα that physically interacts with FOXA2. For this purpose, full length 6myc-LXRα or the truncated LXRα forms shown in Figure 3.31A (464) were expressed in HEK293T cells and the extracts were incubated with glutathione sepharose beads coupled with GST or GST-FOXA2 purified from bacteria (Figure 3.31B). As shown in Figure 3.31C, GST-FOXA2 interacted with the full length LXRα and RXRα, and also with the truncated forms of LXRα, 1-163aa and 30-163aa. Further deletion of the mutant 30-163 reduced (1-127aa) or abolished (1-97aa, 98-163aa and 30-127aa) this interaction. The data from Figure 3.31 indicated that the minimal region of the LXRα protein that is required for interaction with FOXA2 is the region between amino acids

30 and 163 which contains part of the A/B domain and the DNA binding domain (DBD).

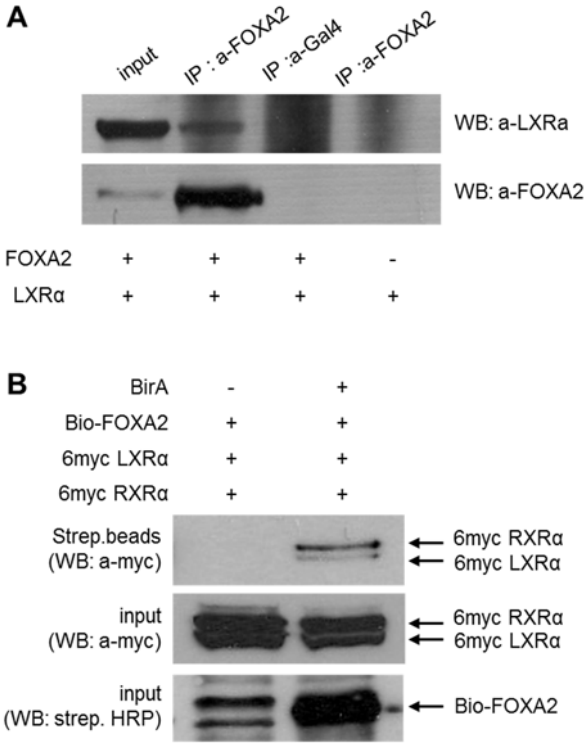

Figure 3.30. FOXA2 physically interacts with the nuclear receptors LXRα and RXRα in vivo. (A) HEK293T cells were transfected with expression vectors for 6myc LXRα and 6myc FOXA2 (10μg each) and subjected to immunoprecipitation (IP) using the anti-FOXA2 antibody or a nonspecific (anti-Gal4) antibody as a control. The immunoprecipitated proteins as well as the starting material (input) were detected by Western blotting using the anti-LXRα antibody or the a-FOXA2 antibody used for immunoprecipitation. The experiment was performed three times and representative images are presented. (B) Protein–protein interaction assay based on in vivo biotinylation was performed using whole cell extracts from HEK293T cells transiently transfected with the expression vectors for Bio-FOXA2 (7,5μg), 6myc LXRα (12,5μg) and 6myc RXRα (7,5μg) in the presence or in the absence of the biotin ligase BirA (7,5μg). Bound proteins as well as a fraction of the starting material (WCE) were detected by Western blotting using the anti-myc antibody for the detection of myc LXRα and myc RXRα or HRP-conjugated streptavidin for the detection of biotinylated FOXA2 protein. The experiment was performed two times and representative images are presented.

In order to map the domain of FOXA2 that is critical for the physical interactions with LXRα, we followed the reverse approach using the GST pull down assays. Specifically, full length 6myc-FOXA2 or the truncated forms shown in Figure 3.32A were expressed in HEK293T cells and the extracts were incubated with glutathione sepharose beads coupled with GST or GST-LXRα purified from bacteria

(Figure 3.32B). As shown in Figure 3.32C, GST- LXRα interacted with the full length FOXA2, and also with the truncated forms of FOXA2, 1-360aa and 1-279aa, which contain the transactivation domain IV/V. In contrast, GST-LXRα did not interact with the FOXA2 mutants that not contain the TA domain IV/V, 95-458aa and 95-360aa. Furthermore, GST-LXRα precipitated with the FOXA2 1-94aa transactivation domain IV/V, but not with the DNA binding domain 144-279aa, the hinge domain 280-360aa or the transactivation II/III domain 361-458aa (Figure 3.32D). The data of Figure 3.32 showed that the domain of FOXA2 that is essential for its physical interactions with LXRα is the transactivation domain IV/V defined by nucleotides 1 and 94.

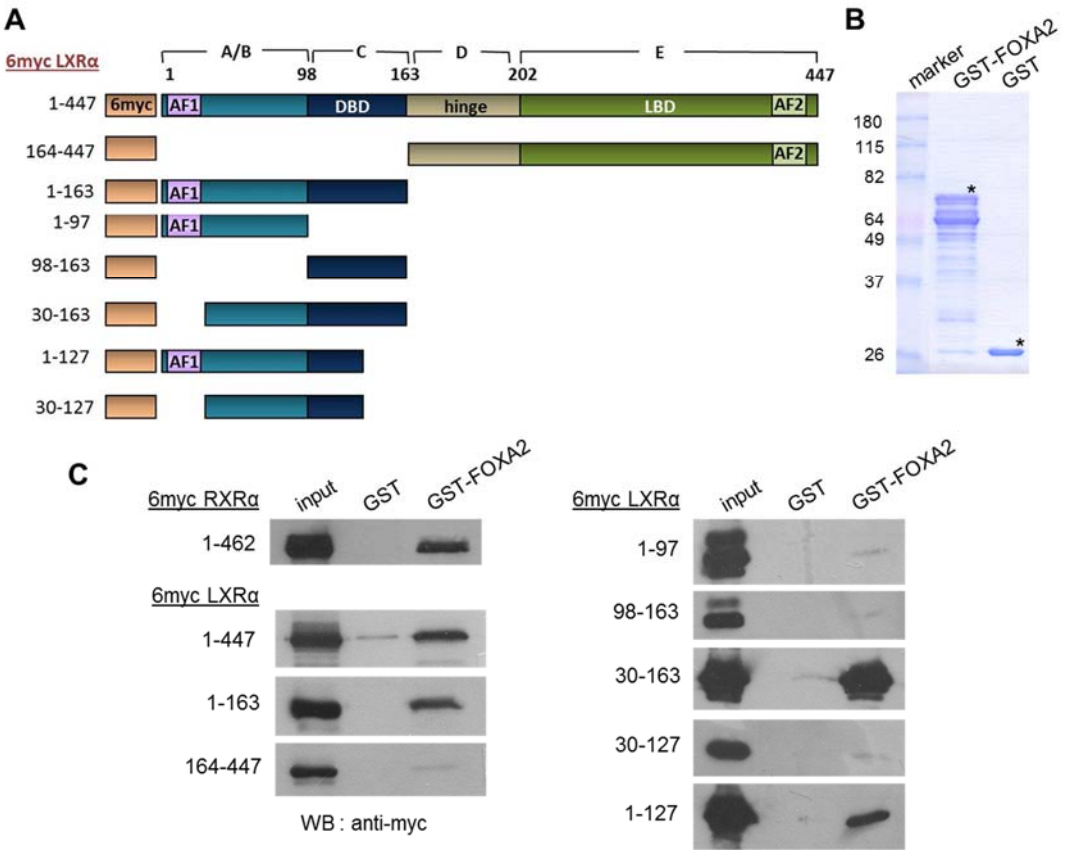

Figure 3.31. Nuclear receptor LXRα physically interacts with FOXA2 in vitro via the aa 30-163 region that contains part of the A/B and the DBD domain. (A) Schematic representation of the various 6myc-LXRα (wild-type and truncated) forms that were used in the GST pull-down experiments of panel C. The amino-terminal A/B domain, the DNA binding domain (DBD), the hinge (D domain) and the ligand binding domain (LBD) are presented with boxes of different colors. The activation functions 1 and 2 (AF1, AF2) of the A/B and E domain respectively, are shown as small boxes. (B) The GST or GST-FOXA2 fusion proteins were expressed in Escherichia coli and coupled to glutathione–Sepharose

beads. The coupling efficiency was monitored by SDS-PAGE and Coomassie brilliant blue staining. Molecular mass marker (expressed in kilodaltons) is shown on the left of the gel. The position of GST and GST-FOXA2 proteins is shown with asterisks. (C) GST and GST-FOXA2 coupled beads were allowed to interact with extracts from HEK293T cells transiently transfected with the expression vectors for RXRα and LXRα (wild-type and truncated forms) (15µg each). Bound proteins as well as a fraction of the starting material (input) were detected by Western blotting using the anti-myc antibody. The experiment was performed at least two times and representative images are presented.

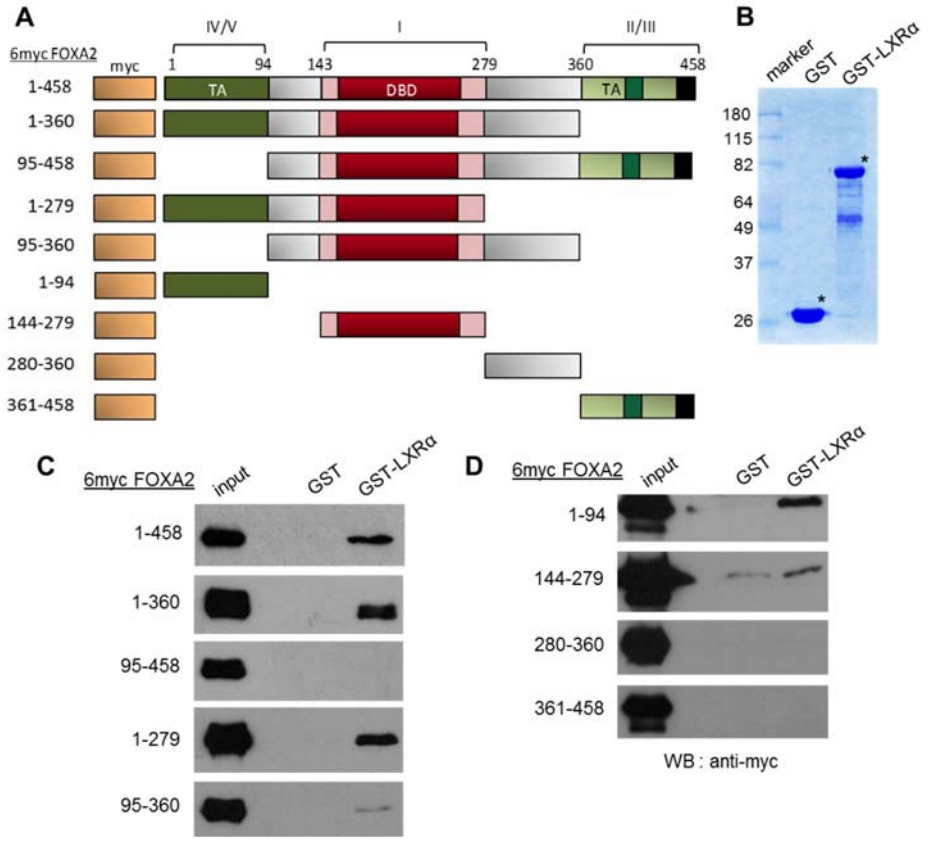

Figure 3.32. The transactivation IV/V domain of FOXA2 is required for the physical interaction with LXRα. (A) Schematic representation of the various 6myc-FOXA2 (wild-type and truncated forms) that were used in the GST pull-down experiments of panels C and D. The FOXA2 amino-terminal transactivation domain IV/V, the DNA binding domain I (DBD) and the carboxy-terminally transactivation domain II/III are shown with boxes of different colors. (B) The GST or GST-LXRα fusion proteins were expressed in Escherichia coli and coupled to glutathione–Sepharose beads. The coupling efficiency was monitored by SDS-PAGE and Coomassie blue staining. Molecular mass marker (expressed in kilodaltons) is shown on the left of the gel. The position of GST and GST-LXRα proteins is shown with asterisks. (C and D) HEK293T cells were transiently transfected with the expression vectors for FOXA2 (wild-type and truncated forms) (15µg each) and extracts were allowed to interact with GST and GST-LXRα coupled beads. Bound proteins as well as a fraction of the starting material (input) were detected by Western blotting using the anti-myc antibody. In panel D, transfected cells were treated with proteasome *inhibitor MG132* (10µM) for 6 hours to increase the stability of the short FOXA2 fragments. The experiments were performed at least two times and representative images are presented.

This finding was confirmed using the GAL4-based transactivation system. For this purpose, the truncated FOXA2 forms 1-94aa and 95-458aa were fused with the DNA binding domain of the yeast transactivator GAL4, generating the constructs GAL4-FOXA2 (1-94) and GAL4-FOXA2 (95-458) (Figure 3.33A, B).

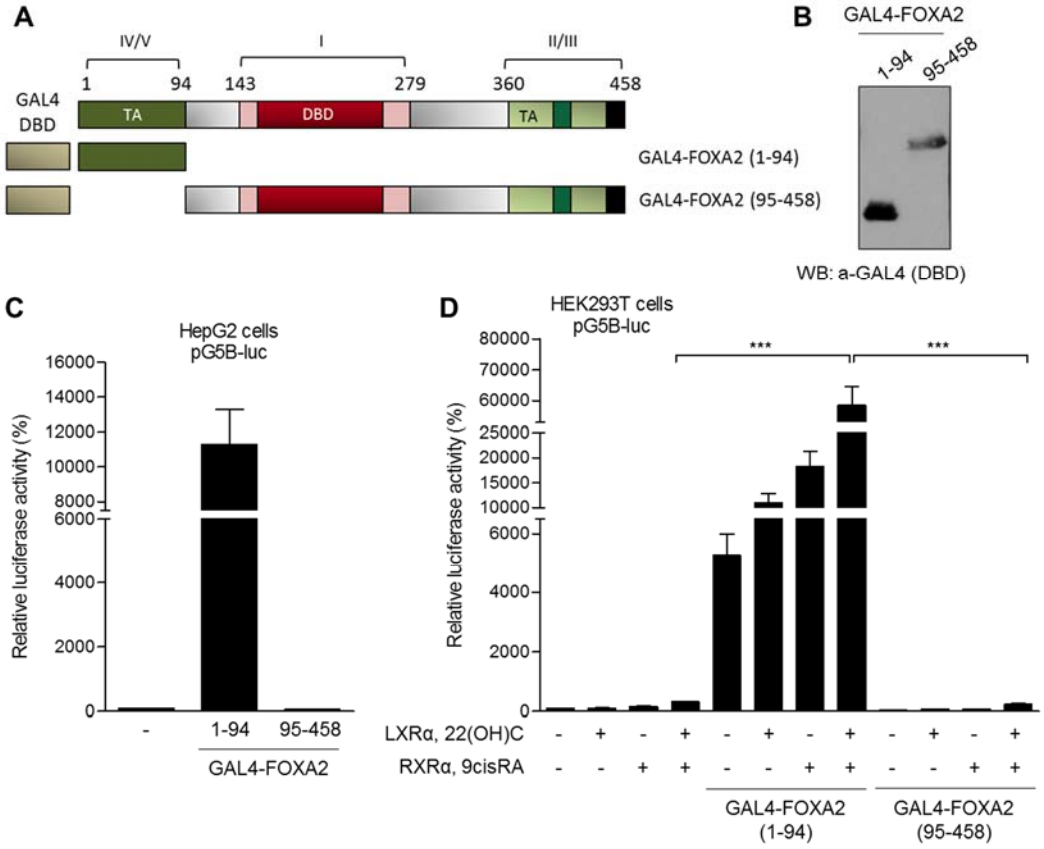

Figure 3.33. Functional interactions between LXRα/RXRα heterodimers and domain IV/V of FOXA2 in a GAL4-based transactivation system. (A) Schematic representation of the truncated FOXA2 forms, fused with the DBD of GAL4, that were utilized in the transactivation experiments of panel C. (B) HEK293T cells were transfected with the truncated GAL4- FOXA2 expression vectors (13μg) and the protein levels of GAL4-FOXA2 were determined by immunoblotting using the anti-GAL4 DBD antibody. (C) HepG2 cells were transiently transfected with the pG5B-Luc reporter plasmid (1μg) along with the β-galactosidase expression vector (1μg) and GAL4-FOXA2 1-94 or 95-458 (1μg). The normalized, relative luciferase activity (±SD) is presented with histograph. (D) HEK293T cells were transiently transfected with the pG5B-Luc reporter plasmid (1μg) along with the β-galactosidase expression vector (1μg), in the presence or in the absence of expression vectors for LXRα, RXRα (0.5μg each) and GAL4-FOXA2 1-94 or 95-458 (1μg each), as indicated at the bottom of the graphs. Transfected cells were treated with the ligands 22(OH)C and 9cisRA (1μM) for 24 hours or left untreated. The normalized, relative luciferase activity (±SD) calculated form three independent experiments performed in duplicate is presented with histographs. ***, $p < 0.001$.

HepG2 cells were transfected with the reporter plasmid pG5B-luc bearing the luciferase gene under the control of a GAL4-responsive artificial promoter (G5B) in the presence of the GAL4-FOXA2 expression vectors. A shown in Figure 3.33C, the GAL4-FOXA2 (1-94), which contains the tranactivation domain IV/V, transactivated strongly the pG5B-luc reporter, but the GAL4-FOXA2 (95-458) did not. Moreover, HEK293T cells were transfected with the reporter plasmid pG5B-luc in the presence or in the absence of the expression vectors GAL4-FOXA2 1-94 or 95-458, and LXRα, RXRα in the presence of their corresponding ligands. As shown in Figure 3.33D, GAL4-FOXA2 (1-94) trasnactivated the G5B promoter and this transactivation was enhanced by ligand activated LXRα or RXRα. Importantly, coexpression of both LXRα and RXRα caused a strong synergistic transactivation of the G5B promoter suggesting that both LXRα and RXRα physically interact with and act as super-activators of the transactivation domain IV/V of FOXA2 (Figure 3.33D). In agreement with the data of Figure 3.32, co-expression of LXRα and RXRα had no effect on the transcriptional activity of FOXA 95-458 which contains transactivation domains I and II/III (Figure 3.33D).

A scheme summarizing the data from the physical and functional interaction experiments of Figure 3.31-3.33 is shown in Figure 3.34.

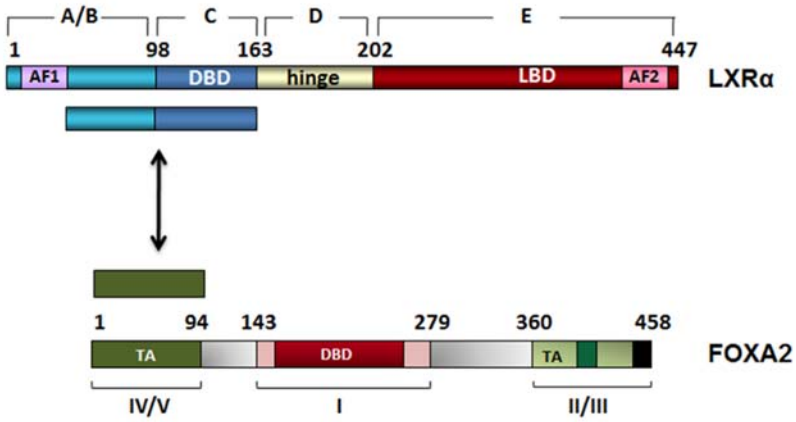

Figure 3.34. Schematic representation of the domains of LXRα and FOXA2 that are required for the physical interactions between them. The double arrow indicates established physical interactions between domains 30-163 of LXRα and 1-94 of FOXA2.

The main finding of the present study is that LXRs, in the presence of increased concentrations of their ligands (oxysterols or synthetic compounds), induce the expression of the human lipoprotein lipase gene in hepatic cells via a novel mechanism that depends on physical and functional interactions between LXRα and the hepatic transcription factor FOXA2/HNF-3β. To our knowledge, this is the first time that this nuclear receptor is reported to activate gene transcription as a super-activator of another transcription factor. The ability of other members of the hormone nuclear receptor superfamily to function as super-activators on promoters that do not contain hormone response elements is not unprecedented however. Nuclear receptors such as the retinoic acid receptor (RAR) (465, 466), the vitamin D receptor (VDR) (467, 468) and the estrogen receptor (469, 470) have all been shown to activate their corresponding target genes not by directly binding to the corresponding promoters but by inducing the transcriptional activity of the ubiquitous transcription factor Specificity Protein 1 (Sp1). In line with these findings, we showed in a previous paper that ligand-activated LXRα activates the promoter of the ATP Binding Cassette Transporter A1 gene via physical and functional interactions with Sp1 bound to the proximal ABCA1 promoter adjacent to a LXRE. For the physical interactions between the two factors, the N-terminal region of LXRα, which included the AF1 and DNA binding domains and two different domains of Sp1: the transactivation domain B and the DNA binding domain were required (464). Similar to the data of the present study, LXRα was able to induce the transcription of a synthetic GAL4-responsive promoter by super-activating a fusion protein consisting of the DNA binding domain of the yeast transactivator GAL4 and full length Sp1 (464).

In the case of the LPL promoter studied in the present study, the key mediator of the induction by LXR ligands is FOXA2 which binds to a FOXA2 responsive element present in the proximal -47/-40 region, as discussed in the previous part. Inhibition of FOXA2 binding to this site abolished the basal activity and the FOXA2-mediated transactivation of the LPL promoter whereas silencing of FOXA2 caused a reduction in the mRNA and protein levels of LPL. We also showed that insulin inhibited the expression of LPL in the liver via a PI3K/AKT/FOXA2 pathway that keeps FOXA2 out of the nucleus. In this part, we revealed a novel role of FOXA2 in LPL gene regulation which is to mediate the induction of this gene by the LXRα. We

showed that LXR agonists increase the mRNA and protein levels of LPL in HepG2 cells and in primary mouse hepatocytes in a FOXA2-dependent manner. Silencing of endogenous FOXA2 using specific FOXA2 siRNA abolished the induction of the LPL gene by LXR agonists in human hepatocytes. In the same way, insulin mimics the FOXA2 siRNA and inhibited the induction of LPL by oxysterols. Importantly, co-expression of FOXA2 and LXRα/RXRα caused a synergistic transactivation of the LPL promoter. Moreover mutations in the FOXA2 site abolished the transactivation of the human LPL promoter by ligand-activated LXRα/RXRα heterodimers and also the FOXA-LXR-RXRα synergistic transactivation of the LPL promoter. However, nuclear receptors LXRα and RXRα did not bind or bound very weakly to the LPL promoter. Synergism of the three factors FOXA-LXR-RXRα is facilitated by physical interactions between them, with the N-terminal regions of both factors (the DBD of LXRα and the transactivation domain IV/V of FOXA2) to be required for this interaction (Figure 3.34). These physical interactions were established using various complementary approaches including co-IPs, in vivo protein biotinylation assays, GST pull down assays and GAL4 transactivation experiments. Figure 3.35 summarizes the combined findings from parts I and II for the coordinated regulation of expression of LPL gene by FOXA2, LXRα and oxysterols in hepatocytes. Liver LPL gene expression is controlled by the interplay between the liver-enriched factor FOXA2 and ligand-dependent nuclear receptors LXRα, RXRα.

Although it was known that oxysterols (generated in the liver by a high cholesterol diet) or synthetic LXR agonists induce strongly the mouse LPL gene in vivo and in vitro (180-182, 471), the regulation of the human LPL gene by LXRs had not been studied. We found one paper reporting the induction of the human LPL gene by LXR/RXR agonists in human endothelial cells along with other genes implicated in lipoprotein metabolism (184). The mechanism by which LXRs induce the mouse LPL gene was studied by Zhang et al. who showed that LXR/RXR heterodimers induce LPL gene expression in the liver by binding in vitro to a distal LXR responsive element (LXRE) present in the first intron of the mouse LPL gene (181). No binding of LXR/RXR heterodimers could be shown on a putative LXRE present in the promoter of the mouse LPL gene upstream of exon 1 (181).

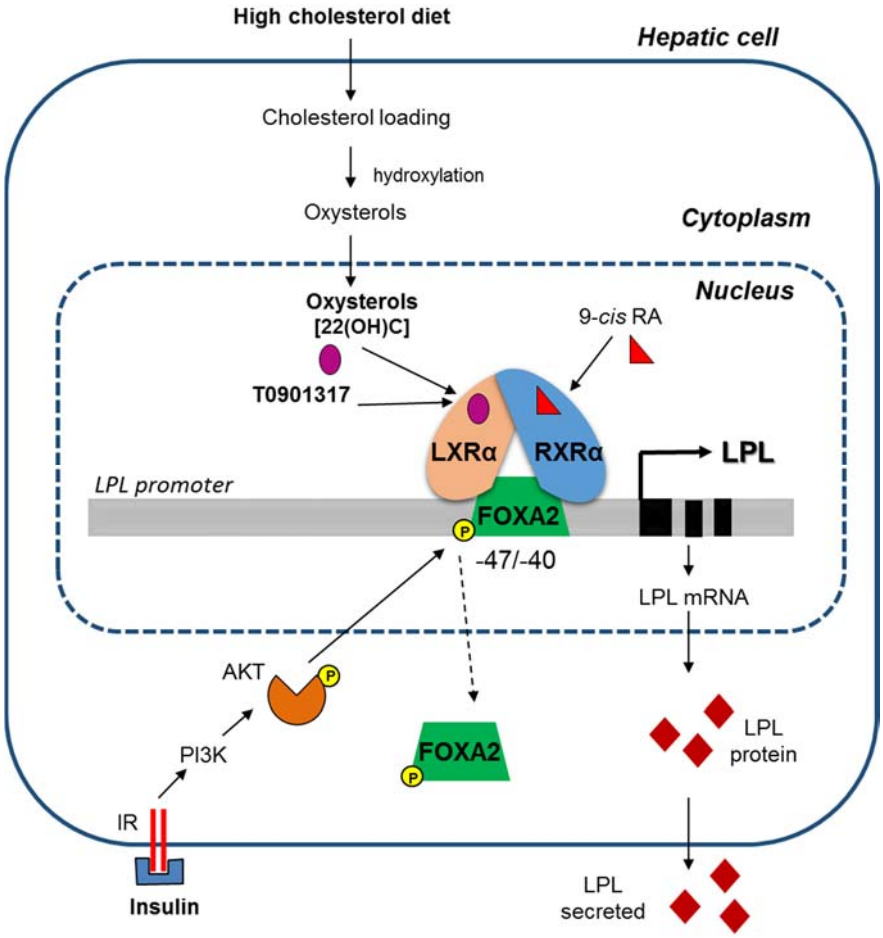

Figure 3.35. Proposed mechanism-model for the induction of LPL gene by oxysterols in hepatic cells, which is based on physical and functional interactions between FOXA2 transcription factor and LXRα/RXRα nuclear receptors. See text for details.

In order to investigate the existence of a similar mechanism in the human LPL gene we performed chromatin immunoprecipitation assays using anti-LXRα or anti-RXRα antibodies and reverse transcription quantitative PCR primers corresponding to the 1st intron of the human LPL gene but no binding of either nuclear receptor could be detected in this region (Figure 3.19). A comparison of the mouse and the human LPL intronic sequences in the region of the LXRE showed that this element is not highly conserved between these two species (Figure 3.36). These data suggested that this intronic LXRE that was identified in the mouse LPL gene is not significant for the regulation of the human LPL gene by oxysterols in hepatic cells and that the mechanism of regulation of the mouse LPL gene may be similar to the mechanism identified in the present study. Indeed, comparison of the mouse and human

sequences in the LPL promoter upstream of exon 1 revealed a perfect match in the region corresponding to the FOXA2 binding site and a very high degree of homology in the flanking regions (Figure 3.22).

Figure 3.36. Sequence alignment of the mouse and human LPL sequences in the intron 1 region. The mouse LPL intron 1 including the LXRE element was aligned with the corresponding human sequence. Identical nucleotides are indicated by vertical lines under the sequences. Numbers refer to distance in base pairs from the transcription start site of the human and mouse genes and boxes show identified transcription factor binding sites for LXR.

The role of lipoprotein lipase in the adult liver and its contribution to lipid homeostasis and the pathogenesis of atherosclerosis has been controversial mainly due to its low levels of expression in this tissue. However, despite this low expression, hepatic LPL is physiologically significant for lipoprotein metabolism as shown by studies in hepatic-specific LPL gene ablation (453) which decreased postprandial TG clearance and elevated plasma TG and cholesterol levels. Furthermore, it was shown that overexpression of LPL specifically in the mouse liver increased liver TG and caused insulin resistance (171). LPL is expressed at high levels in the adipose tissue where it facilitates the hydrolysis of triglycerides of TRLs to fatty acids for uptake by the adipocytes (104, 105). In contrast to the liver, LXRs cannot induce LPL gene in adipose tissue where its mRNA levels are high (312) suggesting a tissue-specific mode of regulation of this gene and the existence of tissue specific transcription factors that could modulate LPL gene regulation by LXRs and oxysterols. One such factor could be the forkhead box protein FOXA2. Furthermore other members of the forkhead box family, such as FOXO1, which share extensive homology with FOXA2 (309) and could theoretically bind to the same DNA element in the proximal LPL promoter and interact with LXR to regulate LPL gene expression in other tissues other than the liver such as macrophages (181) or endothelial cells (184).

FOXO1, also known as FKHR, is a member of the forkhead family of the O subclass. It is a downstream target of the insulin /PI3-K signaling pathway and has a

role in cell cycle control and apoptosis, fertility, stress response, longevity and regulation of metabolism (472-475). FOXO1 is expressed at high levels in insulin-responsive tissues, such as adipose tissue and muscle, and insulin-production tissues, such as pancreatic beta cells (475). Similar to FOXA2, we showed that FOXO1 also interacts physically with LXRα in vivo, by co-immunoprecipitation assays and in vitro, by GST pull down assays. As shown in Figure 3.37A, LXRα was immunoprecipitated along with flag-FOXO1 in HEK293T cells ectopically expressing both factors by an anti-flag antibody but not by a non-specific antibody (anti-Gal4) or when FOXO1 was not expressed. GST pull down assays confirmed this finding, as GST-FOXO1 interacted with the full length 6myc-LXRα (Figure 3.37B). In line with this finding, we showed in part I that FOXA2 does not transactivate the LPL promoter in mouse 3T3-L1 pre-adipocytes and also is not expressed in differentiated adipocytes 3T3L1.

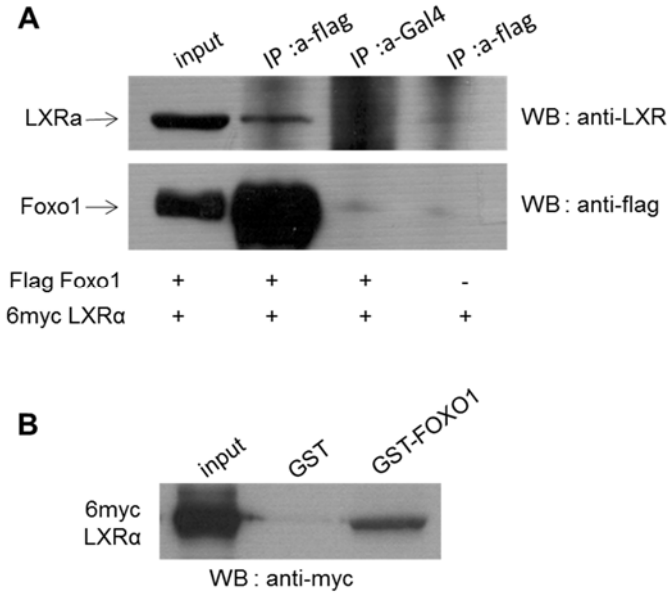

Figure 3.37. FOXO1 physically interacts with the nuclear receptors LXRα in vivo and in vitro. (A) HEK293T cells were transfected with expression vectors for 6myc LXRα and flag FOXO1 (10μg each) and subjected to immunoprecipitation (IP) using the anti-flag antibody or a nonspecific (anti-Gal4) antibody as a control. The immunoprecipitated proteins as well as the starting material (input) were detected by Western blotting using the anti-LXRα antibody or the a-flag antibody used for immunoprecipitation. (B) GST and GST-FOXO1 coupled beads were allowed to interact with extracts from HEK293T cells transiently transfected with the expression vectors for LXRα (15μg). Bound proteins as well as a fraction of the starting material (input) were detected by Western blotting using the anti-myc antibody.

However, the mutations into the FOXA2 element reduced the basal activity of the LPL promoter in pre-adipocytes, indicating the importance of this element for the regulation of LPL gene. These data suggest that FOXO1 and LXRs may cooperate using the FOXA2 element at -47/-40 to regulate the expression of the LPL gene in adipocytes that express this forkhead factor, but this remains to be shown.

Liver X Receptors (LXRs) have a crucial role as sensors of intracellular sterol levels protecting cells, especially macrophages, from cholesterol overload and facilitating the process of reverse cholesterol transport (344, 384, 476, 477). In this context, activation of the LPL gene in the liver by a high fat diet may facilitate the binding of HDL to liver cells and the transport of HDL cholesterol to the hepatocytes for catabolism and elimination (168). Inhibition of FOXA2, and as a consequence of LPL gene by insulin via a PI3K/AKT/FOXA2 pathway could prevent the overexpression of LPL by oxysterols under conditions of cholesterol overload such as a high fat diet, thus protecting liver from the toxic effects of LPL overexpression (insulin resistance) as demonstrated recently in mouse studies (171).

The mechanism of LPL gene regulation by LXRα/FOXA2 in the liver that was unraveled in this study may have wider implications for cholesterol and TG homeostasis. The FOXA2 binding site may serve as a novel LXRE that facilitates the induction of the LPL promoter by oxysterols via FOXA2. In addition to the canonical model of gene activation by LXRs via binding to LXREs, a non-canonical model emerges which does not require the presence of LXREs but it rather depends on physical and functional interactions of LXRs with other DNA-bound transcription factors such as FOXA2.

In conclusion, our study reveals a novel synergistic mechanism of LPL gene induction by LXRs and FOXA2 in the liver in response to intracellular or extracellular signals such as oxysterols and insulin treatment, facilitating the cross talk between the signaling pathways that are induced by these signals. This mechanism may not be restricted to the LPL gene but may have wide implications to other genes involved in cholesterol, triglyceride and glucose metabolism. Understanding in depth the mechanisms by which lipid and glucose metabolic pathways are interconnected in the liver and possibly in other tissues by factors such as LXRs and FOXA2 may open the way to novel therapeutic strategies for humans with complex metabolic conditions such as dyslipidemia, diabetes, Coronary Artery Disease, metabolic syndrome and other lipid disorders that are characterized by low HDL levels.

<u>PART III</u>:

The role of the hepatic factor FOXA2 in the regulation of sterol transporters, ABCG5 and ABCG8, by LXRs in the liver

Excess cholesterol from peripheral tissues is transported via HDL particles to the liver for excretion in the bile as cholesterol or bile acids, a process known as reverse cholesterol transport. Biogenesis of HDL is initiated by the synthesis and secretion of apolipoprotein apoA-I mainly by the liver. ApoA-I interacts with the cholesterol and phospholipid membrane transporter ATP Binding Cassette Transporter A1 (ABCA1) and is gradually lipidated to form nascent discoidal HDL particles. These particles are matured by the enzyme lecithin:cholesterol acyltransferase (LCAT) to spherical HDL which is subsequently remodeled by the ABCG1 transporter in macrophages and various enzymes and transfer proteins including hepatic lipase, phospholipid transfer protein (PLTP) and cholesterol ester transfer protein (CETP). HDL cholesteryl esters are transferred to the liver by Scavenger Receptor Class B Type I (SR-BI) for excretion into the bile by the cholesterol transporters ABCG5 and ABCG8. Almost every step of this process is stimulated by LXRs and their ligands. Various genes that are involved in biogenesis and remodeling of HDL cholesterol, including lipid transporters ABCA1, ABCG1, SR-BI, and transfer proteins CETP, PLTP, contain LXR responsive elements (LXREs) in their promoters (Figure 1.16) and are induced by LXR ligands or high cholesterol diets (403, 405-408, 414, 419-421). Moreover, the lipid transporters ABCG5 and ABCG8 are induced by cholesterol feeding and by treatment with LXR agonists (427, 478, 479). However, no apparent LXR binding sites were found in the intergenic region between the two genes (480).

In this part, we investigated the synergy between FOXA2 and LXRs in the regulation of genes involved in HDL metabolism in the liver, as described in part II. First, we confirmed the positive regulation of various HDL genes by the LXR synthetic ligand, T0901317, in HepG2 cells and in primary mouse hepatocytes, isolated from the livers of C57BL/6 mice. As shown in Figure 3.38A and B, T0901317 treatment increased strongly the mRNA levels of the mouse (panel A) and human (panel B) genes encoding the lipid transporters ABCG1, ABCG5, ABCG8 and the human gene encoding cholesteryl ester transfer protein (CETP) (2nd lane of panels A, B). However, the expression of the genes LIPC and PLTP was not changed by the T0901317 agonist (Figure 3.38A and B).

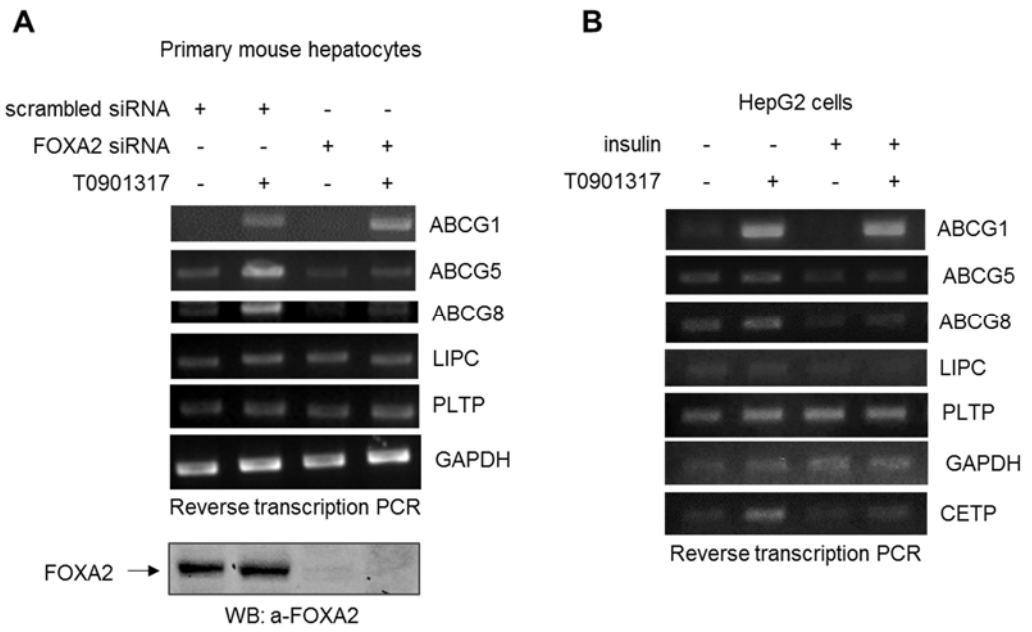

Figure 3.38. Inactivation of the hepatic factor FOXA2 by siRNA silencing or insulin affects the expression of ABCG5 and ABCG8 genes by the LXR agonist T0901317in primary hepatocytes and HepG2 cells. (A) Primary mouse hepatocytes were transfected with 50nM of a scrambled siRNA or a FOXA2 specific siRNA and were treated with the synthetic LXR agonist T0901317 (1μM) for 24 hours or left untreated. Total RNA was extracted and the expression of the HDL metabolism genes was analyzed by reverse transcription PCR. The expression levels of GAPDH gene were used for normalization purposes. Protein levels of FOXA2 were determined by immunoblotting using the anti-FOXA2 antibody (Bottom of the panel). (B) HepG2 cells were treated with insulin (500nM) or/and T0901317 agonist (1μM) for 24 hours or left untreated and total RNA was extracted. The expression of the HDL genes was analyzed by reverse transcription PCR. The expression levels of GAPDH gene were used for normalization purposes.

A previous study had shown that mice heterozygous for the FOXA2 factor have reduced levels of HDL in the plasma (325), suggesting the involvement of FOXA2 in the regulation of HDL genes. Using a database search for putative transcription factor binding sites (www.genomatix.de) we identified putative recognition sites for the FOXA2 hepatic factor in proximity with characterized LXREs in the promoter regions of the human ABCG1, CETP and hepatic lipase (LIPC) genes (data not shown). Next, we investigated the possible requirement of FOXA2 for the oxysterol induction of HDL genes. For this purpose, we silenced the endogenous FOXA2 expression in primary mouse hepatocytes, in the presence or absence of LXR activation by T0901317 and the mRNA levels of HDL genes were determined. As shown in Figure 3.38A, silencing of endogenous FOXA2 by the

FOXA2-specific siRNA reduced the basal expression levels of ABCG5 and ABCG8 genes in mouse primary hepatocytes, without affecting the expression of ABCG1, LIPC and PLTP genes (compare lanes 1 and 3). The FOXA2-specific siRNA inhibited also the T0901317-inducible expression of the ABCG5 and ABCG8 genes (Figure 3.38A, lane 4), indicating that FOXA2 is essential for the upregulation of these lipid transporters by the LXR ligand T0901317 (unpublished data by Ioanna Tiniakou). Similar results were obtained, when HepG2 cells were treated simultaneously with insulin and T0901317 agonist. As shown in Figure 3.38B, insulin reduced strongly both the basal and the T0901317-inducible mRNA levels of the ABCG5, ABCG8 and CETP genes (compare lanes 1, 3 and 4). The findings from Figure 3.38 strongly indicate that induction of the ABCG5, ABCG8 and CETP genes by oxysterols in hepatic cells requires the presence of FOXA2 in the nucleus.

Based on the above data, we focused on the regulation of ABCG5 and ABCG8 genes that respond to both T0901317 and FOXA2 and investigated whether their regulation is similar to the model of LPL regulation by FOXA2 and LXRs, as we showed in part II. The human ABCG5 and ABCG8 genes are located adjacent to each other in a head-to-head configuration on chromosome 2p21 and their first exons are separated by only 140 bp intergenic promoter region. Each gene is composed of 13 exons and 12 introns (478-482). To examine the role of FOXA2 in the promoter activity of ABCG5 and ABCG8 genes, we amplified by polymerase chain reaction from human genomic DNA the human -972/+72 ABCG5 and -939/+12 ABCG8 promoters, both of them including the intergenic region, and cloned them upstream of the luciferase gene (Figure 3.39A). HepG2 cells were transfected with the ABCG5 and ABCG8 promoter constructs along with a plasmid vector expressing FOXA2 and their relative transcriptional activity was determined by luciferase activity assays. As shown in Figure 3.39B, FOXA2 overexpression caused a 5-fold increase in the activity of the ABCG8 promoter and a 1.3-fold increase in the activity of the ABCG5 promoter. This finding indicates that a FOXA2 binding element may exist in the ABCG8 promoter, inside the ABCG5 gene, that facilitates the transactivation of ABCG8 promoter. With transactivation assays, we established also that overexpression of LXRα/RXRα in the presence of their ligands, transactivated highly the promoters of ABCG5 and ABCG8, 12-fold and 9-fold respectively, in HepG2 cells (Figure 3.39C), suggesting that an LXR responsive element (LXRE) may be located in the intergenic promoter region.

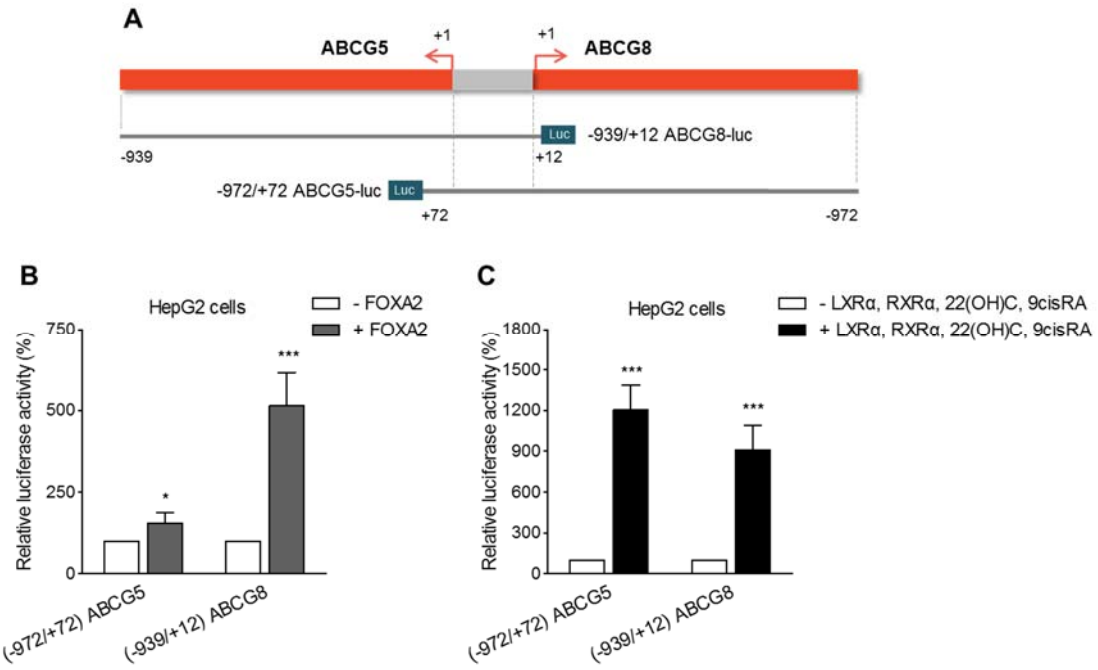

Figure 3.39. FOXA2 and nuclear receptors LXRα/RXRα activate the promoters of ABCG5 and ABCG8 genes in HepG2 cells. (A) Schematic representation of the human promoters of ABCG5 and ABCG8 genes that were cloned upstream of the luciferase reporter gene (Luc) and used in the transactivation experiments of panel B and C. (B) HepG2 cells were transiently transfected with the (−972/+72) ABCG5-luc and (−939/+12) ABCG8-luc reporter plasmids (1μg), along with a β-galactosidase expression plasmid (1μg) in the presence or absence of expression vector for FOXA2 (1μg). (C) HepG2 cells were transiently transfected with the (−972/+72) ABCG5-luc and (−939/+12) ABCG8-luc reporter plasmids (1μg), along with a β-galactosidase expression plasmid (1μg) in the presence or absence of expression vectors for LXRα, RXRα (0.5μg each) and were treated with the ligands 22(OH)C and 9cisRA (1μM each) for 24 hours or left untreated. (B and C) The normalized, relative luciferase activity (±SD) calculated form three independent experiments performed in duplicate is presented with histographs. *, $p<0.05$; ***, $p< 0.001$.

To investigate further the role of LXRs in ABCG5 and ABCG8 gene regulation in hepatic cells, short hairpin RNA (shRNA)-mediated gene silencing combined with lentivirus-mediated gene transfer methodologies were employed. For this purpose, an LXRα, LXRβ and scrambled shRNA (shLXRα, shLXRβ, shcontrol) were cloned in the pSuper vector, as described in the "Materials and Methods" section and the silencing of expression of the corresponding proteins (LXRα and LXRβ) was confirmed by transient transfection assays in HEK293T cells and western blot analysis. Figure 3.40A and B, shows that the transient overexpression of shRNA-producing vectors specific for LXRα (panel A) or LXRβ (panel B), abolished the expression of the exogenous LXRα or LXRβ genes respectively, at the protein level.

The cloned shRNAs were then subcloned into the pLKO.1 vector and lentiviral particles were produced by cotransfection of the specific LXRα or LXRβ or scrambled shRNAs vectors and other lentivirus packaging vectors (Figure 3.41). HepG2 cells were infected with lentiviruses expressing control shRNA, LXRα shRNA or LXRβ shRNA (Figure 3.41) and mRNA levels of endogenous LXR isoforms were determined to evaluate the efficiency of shRNA lentivirus infection.

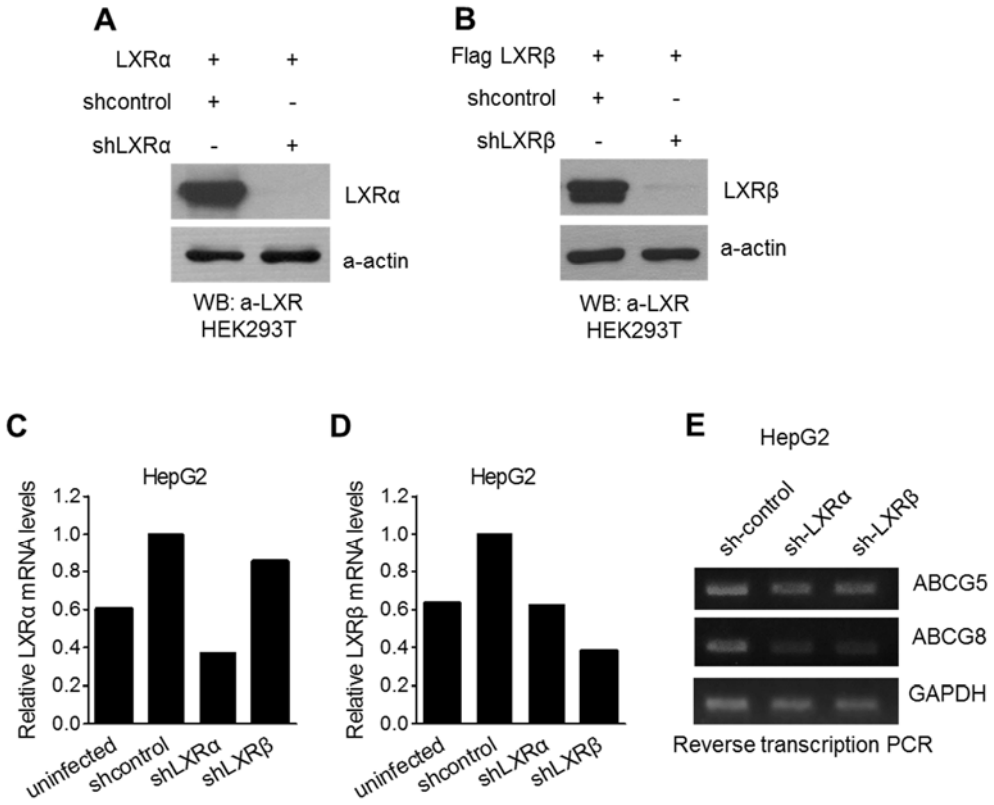

Figure 3.40. Inhibition of the nuclear receptors LXrα or LXRβ by shRNA silencing reduces the expression of ABCG5 and ABCG8 genes in HepG2 cells. (A and B) HEK293T cells were transfected with an LXRα (panel A) or LXRβ (panel B) expression vector (1μg) along with expression vectors for control shRNA or LXRα shRNA or LXRβ shRNA (1μg) and the protein levels of LXRα, LXRβ and actin (loading control) were determined by immunoblotting using the corresponding antibodies. (C-E) HepG2 cells were infected for two days with lentivirus expressing control shRNA or LXRα shRNA or LXRβ shRNA, selected with puromycin and total RNA was extracted. (C and D) LXRα and LXRβ mRNA levels were determined by reverse transcription reverse transcription quantitative PCR and normalized relative to the HPRT mRNA levels. Results are expressed as mean and shown as histographs. (E) The expression of the ABCG5 and ABCG8 genes was analyzed by reverse transcription PCR. The expression levels of GAPDH gene were used for normalization purposes.

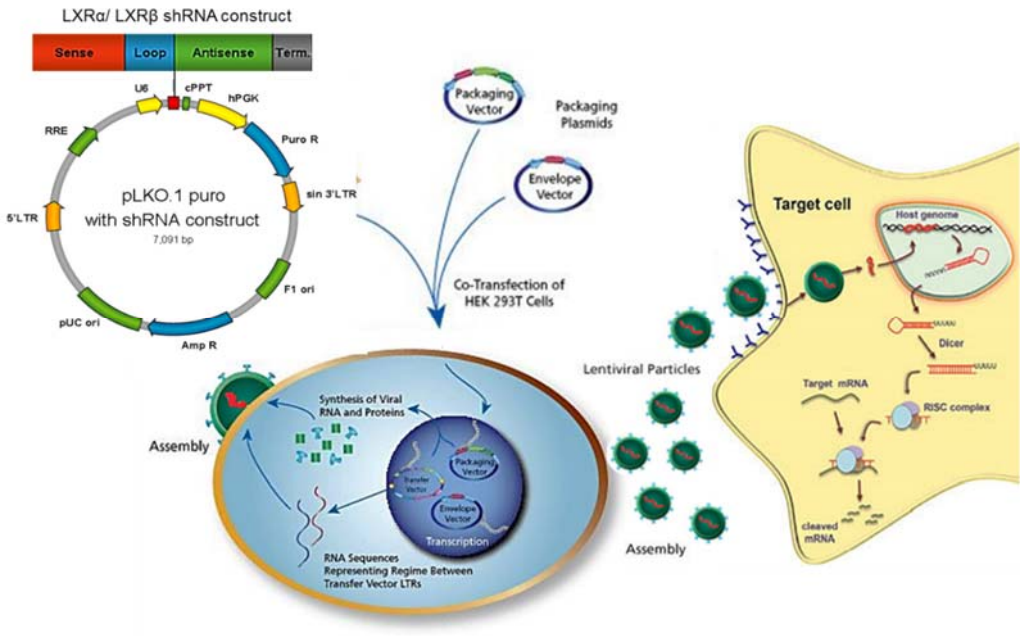

Figure 3.41. Schematic representation of the production of lentiviral particles containing LXRα/LXRβ shRNA and infection of target cells. The specific sequences of shRNAs for LXRα or LXRβ or scrambled were cloned into the pLKO.1 vector. HEK293T cells were cotransfected with the shRNA-producing vectors along with packaging and envelope vectors. Lentiviral particles were assembled and then HepG2 cells were infected by lentiviruses, in order to produce LXRα, LXRβ shRNAs and silence the expression of LXRs. See "Materials and Methods" section for details.

As shown in Figure 3.40C and D, both the shLXRα and shLXRβ lentiviruses reduced the mRNA levels of LXRα (compare bars 2 and 3, panel C) and LXRβ (compare bars 2 and 4, panel D) respectively, by 60%. Silencing the expression of endogenous LXRα or LXRβ in HepG2 cells via the specific shRNA lentiviruses reduced significantly the mRNA levels of ABCG8 and ABCG5 genes (Figure 3.40E) suggesting that LXRs are transcriptional activators of the lipid transporters ABCG8 and ABCG5 in hepatic cells.

The requirement of FOXA2 for the induction of the ABCG5 and ABCG8 genes by T0901317 suggested that FOXA2 and LXRα/RXRα may transactivate the promoters of these genes in a synergistic fashion, as in the case of LPL gene (part II). To test this hypothesis, we transfected HepG2 cells with expression vectors for FOXA2 and LXRα/RXRα individually or in combination and we employed luciferase activity assays using the human -972/+72 ABCG5 and -939/+12 ABCG8 promoters (Figure 3.42A). As shown in Figure 3.42C, overexpression of FOXA2 and ligand-activated LXRα/RXRα transactivated synergistically the -939/+12 ABCG8 promoter.

In contrast, FOXA2 inhibited the induction of the ABCG5 gene by LXRs and oxysterols (Figure 3.42B), indicating an opposite regulation of ABCG5 and ABCG8 promoters by FOXA2 and LXRα/RXRα.

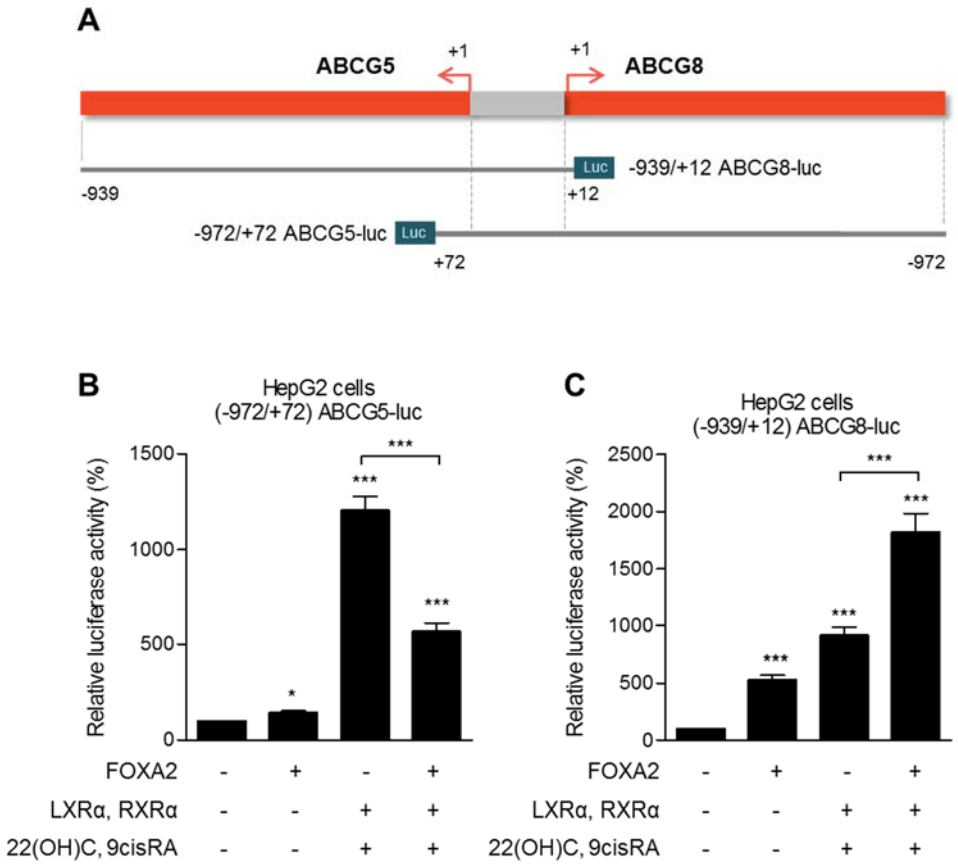

Figure 3.42. Opposite transactivation of the promoters of ABCG5 and ABCG8 genes by FOXA2 and LXRα/RXRα heterodimers. (A) Schematic representation of the human promoters of ABCG5 and ABCG8 genes that share a common small promoter fragment. (B and C) HepG2 cells were transiently transfected with the (−972/+72) ABCG5-luc (panel B) or (−939/+12) ABCG8-luc (panel C) reporter plasmids (1μg), along with a β-galactosidase expression plasmid (1μg) in the presence or absence of expression vectors for FOXA2 (1μg), LXRα, RXRα (0.5μg each) and were treated with the ligands 22(OH)C and 9cisRA (1μM) for 24 hours or left untreated. The normalized, relative luciferase activity (±SD) calculated form three independent experiments performed in duplicate is presented with histographs. (C) *, $p<0.05$; ***, $p< 0.001$.

Our observation that FOXA2 and LXRα/RXRα interact physically and synergistically induce the expression of LPL gene in hepatic cells (part II) is consistent with the data of Figures 3.38-3.42. These findings showed that ABCG5 and ABCG8 genes are induced highly by LXRs and oxysterols, and FOXA2 is critical for the LXRα/RXRα induction, in hepatic cells.

ABCG5 and ABCG8 belong to the family of ABC transporters (ATP-binding cassette), are half-transporters and form an obligate heterodimer to become functional and limit the absorption of dietary cholesterol and plant sterols by mediating the efflux of these sterols from enterocytes back into gut lumen, and by facilitating secretion of cholesterol and plant sterols from hepatocytes into bile (hepatobiliary secretion) (482-485). Consistent with their function, ABCG5 and ABCG8 are expressed almost exclusively on the apical cell surface of hepatocytes and enterocytes (486). Mutations in either of the two genes encoding ABCG5 or ABCG8 cause sitosterolemia, a disorder which is characterized by markedly elevated plasma levels of plant sterols and modest increases in plasma cholesterol, because of the increased absorption of these sterols from the small intestine and the reduced excretion into the bile (478, 479, 482, 487, 488). Due to this accumulation of sterol levels in the circulation, sitosterolemic patients develop atherosclerosis and premature cardiovascular disease (487). Conversely, a gain-of-function mutation in the human ABCG8 gene, D19H, is strongly associated with gallstone disease (489). Moreover, disruption of both ABCG5 and ABCG8 in mice show a reduction in the excretion of cholesterol and plant sterols into bile (425, 490, 491), whereas transgenic mice overexpressing these transporters show enhanced secretion of biliary cholesterol, reduced absorption of dietary sterols and attenuation of diet-induced atherosclerosis (492).

In part I we showed that FOXA2 positively regulates the expression of LPL gene in hepatic cells, via a novel FOXA2 responsive element that is localized in the proximal LPL promoter. In the present study, we investigated the role of FOXA2 hepatic factor in the regulation of ABCG5 and ABCG8 transporter in hepatocytes. Using siRNA specific for FOXA2, we silenced endogenous FOXA2 expression in primary mouse hepatocytes and we observed reduction of the basal expression levels of ABCG5 and ABCG8 genes. Furthermore, overexpression of FOXA2 in HepG2 cells transactivated strongly the promoter of ABCG8 and the promoter of ABCG5 to a lesser extent, indicating a positive role of this factor in the regulation of ABCG5 and ABCG8 expression.

The highly homologous ABCG5 and ABCG8 genes are located adjacent to one another, and both genes are transcribed in opposite directions from independent

transcription start sites that are separated by only ~150 bp of intergenic sequence (479, 493). There is evidence that Hepatocyte nuclear factor 4α (HNF4α) and GATA-binding protein 4 (GATA4) can synergistically stimulate ABCG5 and ABCG8 gene transcription in both directions from the ABCG5/ABCG8 intergenic promoter (494). ABCG5 and ABCG8 genes are regulated also by Liver Receptor Homologue 1 (LRH1) and thyroid hormone (495, 496). However, Liver X receptor is the most important positive regulator of ABCG5 and ABCG8 expression at the transcriptional level (427, 479). Activation of the LXR pathway in response to cholesterol feeding or LXR agonists induces strongly ABCG5 and ABCG8 expression levels in the liver and intestine of wild type mice, but not in LXR knockout mice. LXR activation also promotes increased biliary excretion and reduced cholesterol absorption (426, 478, 479, 497, 498). In agreement with these studies, we showed that T0901317 treatment of HepG2 cells and primary mouse hepatocytes caused a strong induction of mRNA levels of ABCG5, ABCG8 genes. Furthermore, overexpression of LXRα/RXRα and their ligands caused a strong transactivation of the promoters of ABCG5 and ABCG8. We confirmed this LXR activation of ABCG5 and ABCG8 genes, by infecting HepG2 cells with lentiviruses that express shRNAs specific for each LXR isoform. A 60% reduction of the expression of LXRα or LXRβ by the corresponding shLXR lentivirus was observed, causing a reductionin the mRNA levels of ABCG8 and ABCG5 genes in HepG2 cells. Although the regulation of ABCG8 and ABCG5 expression by LXR is well established, no LXR responsive elements (LXREs) have been identified to date. However, our findings indicate that an LXRE may be located in the intergenic promoter region of ABCG8 and ABCG5 or inside the genes in distal regions. A recent study has identified two conserved regions located in introns 1 and 6 of ABCG8, which contain a 22-bp LXRE and this sequence, in conjunction with the previously identified GATA-box and LRH-1 site led to significant expression of a reporter construct (499).

We showed in part II, that in the presence of increased concentrations of oxysterols LXRs induce the expression of the LPL gene in a synergistic fashion with FOXA2 factor, via a novel mechanism that depends on physical and functional interactions between LXRα and FOXA2. Based on this finding, we hypothesized that the model of synergistic induction by oxysterols, LXRα/RXRα and FOXA2 in hepatic cells, which is based on physical interactions between these factors, may be a general mechanism for the regulation of genes involved in HDL metabolism in the liver and specifically

for ABCG8 and ABCG5 genes. We observed that silencing of FOXA2 via the FOXA2-specific siRNA reduced the induction of ABCG5 and ABCG8 genes by the synthetic LXR ligand, T0901317, indicating that FOXA2 is critical for the upregulation of these lipid transporters by the LXR ligands. The synergy between these factors was confirmed also with transactivation assays, which showed that FOXA2 and ligand-activated LXRα/RXRα transactivated synergistically the ABCG8 promoter, but not the ABCG5 promoter. FOXA2 inhibited the induction of the ABCG5 promoter by LXRs and oxysterols in HepG2 cells. If the two transporters form a functional heterodimer, the observed difference in the activation of the promoters would not be expected. It is likely, that more distal FOXA2 elements may be present, perhaps inside the ABCG8 gene, in coding or non-coding regions that are not included in our -972/+72 ABCG5 promoter construct. In this case, FOXA2 cannot bind to the FOXA2 element, but interacts with LXR/RXR receptors and inhibits the induction of the ABCG5 gene by LXRs and oxysterols, by preventing their binding to the LXRE. Furthermore, one more FOXA2 element may be present in the -939/+12 ABCG8 promoter construct, inside the ABCG5 gene, which facilitates the binding of FOXA2 and its interaction with LXRα/RXRα, contributing to the synergistic regulation of ABCG8 gene. These observations suggest that more distal transcription factor binding sites far from the coding regions of the genes may be involved and via DNA looping regulate coordinately the expression of ABCG5 and ABCG8 genes. This remains to be confirmed with future studies characterizing these regulatory regions.

A previous study has shown that disruptions in insulin signaling, resulting in hepatic insulin resistance in mice, lead to upregulation of ABCG5, ABCG8 genes, and increased biliary cholesterol excretion. A response element for FOXO1 transcription factor was identified in the human intergenic promoter of ABCG5 and ABCG8 and the inhibition of hepatic insulin signaling resulted in re-activation of FOXO1. Adenoviral expression of a constitutively active FOXO1 form increased the mRNA levels of ABCG5 and ABCG8 in rat hepatocytes. Of considerable clinical significance, the upregulation of ABCG5 and ABCG8 genes in insulin-resistant liver resulted in the formation of gallstones, thereby linking insulin resistance to the hyperglycemia, dyslipidemia and gallbladder disease (500). In agreement with this study, we showed that insulin treatment in HepG2 cells, which inactivates FOXA2 by nuclear exclusion, caused a strong reduction of basal and also of T0901317-inducible

expression of ABCG5 and ABCG8 genes. Except of the FOXO1 binding site in the intergenic promoter of ABCG5, ABCG8, an additional FOXA2 element may be present in the ABCG5 promoter. Our findings indicate that FOXA2 is required to be present in the nucleus, to induce ABCG5, ABCG8 genes. The increase of ABCG5 and ABCG8 expression in states of insulin resistance/ inhibition of hepatic insulin signaling may be explained by the disinhibition of FOXA2 or/and FOXO1 by insulin and the active FOXA2/FOXO1 that induces expression of these genes.

In the liver, except from cholesterol excretion into the bile via the ABCG5 and ABCG8 transporters, excess cholesterol is converted also to bile acids for excretion in the bile through bile acid transporters (454-456). Importantly, inactivation of FOXA2 in the liver of mice inhibited the expression of bile acid transporters resulting in intrahepatic cholestasis (323). Furthermore, it was also shown that patients with cholestatic syndromes have lower FOXA2 levels in their liver (323). In a previous study we showed that FOXA2 is implicated in the regulation of another ABC gene, in hepatic cells. FOXA2 binds to the proximal promoter of the human ABCA1 gene, at three sites, and compromises the upregulation of ABCA1 gene expression by oxysterol-activated LXRs under conditions of cholesterol loading (329). Thus, FOXA2 emerges as a key regulator of cholesterol and bile acid metabolism in the liver.

The sterol transporters ABCG5/ABCG8 play a key role in reverse cholesterol transport pathway promoting cholesterol removal from the body. Thus it seems logical to assume that overexpression of ABCG5 and ABCG8 should inhibit development of atherosclerosis while deletion of ABCG5 and ABCG8 should promote atherosclerosis. The elevated plant sterols may contribute to cardiovascular disease by disrupting normal cholesterol homeostasis. Sitosterolemic patients are highly sensitive to dietary cholesterol and upon a high-cholesterol diet develop hypercholesterolemia, atherosclerosis and premature cardiovascular disease (479, 482, 487, 488, 501, 502). This was supported by a study showing that overexpression of ABCG5 and ABCG8 in the intestine and liver of an atherogenic (LDLR)-deficient mouse model leads to a reduction of aortic atherosclerotic lesion area in association with reduced plasma cholesterol levels (503). In agreement, SNPs associated with reduced ABCG5 and ABCG8 function and increased phytosterol levels were also associated with increased prevalence of CAD, and one allele that resulted in increased function of the transporters was associated with reduced CAD (504). Therefore, these

observations suggest that ABCG5 and ABCG8 transporters can modulate plasma cholesterol levels and interventions to enhance the ABCG5/8 pathway could protect against CAD in hypercholesterolemic subjects by eliminating more cholesterol in the bile and reducing plasma cholesterol levels.

Taken together, it is quite obvious that ABCG5 and ABCG8 are coordinately modulated by multiple molecular players and transcriptional processes. More work in this field may prove to be key for understanding the regulation and role of these two important genes in lipid metabolism and for identifying new therapeutic drug targets for preventing atherosclerosis, coronary heart disease, diabetes and other metabolic diseases.

4. REFERENCES

1. Zannis VI, Kypreos, K.E., Chroni, A., Kardassis, D., Zanni, E.E. Lipoproteins and atherogenesis. In: Loscalzo J, editor. Molecular mechanisms of atherosclerosis: Taylor & Francis; 2004. p. 11-174.
2. Gotto AM, Jr., Pownall HJ, Havel RJ. Introduction to the plasma lipoproteins. Methods in enzymology. 1986;128:3-41.
3. Hegele RA. Monogenic dyslipidemias: window on determinants of plasma lipoprotein metabolism. Am J Hum Genet. 2001;69(6):1161-77.
4. Ridker PM. LDL cholesterol: controversies and future therapeutic directions. Lancet. 2014;384(9943):607-17.
5. Shelness GS, Sellers JA. Very-low-density lipoprotein assembly and secretion. Curr Opin Lipidol. 2001;12(2):151-7.
6. Hussain MM, Kancha RK, Zhou Z, Luchoomun J, Zu H, Bakillah A. Chylomicron assembly and catabolism: role of apolipoproteins and receptors. Biochim Biophys Acta. 1996;1300(3):151-70.
7. Zannis VI, Chroni A, Krieger M. Role of apoA-I, ABCA1, LCAT, and SR-BI in the biogenesis of HDL. J Mol Med. 2006;84(4):276-94.
8. Karpe F. Postprandial lipoprotein metabolism and atherosclerosis. J Intern Med. 1999;246(4):341-55.
9. Ramasamy I. Recent advances in physiological lipoprotein metabolism. Clin Chem Lab Med. 2014;52(12):1695-727.
10. Kardassis D, Mosialou I, Kanaki M, Tiniakou I, Thymiakou E. Metabolism of HDL and its regulation. Curr Med Chem. 2014;21(25):2864-80.
11. Beisiegel U, Krapp A, Weber W, Olivecrona G. The role of alpha 2M receptor/LRP in chylomicron remnant metabolism. Annals of the New York Academy of Sciences. 1994;737:53-69.
12. Beisiegel U, Weber W, Ihrke G, Herz J, Stanley KK. The LDL-receptor-related protein, LRP, is an apolipoprotein E-binding protein. Nature. 1989;341(6238):162-4.
13. Willnow TE, Sheng Z, Ishibashi S, Herz J. Inhibition of hepatic chylomicron remnant uptake by gene transfer of a receptor antagonist. Science. 1994;264(5164):1471-4.
14. Gordon DA, Jamil H. Progress towards understanding the role of microsomal triglyceride transfer protein in apolipoprotein-B lipoprotein assembly. Biochim Biophys Acta. 2000;1486(1):72-83.
15. Niemeier A, Gafvels M, Heeren J, Meyer N, Angelin B, Beisiegel U. VLDL receptor mediates the uptake of human chylomicron remnants in vitro. J Lipid Res. 1996;37(8):1733-42.
16. Marais AD, Kim JB, Wasserman SM, Lambert G. PCSK9 inhibition in LDL cholesterol reduction: genetics and therapeutic implications of very low plasma lipoprotein levels. Pharmacology & therapeutics. 2015;145:58-66.
17. Zannis VI, Chroni A, Kypreos KE, Kan HY, Cesar TB, Zanni EE, et al. Probing the pathways of chylomicron and HDL metabolism using adenovirus-mediated gene transfer. Curr Opin Lipidol. 2004;15(2):151-66.
18. Zannis VI, Fotakis P, Koukos G, Kardassis D, Ehnholm C, Jauhiainen M, et al. HDL biogenesis, remodeling, and catabolism. Handb Exp Pharmacol. 2015;224:53-111.
19. Denis M, Haidar B, Marcil M, Bouvier M, Krimbou L, Genest J, Jr. Molecular and cellular physiology of apolipoprotein A-I lipidation by the ATP-binding cassette transporter A1 (ABCA1). J Biol Chem. 2004;279(9):7384-94.
20. Jonas A. Lecithin cholesterol acyltransferase. Biochim Biophys Acta. 2000;1529(1-3):245-56.
21. Wang N, Lan D, Chen W, Matsuura F, Tall AR. ATP-binding cassette transporters G1 and G4 mediate cellular cholesterol efflux to high-density lipoproteins. Proc Natl Acad Sci U S A. 2004;101(26):9774-9.

22. Lusa S, Jauhiainen M, Metso J, Somerharju P, Ehnholm C. The mechanism of human plasma phospholipid transfer protein-induced enlargement of high-density lipoprotein particles: evidence for particle fusion. Biochem J. 1996;313 (Pt 1):275-82.
23. Barter PJ, Brewer HB, Jr., Chapman MJ, Hennekens CH, Rader DJ, Tall AR. Cholesteryl ester transfer protein: a novel target for raising HDL and inhibiting atherosclerosis. Arterioscler Thromb Vasc Biol. 2003;23(2):160-7.
24. McCoy MG, Sun GS, Marchadier D, Maugeais C, Glick JM, Rader DJ. Characterization of the lipolytic activity of endothelial lipase. J Lipid Res. 2002;43(6):921-9.
25. Dichek HL, Qian K, Agrawal N. Divergent effects of the catalytic and bridging functions of hepatic lipase on atherosclerosis. Arterioscler Thromb Vasc Biol. 2004;24(9):1696-702.
26. Ishida T, Choi S, Kundu RK, Hirata K, Rubin EM, Cooper AD, et al. Endothelial lipase is a major determinant of HDL level. J Clin Invest. 2003;111(3):347-55.
27. Krieger M. Scavenger receptor class B type I is a multiligand HDL receptor that influences diverse physiologic systems. The Journal of clinical investigation. 2001;108(6):793-7.
28. Wolkoff AW, Cohen DE. Bile acid regulation of hepatic physiology: I. Hepatocyte transport of bile acids. American journal of physiology Gastrointestinal and liver physiology. 2003;284(2):G175-9.
29. Silver DL, Wang N, Xiao X, Tall AR. High density lipoprotein (HDL) particle uptake mediated by scavenger receptor class B type 1 results in selective sorting of HDL cholesterol from protein and polarized cholesterol secretion. J Biol Chem. 2001;276(27):25287-93.
30. Rhainds D, Brissette L. The role of scavenger receptor class B type I (SR-BI) in lipid trafficking. defining the rules for lipid traders. Int J Biochem Cell Biol. 2004;36(1):39-77.
31. van der Velde AE, Brufau G, Groen AK. Transintestinal cholesterol efflux. Curr Opin Lipidol. 2010;21(3):167-71.
32. Besler C, Luscher TF, Landmesser U. Molecular mechanisms of vascular effects of High-density lipoprotein: alterations in cardiovascular disease. EMBO molecular medicine. 2012;4(4):251-68.
33. Singh IM, Shishehbor MH, Ansell BJ. High-density lipoprotein as a therapeutic target: a systematic review. JAMA. 2007;298(7):786-98.
34. Rader DJ, Daugherty A. Translating molecular discoveries into new therapies for atherosclerosis. Nature. 2008;451(7181):904-13.
35. Stary HC. Natural history and histological classification of atherosclerotic lesions: an update. Arterioscler Thromb Vasc Biol. 2000;20(5):1177-8.
36. Barter PJ, Rye KA. High density lipoproteins and coronary heart disease. Atherosclerosis. 1996;121(1):1-12.
37. Chapman MJ, Assmann G, Fruchart JC, Shepherd J, Sirtori C. Raising high-density lipoprotein cholesterol with reduction of cardiovascular risk: the role of nicotinic acid--a position paper developed by the European Consensus Panel on HDL-C. Curr Med Res Opin. 2004;20(8):1253-68.
38. Briel M, Ferreira-Gonzalez I, You JJ, Karanicolas PJ, Akl EA, Wu P, et al. Association between change in high density lipoprotein cholesterol and cardiovascular disease morbidity and mortality: systematic review and meta-regression analysis. BMJ. 2009;338:b92.
39. van der Steeg WA, Holme I, Boekholdt SM, Larsen ML, Lindahl C, Stroes ES, et al. High-density lipoprotein cholesterol, high-density lipoprotein particle size, and apolipoprotein A-I: significance for cardiovascular risk: the IDEAL and EPIC-Norfolk studies. Journal of the American College of Cardiology. 2008;51(6):634-42.
40. Barter P, Gotto AM, LaRosa JC, Maroni J, Szarek M, Grundy SM, et al. HDL cholesterol, very low levels of LDL cholesterol, and cardiovascular events. N Engl J Med. 2007;357(13):1301-10.

41. Emerging Risk Factors C, Di Angelantonio E, Sarwar N, Perry P, Kaptoge S, Ray KK, et al. Major lipids, apolipoproteins, and risk of vascular disease. JAMA. 2009;302(18):1993-2000.
42. Ginsberg HN. Diabetic dyslipidemia: basic mechanisms underlying the common hypertriglyceridemia and low HDL cholesterol levels. Diabetes. 1996;45 Suppl 3:S27-30.
43. Singaraja RR, Van Eck M, Bissada N, Zimetti F, Collins HL, Hildebrand RB, et al. Both hepatic and extrahepatic ABCA1 have discrete and essential functions in the maintenance of plasma high-density lipoprotein cholesterol levels in vivo. Circulation. 2006;114(12):1301-9.
44. Rye KA, Bursill CA, Lambert G, Tabet F, Barter PJ. The metabolism and anti-atherogenic properties of HDL. J Lipid Res. 2009;50 Suppl:S195-200.
45. Davidson WS, Silva RA, Chantepie S, Lagor WR, Chapman MJ, Kontush A. Proteomic analysis of defined HDL subpopulations reveals particle-specific protein clusters: relevance to antioxidative function. Arterioscler Thromb Vasc Biol. 2009;29(6):870-6.
46. Vaisar T, Pennathur S, Green PS, Gharib SA, Hoofnagle AN, Cheung MC, et al. Shotgun proteomics implicates protease inhibition and complement activation in the antiinflammatory properties of HDL. J Clin Invest. 2007;117(3):746-56.
47. Annema W, von Eckardstein A. High-density lipoproteins. Multifunctional but vulnerable protections from atherosclerosis. Circ J. 2013;77(10):2432-48.
48. Mineo C, Shaul PW. Novel biological functions of high-density lipoprotein cholesterol. Circ Res. 2012;111(8):1079-90.
49. Mertens A, Holvoet P. Oxidized LDL and HDL: antagonists in atherothrombosis. FASEB J. 2001;15(12):2073-84.
50. Navab M, Hama SY, Anantharamaiah GM, Hassan K, Hough GP, Watson AD, et al. Normal high density lipoprotein inhibits three steps in the formation of mildly oxidized low density lipoprotein: steps 2 and 3. J Lipid Res. 2000;41(9):1495-508.
51. Barter PJ, Nicholls S, Rye KA, Anantharamaiah GM, Navab M, Fogelman AM. Antiinflammatory properties of HDL. Circ Res. 2004;95(8):764-72.
52. Mineo C, Deguchi H, Griffin JH, Shaul PW. Endothelial and antithrombotic actions of HDL. Circ Res. 2006;98(11):1352-64.
53. Nofer JR, Walter M, Kehrel B, Wierwille S, Tepel M, Seedorf U, et al. HDL3-mediated inhibition of thrombin-induced platelet aggregation and fibrinogen binding occurs via decreased production of phosphoinositide-derived second messengers 1,2-diacylglycerol and inositol 1,4,5-tris-phosphate. Arterioscler Thromb Vasc Biol. 1998;18(6):861-9.
54. Tso C, Martinic G, Fan WH, Rogers C, Rye KA, Barter PJ. High-density lipoproteins enhance progenitor-mediated endothelium repair in mice. Arterioscler Thromb Vasc Biol. 2006;26(5):1144-9.
55. Mineo C, Yuhanna IS, Quon MJ, Shaul PW. High density lipoprotein-induced endothelial nitric-oxide synthase activation is mediated by Akt and MAP kinases. J Biol Chem. 2003;278(11):9142-9.
56. Seetharam D, Mineo C, Gormley AK, Gibson LL, Vongpatanasin W, Chambliss KL, et al. High-density lipoprotein promotes endothelial cell migration and reendothelialization via scavenger receptor-B type I. Circ Res. 2006;98(1):63-72.
57. Nofer JR, Levkau B, Wolinska I, Junker R, Fobker M, von Eckardstein A, et al. Suppression of endothelial cell apoptosis by high density lipoproteins (HDL) and HDL-associated lysosphingolipids. J Biol Chem. 2001;276(37):34480-5.
58. Despres JP. HDL cholesterol studies--more of the same? Nat Rev Cardiol. 2013;10(2):70-2.
59. Mahdy Ali K, Wonnerth A, Huber K, Wojta J. Cardiovascular disease risk reduction by raising HDL cholesterol--current therapies and future opportunities. British journal of pharmacology. 2012;167(6):1177-94.

60. Balder JW, Staels B, Kuivenhoven JA. Pharmacological interventions in human HDL metabolism. Curr Opin Lipidol. 2013;24(6):500-9.
61. Saha SA, Kizhakepunnur LG, Bahekar A, Arora RR. The role of fibrates in the prevention of cardiovascular disease--a pooled meta-analysis of long-term randomized placebo-controlled clinical trials. American heart journal. 2007;154(5):943-53.
62. Jun M, Foote C, Lv J, Neal B, Patel A, Nicholls SJ, et al. Effects of fibrates on cardiovascular outcomes: a systematic review and meta-analysis. Lancet. 2010;375(9729):1875-84.
63. Khoury N, Goldberg AC. The use of fibric Acid derivatives in cardiovascular prevention. Curr Treat Options Cardiovasc Med. 2011;13(4):335-42.
64. Henry RR, Lincoff AM, Mudaliar S, Rabbia M, Chognot C, Herz M. Effect of the dual peroxisome proliferator-activated receptor-alpha/gamma agonist aleglitazar on risk of cardiovascular disease in patients with type 2 diabetes (SYNCHRONY): a phase II, randomised, dose-ranging study. Lancet. 2009;374(9684):126-35.
65. Fruchart JC. Selective peroxisome proliferator-activated receptor alpha modulators (SPPARMalpha): the next generation of peroxisome proliferator-activated receptor alpha-agonists. Cardiovasc Diabetol. 2013;12:82.
66. Blankenhorn DH, Azen SP, Crawford DW, Nessim SA, Sanmarco ME, Selzer RH, et al. Effects of colestipol-niacin therapy on human femoral atherosclerosis. Circulation. 1991;83(2):438-47.
67. Vega GL, Grundy SM. Lipoprotein responses to treatment with lovastatin, gemfibrozil, and nicotinic acid in normolipidemic patients with hypoalphalipoproteinemia. Arch Intern Med. 1994;154(1):73-82.
68. Kamanna VS, Kashyap ML. Mechanism of action of niacin. Am J Cardiol. 2008;101(8A):20B-6B.
69. McTaggart F, Jones P. Effects of statins on high-density lipoproteins: a potential contribution to cardiovascular benefit. Cardiovascular drugs and therapy / sponsored by the International Society of Cardiovascular Pharmacotherapy. 2008;22(4):321-38.
70. Jones PH, Davidson MH, Stein EA, Bays HE, McKenney JM, Miller E, et al. Comparison of the efficacy and safety of rosuvastatin versus atorvastatin, simvastatin, and pravastatin across doses (STELLAR* Trial). Am J Cardiol. 2003;92(2):152-60.
71. Paciaroni M, Bogousslavsky J. Statins and stroke prevention. Expert Rev Cardiovasc Ther. 2009;7(10):1231-43.
72. Barter PJ, Brandrup-Wognsen G, Palmer MK, Nicholls SJ. Effect of statins on HDL-C: a complex process unrelated to changes in LDL-C: analysis of the VOYAGER Database. J Lipid Res. 2010;51(6):1546-53.
73. Martin G, Duez H, Blanquart C, Berezowski V, Poulain P, Fruchart JC, et al. Statin-induced inhibition of the Rho-signaling pathway activates PPARalpha and induces HDL apoA-I. J Clin Invest. 2001;107(11):1423-32.
74. Inazu A, Brown ML, Hesler CB, Agellon LB, Koizumi J, Takata K, et al. Increased high-density lipoprotein levels caused by a common cholesteryl-ester transfer protein gene mutation. N Engl J Med. 1990;323(18):1234-8.
75. Kastelein JJ, van Leuven SI, Burgess L, Evans GW, Kuivenhoven JA, Barter PJ, et al. Effect of torcetrapib on carotid atherosclerosis in familial hypercholesterolemia. N Engl J Med. 2007;356(16):1620-30.
76. Schwartz GG, Olsson AG, Abt M, Ballantyne CM, Barter PJ, Brumm J, et al. Effects of dalcetrapib in patients with a recent acute coronary syndrome. N Engl J Med. 2012;367(22):2089-99.
77. Voight BF, Peloso GM, Orho-Melander M, Frikke-Schmidt R, Barbalic M, Jensen MK, et al. Plasma HDL cholesterol and risk of myocardial infarction: a mendelian randomisation study. Lancet. 2012;380(9841):572-80.

78. Navab M, Anantharamaiah GM, Hama S, Garber DW, Chaddha M, Hough G, et al. Oral administration of an Apo A-I mimetic Peptide synthesized from D-amino acids dramatically reduces atherosclerosis in mice independent of plasma cholesterol. Circulation. 2002;105(3):290-2.
79. Navab M, Anantharamaiah GM, Reddy ST, Hama S, Hough G, Grijalva VR, et al. Oral D-4F causes formation of pre-beta high-density lipoprotein and improves high-density lipoprotein-mediated cholesterol efflux and reverse cholesterol transport from macrophages in apolipoprotein E-null mice. Circulation. 2004;109(25):3215-20.
80. Chattopadhyay A, Navab M, Hough G, Gao F, Meriwether D, Grijalva V, et al. A novel approach to oral apoA-I mimetic therapy. J Lipid Res. 2013;54(4):995-1010.
81. Badimon JJ, Badimon L, Galvez A, Dische R, Fuster V. High density lipoprotein plasma fractions inhibit aortic fatty streaks in cholesterol-fed rabbits. Laboratory investigation; a journal of technical methods and pathology. 1989;60(3):455-61.
82. Badimon JJ, Badimon L, Fuster V. Regression of atherosclerotic lesions by high density lipoprotein plasma fraction in the cholesterol-fed rabbit. J Clin Invest. 1990;85(4):1234-41.
83. Nissen SE, Tsunoda T, Tuzcu EM, Schoenhagen P, Cooper CJ, Yasin M, et al. Effect of recombinant ApoA-I Milano on coronary atherosclerosis in patients with acute coronary syndromes: a randomized controlled trial. JAMA. 2003;290(17):2292-300.
84. Easton R, Gille A, D'Andrea D, Davis R, Wright SD, Shear C. A multiple ascending dose study of CSL112, an infused formulation of ApoA-I. J Clin Pharmacol. 2014;54(3):301-10.
85. Terasaka N, Hiroshima A, Koieyama T, Ubukata N, Morikawa Y, Nakai D, et al. T-0901317, a synthetic liver X receptor ligand, inhibits development of atherosclerosis in LDL receptor-deficient mice. FEBS Lett. 2003;536(1-3):6-11.
86. Calkin AC, Tontonoz P. Transcriptional integration of metabolism by the nuclear sterol-activated receptors LXR and FXR. Nat Rev Mol Cell Biol. 2012;13(4):213-24.
87. Deeb SS, Peng RL. Structure of the human lipoprotein lipase gene. Biochemistry. 1989;28(10):4131-5.
88. Holmes RS, Vandeberg JL, Cox LA. Comparative studies of vertebrate lipoprotein lipase: a key enzyme of very low density lipoprotein metabolism. Comp Biochem Physiol Part D Genomics Proteomics. 2011;6(2):224-34.
89. Kirchgessner TG, Chuat JC, Heinzmann C, Etienne J, Guilhot S, Svenson K, et al. Organization of the human lipoprotein lipase gene and evolution of the lipase gene family. Proc Natl Acad Sci U S A. 1989;86(24):9647-51.
90. Wion KL, Kirchgessner TG, Lusis AJ, Schotz MC, Lawn RM. Human lipoprotein lipase complementary DNA sequence. Science. 1987;235(4796):1638-41.
91. Hide WA, Chan L, Li WH. Structure and evolution of the lipase superfamily. J Lipid Res. 1992;33(2):167-78.
92. Wong H, Schotz MC. The lipase gene family. J Lipid Res. 2002;43(7):993-9.
93. Wong H, Davis RC, Thuren T, Goers JW, Nikazy J, Waite M, et al. Lipoprotein lipase domain function. J Biol Chem. 1994;269(14):10319-23.
94. McIlhargey TL, Yang Y, Wong H, Hill JS. Identification of a lipoprotein lipase cofactor-binding site by chemical cross-linking and transfer of apolipoprotein C-II-responsive lipolysis from lipoprotein lipase to hepatic lipase. J Biol Chem. 2003;278(25):23027-35.
95. Emmerich J, Beg OU, Peterson J, Previato L, Brunzell JD, Brewer HB, Jr., et al. Human lipoprotein lipase. Analysis of the catalytic triad by site-directed mutagenesis of Ser-132, Asp-156, and His-241. J Biol Chem. 1992;267(6):4161-5.
96. Dugi KA, Dichek HL, Talley GD, Brewer HB, Jr., Santamarina-Fojo S. Human lipoprotein lipase: the loop covering the catalytic site is essential for interaction with lipid substrates. J Biol Chem. 1992;267(35):25086-91.

97. Wang H, Eckel RH. Lipoprotein lipase: from gene to obesity. Am J Physiol Endocrinol Metab. 2009;297(2):E271-88.
98. Hata A, Ridinger DN, Sutherland S, Emi M, Shuhua Z, Myers RL, et al. Binding of lipoprotein lipase to heparin. Identification of five critical residues in two distinct segments of the amino-terminal domain. J Biol Chem. 1993;268(12):8447-57.
99. Ma Y, Henderson HE, Liu MS, Zhang H, Forsythe IJ, Clarke-Lewis I, et al. Mutagenesis in four candidate heparin binding regions (residues 279-282, 291-304, 390-393, and 439-448) and identification of residues affecting heparin binding of human lipoprotein lipase. J Lipid Res. 1994;35(11):2049-59.
100. Osborne JC, Jr., Bengtsson-Olivecrona G, Lee NS, Olivecrona T. Studies on inactivation of lipoprotein lipase: role of the dimer to monomer dissociation. Biochemistry. 1985;24(20):5606-11.
101. Wong H, Yang D, Hill JS, Davis RC, Nikazy J, Schotz MC. A molecular biology-based approach to resolve the subunit orientation of lipoprotein lipase. Proc Natl Acad Sci U S A. 1997;94(11):5594-8.
102. Griffon N, Budreck EC, Long CJ, Broedl UC, Marchadier DH, Glick JM, et al. Substrate specificity of lipoprotein lipase and endothelial lipase: studies of lid chimeras. J Lipid Res. 2006;47(8):1803-11.
103. Wang CS, Hartsuck J, McConathy WJ. Structure and functional properties of lipoprotein lipase. Biochim Biophys Acta. 1992;1123(1):1-17.
104. Camps L, Reina M, Llobera M, Bengtsson-Olivecrona G, Olivecrona T, Vilaro S. Lipoprotein lipase in lungs, spleen, and liver: synthesis and distribution. J Lipid Res. 1991;32(12):1877-88.
105. Camps L, Reina M, Llobera M, Vilaro S, Olivecrona T. Lipoprotein lipase: cellular origin and functional distribution. Am J Physiol. 1990;258(4 Pt 1):C673-81.
106. Goldberg IJ, Soprano DR, Wyatt ML, Vanni TM, Kirchgessner TG, Schotz MC. Localization of lipoprotein lipase mRNA in selected rat tissues. J Lipid Res. 1989;30(10):1569-77.
107. Chajek T, Stein O, Stein Y. Pre- and post-natal development of lipoprotein lipase and hepatic triglyceride hydrolase activity in rat tissues. Atherosclerosis. 1977;26(4):549-61.
108. Mead JR, Irvine SA, Ramji DP. Lipoprotein lipase: structure, function, regulation, and role in disease. J Mol Med (Berl). 2002;80(12):753-69.
109. Braun JE, Severson DL. Regulation of the synthesis, processing and translocation of lipoprotein lipase. Biochem J. 1992;287 (Pt 2):337-47.
110. Enerback S, Gimble JM. Lipoprotein lipase gene expression: physiological regulators at the transcriptional and post-transcriptional level. Biochim Biophys Acta. 1993;1169(2):107-25.
111. Peterfy M, Ben-Zeev O, Mao HZ, Weissglas-Volkov D, Aouizerat BE, Pullinger CR, et al. Mutations in LMF1 cause combined lipase deficiency and severe hypertriglyceridemia. Nat Genet. 2007;39(12):1483-7.
112. Peterfy M. Lipase maturation factor 1: a lipase chaperone involved in lipid metabolism. Biochim Biophys Acta. 2012;1821(5):790-4.
113. Ben-Zeev O, Hosseini M, Lai CM, Ehrhardt N, Wong H, Cefalu AB, et al. Lipase maturation factor 1 is required for endothelial lipase activity. J Lipid Res. 2011;52(6):1162-9.
114. Sha H, Sun S, Francisco AB, Ehrhardt N, Xue Z, Liu L, et al. The ER-associated degradation adaptor protein Sel1L regulates LPL secretion and lipid metabolism. Cell Metab. 2014;20(3):458-70.
115. Klinger SC, Glerup S, Raarup MK, Mari MC, Nyegaard M, Koster G, et al. SorLA regulates the activity of lipoprotein lipase by intracellular trafficking. J Cell Sci. 2011;124(Pt 7):1095-105.

116. Beigneux AP, Davies BS, Gin P, Weinstein MM, Farber E, Qiao X, et al. Glycosylphosphatidylinositol-anchored high-density lipoprotein-binding protein 1 plays a critical role in the lipolytic processing of chylomicrons. Cell Metab. 2007;5(4):279-91.
117. Wang Y, Zhang D, Chiu AP, Wan A, Neumaier K, Vlodavsky I, et al. Endothelial heparanase regulates heart metabolism by stimulating lipoprotein lipase secretion from cardiomyocytes. Arterioscler Thromb Vasc Biol. 2013;33(5):894-902.
118. Wang Y, Rodrigues B. Intrinsic and extrinsic regulation of cardiac lipoprotein lipase following diabetes. Biochim Biophys Acta. 2015;1851(2):163-71.
119. Chajek-Shaul T, Friedman G, Bengtsson-Olivecrona G, Vlodavsky I, Bar-Shavit R. Interaction of lipoprotein lipase with subendothelial extracellular matrix. Biochim Biophys Acta. 1990;1042(2):168-75.
120. Davies BS, Beigneux AP, Barnes RH, 2nd, Tu Y, Gin P, Weinstein MM, et al. GPIHBP1 is responsible for the entry of lipoprotein lipase into capillaries. Cell Metab. 2010;12(1):42-52.
121. Gin P, Yin L, Davies BS, Weinstein MM, Ryan RO, Bensadoun A, et al. The acidic domain of GPIHBP1 is important for the binding of lipoprotein lipase and chylomicrons. J Biol Chem. 2008;283(43):29554-62.
122. Goulbourne CN, Gin P, Tatar A, Nobumori C, Hoenger A, Jiang H, et al. The GPIHBP1-LPL complex is responsible for the margination of triglyceride-rich lipoproteins in capillaries. Cell Metab. 2014;19(5):849-60.
123. Mysling S, Kristensen KK, Larsson M, Beigneux AP, Gardsvoll H, Fong LG, et al. The acidic domain of the endothelial membrane protein GPIHBP1 stabilizes lipoprotein lipase activity by preventing unfolding of its catalytic domain. Elife. 2016;5:e12095.
124. Olivecrona G. Role of lipoprotein lipase in lipid metabolism. Curr Opin Lipidol. 2016;27(3):233-41.
125. Cryer A. Tissue lipoprotein lipase activity and its action in lipoprotein metabolism. Int J Biochem. 1981;13(5):525-41.
126. Goldberg IJ, Merkel M. Lipoprotein lipase: physiology, biochemistry, and molecular biology. Front Biosci. 2001;6:D388-405.
127. Eckel RH. Lipoprotein lipase. A multifunctional enzyme relevant to common metabolic diseases. N Engl J Med. 1989;320(16):1060-8.
128. Catapano AL. Apolipoprotein C-II and lipoprotein lipase activity. Ric Clin Lab. 1982;12(1):35-40.
129. Breckenridge WC, Alaupovic P, Cox DW, Little JA. Apolipoprotein and lipoprotein concentrations in familial apolipoprotein C-II deficiency. Atherosclerosis. 1982;44(2):223-35.
130. Olivecrona G, Beisiegel U. Lipid binding of apolipoprotein CII is required for stimulation of lipoprotein lipase activity against apolipoprotein CII-deficient chylomicrons. Arterioscler Thromb Vasc Biol. 1997;17(8):1545-9.
131. Merkel M, Kako Y, Radner H, Cho IS, Ramasamy R, Brunzell JD, et al. Catalytically inactive lipoprotein lipase expression in muscle of transgenic mice increases very low density lipoprotein uptake: direct evidence that lipoprotein lipase bridging occurs in vivo. Proc Natl Acad Sci U S A. 1998;95(23):13841-6.
132. Beisiegel U, Weber W, Bengtsson-Olivecrona G. Lipoprotein lipase enhances the binding of chylomicrons to low density lipoprotein receptor-related protein. Proc Natl Acad Sci U S A. 1991;88(19):8342-6.
133. Medh JD, Bowen SL, Fry GL, Ruben S, Andracki M, Inoue I, et al. Lipoprotein lipase binds to low density lipoprotein receptors and induces receptor-mediated catabolism of very low density lipoproteins in vitro. J Biol Chem. 1996;271(29):17073-80.
134. Merkel M, Heeren J, Dudeck W, Rinninger F, Radner H, Breslow JL, et al. Inactive lipoprotein lipase (LPL) alone increases selective cholesterol ester uptake in vivo, whereas in

the presence of active LPL it also increases triglyceride hydrolysis and whole particle lipoprotein uptake. J Biol Chem. 2002;277(9):7405-11.
135. Rinninger F, Kaiser T, Mann WA, Meyer N, Greten H, Beisiegel U. Lipoprotein lipase mediates an increase in the selective uptake of high density lipoprotein-associated cholesteryl esters by hepatic cells in culture. J Lipid Res. 1998;39(7):1335-48.
136. Takahashi S, Suzuki J, Kohno M, Oida K, Tamai T, Miyabo S, et al. Enhancement of the binding of triglyceride-rich lipoproteins to the very low density lipoprotein receptor by apolipoprotein E and lipoprotein lipase. J Biol Chem. 1995;270(26):15747-54.
137. Preiss-Landl K, Zimmermann R, Hammerle G, Zechner R. Lipoprotein lipase: the regulation of tissue specific expression and its role in lipid and energy metabolism. Curr Opin Lipidol. 2002;13(5):471-81.
138. Murthy V, Julien P, Gagne C. Molecular pathobiology of the human lipoprotein lipase gene. Pharmacol Ther. 1996;70(2):101-35.
139. Santamarina-Fojo S. The familial chylomicronemia syndrome. Endocrinol Metab Clin North Am. 1998;27(3):551-67, viii.
140. Santamarina-Fojo S, Brewer HB, Jr. The familial hyperchylomicronemia syndrome. New insights into underlying genetic defects. JAMA. 1991;265(7):904-8.
141. Benlian P, De Gennes JL, Foubert L, Zhang H, Gagne SE, Hayden M. Premature atherosclerosis in patients with familial chylomicronemia caused by mutations in the lipoprotein lipase gene. N Engl J Med. 1996;335(12):848-54.
142. Nordestgaard BG, Abildgaard S, Wittrup HH, Steffensen R, Jensen G, Tybjaerg-Hansen A. Heterozygous lipoprotein lipase deficiency: frequency in the general population, effect on plasma lipid levels, and risk of ischemic heart disease. Circulation. 1997;96(6):1737-44.
143. Reymer PW, Gagne E, Groenemeyer BE, Zhang H, Forsyth I, Jansen H, et al. A lipoprotein lipase mutation (Asn291Ser) is associated with reduced HDL cholesterol levels in premature atherosclerosis. Nat Genet. 1995;10(1):28-34.
144. Breckenridge WC, Little JA, Steiner G, Chow A, Poapst M. Hypertriglyceridemia associated with deficiency of apolipoprotein C-II. N Engl J Med. 1978;298(23):1265-73.
145. Fojo SS, Brewer HB. Hypertriglyceridaemia due to genetic defects in lipoprotein lipase and apolipoprotein C-II. J Intern Med. 1992;231(6):669-77.
146. Johansen CT, Kathiresan S, Hegele RA. Genetic determinants of plasma triglycerides. J Lipid Res. 2011;52(2):189-206.
147. Johansen CT, Hegele RA. Genetic bases of hypertriglyceridemic phenotypes. Curr Opin Lipidol. 2011;22(4):247-53.
148. Yagyu H, Ishibashi S, Chen Z, Osuga J, Okazaki M, Perrey S, et al. Overexpressed lipoprotein lipase protects against atherosclerosis in apolipoprotein E knockout mice. J Lipid Res. 1999;40(9):1677-85.
149. Shimada M, Ishibashi S, Inaba T, Yagyu H, Harada K, Osuga JI, et al. Suppression of diet-induced atherosclerosis in low density lipoprotein receptor knockout mice overexpressing lipoprotein lipase. Proc Natl Acad Sci U S A. 1996;93(14):7242-6.
150. Li Y, He PP, Zhang DW, Zheng XL, Cayabyab FS, Yin WD, et al. Lipoprotein lipase: from gene to atherosclerosis. Atherosclerosis. 2014;237(2):597-608.
151. Clee SM, Bissada N, Miao F, Miao L, Marais AD, Henderson HE, et al. Plasma and vessel wall lipoprotein lipase have different roles in atherosclerosis. J Lipid Res. 2000;41(4):521-31.
152. Kobayashi J, Mabuchi H. Lipoprotein lipase and atherosclerosis. Ann Clin Biochem. 2015;52(Pt 6):632-7.
153. Gagne SE, Larson MG, Pimstone SN, Schaefer EJ, Kastelein JJ, Wilson PW, et al. A common truncation variant of lipoprotein lipase (Ser447X) confers protection against coronary heart disease: the Framingham Offspring Study. Clin Genet. 1999;55(6):450-4.

154. Kageyama H, Hirano T, Okada K, Ebara T, Kageyama A, Murakami T, et al. Lipoprotein lipase mRNA in white adipose tissue but not in skeletal muscle is increased by pioglitazone through PPAR-gamma. Biochem Biophys Res Commun. 2003;305(1):22-7.
155. Nagashima K, Lopez C, Donovan D, Ngai C, Fontanez N, Bensadoun A, et al. Effects of the PPARgamma agonist pioglitazone on lipoprotein metabolism in patients with type 2 diabetes mellitus. J Clin Invest. 2005;115(5):1323-32.
156. Schneider JG, von Eynatten M, Parhofer KG, Volkmer JE, Schiekofer S, Hamann A, et al. Atorvastatin improves diabetic dyslipidemia and increases lipoprotein lipase activity in vivo. Atherosclerosis. 2004;175(2):325-31.
157. Hitsumoto T, Ohsawa H, Uchi T, Noike H, Kanai M, Yoshinuma M, et al. Preheparin serum lipoprotein lipase mass is negatively related to coronary atherosclerosis. Atherosclerosis. 2000;153(2):391-6.
158. Lindqvist P, Ostlund-Lindqvist AM, Witztum JL, Steinberg D, Little JA. The role of lipoprotein lipase in the metabolism of triglyceride-rich lipoproteins by macrophages. J Biol Chem. 1983;258(15):9086-92.
159. Mead JR, Ramji DP. The pivotal role of lipoprotein lipase in atherosclerosis. Cardiovasc Res. 2002;55(2):261-9.
160. Cohn JS, Marcoux C, Davignon J. Detection, quantification, and characterization of potentially atherogenic triglyceride-rich remnant lipoproteins. Arterioscler Thromb Vasc Biol. 1999;19(10):2474-86.
161. Kawashima RL, Medh JD. Down-regulation of lipoprotein lipase increases ABCA1-mediated cholesterol efflux in THP-1 macrophages. Biochem Biophys Res Commun. 2014;450(4):1416-21.
162. Yang Y, Thyagarajan N, Coady BM, Brown RJ. Cholesterol efflux from THP-1 macrophages is impaired by the fatty acid component from lipoprotein hydrolysis by lipoprotein lipase. Biochem Biophys Res Commun. 2014;451(4):632-6.
163. He PP, OuYang XP, Li Y, Lv YC, Wang ZB, Yao F, et al. MicroRNA-590 Inhibits Lipoprotein Lipase Expression and Prevents Atherosclerosis in apoE Knockout Mice. PLoS One. 2015;10(9):e0138788.
164. Coleman T, Seip RL, Gimble JM, Lee D, Maeda N, Semenkovich CF. COOH-terminal disruption of lipoprotein lipase in mice is lethal in homozygotes, but heterozygotes have elevated triglycerides and impaired enzyme activity. J Biol Chem. 1995;270(21):12518-25.
165. Weinstock PH, Bisgaier CL, Aalto-Setala K, Radner H, Ramakrishnan R, Levak-Frank S, et al. Severe hypertriglyceridemia, reduced high density lipoprotein, and neonatal death in lipoprotein lipase knockout mice. Mild hypertriglyceridemia with impaired very low density lipoprotein clearance in heterozygotes. J Clin Invest. 1995;96(6):2555-68.
166. Li YX, Han TT, Liu Y, Zheng S, Zhang Y, Liu W, et al. Insulin resistance caused by lipotoxicity is related to oxidative stress and endoplasmic reticulum stress in LPL gene knockout heterozygous mice. Atherosclerosis. 2015;239(1):276-82.
167. Marshall BA, Tordjman K, Host HH, Ensor NJ, Kwon G, Marshall CA, et al. Relative hypoglycemia and hyperinsulinemia in mice with heterozygous lipoprotein lipase (LPL) deficiency. Islet LPL regulates insulin secretion. J Biol Chem. 1999;274(39):27426-32.
168. Strauss JG, Frank S, Kratky D, Hammerle G, Hrzenjak A, Knipping G, et al. Adenovirus-mediated rescue of lipoprotein lipase-deficient mice. Lipolysis of triglyceride-rich lipoproteins is essential for high density lipoprotein maturation in mice. J Biol Chem. 2001;276(39):36083-90.
169. Shimada M, Shimano H, Gotoda T, Yamamoto K, Kawamura M, Inaba T, et al. Overexpression of human lipoprotein lipase in transgenic mice. Resistance to diet-induced hypertriglyceridemia and hypercholesterolemia. J Biol Chem. 1993;268(24):17924-9.

170. Shibasaki M, Bujo H, Takahashi K, Murakami K, Unoki H, Saito Y. Catalytically inactive lipoprotein lipase overexpression increases insulin sensitivity in mice. Horm Metab Res. 2006;38(8):491-6.
171. Kim JK, Fillmore JJ, Chen Y, Yu C, Moore IK, Pypaert M, et al. Tissue-specific overexpression of lipoprotein lipase causes tissue-specific insulin resistance. Proc Natl Acad Sci U S A. 2001;98(13):7522-7.
172. Merkel M, Weinstock PH, Chajek-Shaul T, Radner H, Yin B, Breslow JL, et al. Lipoprotein lipase expression exclusively in liver. A mouse model for metabolism in the neonatal period and during cachexia. J Clin Invest. 1998;102(5):893-901.
173. Schoonjans K, Peinado-Onsurbe J, Lefebvre AM, Heyman RA, Briggs M, Deeb S, et al. PPARalpha and PPARgamma activators direct a distinct tissue-specific transcriptional response via a PPRE in the lipoprotein lipase gene. EMBO J. 1996;15(19):5336-48.
174. Michaud SE, Renier G. Direct regulatory effect of fatty acids on macrophage lipoprotein lipase: potential role of PPARs. Diabetes. 2001;50(3):660-6.
175. Blanchard PG, Festuccia WT, Houde VP, St-Pierre P, Brule S, Turcotte V, et al. Major involvement of mTOR in the PPARgamma-induced stimulation of adipose tissue lipid uptake and fat accretion. J Lipid Res. 2012;53(6):1117-25.
176. Laplante M, Sell H, MacNaul KL, Richard D, Berger JP, Deshaies Y. PPAR-gamma activation mediates adipose depot-specific effects on gene expression and lipoprotein lipase activity: mechanisms for modulation of postprandial lipemia and differential adipose accretion. Diabetes. 2003;52(2):291-9.
177. Vidal-Puig A, Jimenez-Linan M, Lowell BB, Hamann A, Hu E, Spiegelman B, et al. Regulation of PPAR gamma gene expression by nutrition and obesity in rodents. J Clin Invest. 1996;97(11):2553-61.
178. Chawla A, Lee CH, Barak Y, He W, Rosenfeld J, Liao D, et al. PPARdelta is a very low-density lipoprotein sensor in macrophages. Proc Natl Acad Sci U S A. 2003;100(3):1268-73.
179. Gbaguidi FG, Chinetti G, Milosavljevic D, Teissier E, Chapman J, Olivecrona G, et al. Peroxisome proliferator-activated receptor (PPAR) agonists decrease lipoprotein lipase secretion and glycated LDL uptake by human macrophages. FEBS Lett. 2002;512(1-3):85-90.
180. Peng D, Hiipakka RA, Xie JT, Reardon CA, Getz GS, Liao S. Differential effects of activation of liver X receptor on plasma lipid homeostasis in wild-type and lipoprotein clearance-deficient mice. Atherosclerosis. 2010;208(1):126-33.
181. Zhang Y, Repa JJ, Gauthier K, Mangelsdorf DJ. Regulation of lipoprotein lipase by the oxysterol receptors, LXRαlpha and LXRβeta. The Journal of biological chemistry. 2001;276(46):43018-24.
182. Zou Y, Du H, Yin M, Zhang L, Mao L, Xiao N, et al. Effects of high dietary fat and cholesterol on expression of PPAR alpha, LXR alpha, and their responsive genes in the liver of apoE and LDLR double deficient mice. Mol Cell Biochem. 2009;323(1-2):195-205.
183. Beyea MM, Heslop CL, Sawyez CG, Edwards JY, Markle JG, Hegele RA, et al. Selective up-regulation of LXR-regulated genes ABCA1, ABCG1, and APOE in macrophages through increased endogenous synthesis of 24(S),25-epoxycholesterol. J Biol Chem. 2007;282(8):5207-16.
184. Norata GD, Ongari M, Uboldi P, Pellegatta F, Catapano AL. Liver X receptor and retinoic X receptor agonists modulate the expression of genes involved in lipid metabolism in human endothelial cells. Int J Mol Med. 2005;16(4):717-22.
185. Enerback S, Semb H, Tavernier J, Bjursell G, Olivecrona T. Tissue-specific regulation of guinea pig lipoprotein lipase; effects of nutritional state and of tumor necrosis factor on mRNA levels in adipose tissue, heart and liver. Gene. 1988;64(1):97-106.
186. Fruchart JC, Duriez P. Mode of action of fibrates in the regulation of triglyceride and HDL-cholesterol metabolism. Drugs Today (Barc). 2006;42(1):39-64.

187. Previato L, Parrott CL, Santamarina-Fojo S, Brewer HB, Jr. Transcriptional regulation of the human lipoprotein lipase gene in 3T3-L1 adipocytes. J Biol Chem. 1991;266(28):18958-63.
188. Yang WS, Nevin DN, Peng R, Brunzell JD, Deeb SS. A mutation in the promoter of the lipoprotein lipase (LPL) gene in a patient with familial combined hyperlipidemia and low LPL activity. Proc Natl Acad Sci U S A. 1995;92(10):4462-6.
189. Nakshatri H, Nakshatri P, Currie RA. Interaction of Oct-1 with TFIIB. Implications for a novel response elicited through the proximal octamer site of the lipoprotein lipase promoter. J Biol Chem. 1995;270(33):19613-23.
190. Currie RA, Eckel RH. Characterization of a high affinity octamer transcription factor binding site in the human lipoprotein lipase promoter. Arch Biochem Biophys. 1992;298(2):630-9.
191. Morin CL, Schlaepfer IR, Eckel RH. Tumor necrosis factor-alpha eliminates binding of NF-Y and an octamer-binding protein to the lipoprotein lipase promoter in 3T3-L1 adipocytes. J Clin Invest. 1995;95(4):1684-9.
192. Tengku-Muhammad TS, Cryer A, Ramji DP. Synergism between interferon gamma and tumour necrosis factor alpha in the regulation of lipoprotein lipase in the macrophage J774.2 cell line. Cytokine. 1998;10(1):38-48.
193. Yang WS, Deeb SS. Sp1 and Sp3 transactivate the human lipoprotein lipase gene promoter through binding to a CT element: synergy with the sterol regulatory element binding protein and reduced transactivation of a naturally occurring promoter variant. J Lipid Res. 1998;39(10):2054-64.
194. Hughes TR, Tengku-Muhammad TS, Irvine SA, Ramji DP. A novel role of Sp1 and Sp3 in the interferon-gamma -mediated suppression of macrophage lipoprotein lipase gene transcription. J Biol Chem. 2002;277(13):11097-106.
195. Schoonjans K, Gelman L, Haby C, Briggs M, Auwerx J. Induction of LPL gene expression by sterols is mediated by a sterol regulatory element and is independent of the presence of multiple E boxes. J Mol Biol. 2000;304(3):323-34.
196. Staels B, Martin G, Martinez M, Albert C, Peinado-Onsurbe J, Saladin R, et al. Expression and regulation of the lipoprotein lipase gene in human adrenal cortex. J Biol Chem. 1996;271(29):17425-32.
197. Homma H, Kurachi H, Nishio Y, Takeda T, Yamamoto T, Adachi K, et al. Estrogen suppresses transcription of lipoprotein lipase gene. Existence of a unique estrogen response element on the lipoprotein lipase promoter. J Biol Chem. 2000;275(15):11404-11.
198. Irvine SA, Foka P, Rogers SA, Mead JR, Ramji DP. A critical role for the Sp1-binding sites in the transforming growth factor-beta-mediated inhibition of lipoprotein lipase gene expression in macrophages. Nucleic Acids Res. 2005;33(5):1423-34.
199. Tanuma Y, Nakabayashi H, Esumi M, Endo H. A silencer element for the lipoprotein lipase gene promoter and cognate double- and single-stranded DNA-binding proteins. Mol Cell Biol. 1995;15(1):517-23.
200. Jong MC, Hofker MH, Havekes LM. Role of ApoCs in lipoprotein metabolism: functional differences between ApoC1, ApoC2, and ApoC3. Arterioscler Thromb Vasc Biol. 1999;19(3):472-84.
201. LaRosa JC, Levy RI, Herbert P, Lux SE, Fredrickson DS. A specific apoprotein activator for lipoprotein lipase. Biochem Biophys Res Commun. 1970;41(1):57-62.
202. Nilsson SK, Heeren J, Olivecrona G, Merkel M. Apolipoprotein A-V; a potent triglyceride reducer. Atherosclerosis. 2011;219(1):15-21.
203. Shachter NS, Hayek T, Leff T, Smith JD, Rosenberg DW, Walsh A, et al. Overexpression of apolipoprotein CII causes hypertriglyceridemia in transgenic mice. J Clin Invest. 1994;93(4):1683-90.

204. Lookene A, Beckstead JA, Nilsson S, Olivecrona G, Ryan RO. Apolipoprotein A-V-heparin interactions: implications for plasma lipoprotein metabolism. J Biol Chem. 2005;280(27):25383-7.
205. Shu X, Nelbach L, Weinstein MM, Burgess BL, Beckstead JA, Young SG, et al. Intravenous injection of apolipoprotein A-V reconstituted high-density lipoprotein decreases hypertriglyceridemia in apoav-/- mice and requires glycosylphosphatidylinositol-anchored high-density lipoprotein-binding protein 1. Arterioscler Thromb Vasc Biol. 2010;30(12):2504-9.
206. Fruchart-Najib J, Bauge E, Niculescu LS, Pham T, Thomas B, Rommens C, et al. Mechanism of triglyceride lowering in mice expressing human apolipoprotein A5. Biochem Biophys Res Commun. 2004;319(2):397-404.
207. Kao JT, Wen HC, Chien KL, Hsu HC, Lin SW. A novel genetic variant in the apolipoprotein A5 gene is associated with hypertriglyceridemia. Hum Mol Genet. 2003;12(19):2533-9.
208. Albers K, Schlein C, Wenner K, Lohse P, Bartelt A, Heeren J, et al. Homozygosity for a partial deletion of apoprotein A-V signal peptide results in intracellular missorting of the protein and chylomicronemia in a breast-fed infant. Atherosclerosis. 2014;233(1):97-103.
209. Priore Oliva C, Pisciotta L, Li Volti G, Sambataro MP, Cantafora A, Bellocchio A, et al. Inherited apolipoprotein A-V deficiency in severe hypertriglyceridemia. Arterioscler Thromb Vasc Biol. 2005;25(2):411-7.
210. Berbee JF, van der Hoogt CC, Sundararaman D, Havekes LM, Rensen PC. Severe hypertriglyceridemia in human APOC1 transgenic mice is caused by apoC-I-induced inhibition of LPL. J Lipid Res. 2005;46(2):297-306.
211. Jong MC, Dahlmans VE, Hofker MH, Havekes LM. Nascent very-low-density lipoprotein triacylglycerol hydrolysis by lipoprotein lipase is inhibited by apolipoprotein E in a dose-dependent manner. Biochem J. 1997;328 (Pt 3):745-50.
212. McConathy WJ, Gesquiere JC, Bass H, Tartar A, Fruchart JC, Wang CS. Inhibition of lipoprotein lipase activity by synthetic peptides of apolipoprotein C-III. J Lipid Res. 1992;33(7):995-1003.
213. Pollin TI, Damcott CM, Shen H, Ott SH, Shelton J, Horenstein RB, et al. A null mutation in human APOC3 confers a favorable plasma lipid profile and apparent cardioprotection. Science. 2008;322(5908):1702-5.
214. Larsson M, Vorrsjo E, Talmud P, Lookene A, Olivecrona G. Apolipoproteins C-I and C-III inhibit lipoprotein lipase activity by displacement of the enzyme from lipid droplets. J Biol Chem. 2013;288(47):33997-4008.
215. Gerritsen G, Rensen PC, Kypreos KE, Zannis VI, Havekes LM, Willems van Dijk K. ApoC-III deficiency prevents hyperlipidemia induced by apoE overexpression. J Lipid Res. 2005;46(7):1466-73.
216. Mensenkamp AR, Jong MC, van Goor H, van Luyn MJ, Bloks V, Havinga R, et al. Apolipoprotein E participates in the regulation of very low density lipoprotein-triglyceride secretion by the liver. J Biol Chem. 1999;274(50):35711-8.
217. Koster A, Chao YB, Mosior M, Ford A, Gonzalez-DeWhitt PA, Hale JE, et al. Transgenic angiopoietin-like (angptl)4 overexpression and targeted disruption of angptl4 and angptl3: regulation of triglyceride metabolism. Endocrinology. 2005;146(11):4943-50.
218. Li C. Genetics and regulation of angiopoietin-like proteins 3 and 4. Curr Opin Lipidol. 2006;17(2):152-6.
219. Mandard S, Zandbergen F, van Straten E, Wahli W, Kuipers F, Muller M, et al. The fasting-induced adipose factor/angiopoietin-like protein 4 is physically associated with lipoproteins and governs plasma lipid levels and adiposity. J Biol Chem. 2006;281(2):934-44.

220. Xu A, Lam MC, Chan KW, Wang Y, Zhang J, Hoo RL, et al. Angiopoietin-like protein 4 decreases blood glucose and improves glucose tolerance but induces hyperlipidemia and hepatic steatosis in mice. Proc Natl Acad Sci U S A. 2005;102(17):6086-91.
221. Wang Y, Quagliarini F, Gusarova V, Gromada J, Valenzuela DM, Cohen JC, et al. Mice lacking ANGPTL8 (Betatrophin) manifest disrupted triglyceride metabolism without impaired glucose homeostasis. Proc Natl Acad Sci U S A. 2013;110(40):16109-14.
222. Fujimoto K, Koishi R, Shimizugawa T, Ando Y. Angptl3-null mice show low plasma lipid concentrations by enhanced lipoprotein lipase activity. Exp Anim. 2006;55(1):27-34.
223. Sukonina V, Lookene A, Olivecrona T, Olivecrona G. Angiopoietin-like protein 4 converts lipoprotein lipase to inactive monomers and modulates lipase activity in adipose tissue. Proc Natl Acad Sci U S A. 2006;103(46):17450-5.
224. Yau MH, Wang Y, Lam KS, Zhang J, Wu D, Xu A. A highly conserved motif within the NH2-terminal coiled-coil domain of angiopoietin-like protein 4 confers its inhibitory effects on lipoprotein lipase by disrupting the enzyme dimerization. J Biol Chem. 2009;284(18):11942-52.
225. Lafferty MJ, Bradford KC, Erie DA, Neher SB. Angiopoietin-like protein 4 inhibition of lipoprotein lipase: evidence for reversible complex formation. J Biol Chem. 2013;288(40):28524-34.
226. Dijk W, Beigneux AP, Larsson M, Bensadoun A, Young SG, Kersten S. Angiopoietin-like 4 promotes intracellular degradation of lipoprotein lipase in adipocytes. J Lipid Res. 2016;57(9):1670-83.
227. Zhang R. Lipasin, a novel nutritionally-regulated liver-enriched factor that regulates serum triglyceride levels. Biochem Biophys Res Commun. 2012;424(4):786-92.
228. Shan L, Yu XC, Liu Z, Hu Y, Sturgis LT, Miranda ML, et al. The angiopoietin-like proteins ANGPTL3 and ANGPTL4 inhibit lipoprotein lipase activity through distinct mechanisms. J Biol Chem. 2009;284(3):1419-24.
229. Sonnenburg WK, Yu D, Lee EC, Xiong W, Gololobov G, Key B, et al. GPIHBP1 stabilizes lipoprotein lipase and prevents its inhibition by angiopoietin-like 3 and angiopoietin-like 4. J Lipid Res. 2009;50(12):2421-9.
230. Quagliarini F, Wang Y, Kozlitina J, Grishin NV, Hyde R, Boerwinkle E, et al. Atypical angiopoietin-like protein that regulates ANGPTL3. Proc Natl Acad Sci U S A. 2012;109(48):19751-6.
231. Geldenhuys WJ, Lin L, Darvesh AS, Sadana P. Emerging strategies of targeting lipoprotein lipase for metabolic and cardiovascular diseases. Drug Discov Today. 2016.
232. Kersten S. Physiological regulation of lipoprotein lipase. Biochim Biophys Acta. 2014;1841(7):919-33.
233. Teusink B, Voshol PJ, Dahlmans VE, Rensen PC, Pijl H, Romijn JA, et al. Contribution of fatty acids released from lipolysis of plasma triglycerides to total plasma fatty acid flux and tissue-specific fatty acid uptake. Diabetes. 2003;52(3):614-20.
234. Ong JM, Kirchgessner TG, Schotz MC, Kern PA. Insulin increases the synthetic rate and messenger RNA level of lipoprotein lipase in isolated rat adipocytes. J Biol Chem. 1988;263(26):12933-8.
235. Picard F, Naimi N, Richard D, Deshaies Y. Response of adipose tissue lipoprotein lipase to the cephalic phase of insulin secretion. Diabetes. 1999;48(3):452-9.
236. Semenkovich CF, Wims M, Noe L, Etienne J, Chan L. Insulin regulation of lipoprotein lipase activity in 3T3-L1 adipocytes is mediated at posttranscriptional and posttranslational levels. J Biol Chem. 1989;264(15):9030-8.
237. Yamada T, Ozaki N, Kato Y, Miura Y, Oiso Y. Insulin downregulates angiopoietin-like protein 4 mRNA in 3T3-L1 adipocytes. Biochem Biophys Res Commun. 2006;347(4):1138-44.
238. Ladu MJ, Kapsas H, Palmer WK. Regulation of lipoprotein lipase in adipose and muscle tissues during fasting. Am J Physiol. 1991;260(5 Pt 2):R953-9.

239. Sugden MC, Holness MJ, Howard RM. Changes in lipoprotein lipase activities in adipose tissue, heart and skeletal muscle during continuous or interrupted feeding. Biochem J. 1993;292 (Pt 1):113-9.
240. Farese RV, Jr., Yost TJ, Eckel RH. Tissue-specific regulation of lipoprotein lipase activity by insulin/glucose in normal-weight humans. Metabolism. 1991;40(2):214-6.
241. Dutton S, Trayhurn P. Regulation of angiopoietin-like protein 4/fasting-induced adipose factor (Angptl4/FIAF) expression in mouse white adipose tissue and 3T3-L1 adipocytes. Br J Nutr. 2008;100(1):18-26.
242. Lichtenstein L, Berbee JF, van Dijk SJ, van Dijk KW, Bensadoun A, Kema IP, et al. Angptl4 upregulates cholesterol synthesis in liver via inhibition of LPL- and HL-dependent hepatic cholesterol uptake. Arterioscler Thromb Vasc Biol. 2007;27(11):2420-7.
243. Greiwe JS, Holloszy JO, Semenkovich CF. Exercise induces lipoprotein lipase and GLUT-4 protein in muscle independent of adrenergic-receptor signaling. J Appl Physiol (1985). 2000;89(1):176-81.
244. Pilegaard H, Keller C, Steensberg A, Helge JW, Pedersen BK, Saltin B, et al. Influence of pre-exercise muscle glycogen content on exercise-induced transcriptional regulation of metabolic genes. J Physiol. 2002;541(Pt 1):261-71.
245. Seip RL, Mair K, Cole TG, Semenkovich CF. Induction of human skeletal muscle lipoprotein lipase gene expression by short-term exercise is transient. Am J Physiol. 1997;272(2 Pt 1):E255-61.
246. Vissing K, Andersen JL, Schjerling P. Are exercise-induced genes induced by exercise? FASEB J. 2005;19(1):94-6.
247. Ruge T, Bergo M, Hultin M, Olivecrona G, Olivecrona T. Nutritional regulation of binding sites for lipoprotein lipase in rat heart. Am J Physiol Endocrinol Metab. 2000;278(2):E211-8.
248. Ruge T, Wu G, Olivecrona T, Olivecrona G. Nutritional regulation of lipoprotein lipase in mice. Int J Biochem Cell Biol. 2004;36(2):320-9.
249. Sambandam N, Abrahani MA, St Pierre E, Al-Atar O, Cam MC, Rodrigues B. Localization of lipoprotein lipase in the diabetic heart: regulation by acute changes in insulin. Arterioscler Thromb Vasc Biol. 1999;19(6):1526-34.
250. Georgiadi A, Lichtenstein L, Degenhardt T, Boekschoten MV, van Bilsen M, Desvergne B, et al. Induction of cardiac Angptl4 by dietary fatty acids is mediated by peroxisome proliferator-activated receptor beta/delta and protects against fatty acid-induced oxidative stress. Circ Res. 2010;106(11):1712-21.
251. Cheng Y, Hauton D. Cold acclimation induces physiological cardiac hypertrophy and increases assimilation of triacylglycerol metabolism through lipoprotein lipase. Biochim Biophys Acta. 2008;1781(10):618-26.
252. Bartelt A, Bruns OT, Reimer R, Hohenberg H, Ittrich H, Peldschus K, et al. Brown adipose tissue activity controls triglyceride clearance. Nat Med. 2011;17(2):200-5.
253. Mantha L, Deshaies Y. beta-Adrenergic modulation of triglyceridemia under increased energy expenditure. Am J Physiol. 1998;274(6 Pt 2):R1769-76.
254. Cannon B, Nedergaard J. Brown adipose tissue: function and physiological significance. Physiol Rev. 2004;84(1):277-359.
255. Goldman R, Sopher O. Control of lipoprotein lipase secretion in mouse macrophages. Biochim Biophys Acta. 1989;1001(2):120-6.
256. Yin B, Loike JD, Kako Y, Weinstock PH, Breslow JL, Silverstein SC, et al. Lipoprotein lipase regulates Fc receptor-mediated phagocytosis by macrophages maintained in glucose-deficient medium. J Clin Invest. 1997;100(3):649-57.
257. Hill MR, Kelly K, Wu X, Wanker F, Bass H, Morgan C, et al. Lipopolysaccharide regulation of lipoprotein lipase expression in murine macrophages. Infect Immun. 1995;63(3):858-64.

258. Sopher O, Goldman R. Bacterial lipopolysaccharide suppresses the expression of lipoprotein lipase in murine macrophages: a process independent of tumor necrosis factor or interleukin 1. Immunol Lett. 1987;15(3):261-5.
259. Tengku-Muhammad TS, Hughes TR, Cryer A, Ramji DP. Differential regulation of lipoprotein lipase in the macrophage J774.2 cell line by cytokines. Cytokine. 1996;8(7):525-33.
260. Kaestner KH, Knochel W, Martinez DE. Unified nomenclature for the winged helix/forkhead transcription factors. Genes Dev. 2000;14(2):142-6.
261. Weigel D, Jurgens G, Kuttner F, Seifert E, Jackle H. The homeotic gene fork head encodes a nuclear protein and is expressed in the terminal regions of the Drosophila embryo. Cell. 1989;57(4):645-58.
262. Weigel D, Jackle H. The fork head domain: a novel DNA binding motif of eukaryotic transcription factors? Cell. 1990;63(3):455-6.
263. Lai E, Prezioso VR, Tao WF, Chen WS, Darnell JE, Jr. Hepatocyte nuclear factor 3 alpha belongs to a gene family in mammals that is homologous to the Drosophila homeotic gene fork head. Genes Dev. 1991;5(3):416-27.
264. Wang DY, Kumar S, Hedges SB. Divergence time estimates for the early history of animal phyla and the origin of plants, animals and fungi. Proc Biol Sci. 1999;266(1415):163-71.
265. Lai E, Clark KL, Burley SK, Darnell JE, Jr. Hepatocyte nuclear factor 3/fork head or "winged helix" proteins: a family of transcription factors of diverse biologic function. Proceedings of the National Academy of Sciences of the United States of America. 1993;90(22):10421-3.
266. Hannenhalli S, Kaestner KH. The evolution of Fox genes and their role in development and disease. Nat Rev Genet. 2009;10(4):233-40.
267. Kaestner KH, Katz J, Liu Y, Drucker DJ, Schutz G. Inactivation of the winged helix transcription factor HNF3alpha affects glucose homeostasis and islet glucagon gene expression in vivo. Genes Dev. 1999;13(4):495-504.
268. Tuteja G, Kaestner KH. Forkhead transcription factors II. Cell. 2007;131(1):192.
269. Tuteja G, Kaestner KH. SnapShot: forkhead transcription factors I. Cell. 2007;130(6):1160.
270. Cirillo LA, Barton MC. Many forkheads in the road to regulation. Symposium on forkhead transcription factor networks in development, signalling and disease. EMBO Rep. 2008;9(8):721-4.
271. Costa RH, Grayson DR, Darnell JE, Jr. Multiple hepatocyte-enriched nuclear factors function in the regulation of transthyretin and alpha 1-antitrypsin genes. Molecular and cellular biology. 1989;9(4):1415-25.
272. Sekiya S, Suzuki A. Direct conversion of mouse fibroblasts to hepatocyte-like cells by defined factors. Nature. 2011;475(7356):390-3.
273. Smale ST. Pioneer factors in embryonic stem cells and differentiation. Curr Opin Genet Dev. 2010;20(5):519-26.
274. Tan Y, Xie Z, Ding M, Wang Z, Yu Q, Meng L, et al. Increased levels of FoxA1 transcription factor in pluripotent P19 embryonal carcinoma cells stimulate neural differentiation. Stem Cells Dev. 2010;19(9):1365-74.
275. Xu J, Watts JA, Pope SD, Gadue P, Kamps M, Plath K, et al. Transcriptional competence and the active marking of tissue-specific enhancers by defined transcription factors in embryonic and induced pluripotent stem cells. Genes Dev. 2009;23(24):2824-38.
276. Overdier DG, Porcella A, Costa RH. The DNA-binding specificity of the hepatocyte nuclear factor 3/forkhead domain is influenced by amino-acid residues adjacent to the recognition helix. Molecular and cellular biology. 1994;14(4):2755-66.

277. Rada-Iglesias A, Wallerman O, Koch C, Ameur A, Enroth S, Clelland G, et al. Binding sites for metabolic disease related transcription factors inferred at base pair resolution by chromatin immunoprecipitation and genomic microarrays. Human molecular genetics. 2005;14(22):3435-47.
278. Gerrish K, Gannon M, Shih D, Henderson E, Stoffel M, Wright CV, et al. Pancreatic beta cell-specific transcription of the pdx-1 gene. The role of conserved upstream control regions and their hepatic nuclear factor 3beta sites. The Journal of biological chemistry. 2000;275(5):3485-92.
279. Clark KL, Halay ED, Lai E, Burley SK. Co-crystal structure of the HNF-3/fork head DNA-recognition motif resembles histone H5. Nature. 1993;364(6436):412-20.
280. Benayoun BA, Caburet S, Veitia RA. Forkhead transcription factors: key players in health and disease. Trends Genet. 2011;27(6):224-32.
281. Li C, Tucker PW. DNA-binding properties and secondary structural model of the hepatocyte nuclear factor 3/fork head domain. Proceedings of the National Academy of Sciences of the United States of America. 1993;90(24):11583-7.
282. Qian X, Costa RH. Analysis of hepatocyte nuclear factor-3 beta protein domains required for transcriptional activation and nuclear targeting. Nucleic acids research. 1995;23(7):1184-91.
283. Pani L, Overdier DG, Porcella A, Qian X, Lai E, Costa RH. Hepatocyte nuclear factor 3 beta contains two transcriptional activation domains, one of which is novel and conserved with the Drosophila fork head protein. Molecular and cellular biology. 1992;12(9):3723-32.
284. Cirillo LA, Lin FR, Cuesta I, Friedman D, Jarnik M, Zaret KS. Opening of compacted chromatin by early developmental transcription factors HNF3 (FoxA) and GATA-4. Mol Cell. 2002;9(2):279-89.
285. Romanelli MG, Tato L, Lorenzi P, Morandi C. Nuclear localization domains in human thyroid transcription factor 2. Biochimica et biophysica acta. 2003;1643(1-3):55-64.
286. Friedman JR, Kaestner KH. The Foxa family of transcription factors in development and metabolism. Cell Mol Life Sci. 2006;63(19-20):2317-28.
287. Wolfrum C, Besser D, Luca E, Stoffel M. Insulin regulates the activity of forkhead transcription factor Hnf-3beta/Foxa-2 by Akt-mediated phosphorylation and nuclear/cytosolic localization. Proceedings of the National Academy of Sciences of the United States of America. 2003;100(20):11624-9.
288. Besnard V, Wert SE, Hull WM, Whitsett JA. Immunohistochemical localization of Foxa1 and Foxa2 in mouse embryos and adult tissues. Gene Expr Patterns. 2004;5(2):193-208.
289. Monaghan AP, Kaestner KH, Grau E, Schutz G. Postimplantation expression patterns indicate a role for the mouse forkhead/HNF-3 alpha, beta and gamma genes in determination of the definitive endoderm, chordamesoderm and neuroectoderm. Development. 1993;119(3):567-78.
290. Sasaki H, Hogan BL. Differential expression of multiple fork head related genes during gastrulation and axial pattern formation in the mouse embryo. Development. 1993;118(1):47-59.
291. Ruiz i Altaba A, Prezioso VR, Darnell JE, Jessell TM. Sequential expression of HNF-3 beta and HNF-3 alpha by embryonic organizing centers: the dorsal lip/node, notochord and floor plate. Mech Dev. 1993;44(2-3):91-108.
292. Hwang JT, Kelly GM. GATA6 and FOXA2 regulate Wnt6 expression during extraembryonic endoderm formation. Stem Cells Dev. 2012;21(17):3220-32.
293. Mirosevich J, Gao N, Matusik RJ. Expression of Foxa transcription factors in the developing and adult murine prostate. Prostate. 2005;62(4):339-52.

294. Ang SL, Wierda A, Wong D, Stevens KA, Cascio S, Rossant J, et al. The formation and maintenance of the definitive endoderm lineage in the mouse: involvement of HNF3/forkhead proteins. Development. 1993;119(4):1301-15.
295. Kaestner KH, Hiemisch H, Luckow B, Schutz G. The HNF-3 gene family of transcription factors in mice: gene structure, cDNA sequence, and mRNA distribution. Genomics. 1994;20(3):377-85.
296. Stott SR, Metzakopian E, Lin W, Kaestner KH, Hen R, Ang SL. Foxa1 and foxa2 are required for the maintenance of dopaminergic properties in ventral midbrain neurons at late embryonic stages. J Neurosci. 2013;33(18):8022-34.
297. Lee CS, Friedman JR, Fulmer JT, Kaestner KH. The initiation of liver development is dependent on Foxa transcription factors. Nature. 2005;435(7044):944-7.
298. Ang SL, Rossant J. HNF-3 beta is essential for node and notochord formation in mouse development. Cell. 1994;78(4):561-74.
299. Weinstein DC, Ruiz i Altaba A, Chen WS, Hoodless P, Prezioso VR, Jessell TM, et al. The winged-helix transcription factor HNF-3 beta is required for notochord development in the mouse embryo. Cell. 1994;78(4):575-88.
300. Kittappa R, Chang WW, Awatramani RB, McKay RD. The foxa2 gene controls the birth and spontaneous degeneration of dopamine neurons in old age. PLoS Biol. 2007;5(12):e325.
301. Bramswig NC, Everett LJ, Schug J, Dorrell C, Liu C, Luo Y, et al. Epigenomic plasticity enables human pancreatic alpha to beta cell reprogramming. The Journal of clinical investigation. 2013;123(3):1275-84.
302. Behr R, Brestelli J, Fulmer JT, Miyawaki N, Kleyman TR, Kaestner KH. Mild nephrogenic diabetes insipidus caused by Foxa1 deficiency. The Journal of biological chemistry. 2004;279(40):41936-41.
303. Shih DQ, Navas MA, Kuwajima S, Duncan SA, Stoffel M. Impaired glucose homeostasis and neonatal mortality in hepatocyte nuclear factor 3alpha-deficient mice. Proceedings of the National Academy of Sciences of the United States of America. 1999;96(18):10152-7.
304. Gao N, Ishii K, Mirosevich J, Kuwajima S, Oppenheimer SR, Roberts RL, et al. Forkhead box A1 regulates prostate ductal morphogenesis and promotes epithelial cell maturation. Development. 2005;132(15):3431-43.
305. Kaestner KH, Hiemisch H, Schutz G. Targeted disruption of the gene encoding hepatocyte nuclear factor 3gamma results in reduced transcription of hepatocyte-specific genes. Molecular and cellular biology. 1998;18(7):4245-51.
306. Shen W, Scearce LM, Brestelli JE, Sund NJ, Kaestner KH. Foxa3 (hepatocyte nuclear factor 3gamma) is required for the regulation of hepatic GLUT2 expression and the maintenance of glucose homeostasis during a prolonged fast. The Journal of biological chemistry. 2001;276(46):42812-7.
307. Zaret KS, Carroll JS. Pioneer transcription factors: establishing competence for gene expression. Genes Dev. 2011;25(21):2227-41.
308. Sekiya T, Muthurajan UM, Luger K, Tulin AV, Zaret KS. Nucleosome-binding affinity as a primary determinant of the nuclear mobility of the pioneer transcription factor FoxA. Genes Dev. 2009;23(7):804-9.
309. Golson ML, Kaestner KH. Fox transcription factors: from development to disease. Development. 2016;143(24):4558-70.
310. Zaret KS, Caravaca JM, Tulin A, Sekiya T. Nuclear mobility and mitotic chromosome binding: similarities between pioneer transcription factor FoxA and linker histone H1. Cold Spring Harb Symp Quant Biol. 2010;75:219-26.

311. Cirillo LA, McPherson CE, Bossard P, Stevens K, Cherian S, Shim EY, et al. Binding of the winged-helix transcription factor HNF3 to a linker histone site on the nucleosome. EMBO J. 1998;17(1):244-54.
312. Zhang L, Rubins NE, Ahima RS, Greenbaum LE, Kaestner KH. Foxa2 integrates the transcriptional response of the hepatocyte to fasting. Cell metabolism. 2005;2(2):141-8.
313. Gao N, Zhang J, Rao MA, Case TC, Mirosevich J, Wang Y, et al. The role of hepatocyte nuclear factor-3 alpha (Forkhead Box A1) and androgen receptor in transcriptional regulation of prostatic genes. Mol Endocrinol. 2003;17(8):1484-507.
314. Carroll JS, Liu XS, Brodsky AS, Li W, Meyer CA, Szary AJ, et al. Chromosome-wide mapping of estrogen receptor binding reveals long-range regulation requiring the forkhead protein FoxA1. Cell. 2005;122(1):33-43.
315. Hurtado A, Holmes KA, Ross-Innes CS, Schmidt D, Carroll JS. FOXA1 is a key determinant of estrogen receptor function and endocrine response. Nat Genet. 2011;43(1):27-33.
316. Nussey S, Whitehead S. Endocrinology: An Integrated Approach. Oxford2001.
317. Guignot L, Mithieux G. Mechanisms by which insulin, associated or not with glucose, may inhibit hepatic glucose production in the rat. Am J Physiol. 1999;277(6 Pt 1):E984-9.
318. Pandey AK, Bhardwaj V, Datta M. Tumour necrosis factor-alpha attenuates insulin action on phosphoenolpyruvate carboxykinase gene expression and gluconeogenesis by altering the cellular localization of Foxa2 in HepG2 cells. FEBS J. 2009;276(14):3757-69.
319. von Meyenn F, Porstmann T, Gasser E, Selevsek N, Schmidt A, Aebersold R, et al. Glucagon-induced acetylation of Foxa2 regulates hepatic lipid metabolism. Cell metabolism. 2013;17(3):436-47.
320. Lee CS, Sund NJ, Behr R, Herrera PL, Kaestner KH. Foxa2 is required for the differentiation of pancreatic alpha-cells. Dev Biol. 2005;278(2):484-95.
321. Lantz KA, Vatamaniuk MZ, Brestelli JE, Friedman JR, Matschinsky FM, Kaestner KH. Foxa2 regulates multiple pathways of insulin secretion. The Journal of clinical investigation. 2004;114(4):512-20.
322. Sund NJ, Vatamaniuk MZ, Casey M, Ang SL, Magnuson MA, Stoffers DA, et al. Tissue-specific deletion of Foxa2 in pancreatic beta cells results in hyperinsulinemic hypoglycemia. Genes Dev. 2001;15(13):1706-15.
323. Bochkis IM, Rubins NE, White P, Furth EE, Friedman JR, Kaestner KH. Hepatocyte-specific ablation of Foxa2 alters bile acid homeostasis and results in endoplasmic reticulum stress. Nature medicine. 2008;14(8):828-36.
324. Wolfrum C, Asilmaz E, Luca E, Friedman JM, Stoffel M. Foxa2 regulates lipid metabolism and ketogenesis in the liver during fasting and in diabetes. Nature. 2004;432(7020):1027-32.
325. Wolfrum C, Howell JJ, Ndungo E, Stoffel M. Foxa2 activity increases plasma high density lipoprotein levels by regulating apolipoprotein M. The Journal of biological chemistry. 2008;283(24):16940-9.
326. Wolfrum C, Stoffel M. Coactivation of Foxa2 through Pgc-1beta promotes liver fatty acid oxidation and triglyceride/VLDL secretion. Cell metabolism. 2006;3(2):99-110.
327. Wolfrum C, Shih DQ, Kuwajima S, Norris AW, Kahn CR, Stoffel M. Role of Foxa-2 in adipocyte metabolism and differentiation. The Journal of clinical investigation. 2003;112(3):345-56.
328. Xu N, Nilsson-Ehle P, Hurtig M, Ahren B. Both leptin and leptin-receptor are essential for apolipoprotein M expression in vivo. Biochemical and biophysical research communications. 2004;321(4):916-21.
329. Thymiakou E, Kardassis D. Novel mechanism of transcriptional repression of the human ATP binding cassette transporter A1 gene in hepatic cells by the winged

helix/forkhead box transcription factor A2. Biochimica et biophysica acta. 2014;1839(6):526-36.
330. Steneberg P, Rubins N, Bartoov-Shifman R, Walker MD, Edlund H. The FFA receptor GPR40 links hyperinsulinemia, hepatic steatosis, and impaired glucose homeostasis in mouse. Cell metabolism. 2005;1(4):245-58.
331. Wederell ED, Bilenky M, Cullum R, Thiessen N, Dagpinar M, Delaney A, et al. Global analysis of in vivo Foxa2-binding sites in mouse adult liver using massively parallel sequencing. Nucleic Acids Res. 2008;36(14):4549-64.
332. Bochkis IM, Schug J, Rubins NE, Chopra AR, O'Malley BW, Kaestner KH. Foxa2-dependent hepatic gene regulatory networks depend on physiological state. Physiological genomics. 2009;38(2):186-95.
333. Bochkis IM, Schug J, Ye DZ, Kurinna S, Stratton SA, Barton MC, et al. Genome-wide location analysis reveals distinct transcriptional circuitry by paralogous regulators Foxa1 and Foxa2. PLoS genetics. 2012;8(6):e1002770.
334. Wallerman O, Motallebipour M, Enroth S, Patra K, Bysani MS, Komorowski J, et al. Molecular interactions between HNF4a, FOXA2 and GABP identified at regulatory DNA elements through ChIP-sequencing. Nucleic acids research. 2009;37(22):7498-508.
335. Beato M. Transcriptional control by nuclear receptors. FASEB J. 1991;5(7):2044-51.
336. Mangelsdorf DJ, Thummel C, Beato M, Herrlich P, Schutz G, Umesono K, et al. The nuclear receptor superfamily: the second decade. Cell. 1995;83(6):835-9.
337. Peet DJ, Janowski BA, Mangelsdorf DJ. The LXRs: a new class of oxysterol receptors. Curr Opin Genet Dev. 1998;8(5):571-5.
338. Mangelsdorf DJ, Evans RM. The RXR heterodimers and orphan receptors. Cell. 1995;83(6):841-50.
339. Kastner P, Mark M, Chambon P. Nonsteroid nuclear receptors: what are genetic studies telling us about their role in real life? Cell. 1995;83(6):859-69.
340. Willy PJ, Umesono K, Ong ES, Evans RM, Heyman RA, Mangelsdorf DJ. LXR, a nuclear receptor that defines a distinct retinoid response pathway. Genes Dev. 1995;9(9):1033-45.
341. Dalen KT, Ulven SM, Bamberg K, Gustafsson JA, Nebb HI. Expression of the insulin-responsive glucose transporter GLUT4 in adipocytes is dependent on liver X receptor alpha. The Journal of biological chemistry. 2003;278(48):48283-91.
342. Cha JY, Repa JJ. The liver X receptor (LXR) and hepatic lipogenesis. The carbohydrate-response element-binding protein is a target gene of LXR. The Journal of biological chemistry. 2007;282(1):743-51.
343. Laffitte BA, Chao LC, Li J, Walczak R, Hummasti S, Joseph SB, et al. Activation of liver X receptor improves glucose tolerance through coordinate regulation of glucose metabolism in liver and adipose tissue. Proceedings of the National Academy of Sciences of the United States of America. 2003;100(9):5419-24.
344. Joseph SB, Castrillo A, Laffitte BA, Mangelsdorf DJ, Tontonoz P. Reciprocal regulation of inflammation and lipid metabolism by liver X receptors. Nat Med. 2003;9(2):213-9.
345. Castrillo A, Joseph SB, Vaidya SA, Haberland M, Fogelman AM, Cheng G, et al. Crosstalk between LXR and toll-like receptor signaling mediates bacterial and viral antagonism of cholesterol metabolism. Mol Cell. 2003;12(4):805-16.
346. Korach-Andre M, Gustafsson JA. Liver X receptors as regulators of metabolism. Biomol Concepts. 2015;6(3):177-90.
347. Repa JJ, Mangelsdorf DJ. The role of orphan nuclear receptors in the regulation of cholesterol homeostasis. Annu Rev Cell Dev Biol. 2000;16:459-81.
348. Auboeuf D, Rieusset J, Fajas L, Vallier P, Frering V, Riou JP, et al. Tissue distribution and quantification of the expression of mRNAs of peroxisome proliferator-activated receptors and liver X receptor-alpha in humans: no alteration in adipose tissue of obese and NIDDM patients. Diabetes. 1997;46(8):1319-27.

349. Annicotte JS, Schoonjans K, Auwerx J. Expression of the liver X receptor alpha and beta in embryonic and adult mice. Anat Rec A Discov Mol Cell Evol Biol. 2004;277(2):312-6.
350. Warnmark A, Treuter E, Wright AP, Gustafsson JA. Activation functions 1 and 2 of nuclear receptors: molecular strategies for transcriptional activation. Mol Endocrinol. 2003;17(10):1901-9.
351. Jin L, Li Y. Structural and functional insights into nuclear receptor signaling. Adv Drug Deliv Rev. 2010;62(13):1218-26.
352. Apfel R, Benbrook D, Lernhardt E, Ortiz MA, Salbert G, Pfahl M. A novel orphan receptor specific for a subset of thyroid hormone-responsive elements and its interaction with the retinoid/thyroid hormone receptor subfamily. Molecular and cellular biology. 1994;14(10):7025-35.
353. Ulven SM, Dalen KT, Gustafsson JA, Nebb HI. LXR is crucial in lipid metabolism. Prostaglandins Leukot Essent Fatty Acids. 2005;73(1):59-63.
354. Lehmann JM, Kliewer SA, Moore LB, Smith-Oliver TA, Oliver BB, Su JL, et al. Activation of the nuclear receptor LXR by oxysterols defines a new hormone response pathway. The Journal of biological chemistry. 1997;272(6):3137-40.
355. Janowski BA, Willy PJ, Devi TR, Falck JR, Mangelsdorf DJ. An oxysterol signalling pathway mediated by the nuclear receptor LXR alpha. Nature. 1996;383(6602):728-31.
356. Janowski BA, Grogan MJ, Jones SA, Wisely GB, Kliewer SA, Corey EJ, et al. Structural requirements of ligands for the oxysterol liver X receptors LXRαlpha and LXRβeta. Proceedings of the National Academy of Sciences of the United States of America. 1999;96(1):266-71.
357. Bjorkhem I, Meaney S, Diczfalusy U. Oxysterols in human circulation: which role do they have? Curr Opin Lipidol. 2002;13(3):247-53.
358. Fu X, Menke JG, Chen Y, Zhou G, MacNaul KL, Wright SD, et al. 27-hydroxycholesterol is an endogenous ligand for liver X receptor in cholesterol-loaded cells. The Journal of biological chemistry. 2001;276(42):38378-87.
359. Song C, Hiipakka RA, Liao S. Selective activation of liver X receptor alpha by 6alpha-hydroxy bile acids and analogs. Steroids. 2000;65(8):423-7.
360. Swahn BM, Macsari I, Viklund J, Ohberg L, Sjodin J, Neelissen J, et al. Liver X receptor agonists with selectivity for LXRβeta; N-aryl-3,3,3-trifluoro-2-hydroxy-2-methylpropionamides. Bioorg Med Chem Lett. 2009;19(7):2009-12.
361. Hu B, Unwalla R, Collini M, Quinet E, Feingold I, Goos-Nilsson A, et al. Discovery and SAR of cinnolines/quinolines as liver X receptor (LXR) agonists with binding selectivity for LXRβeta. Bioorg Med Chem. 2009;17(10):3519-27.
362. Mitro N, Mak PA, Vargas L, Godio C, Hampton E, Molteni V, et al. The nuclear receptor LXR is a glucose sensor. Nature. 2007;445(7124):219-23.
363. Denechaud PD, Bossard P, Lobaccaro JM, Millatt L, Staels B, Girard J, et al. ChREBP, but not LXRs, is required for the induction of glucose-regulated genes in mouse liver. The Journal of clinical investigation. 2008;118(3):956-64.
364. Patel MD, Thompson PD. Phytosterols and vascular disease. Atherosclerosis. 2006;186(1):12-9.
365. Kaneko E, Matsuda M, Yamada Y, Tachibana Y, Shimomura I, Makishima M. Induction of intestinal ATP-binding cassette transporters by a phytosterol-derived liver X receptor agonist. The Journal of biological chemistry. 2003;278(38):36091-8.
366. Schultz JR, Tu H, Luk A, Repa JJ, Medina JC, Li L, et al. Role of LXRs in control of lipogenesis. Genes Dev. 2000;14(22):2831-8.
367. Collins JL, Fivush AM, Watson MA, Galardi CM, Lewis MC, Moore LB, et al. Identification of a nonsteroidal liver X receptor agonist through parallel array synthesis of tertiary amines. J Med Chem. 2002;45(10):1963-6.

368. Molteni V, Li X, Nabakka J, Liang F, Wityak J, Koder A, et al. N-Acylthiadiazolines, a new class of liver X receptor agonists with selectivity for LXRβeta. J Med Chem. 2007;50(17):4255-9.
369. Houck KA, Borchert KM, Hepler CD, Thomas JS, Bramlett KS, Michael LF, et al. T0901317 is a dual LXR/FXR agonist. Mol Genet Metab. 2004;83(1-2):184-7.
370. Mitro N, Vargas L, Romeo R, Koder A, Saez E. T0901317 is a potent PXR ligand: implications for the biology ascribed to LXR. FEBS Lett. 2007;581(9):1721-6.
371. Joseph SB, McKilligin E, Pei L, Watson MA, Collins AR, Laffitte BA, et al. Synthetic LXR ligand inhibits the development of atherosclerosis in mice. Proceedings of the National Academy of Sciences of the United States of America. 2002;99(11):7604-9.
372. Michael DR, Ashlin TG, Buckley ML, Ramji DP. Liver X receptors, atherosclerosis and inflammation. Curr Atheroscler Rep. 2012;14(3):284-93.
373. Katz A, Udata C, Ott E, Hickey L, Burczynski ME, Burghart P, et al. Safety, pharmacokinetics, and pharmacodynamics of single doses of LXR-623, a novel liver X-receptor agonist, in healthy participants. J Clin Pharmacol. 2009;49(6):643-9.
374. Quinet EM, Basso MD, Halpern AR, Yates DW, Steffan RJ, Clerin V, et al. LXR ligand lowers LDL cholesterol in primates, is lipid neutral in hamster, and reduces atherosclerosis in mouse. Journal of lipid research. 2009;50(12):2358-70.
375. DiBlasio-Smith EA, Arai M, Quinet EM, Evans MJ, Kornaga T, Basso MD, et al. Discovery and implementation of transcriptional biomarkers of synthetic LXR agonists in peripheral blood cells. J Transl Med. 2008;6:59.
376. Forman BM, Ruan B, Chen J, Schroepfer GJ, Jr., Evans RM. The orphan nuclear receptor LXRαlpha is positively and negatively regulated by distinct products of mevalonate metabolism. Proceedings of the National Academy of Sciences of the United States of America. 1997;94(20):10588-93.
377. Gan X, Kaplan R, Menke JG, MacNaul K, Chen Y, Sparrow CP, et al. Dual mechanisms of ABCA1 regulation by geranylgeranyl pyrophosphate. The Journal of biological chemistry. 2001;276(52):48702-8.
378. Ou J, Tu H, Shan B, Luk A, DeBose-Boyd RA, Bashmakov Y, et al. Unsaturated fatty acids inhibit transcription of the sterol regulatory element-binding protein-1c (SREBP-1c) gene by antagonizing ligand-dependent activation of the LXR. Proceedings of the National Academy of Sciences of the United States of America. 2001;98(11):6027-32.
379. Yoshikawa T, Shimano H, Yahagi N, Ide T, Amemiya-Kudo M, Matsuzaka T, et al. Polyunsaturated fatty acids suppress sterol regulatory element-binding protein 1c promoter activity by inhibition of liver X receptor (LXR) binding to LXR response elements. The Journal of biological chemistry. 2002;277(3):1705-11.
380. Berrodin TJ, Shen Q, Quinet EM, Yudt MR, Freedman LP, Nagpal S. Identification of 5alpha, 6alpha-epoxycholesterol as a novel modulator of liver X receptor activity. Mol Pharmacol. 2010;78(6):1046-58.
381. Song C, Hiipakka RA, Liao S. Auto-oxidized cholesterol sulfates are antagonistic ligands of liver X receptors: implications for the development and treatment of atherosclerosis. Steroids. 2001;66(6):473-9.
382. Lee JM, Gang GT, Kim DK, Kim YD, Koo SH, Lee CH, et al. Ursodeoxycholic acid inhibits liver X receptor alpha-mediated hepatic lipogenesis via induction of the nuclear corepressor SMILE. The Journal of biological chemistry. 2014;289(2):1079-91.
383. Rastinejad F. Retinoid X receptor and its partners in the nuclear receptor family. Curr Opin Struct Biol. 2001;11(1):33-8.
384. Lee SD, Tontonoz P. Liver X receptors at the intersection of lipid metabolism and atherogenesis. Atherosclerosis. 2015;242(1):29-36.
385. Repa JJ, Mangelsdorf DJ. The liver X receptor gene team: potential new players in atherosclerosis. Nat Med. 2002;8(11):1243-8.

386. Lin CY, Vedin LL, Steffensen KR. The emerging roles of liver X receptors and their ligands in cancer. Expert Opin Ther Targets. 2016;20(1):61-71.
387. Chen JD, Evans RM. A transcriptional co-repressor that interacts with nuclear hormone receptors. Nature. 1995;377(6548):454-7.
388. Horlein AJ, Naar AM, Heinzel T, Torchia J, Gloss B, Kurokawa R, et al. Ligand-independent repression by the thyroid hormone receptor mediated by a nuclear receptor co-repressor. Nature. 1995;377(6548):397-404.
389. Svensson S, Ostberg T, Jacobsson M, Norstrom C, Stefansson K, Hallen D, et al. Crystal structure of the heterodimeric complex of LXRαlpha and RXRbeta ligand-binding domains in a fully agonistic conformation. EMBO J. 2003;22(18):4625-33.
390. Wagner BL, Valledor AF, Shao G, Daige CL, Bischoff ED, Petrowski M, et al. Promoter-specific roles for liver X receptor/corepressor complexes in the regulation of ABCA1 and SREBP1 gene expression. Molecular and cellular biology. 2003;23(16):5780-9.
391. Oberkofler H, Schraml E, Krempler F, Patsch W. Potentiation of liver X receptor transcriptional activity by peroxisome-proliferator-activated receptor gamma co-activator 1 alpha. Biochem J. 2003;371(Pt 1):89-96.
392. Huuskonen J, Fielding PE, Fielding CJ. Role of p160 coactivator complex in the activation of liver X receptor. Arterioscler Thromb Vasc Biol. 2004;24(4):703-8.
393. Glass CK, Rosenfeld MG. The coregulator exchange in transcriptional functions of nuclear receptors. Genes Dev. 2000;14(2):121-41.
394. Venteclef N, Jakobsson T, Ehrlund A, Damdimopoulos A, Mikkonen L, Ellis E, et al. GPS2-dependent corepressor/SUMO pathways govern anti-inflammatory actions of LRH-1 and LXRβeta in the hepatic acute phase response. Genes Dev. 2010;24(4):381-95.
395. Ghisletti S, Huang W, Ogawa S, Pascual G, Lin ME, Willson TM, et al. Parallel SUMOylation-dependent pathways mediate gene- and signal-specific transrepression by LXRs and PPARgamma. Mol Cell. 2007;25(1):57-70.
396. Venteclef N, Jakobsson T, Steffensen KR, Treuter E. Metabolic nuclear receptor signaling and the inflammatory acute phase response. Trends Endocrinol Metab. 2011;22(8):333-43.
397. Gabbi C, Warner M, Gustafsson JA. Action mechanisms of Liver X Receptors. Biochemical and biophysical research communications. 2014;446(3):647-50.
398. Jakobsson T, Treuter E, Gustafsson JA, Steffensen KR. Liver X receptor biology and pharmacology: new pathways, challenges and opportunities. Trends Pharmacol Sci. 2012;33(7):394-404.
399. Cavelier C, Lorenzi I, Rohrer L, von Eckardstein A. Lipid efflux by the ATP-binding cassette transporters ABCA1 and ABCG1. Biochimica et biophysica acta. 2006;1761(7):655-66.
400. Zhao SP, Yu BL, Xie XZ, Dong SZ, Dong J. Dual effects of oxidized low-density lipoprotein on LXR-ABCA1-apoA-I pathway in 3T3-L1 cells. Int J Cardiol. 2008;128(1):42-7.
401. Kotokorpi P, Ellis E, Parini P, Nilsson LM, Strom S, Steffensen KR, et al. Physiological differences between human and rat primary hepatocytes in response to liver X receptor activation by 3-[3-[N-(2-chloro-3-trifluoromethylbenzyl)-(2,2-diphenylethyl)amino]propyloxy]phe nylacetic acid hydrochloride (GW3965). Mol Pharmacol. 2007;72(4):947-55.
402. Schwartz K, Lawn RM, Wade DP. ABC1 gene expression and ApoA-I-mediated cholesterol efflux are regulated by LXR. Biochemical and biophysical research communications. 2000;274(3):794-802.
403. Sparrow CP, Baffic J, Lam MH, Lund EG, Adams AD, Fu X, et al. A potent synthetic LXR agonist is more effective than cholesterol loading at inducing ABCA1 mRNA and stimulating cholesterol efflux. The Journal of biological chemistry. 2002;277(12):10021-7.

404. Muscat GE, Wagner BL, Hou J, Tangirala RK, Bischoff ED, Rohde P, et al. Regulation of cholesterol homeostasis and lipid metabolism in skeletal muscle by liver X receptors. The Journal of biological chemistry. 2002;277(43):40722-8.
405. Repa JJ, Turley SD, Lobaccaro JA, Medina J, Li L, Lustig K, et al. Regulation of absorption and ABC1-mediated efflux of cholesterol by RXR heterodimers. Science. 2000;289(5484):1524-9.
406. Costet P, Luo Y, Wang N, Tall AR. Sterol-dependent transactivation of the ABC1 promoter by the liver X receptor/retinoid X receptor. The Journal of biological chemistry. 2000;275(36):28240-5.
407. Sabol SL, Brewer HB, Jr., Santamarina-Fojo S. The human ABCG1 gene: identification of LXR response elements that modulate expression in macrophages and liver. Journal of lipid research. 2005;46(10):2151-67.
408. Kennedy MA, Venkateswaran A, Tarr PT, Xenarios I, Kudoh J, Shimizu N, et al. Characterization of the human ABCG1 gene: liver X receptor activates an internal promoter that produces a novel transcript encoding an alternative form of the protein. The Journal of biological chemistry. 2001;276(42):39438-47.
409. Engel T, Lorkowski S, Lueken A, Rust S, Schluter B, Berger G, et al. The human ABCG4 gene is regulated by oxysterols and retinoids in monocyte-derived macrophages. Biochemical and biophysical research communications. 2001;288(2):483-8.
410. Rigamonti E, Helin L, Lestavel S, Mutka AL, Lepore M, Fontaine C, et al. Liver X receptor activation controls intracellular cholesterol trafficking and esterification in human macrophages. Circ Res. 2005;97(7):682-9.
411. Zelcer N, Hong C, Boyadjian R, Tontonoz P. LXR regulates cholesterol uptake through Idol-dependent ubiquitination of the LDL receptor. Science. 2009;325(5936):100-4.
412. Calkin AC, Goult BT, Zhang L, Fairall L, Hong C, Schwabe JW, et al. FERM-dependent E3 ligase recognition is a conserved mechanism for targeted degradation of lipoprotein receptors. Proceedings of the National Academy of Sciences of the United States of America. 2011;108(50):20107-12.
413. Zhang L, Reue K, Fong LG, Young SG, Tontonoz P. Feedback regulation of cholesterol uptake by the LXR-IDOL-LDLR axis. Arterioscler Thromb Vasc Biol. 2012;32(11):2541-6.
414. Malerod L, Juvet LK, Hanssen-Bauer A, Eskild W, Berg T. Oxysterol-activated LXRαlpha/RXR induces hSR-BI-promoter activity in hepatoma cells and preadipocytes. Biochemical and biophysical research communications. 2002;299(5):916-23.
415. Kardassis D, Drosatos, C., Zannis, V. Regulation of Genes Involved in the Biogenesis and the Remodeling of HDL. High-Density Lipoproteins From Basic Biology to Clinical Aspects: Wiley-VCH, Weinheim; 2007. p. 237-53.
416. Mak PA, Laffitte BA, Desrumaux C, Joseph SB, Curtiss LK, Mangelsdorf DJ, et al. Regulated expression of the apolipoprotein E/C-I/C-IV/C-II gene cluster in murine and human macrophages. A critical role for nuclear liver X receptors alpha and beta. The Journal of biological chemistry. 2002;277(35):31900-8.
417. Laffitte BA, Repa JJ, Joseph SB, Wilpitz DC, Kast HR, Mangelsdorf DJ, et al. LXRs control lipid-inducible expression of the apolipoprotein E gene in macrophages and adipocytes. Proceedings of the National Academy of Sciences of the United States of America. 2001;98(2):507-12.
418. Wouters K, Shiri-Sverdlov R, van Gorp PJ, van Bilsen M, Hofker MH. Understanding hyperlipidemia and atherosclerosis: lessons from genetically modified apoe and ldlr mice. Clin Chem Lab Med. 2005;43(5):470-9.
419. Luo Y, Tall AR. Sterol upregulation of human CETP expression in vitro and in transgenic mice by an LXR element. The Journal of clinical investigation. 2000;105(4):513-20.

420. Cao G, Beyer TP, Yang XP, Schmidt RJ, Zhang Y, Bensch WR, et al. Phospholipid transfer protein is regulated by liver X receptors in vivo. The Journal of biological chemistry. 2002;277(42):39561-5.
421. Laffitte BA, Joseph SB, Chen M, Castrillo A, Repa J, Wilpitz D, et al. The phospholipid transfer protein gene is a liver X receptor target expressed by macrophages in atherosclerotic lesions. Molecular and cellular biology. 2003;23(6):2182-91.
422. Menke JG, Macnaul KL, Hayes NS, Baffic J, Chao YS, Elbrecht A, et al. A novel liver X receptor agonist establishes species differences in the regulation of cholesterol 7alpha-hydroxylase (CYP7a). Endocrinology. 2002;143(7):2548-58.
423. Chiang JY, Kimmel R, Stroup D. Regulation of cholesterol 7alpha-hydroxylase gene (CYP7A1) transcription by the liver orphan receptor (LXRαlpha). Gene. 2001;262(1-2):257-65.
424. Goodwin B, Watson MA, Kim H, Miao J, Kemper JK, Kliewer SA. Differential regulation of rat and human CYP7A1 by the nuclear oxysterol receptor liver X receptor-alpha. Mol Endocrinol. 2003;17(3):386-94.
425. Yu L, Hammer RE, Li-Hawkins J, Von Bergmann K, Lutjohann D, Cohen JC, et al. Disruption of Abcg5 and Abcg8 in mice reveals their crucial role in biliary cholesterol secretion. Proceedings of the National Academy of Sciences of the United States of America. 2002;99(25):16237-42.
426. Yu L, York J, von Bergmann K, Lutjohann D, Cohen JC, Hobbs HH. Stimulation of cholesterol excretion by the liver X receptor agonist requires ATP-binding cassette transporters G5 and G8. J Biol Chem. 2003;278(18):15565-70.
427. Repa JJ, Berge KE, Pomajzl C, Richardson JA, Hobbs H, Mangelsdorf DJ. Regulation of ATP-binding cassette sterol transporters ABCG5 and ABCG8 by the liver X receptors alpha and beta. J Biol Chem. 2002;277(21):18793-800.
428. Wang A, Kurdistani SK, Grunstein M. Requirement of Hos2 histone deacetylase for gene activity in yeast. Science. 2002;298(5597):1412-4.
429. Duval C, Touche V, Tailleux A, Fruchart JC, Fievet C, Clavey V, et al. Niemann-Pick C1 like 1 gene expression is down-regulated by LXR activators in the intestine. Biochemical and biophysical research communications. 2006;340(4):1259-63.
430. Plosch T, Kok T, Bloks VW, Smit MJ, Havinga R, Chimini G, et al. Increased hepatobiliary and fecal cholesterol excretion upon activation of the liver X receptor is independent of ABCA1. The Journal of biological chemistry. 2002;277(37):33870-7.
431. Eberle D, Hegarty B, Bossard P, Ferre P, Foufelle F. SREBP transcription factors: master regulators of lipid homeostasis. Biochimie. 2004;86(11):839-48.
432. Peet DJ, Turley SD, Ma W, Janowski BA, Lobaccaro JM, Hammer RE, et al. Cholesterol and bile acid metabolism are impaired in mice lacking the nuclear oxysterol receptor LXR alpha. Cell. 1998;93(5):693-704.
433. Repa JJ, Liang G, Ou J, Bashmakov Y, Lobaccaro JM, Shimomura I, et al. Regulation of mouse sterol regulatory element-binding protein-1c gene (SREBP-1c) by oxysterol receptors, LXRαlpha and LXRβeta. Genes Dev. 2000;14(22):2819-30.
434. Yoshikawa T, Shimano H, Amemiya-Kudo M, Yahagi N, Hasty AH, Matsuzaka T, et al. Identification of liver X receptor-retinoid X receptor as an activator of the sterol regulatory element-binding protein 1c gene promoter. Molecular and cellular biology. 2001;21(9):2991-3000.
435. Horton JD, Goldstein JL, Brown MS. SREBPs: activators of the complete program of cholesterol and fatty acid synthesis in the liver. The Journal of clinical investigation. 2002;109(9):1125-31.
436. Chu K, Miyazaki M, Man WC, Ntambi JM. Stearoyl-coenzyme A desaturase 1 deficiency protects against hypertriglyceridemia and increases plasma high-density lipoprotein cholesterol induced by liver X receptor activation. Molecular and cellular biology. 2006;26(18):6786-98.

437. Joseph SB, Laffitte BA, Patel PH, Watson MA, Matsukuma KE, Walczak R, et al. Direct and indirect mechanisms for regulation of fatty acid synthase gene expression by liver X receptors. The Journal of biological chemistry. 2002;277(13):11019-25.
438. Talukdar S, Hillgartner FB. The mechanism mediating the activation of acetyl-coenzyme A carboxylase-alpha gene transcription by the liver X receptor agonist T0-901317. Journal of lipid research. 2006;47(11):2451-61.
439. Wang Y, Kurdi-Haidar B, Oram JF. LXR-mediated activation of macrophage stearoyl-CoA desaturase generates unsaturated fatty acids that destabilize ABCA1. Journal of lipid research. 2004;45(5):972-80.
440. Grefhorst A, Elzinga BM, Voshol PJ, Plosch T, Kok T, Bloks VW, et al. Stimulation of lipogenesis by pharmacological activation of the liver X receptor leads to production of large, triglyceride-rich very low density lipoprotein particles. The Journal of biological chemistry. 2002;277(37):34182-90.
441. Quinet EM, Savio DA, Halpern AR, Chen L, Schuster GU, Gustafsson JA, et al. Liver X receptor (LXR)-beta regulation in LXRαlpha-deficient mice: implications for therapeutic targeting. Mol Pharmacol. 2006;70(4):1340-9.
442. Korach-Andre M, Parini P, Larsson L, Arner A, Steffensen KR, Gustafsson JA. Separate and overlapping metabolic functions of LXRαlpha and LXRβeta in C57Bl/6 female mice. Am J Physiol Endocrinol Metab. 2010;298(2):E167-78.
443. Stulnig TM, Steffensen KR, Gao H, Reimers M, Dahlman-Wright K, Schuster GU, et al. Novel roles of liver X receptors exposed by gene expression profiling in liver and adipose tissue. Mol Pharmacol. 2002;62(6):1299-305.
444. Commerford SR, Vargas L, Dorfman SE, Mitro N, Rocheford EC, Mak PA, et al. Dissection of the insulin-sensitizing effect of liver X receptor ligands. Mol Endocrinol. 2007;21(12):3002-12.
445. Grefhorst A, van Dijk TH, Hammer A, van der Sluijs FH, Havinga R, Havekes LM, et al. Differential effects of pharmacological liver X receptor activation on hepatic and peripheral insulin sensitivity in lean and ob/ob mice. Am J Physiol Endocrinol Metab. 2005;289(5):E829-38.
446. Efanov AM, Sewing S, Bokvist K, Gromada J. Liver X receptor activation stimulates insulin secretion via modulation of glucose and lipid metabolism in pancreatic beta-cells. Diabetes. 2004;53 Suppl 3:S75-8.
447. Efanov AM, Barrett DG, Brenner MB, Briggs SL, Delaunois A, Durbin JD, et al. A novel glucokinase activator modulates pancreatic islet and hepatocyte function. Endocrinology. 2005;146(9):3696-701.
448. Zitzer H, Wente W, Brenner MB, Sewing S, Buschard K, Gromada J, et al. Sterol regulatory element-binding protein 1 mediates liver X receptor-beta-induced increases in insulin secretion and insulin messenger ribonucleic acid levels. Endocrinology. 2006;147(8):3898-905.
449. Cao G, Liang Y, Broderick CL, Oldham BA, Beyer TP, Schmidt RJ, et al. Antidiabetic action of a liver x receptor agonist mediated by inhibition of hepatic gluconeogenesis. The Journal of biological chemistry. 2003;278(2):1131-6.
450. Prokova V, Mavridou S, Papakosta P, Kardassis D. Characterization of a novel transcriptionally active domain in the transforming growth factor beta-regulated Smad3 protein. Nucleic acids research. 2005;33(12):3708-21.
451. Kirchgessner TG, LeBoeuf RC, Langner CA, Zollman S, Chang CH, Taylor BA, et al. Genetic and developmental regulation of the lipoprotein lipase gene: loci both distal and proximal to the lipoprotein lipase structural gene control enzyme expression. J Biol Chem. 1989;264(3):1473-82.

452. Staels B, Auwerx J. Perturbation of developmental gene expression in rat liver by fibric acid derivatives: lipoprotein lipase and alpha-fetoprotein as models. Development. 1992;115(4):1035-43.
453. Liu G, Xu JN, Liu D, Ding Q, Liu MN, Chen R, et al. Regulation of plasma lipid homeostasis by hepatic lipoprotein lipase in adult mice. J Lipid Res. 2016;57(7):1155-61.
454. Kullak-Ublick GA, Stieger B, Meier PJ. Enterohepatic bile salt transporters in normal physiology and liver disease. Gastroenterology. 2004;126(1):322-42.
455. Eloranta JJ, Kullak-Ublick GA. Coordinate transcriptional regulation of bile acid homeostasis and drug metabolism. Archives of biochemistry and biophysics. 2005;433(2):397-412.
456. Mennone A, Soroka CJ, Cai SY, Harry K, Adachi M, Hagey L, et al. Mrp4-/- mice have an impaired cytoprotective response in obstructive cholestasis. Hepatology (Baltimore, Md. 2006;43(5):1013-21.
457. Yang WS, Nevin DN, Iwasaki L, Peng R, Brown BG, Brunzell JD, et al. Regulatory mutations in the human lipoprotein lipase gene in patients with familial combined hyperlipidemia and coronary artery disease. J Lipid Res. 1996;37(12):2627-37.
458. Wang P, Jin T. Oct-1 functions as a sensor for metabolic and stress signals. Islets. 2010;2(1):46-8.
459. Wang P, Wang Q, Sun J, Wu J, Li H, Zhang N, et al. POU homeodomain protein Oct-1 functions as a sensor for cyclic AMP. The Journal of biological chemistry. 2009;284(39):26456-65.
460. Kang J, Gemberling M, Nakamura M, Whitby FG, Handa H, Fairbrother WG, et al. A general mechanism for transcription regulation by Oct1 and Oct4 in response to genotoxic and oxidative stress. Genes & development. 2009;23(2):208-22.
461. Uyeda K, Repa JJ. Carbohydrate response element binding protein, ChREBP, a transcription factor coupling hepatic glucose utilization and lipid synthesis. Cell metabolism. 2006;4(2):107-10.
462. Sirek AS, Liu L, Naples M, Adeli K, Ng DS, Jin T. Insulin stimulates the expression of carbohydrate response element binding protein (ChREBP) by attenuating the repressive effect of Pit-1, Oct-1/Oct-2, and Unc-86 homeodomain protein octamer transcription factor-1. Endocrinology. 2009;150(8):3483-92.
463. de Boer E, Rodriguez P, Bonte E, Krijgsveld J, Katsantoni E, Heck A, et al. Efficient biotinylation and single-step purification of tagged transcription factors in mammalian cells and transgenic mice. Proceedings of the National Academy of Sciences of the United States of America. 2003;100(13):7480-5.
464. Thymiakou E, Zannis VI, Kardassis D. Physical and functional interactions between liver X receptor/retinoid X receptor and Sp1 modulate the transcriptional induction of the human ATP binding cassette transporter A1 gene by oxysterols and retinoids. Biochemistry. 2007;46(41):11473-83.
465. Husmann M, Dragneva Y, Romahn E, Jehnichen P. Nuclear receptors modulate the interaction of Sp1 and GC-rich DNA via ternary complex formation. The Biochemical journal. 2000;352 Pt 3:763-72.
466. Suzuki Y, Shimada J, Shudo K, Matsumura M, Crippa MP, Kojima S. Physical interaction between retinoic acid receptor and Sp1: mechanism for induction of urokinase by retinoic acid. Blood. 1999;93(12):4264-76.
467. Huang YC, Chen JY, Hung WC. Vitamin D3 receptor/Sp1 complex is required for the induction of p27Kip1 expression by vitamin D3. Oncogene. 2004;23(28):4856-61.
468. Cheng HT, Chen JY, Huang YC, Chang HC, Hung WC. Functional role of VDR in the activation of p27Kip1 by the VDR/Sp1 complex. Journal of cellular biochemistry. 2006;98(6):1450-6.

469. Kim K, Thu N, Saville B, Safe S. Domains of estrogen receptor alpha (ERalpha) required for ERalpha/Sp1-mediated activation of GC-rich promoters by estrogens and antiestrogens in breast cancer cells. Molecular endocrinology. 2003;17(5):804-17.
470. Sun G, Porter W, Safe S. Estrogen-induced retinoic acid receptor alpha 1 gene expression: role of estrogen receptor-Sp1 complex. Molecular endocrinology. 1998;12(6):882-90.
471. Heverin M, Ali Z, Olin M, Tillander V, Joibari MM, Makoveichuk E, et al. On the regulatory importance of 27-hydroxycholesterol in mouse liver. The Journal of steroid biochemistry and molecular biology. 2016.
472. Huang H, Tindall DJ. Dynamic FoxO transcription factors. J Cell Sci. 2007;120(Pt 15):2479-87.
473. Maiese K, Chong ZZ, Shang YC. OutFOXOing disease and disability: the therapeutic potential of targeting FoxO proteins. Trends Mol Med. 2008;14(5):219-27.
474. Gross DN, Wan M, Birnbaum MJ. The role of FOXO in the regulation of metabolism. Curr Diab Rep. 2009;9(3):208-14.
475. Gross DN, van den Heuvel AP, Birnbaum MJ. The role of FoxO in the regulation of metabolism. Oncogene. 2008;27(16):2320-36.
476. Tontonoz P, Mangelsdorf DJ. Liver X receptor signaling pathways in cardiovascular disease. Mol Endocrinol. 2003;17(6):985-93.
477. Zhao C, Dahlman-Wright K. Liver X receptor in cholesterol metabolism. J Endocrinol. 2010;204(3):233-40.
478. Berge KE, Tian H, Graf GA, Yu L, Grishin NV, Schultz J, et al. Accumulation of dietary cholesterol in sitosterolemia caused by mutations in adjacent ABC transporters. Science. 2000;290(5497):1771-5.
479. Patel SB. Recent advances in understanding the STSL locus and ABCG5/ABCG8 biology. Curr Opin Lipidol. 2014;25(3):169-75.
480. Lu K, Lee MH, Yu H, Zhou Y, Sandell SA, Salen G, et al. Molecular cloning, genomic organization, genetic variations, and characterization of murine sterolin genes Abcg5 and Abcg8. J Lipid Res. 2002;43(4):565-78.
481. Lu K, Lee MH, Hazard S, Brooks-Wilson A, Hidaka H, Kojima H, et al. Two genes that map to the STSL locus cause sitosterolemia: genomic structure and spectrum of mutations involving sterolin-1 and sterolin-2, encoded by ABCG5 and ABCG8, respectively. Am J Hum Genet. 2001;69(2):278-90.
482. Yu XH, Qian K, Jiang N, Zheng XL, Cayabyab FS, Tang CK. ABCG5/ABCG8 in cholesterol excretion and atherosclerosis. Clin Chim Acta. 2014;428:82-8.
483. Brown JM, Yu L. Opposing Gatekeepers of Apical Sterol Transport: Niemann-Pick C1-Like 1 (NPC1L1) and ATP-Binding Cassette Transporters G5 and G8 (ABCG5/ABCG8). Immunol Endocr Metab Agents Med Chem. 2009;9(1):18-29.
484. Graf GA, Yu L, Li WP, Gerard R, Tuma PL, Cohen JC, et al. ABCG5 and ABCG8 are obligate heterodimers for protein trafficking and biliary cholesterol excretion. J Biol Chem. 2003;278(48):48275-82.
485. Dikkers A, Tietge UJ. Biliary cholesterol secretion: more than a simple ABC. World J Gastroenterol. 2010;16(47):5936-45.
486. Graf GA, Li WP, Gerard RD, Gelissen I, White A, Cohen JC, et al. Coexpression of ATP-binding cassette proteins ABCG5 and ABCG8 permits their transport to the apical surface. J Clin Invest. 2002;110(5):659-69.
487. Salen G, Patel S, Batta AK. Sitosterolemia. Cardiovasc Drug Rev. 2002;20(4):255-70.
488. Salen G, Shefer S, Nguyen L, Ness GC, Tint GS, Shore V. Sitosterolemia. J Lipid Res. 1992;33(7):945-55.

489. von Kampen O, Buch S, Nothnagel M, Azocar L, Molina H, Brosch M, et al. Genetic and functional identification of the likely causative variant for cholesterol gallstone disease at the ABCG5/8 lithogenic locus. Hepatology. 2013;57(6):2407-17.
490. Klett EL, Lu K, Kosters A, Vink E, Lee MH, Altenburg M, et al. A mouse model of sitosterolemia: absence of Abcg8/sterolin-2 results in failure to secrete biliary cholesterol. BMC Med. 2004;2:5.
491. Plosch T, Bloks VW, Terasawa Y, Berdy S, Siegler K, Van Der Sluijs F, et al. Sitosterolemia in ABC-transporter G5-deficient mice is aggravated on activation of the liver-X receptor. Gastroenterology. 2004;126(1):290-300.
492. Yu L, Li-Hawkins J, Hammer RE, Berge KE, Horton JD, Cohen JC, et al. Overexpression of ABCG5 and ABCG8 promotes biliary cholesterol secretion and reduces fractional absorption of dietary cholesterol. J Clin Invest. 2002;110(5):671-80.
493. Brown JM, Yu L. Protein mediators of sterol transport across intestinal brush border membrane. Subcell Biochem. 2010;51:337-80.
494. Sumi K, Tanaka T, Uchida A, Magoori K, Urashima Y, Ohashi R, et al. Cooperative interaction between hepatocyte nuclear factor 4 alpha and GATA transcription factors regulates ATP-binding cassette sterol transporters ABCG5 and ABCG8. Mol Cell Biol. 2007;27(12):4248-60.
495. Freeman LA, Kennedy A, Wu J, Bark S, Remaley AT, Santamarina-Fojo S, et al. The orphan nuclear receptor LRH-1 activates the ABCG5/ABCG8 intergenic promoter. J Lipid Res. 2004;45(7):1197-206.
496. Bonde Y, Plosch T, Kuipers F, Angelin B, Rudling M. Stimulation of murine biliary cholesterol secretion by thyroid hormone is dependent on a functional ABCG5/G8 complex. Hepatology. 2012;56(5):1828-37.
497. Calpe-Berdiel L, Rotllan N, Fievet C, Roig R, Blanco-Vaca F, Escola-Gil JC. Liver X receptor-mediated activation of reverse cholesterol transport from macrophages to feces in vivo requires ABCG5/G8. J Lipid Res. 2008;49(9):1904-11.
498. van der Veen JN, Havinga R, Bloks VW, Groen AK, Kuipers F. Cholesterol feeding strongly reduces hepatic VLDL-triglyceride production in mice lacking the liver X receptor alpha. J Lipid Res. 2007;48(2):337-47.
499. Back SS, Kim J, Choi D, Lee ES, Choi SY, Han K. Cooperative transcriptional activation of ATP-binding cassette sterol transporters ABCG5 and ABCG8 genes by nuclear receptors including Liver-X-Receptor. BMB Rep. 2013;46(6):322-7.
500. Biddinger SB, Haas JT, Yu BB, Bezy O, Jing E, Zhang W, et al. Hepatic insulin resistance directly promotes formation of cholesterol gallstones. Nat Med. 2008;14(7):778-82.
501. Bhattacharyya AK, Connor WE. Beta-sitosterolemia and xanthomatosis. A newly described lipid storage disease in two sisters. J Clin Invest. 1974;53(4):1033-43.
502. Belamarich PF, Deckelbaum RJ, Starc TJ, Dobrin BE, Tint GS, Salen G. Response to diet and cholestyramine in a patient with sitosterolemia. Pediatrics. 1990;86(6):977-81.
503. Wilund KR, Yu L, Xu F, Hobbs HH, Cohen JC. High-level expression of ABCG5 and ABCG8 attenuates diet-induced hypercholesterolemia and atherosclerosis in Ldlr-/- mice. J Lipid Res. 2004;45(8):1429-36.
504. Teupser D, Baber R, Ceglarek U, Scholz M, Illig T, Gieger C, et al. Genetic regulation of serum phytosterol levels and risk of coronary artery disease. Circ Cardiovasc Genet. 2010;3(4):331-9.

5. PUBLICATIONS

Biochimica et Biophysica Acta 1860 (2017) 327–336

Contents lists available at ScienceDirect

Biochimica et Biophysica Acta

journal homepage: www.elsevier.com/locate/bbagrm

Regulation of the human lipoprotein lipase gene by the forkhead box transcription factor FOXA2/HNF-3β in hepatic cells

Maria Kanaki, Dimitris Kardassis *

Laboratory of Biochemistry, University of Crete Medical School and Institute of Molecular Biology and Biotechnology, Foundation for Research and Technology-Hellas, Heraklion 71003, Greece

ARTICLE INFO

Article history:
Received 21 November 2016
Received in revised form 13 January 2017
Accepted 13 January 2017
Available online xxxx

Keywords:
Lipoprotein lipase
Promoter
FOXA2
HNF-3β
Transcriptional activation
Insulin
Liver
Triglycerides
Lipoproteins

ABSTRACT

Lipoprotein lipase (LPL) plays a major role in the hydrolysis of triglycerides (TG) from circulating TG-rich lipoproteins. The role of LPL in the liver has been controversial but recent studies in mice with liver LPL overexpression or deficiency have revealed important new roles of the enzyme in glucose and lipid metabolism. The objective of this study was to identify regulatory elements and factors that control the transcription of the human LPL gene in hepatocytes. Deletion analysis of the human LPL promoter revealed that the proximal region which harbors a binding site for the forkhead box transcription factor FOXA2/HNF-3β at position −47/−40 is important for its hepatic cell activity. Silencing of FOXA2 in HepG2 cells reduced the LPL mRNA and protein levels. Direct binding of FOXA2 to the novel binding site was established in vitro and ex vivo. Mutagenesis of the FOXA2 site reduced the basal activity and abolished the FOXA2-mediated transactivation of the LPL promoter. Insulin decreased LPL mRNA levels in HepG2 cells and this was associated with phosphorylation of AKT and nuclear export of FOXA2. In summary, the data of the present study combined with previous findings on the role of FOXA2 in HDL metabolism and gluconeogenesis, suggest that FOXA2 is a key regulator of lipid and glucose homeostasis in the adult liver. Understanding the mechanisms by which FOXA2 exerts its functions in hepatocytes may open the way to novel therapeutic strategies for patients with metabolic diseases such as dyslipidemia, diabetes and the metabolic syndrome.

1. Introduction

Lipoprotein lipase (LPL) plays an important role in lipoprotein metabolism by catalyzing the hydrolysis of triglycerides (TG) in plasma TG-rich lipoproteins including very low density lipoproteins (VLDL) and chylomicrons. Apolipoprotein CII (apoC-II) is a cofactor of this enzyme [1]. LPL is synthesized by various tissues such as the adipose tissue, skeletal muscle and heart but can be found at lower levels in many other tissues including macrophages, kidney, brain, adrenals, lung and embryonic liver [2–6]. Following its secretion, LPL is attached to endothelial cells via heparin sulfate proteoglycans (HSPGs) with the help of a protein called glycosylphosphatidylinositol anchored high density lipoprotein binding protein 1 (GPIHBP1) [1,3]. It has been shown that LPL can act as a ligand of lipoprotein receptors such as the LDL receptor or the LDL receptor-related protein 1 (LRP1) suggesting that it could contribute to lipoprotein catabolism in the liver [7–9].

Mice with total LPL deficiency die immediately after birth from hypertriglyceridemia [10,11]. On the other hand, overexpression of LPL in mice was associated with higher LPL activity, decreased plasma TG and reduced atherosclerosis due to the reduction in lipoprotein remnants [12–14]. Previous studies have shown that deficiencies in LPL or apoC-II in humans are associated with hypertriglyceridemia, reduced levels of high density lipoprotein cholesterol (HDL), familial chylomicronemia or/and premature atherosclerosis [15–19]. Patients with familial LPL deficiency are characterized by very low or absence of LPL activity due to loss-of-function mutations in the LPL gene. Mutations in the homozygous or compound heterozygous form result in markedly decreased or absent LPL activity with consequent extremely low levels of HDL cholesterol, severe hypertriglyceridemia and pancreatitis. Heterozygous LPL deficiency usually results in normal to moderately elevated plasma triglyceride concentrations as a result of a decrease in the LPL activity but this can lead to more severe hypertriglyceridemia when there are other conditions like diabetes or high alcohol intake [20–26].

Members of the peroxisome proliferator activated receptor (PPAR) family of hormone nuclear receptors such as PPARα and PPARγ regulate the activity of the LPL promoter in response to fibrates, fatty acids or fasting [27–32]. The oxysterol receptor Liver X Receptor (LXR) was shown to bind to a responsive element in the first intron of the mouse LPL gene and to facilitate the induction of LPL gene in response to a

* Corresponding author at: Laboratory of Biochemistry, Department of Basic Medical Sciences, University of Crete Medical School, Heraklion 71003, Greece.
E-mail address: kardasis@imbb.forth.gr (D. Kardassis).

http://dx.doi.org/10.1016/j.bbagrm.2017.01.007
1874-9399/

high cholesterol diet or to a synthetic LXR agonist in the liver and macrophages, but not in muscle or adipose tissue where the expression of LPL is constitutively high [33].

In adult mice LPL gene expression in the liver is low compared with other tissues [34]. However, hepatic LPL was recently shown to play an important physiological role in plasma lipid homeostasis in adult mice because ablation of hepatic LPL decreased significantly plasma LPL content and elevated plasma TG and cholesterol levels [34].

Forkhead box A2 (FOXA2)/Hepatocyte Nuclear Factor 3β (HNF3β) belongs to the forkhead box family of liver transcription factors that includes also FOXA1 and FOXA3 (or HNF3α, HNF3γ) [35]. These factors contain a conserved DNA binding domain and bind as monomers to DNA elements having homology with the consensus sequence 5′-T(G/A)TTT(A/G)(C/T)T-3′ [36,37]. FOXA2 is expressed at high levels in the liver and at lower levels in other tissues [38]. Mice with total ablation of FOXA2 die early during embryogenesis due to developmental defects [39,40].

FOXA2 plays a critical role in glucose homeostasis in the liver, by controlling the expression of gluconeogenesis genes in response to insulin, including phosphoenolpyruvate carboxykinase (PEPCK) and glucose-6-phosphatase (G6Pase) [41–43]. During fasting, liver FOXA2 enhances the catabolism of fatty acids and the secretion of VLDL and HDL by activating genes involved in these pathways [44–47]. Furthermore, liver-specific FOXA2 ablation in mice revealed that FOXA2 plays an important role in bile acid homeostasis because it regulates the expression of genes of bile acid metabolism such as bile acid transporters [48]. Mice with FOXA2 haploinsufficiency or with hyperinsulinemia caused by mutations in leptin signaling exhibited decreased pre-β HDL levels in the plasma and this has been correlated with low levels of expression of the apolipoprotein M (apoM) gene which is a FOXA2 target [45,49]. In a previous study we had shown that FOXA2 inhibits the expression of the cholesterol and phospholipid transporter ATP binding cassette transporter 1 (ABCA1) in hepatic cells thus regulating HDL biogenesis [50].

Several studies have used genome wide analyses (ChIP-Seq, ChIP-chip) in liver-derived cell lines and liver samples from wild type or hepatocyte-specific FOXA2 deficient mice and identified many FOXA2 binding sites within the promoters or introns of genes involved in lipid and triglyceride metabolism [37,48,51–53]. Furthermore, gene chip expression analysis of FOXA2-induced genes in livers from mice expressing constitutively active FOXA2 showed increased expression levels of genes involved in β-oxidation, ketogenesis, and TG metabolism including the LPL gene [44].

The objective of this study was to identify cis-acting DNA elements and transcription factors that control the expression of the human LPL gene in hepatocytes.

2. Materials and methods

Materials and a more detailed description of methodologies used in this study can be found in the Supplement.

2.1. Plasmid constructions

The human LPL promoter plasmids (−883/+39) LPL-Luc, (−669/+39) LPL-Luc, (−466/+39) LPL-Luc, (−262/+39) LPL-Luc, (−109/+39) LPL-Luc and (−28/+39) LPL-luc were generated by PCR amplification and cloned at the *Xho*I-*Hin*dIII sites of pBluescript vector bearing the luciferase gene. The (−883/+39) mut LPL-luc and (−109/+39) mut LPL-luc constructs which bear mutations in the FOXA2 binding site of the LPL promoter were generated by site-directed mutagenesis using the QuickChange Site-Directed Mutagenesis Kit. All oligonucleotides used as primers in PCR amplification or in mutagenesis were synthesized at the microchemical facility of the Institute of Molecular Biology and Biotechnology (IMBB) (Heraklion, Greece), and their sequence is shown in Table 1. The expression vector CMV-rFOXA2 was described previously [50].

2.2. Cell culture and treatments

Human hepatoma HepG2 cells and human embryonic kidney cells (HEK293T) were cultured in Dulbecco's modified Eagle's medium (DMEM high glucose) supplemented with 10% fetal bovine serum (FBS), L-glutamine, and penicillin/streptomycin at 37 °C in a 5% CO_2 atmosphere. For the treatment of HepG2 cells with insulin, cells were plated in DMEM low glucose + Glutamax supplemented with 10% fetal bovine serum and penicillin/streptomycin, serum-starved for 18 h with DMEM low glucose + Glutamax supplemented with penicillin/streptomycin and stimulated with insulin for 24 h at a final concentration of 500 nM. Mouse 3T3-L1 pre-adipocytes were grown in DMEM (high glucose) supplemented with 10% newborn calf serum (NBCS), L-glutamine, 1% sodium pyruvate and penicillin/streptomycin (Normal Growth Medium) at 37 °C in a 5% CO_2 atmosphere. For adipocyte differentiation, 3T3-L1 cells were maintained for 1 day in normal growth medium and then switched for 2 days to differentiation medium, a mixture of DMEM supplemented with 10% FBS, 1% sodium pyruvate, penicillin/streptomycin, 0.17 μM insulin, 0.25 μM dexamethasone and 0.5 mM isobutylmethylxanthine (IBMX). After this time cells were cultivated in differentiation medium without the inducers dexamethasone and IBMX for 2–3 days. About 2 days after removal of dexamethasone and IBMX, adipocyte colonies began to be visible as regions containing rounded cells with numerous intracellular lipid droplets. Then the medium of cells was switched again to the differentiation medium supplemented with the inducers (dexamethasone and IBMX) for 2 more days. The cells were maintained for 1 day in differentiation medium without the inducers and the next day cells were harvested.

2.3. Transient transfections, siRNA silencing and reporter assays

Transient transfections in HepG2 and HEK293T cells were performed using the calcium phosphate [$Ca_3(PO_4)_2$] co-precipitation method. Lipofectamine 2000 reagent was used in HepG2 cells that were transfected with FOXA2 expression vector for protein and RNA extraction, according to the manufacturer's instructions. Transient transfections in 3T3-L1 cells and insulin treated HepG2 cells were performed using Lipofectamine 2000. HepG2 and HEK293T cells were treated with scrambled siRNA or siRNA against FOXA2 for 40 h using Lipofectamine RNAiMAX according to the manufacturer's instructions. The silencing efficiency of FOXA2 was confirmed by western blotting or/and qPCR. Luciferase assays were performed 40 h post transfections using the luciferase assay kit from Promega Corp. Normalization for transfection efficiency was performed by β-galactosidase assays.

2.4. RNA isolation, reverse transcription, PCR and quantitative PCR (qPCR)

Total RNA was prepared from HepG2, HEK293T or 3T3-L1 cells using Trizol reagent according to the manufacturer's instructions. All oligonucleotide sequences used as primers in qPCR or PCR experiments are shown in Table 1.

2.5. Chromatin Immunoprecipitation (ChIP) and DNA Affinity Precipitation (DNAP) assays

Chromatin Immunoprecipitation and DNA Affinity Precipitation Assays were performed as described previously [50]. The oligonucleotides used as primers in these assays are shown in Table 1.

2.6. Statistical analysis

Results are expressed as mean ± S.D. Statistical significance was determined using two-tailed Student's *t*-test. Differences with $p < 0.05$

Table 1
Oligonucleotides used in PCR cloning, mutagenesis, PCR, qPCR, DNA affinity precipitation (DNAP), chromatin immunoprecipitation (ChIP) assays and siRNA-mediated silencing.[a]

Name	Sequence	Purpose
LPL −883 Fw	5′ - CCGCTCGAGCAGAGTTGTGCAGCATCAGCAT - 3′	Cloning of the LPL promoter, starting at position −883
LPL −669 Fw	5′ - CCGCTCGAGACGGCTTTAGATTATTTGACCTCG - 3′	Cloning of the LPL promoter, starting at position −669
LPL −466 Fw	5′ - CCGCTCGAGACGCAATGTGTGTCCCTCTAT - 3′	Cloning of the LPL promoter, starting at position −466 and DNAP
LPL −262 Fw	5′ - CCGCTCGAGACCTGTGTTTGGTGCTTAGACA - 3′	Cloning of the LPL promoter, starting at position −262 and DNAP
LPL −109 Fw	5′ - CCGCTCGAGTAGAAGTGAATTTAGGTCCCTC - 3′	Cloning of the LPL promoter, starting at position −109 and DNAP
LPL −28 Fw	5′ - CCGCTCGAGACATAAGCAGCCTTGGCGTGAAAA - 3′	Cloning of the LPL promoter, starting at position −28 and DNAP
LPL +39 Rev	5′ - CCCAAGCTTTTCCCTTGAGGAGGAGGAAGAG - 3′	Cloning of the LPL promoter, ending at position +39
LPL-FOXA2-Mut-Fw	5′ - ATAGGTGATGAGGTT**CCCGG**GCATATTTCCAGTCA - 3′	Mutagenesis of the FOXA2 site of the LPL promoter
LPL-FOXA2-Mut-Rev	5′ - TGACTGGAAATATGC**CCGGG**AACCTCATCACCTAT - 3′	Mutagenesis of the FOXA2 site of the LPL promoter
LPL-39T/C-Fw	5′ - GGTGATGAGGTTTATTTGCA**C**ATTTCCAGTCACATAAGCAG - 3′	Mutagenesis of the LPL promoter at -39C
LPL-39T/C-Rev	5′ - CTGCTTATGTGACTGGAAAT**G**TGCAAATAAACCTCATCACC - 3′	Mutagenesis of the LPL promoter at -39C
mLPL Fw	5′ - TACAGCCTTGGAGCCCATGCT - 3′	PCR analysis of mLPL cDNA
mLPL Rev	5′ - GAAGAGATGAATGGAGCGCTCGT - 3′	PCR analysis of mLPL cDNA
mFOXA2 Fw	5′ - CGTGAAGATGGAAGGGCACGAGC - 3′	PCR analysis of mFOXA2 cDNA
mFOXA2 Rev	5′ - TTCATGTTGGCGTAGGGGGCAAG - 3′	PCR analysis of mFOXA2 cDNA
mGAPDH Fw	5′ - ACCACAGTCCATGCCATCAC - 3′	PCR analysis of mGAPDH cDNA
mGAPDH Rev	5′ - TCCACCACCCTGTTGCTGTA - 3′	PCR analysis of mGAPDH cDNA
hLPL Fw	5′ - AGCATTACCCAGTGTCCGC - 3′	qPCR analysis of hLPL cDNA
hLPL Rev	5′ - GGGCTCCAAGGCTGTATCC - 3′	qPCR analysis of hLPL cDNA
hGUSB Fw	5′ - CACAAGAGTGGTGCTGAGGA - 3′	qPCR analysis of hGUSB cDNA
hGUSB Rev	5′ - ACCAGGTTGCTGATGTCGG - 3′	qPCR analysis of hGUSB cDNA
hFOXA2 Fw	5′ - CTGGGAGCGGTGAAGATGG - 3′	qPCR analysis of hFOXA2 cDNA
hFOXA2 Rev	5′ - CATGTTGCTCACGGAGGAGT - 3′	qPCR analysis of hFOXA2 cDNA
LPL +39 Rev-Bio	5′ - Bio-TTCCCTTGAGGAGGAGGAAGAGGGGGAAT - 3′	DNAP, 5′ biotinylated
LPL −141 ChIP Fw	5′ - GGTTGATCCTCATTACTGTTTGCT - 3′	ChIP analysis of the LPL promoter, starting at position −141
LPL −10 ChIP Rev	5′ - ACGCCAAGGCTGCTTATGT - 3′	ChIP analysis of the LPL promoter, ending at position −10
LPL intron2 ChIP Fw	5′ - GACGGTGCCACTTCCTATCA - 3′	ChIP analysis of the 2nd intron of LPL
LPL intron2 ChIP Rev	5′ - TGCACAGACCCAACTCAGTC - 3′	ChIP analysis of the 2nd intron of LPL
FOXA2 siRNA	5′ - CAGCAGAGCCCCAACAAGA - 3′	siRNA silencing of human FOXA2 gene
Scrambled siRNA	5′ - CAGTCGCGTTTGCGACTGG - 3′	non-specific siRNA (control)

[a] *Xho*I (CTCGAG) and *Hin*dIII (AAGCTT) sites are underlined. Nucleotide substitutions in the primers used for site-directed mutagenesis are in bold.

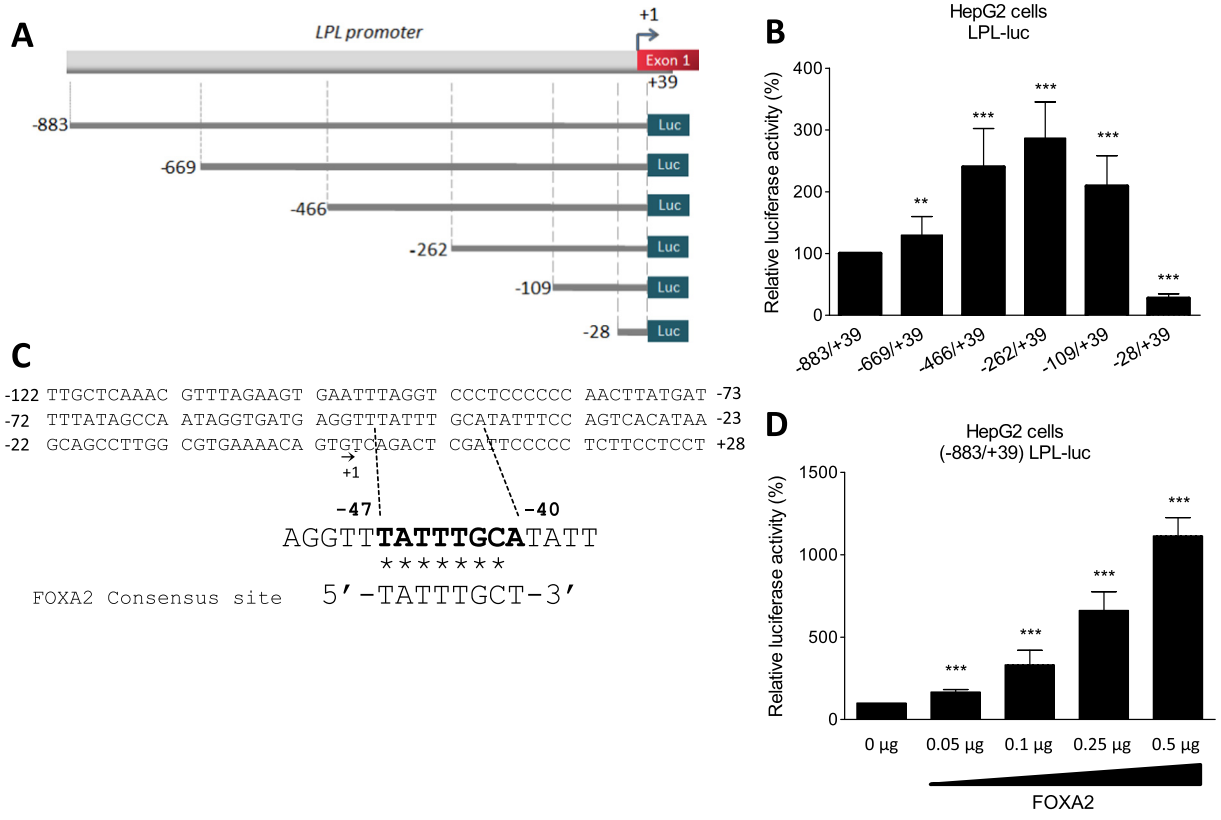

Fig. 1. The human LPL promoter contains a putative FOXA2 binding element. (A) Schematic representation of the 5′-deletion fragments of the (−883/+39) human LPL promoter that were used in the transactivation experiments of panel B. (B) HepG2 cells were transiently transfected with the indicated LPL-luc reporter plasmids (1 μg) along with a β-galactosidase expression plasmid (1 μg) which was included in each sample for normalization of transfection variability. Luciferase activity was normalized to β-galactosidase activity and presented with histographs. Each value represents the average (±SD) from eight independent experiments performed in duplicate. (C) Sequence of the proximal human LPL promoter region −122/+28. The putative FOXA2 binding site in the −47/−40 region is in bold letters. Homology of the putative FOXA2 binding site of the LPL promoter with the FOXA2 consensus site is indicated with the asterisks. (D) HepG2 cells were transiently transfected with the (−883/+39) LPL-luc reporter plasmid (1 μg) along with increasing concentrations (0.05–0.5 μg) of a FOXA2 expression vector. The normalized relative luciferase activity is presented with histographs. Each value represents the average (±SD) from at least three independent experiments performed in duplicate. **, $p < 0.01$; ***, $p < 0.001$.

were considered to be statistically significant. Analysis was performed using GraphPad Prism software (GraphPad Software Inc., La Jolla, CA).

3. Results

3.1. Functional analysis of the human LPL promoter in hepatic cells reveals a putative FOXA2 binding site in the proximal region

In order to identify and characterize regulatory elements that are critical for the expression of the human LPL gene, we amplified by polymerase chain reaction from human genomic DNA the human −883/+39 LPL promoter and generated a series of 5′ deletions: −669/+39, −466/+39, −262/+39, −109/+39 and −28/+39 (Fig. 1A). These LPL promoter fragments were cloned upstream of the luciferase reporter gene and their relative transcriptional activity was determined by luciferase assays in human hepatoblastoma HepG2 cells. As shown in Fig. 1B, serial deletions of the LPL promoter from position −883 to position −262 were associated with a step-wise increase in the activity of the promoter suggesting the presence of inhibitory regulatory region(s) in the area defined by nucleotides −883 and −262. Further deletion to nucleotide −109 caused a small reduction in promoter activity. Importantly, deletion of the LPL promoter from nucleotides −109 to −28 abolished the activity of the LPL promoter suggesting the presence of positive regulatory elements within the −109/−28 region (Fig. 1B).

The proximal −122/+28 region of the human LPL promoter contains one putative binding site for the hepatocyte-specific transcription factor FOXA2 at position −47/−40 having homology (7/8 nucleotides) with the consensus FOXA2 recognition sequence 5′-T(G/A)TTT(A/G)(C/T)T-3′ (Fig. 1C) [37]. Overexpression of FOXA2 in HepG2 cells increased the activity of the −883/+39 LPL promoter in a dose-dependent manner (Fig. 1D). Similar dose-dependent transactivation of the −883/+39 LPL promoter was observed in HEK293T cells (that do not express endogenous FOXA2) when FOXA2 was exogenously overexpressed (Fig. S1A). Collectively, the data of Fig. 1 showed that the forkhead box transcription factor FOXA2 has the ability to transactivate the human LPL promoter in hepatic cells and this transactivation may be facilitated via a putative FOXA2 responsive element present in the proximal LPL promoter.

3.2. FOXA2 is important for LPL gene expression in hepatic cells

The role of FOXA2 in LPL gene expression in hepatic cells was investigated further by gene silencing experiments. HepG2 cells were transfected with a FOXA2-specific siRNA or a non-specific siRNA (scrambled) and the mRNA and protein levels of FOXA2 and LPL were determined by reverse transcription qPCR and Western blotting respectively. The siRNA specific for FOXA2 abolished the expression of the FOXA2 gene in HepG2 cells and this silencing was associated with a 65% decrease in LPL mRNA (Fig. 2A) and 75% decrease in LPL protein levels (Fig. 2B and C). Furthermore, silencing of endogenous FOXA2 in HepG2 cells caused a 50% decrease in the activity of the −883/+39 LPL promoter relative to the same concentration of a scrambled siRNA

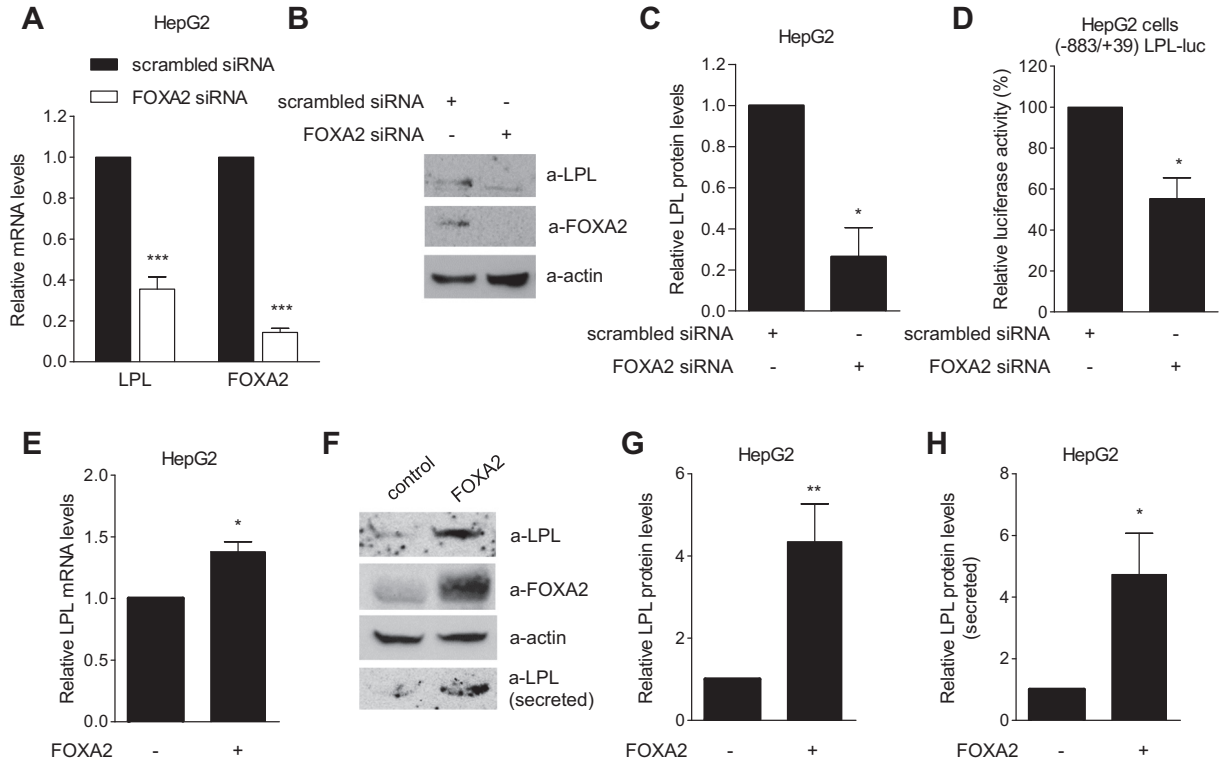

Fig. 2. FOXA2 is a positive regulator of LPL gene expression in HepG2 cells. (A) HepG2 cells were transfected with 50 nM of scrambled si-RNA or FOXA2 specific si-RNA, total RNA was extracted and LPL and FOXA2 mRNA levels were determined by reverse transcription qPCR. LPL and FOXA2 mRNA levels were normalized relative to the GUSB mRNA levels. Results are expressed as mean (±SD) from at least three independent experiments and shown as a histograph. (B) HepG2 cells were transfected with 50 nM of scrambled si-RNA or FOXA2 si-RNA and the protein levels of LPL, FOXA2 and actin (loading control) were determined by immunoblotting using the corresponding antibodies. The experiment was performed three times and representative images are presented. (C) Levels of LPL and actin were quantified by densitometry and the normalized relative protein levels are shown as a histograph. (D) HepG2 cells were transiently transfected with the (−883/+39) LPL-luc reporter plasmid (0.8 μg) in the presence of 200 nM of scrambled si-RNA or FOXA2 si-RNA. Each value of luciferase activity represents the average (±SD) from three independent experiments performed in duplicate. (E) HepG2 cells were transiently transfected with a FOXA2 expression vector (6 μg) and RNA was extracted. LPL mRNA levels were determined by reverse transcription qPCR, normalized relative to the mRNA levels of the GUSB gene and shown as a histograph. (F) HepG2 cells were transiently transfected with a FOXA2 expression vector (8 μg) and the intracellular protein levels of LPL, FOXA2 and actin (loading control) as well as of the secreted LPL were determined by immunoblotting using the corresponding antibodies. The experiment was performed at least three times and representative images are presented. (G, H) Levels of intracellular LPL and actin were quantified by densitometry and the normalized relative protein levels or the secreted LPL protein levels are shown. (C, E, G and H) Results are expressed as mean (±SD) from at least three independent experiments. *, $p < 0.05$; **, $p < 0.01$; ***, $p < 0.001$.

(Fig. 2D). Similar results were obtained in HEK293T cells that had been co-transfected with the FOXA2 expression vector and siRNA for FOXA2 (Fig. S1C–D)

In line with the data of Fig. 2A–D, overexpression of FOXA2 in HepG2 cells was associated with a 1.4-fold increase in the LPL mRNA levels (Fig. 2E) and a much stronger increase (~4-fold) in the protein levels of LPL, both the intracellular (Fig. 2F and G) and the secreted forms (Fig. 2F and H). Similar increase in LPL mRNA levels was obtained in HEK293T cells transfected with the FOXA2 expression vector (Fig. S1B).

In summary, the findings of Fig. 2 and Fig. S1 indicated that transcription factor FOXA2 plays a positive role in LPL gene expression.

3.3. FOXA2 binds to the proximal −47/−40 region of the LPL promoter in vitro and ex vivo

To identify regulatory regions in the LPL promoter that could serve as binding sites for FOXA2 and could facilitate the transactivation of the LPL promoter by FOXA2, we used the LPL promoter plasmids shown in Fig. 1A in transient transfections in HepG2 cells along with an expression vector for wild type FOXA2 or an empty vector as a control. As shown in Fig. 3A, ectopically overexpressed FOXA2 transactivated the −883/+39, −669/+39, −466/+39, −262/+39 and −109/+39 LPL promoter fragments in HepG2 cells. The proximal LPL promoter between nucleotides −109/+39, that contains the putative −47/−40 FOXA2 element, was the shortest LPL promoter fragment that was responsive to FOXA2 overexpression because further deletion to nucleotide −28 abolished the transactivation by FOXA2 (the transactivation of the −28/+39 LPL promoter by FOXA2, although statistically significant, was comparable to the transactivation of the empty luciferase vector) (Fig. 3A).

Next, we used the chromatin immunoprecipitation assay in order to monitor the recruitment of FOXA2 to the LPL promoter ex vivo. This experiment was performed in HepG2 cells and for the qPCR assays we used primers that recognize either the proximal −141/−10 region of the LPL promoter bearing the putative FOXA2 site or a non-related distal region in the 2nd intron of this gene. As shown in Fig. 3B, endogenous FOXA2 was found to be recruited to the proximal LPL promoter but not to the unrelated region in HepG2 cells.

Direct binding of FOXA2 to the proximal human LPL promoter was confirmed using the DNA affinity precipitation assay. For this purpose, biotinylated PCR fragments corresponding to the LPL promoter regions −466/+39, −262/+39, −109/+39 and −28/+39 (Fig. 4A) were amplified, coupled to streptavidin dynabeads and incubated with extracts from HEK293T cells expressing FOXA2 exogenously. As shown in Fig. 4B and C, FOXA2 bound very strongly to the −466/+39, −262/+39 and −109/+39 LPL promoter fragments but did not bind to the −28/+39 fragment lacking the putative FOXA2 site. In control experiments it was shown that FOXA2 did not bind to the streptavidin dynabeads (2nd lane, no oligo). To confirm that the site at −47/−40 is a true FOXA2 binding element, we substituted five nucleotides in this site thus creating a DNA sequence that differed significantly from the consensus FOXA2 recognition element 5′-T(G/A)TTT(A/G)(C/T)T-3′ [37]. The mutations that were introduced are shown in Fig. 4A. As shown in Fig. 4C, these mutations abolished the interaction of FOXA2 with the −109/+39 LPL promoter fragment (compare lanes 4 and 5). Similar results were obtained when the DNAP assays were performed using endogenous FOXA2 present in nuclear extracts from HepG2 cells (Fig. 4D). To investigate the functional importance of the proximal FOXA2 element for the FOXA2-mediated transactivation of the LPL promoter, we introduced the same mutations into the −883/+39 LPL promoter, creating the reporter plasmid (−883/+39) LPL-Luc (mut) (Fig. 5A). Mutagenesis of this FOXA2 site decreased the basal activity of the LPL promoter by 60% relative to the wild type promoter in HepG2 cells (Fig. 5B). Furthermore, the transactivation of the mutated LPL promoter by FOXA2 was compromised (Fig. 5B).

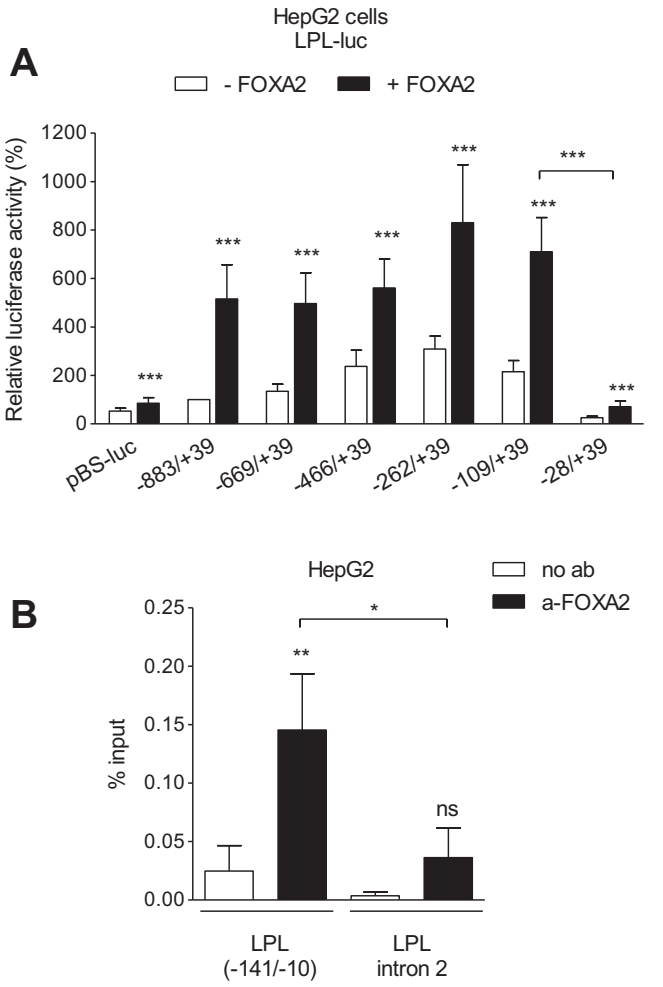

Fig. 3. FOXA2 binds to the proximal human LPL promoter ex vivo. (A) Transactivation of the human LPL promoter by FOXA2 requires the proximal −109/−28 region which contains the putative FOXA2 binding site. HepG2 cells were transiently transfected with the hLPL-luc reporter plasmids (1 μg), shown in Fig. 1A, along with a FOXA2 expression vector (0.25 μg). Each value of luciferase activity represents the average (±SD) from at least four independent experiments performed in duplicate. (B) Chromatin immunoprecipitation in HepG2 cells using an anti-FOXA2 antibody or no antibody as negative control (no ab). The precipitation of the LPL promoter was detected by qPCR using primers that are complementary to the proximal (−141/−10) region of the human LPL promoter or to a distal region in the 2nd intron of the LPL gene. Results from qPCR are expressed as binding relative to the input (%). Each value represents the average (±SD) from four independent experiments. *, $p < 0.05$; **, $p < 0.01$; ***, $p < 0.001$; ns, not significant.

Overall, the findings of Figs. 3–5 established the presence of a novel FOXA2 binding site in the proximal −47/−40 region of the human LPL promoter that binds FOXA2 with high efficiency and specificity and is critical for the basal and the FOXA2-inducible activity of the LPL promoter in hepatic cells.

3.4. The −39T/C mutation in the human LPL promoter reduces basal promoter activity but does not affect FOXA2 binding and transactivation

In a previous study [54] it was shown that a natural mutation in the proximal LPL promoter, a T to C substitution at nucleotide −39 (−39T/C), was identified in a patient with familial combined hyperlipidemia and low LPL activity. The −39T/C substitution which is localized within a binding site for the transcription factor Oct-1, was shown to be associated with a 85% reduction in LPL promoter activity in human macrophages but its effect on hepatic LPL expression was unknown [54,55]. We hypothesized that the close proximity of this substitution to the FOXA2 site could affect the binding of FOXA2 and the FOXA2-mediated

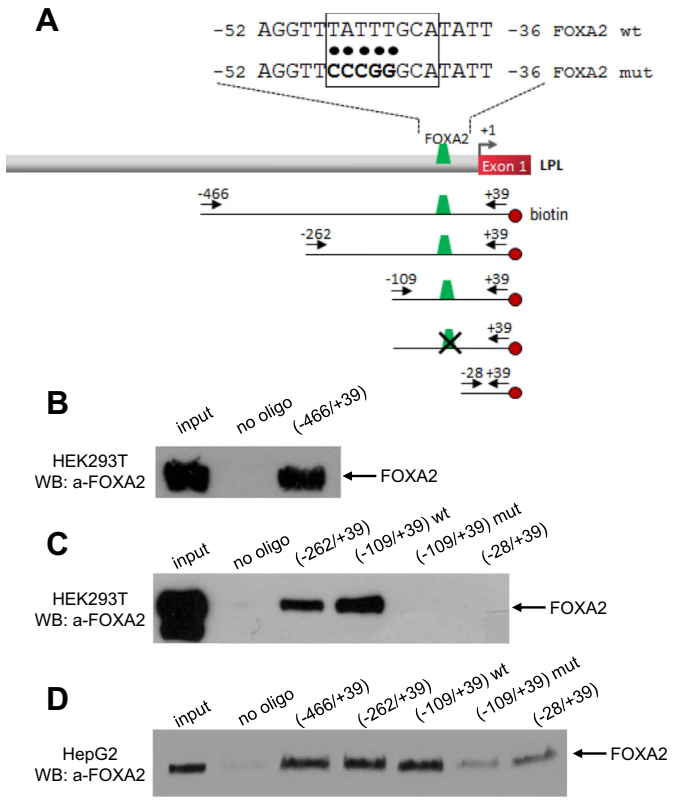

Fig. 4. FOXA2 binds to the proximal region (−47/−40) of human LPL promoter in vitro. (A) Schematic representation of the human LPL promoter showing the biotinylated promoter fragments used for the experiments of panels B–D and the primer sets (arrows) used for the amplification of the fragments. Five nucleotide substitutions in the FOXA2 site are indicated with the black dots and in bold. (B and C) DNA-affinity precipitation experiments using whole cell extracts from HEK293T cells expressing FOXA2 and the following biotinylated fragments of the human LPL promoter: −466/+39, −262/+39, −109/+39 (wild type or mutated) and −28/+39. DNA-bound FOXA2 was detected by Western blotting using a specific anti-FOXA2 antibody. (D) DNA-affinity precipitation using nuclear extracts from HepG2 cells and biotinylated PCR fragments corresponding to the −466/+39, −262/+39, −109/+39 (wild type or mutated) and −28/+39 region of the human LPL promoter. DNA-bound FOXA2 was detected by Western blotting using the a-FOXA2 antibody. The experiments in B–D were performed at least two times and representative images are presented.

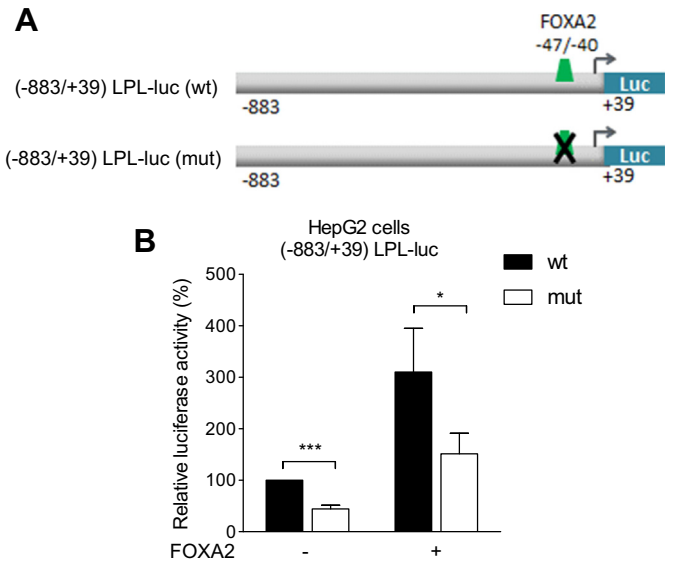

Fig. 5. Mutations in the FOXA2 binding site reduce basal LPL promoter activity and FOXA2 transactivation. (A) Schematic representation of the wild type LPL promoter construct and the corresponding construct bearing the mutations in the FOXA2 site that are shown in Fig. 4A. (B) HepG2 cells were transiently transfected with the (−883/+39) LPL-luc (wt) or (−883/+39) LPL-luc (mut) reporter plasmids (1 μg), in the presence or in the absence of the expression vector for FOXA2 (0.25 μg). The normalized, relative luciferase activity (±SD) calculated from three independent experiments performed in duplicate is presented. *, $p < 0.05$; ***, $p < 0.001$.

transactivation of the LPL promoter thus reducing the levels of expression of the LPL gene in hepatic cells. To address this question, we initially performed DNAP assays using biotinylated fragments corresponding to either the wild type −109/+39 LPL promoter or the promoter bearing the T/C substitution at position −39 (Fig. 6A). The −39T/C substitution did not affect the binding of FOXA2 expressed endogenously in HepG2 cells (Fig. 6B, compare lanes 4 and 5 with lane 3) or exogenously in HEK293T cells (Fig. 6C, compare lanes 4 and 5 with lane 3). To study further the effect of this mutation on LPL promoter activity, we generated a mutated −883/+39 LPL promoter bearing the −39T/C substitution and we cloned it upstream of the luciferase gene (Fig. 7A). As shown in Fig. 7B, the −39T/C mutation reduced the basal activity of the −883/+39 LPL promoter by 60% but did not affect the FOXA2-mediated transactivation of the LPL promoter in HepG2 cells.

The combined data of Figs. 6 and 7 indicate that the −39T/C mutation in the human LPL promoter reduces basal promoter activity but does not affect FOXA2 binding and transactivation in hepatic cells.

3.5. Reduction in LPL mRNA levels and LPL promoter activity by insulin in HepG2 cells due to an insulin-mediated nuclear export of FOXA2

It has been shown previously that the activity of FOXA2 is regulated via phosphorylation by AKT kinase in response to insulin which causes the export of FOXA2 from the nucleus leading to the inhibition of the expression of FOXA2 target genes [44]. To examine whether this mechanism applies to the hepatic regulation of the LPL gene, we treated HepG2 cells with insulin and we determined the mRNA levels of LPL as well as the intracellular localization of FOXA2. As shown in Fig. 8A and D, insulin induced the phosphorylation of AKT kinase and this induction was associated with a decrease in the nuclear localization and an increase in the cytoplasmic localization of endogenous FOXA2 in HepG2 cells (Fig. 8A–C). Cytoplasmic sequestration of FOXA2 by insulin treatment was associated with a reduction in the mRNA levels of LPL (Fig. 8E) and an inhibition in the activity of the −883/+39 LPL promoter (Fig. 8G). The mRNA levels of the FOXA2 gene were not affected by the insulin treatment (Fig. 8F). The data of Fig. 8 suggest that the phosphorylation of FOXA2 by the insulin/PI3K/AKT pathway and its nuclear export in HepG2 cells inhibits the expression of the LPL gene.

4. Discussion

4.1. The role of liver LPL in plasma lipoprotein metabolism

Lipoprotein Lipase is a member of the triglyceride lipase gene family that catalyzes the hydrolysis of TG-rich lipoproteins such as VLDL and chylomicrons [1]. LPL is synthesized by parenchymal cells in adipose tissue, skeletal muscle and heart but can be found at lower levels in many other tissues, including macrophages, kidney, brain, adrenals, lung and embryonic liver [2–6]. In adult mice LPL gene expression in the liver is low compared with other tissues [34] but the physiological role of liver LPL still remains controversial. Previous studies have addressed the physiological role of LPL in the liver. Merkel et al. created a transgenic mouse model that expresses LPL specifically in the liver [56]. These mice had increased plasma ketones and glucose and large amounts of intracellular lipid droplets in their livers. Expression of LPL in the adult was associated with slower turnover of VLDL and increased production of VLDL TG [56]. Kim et al. showed that liver-specific overexpression of LPL in mice leads to an increase in liver TG content and insulin resistance associated with defects in insulin activation of insulin receptor substrate-2 (IRS2) associated phosphatidylinositol 3-kinase (PI3K) activity

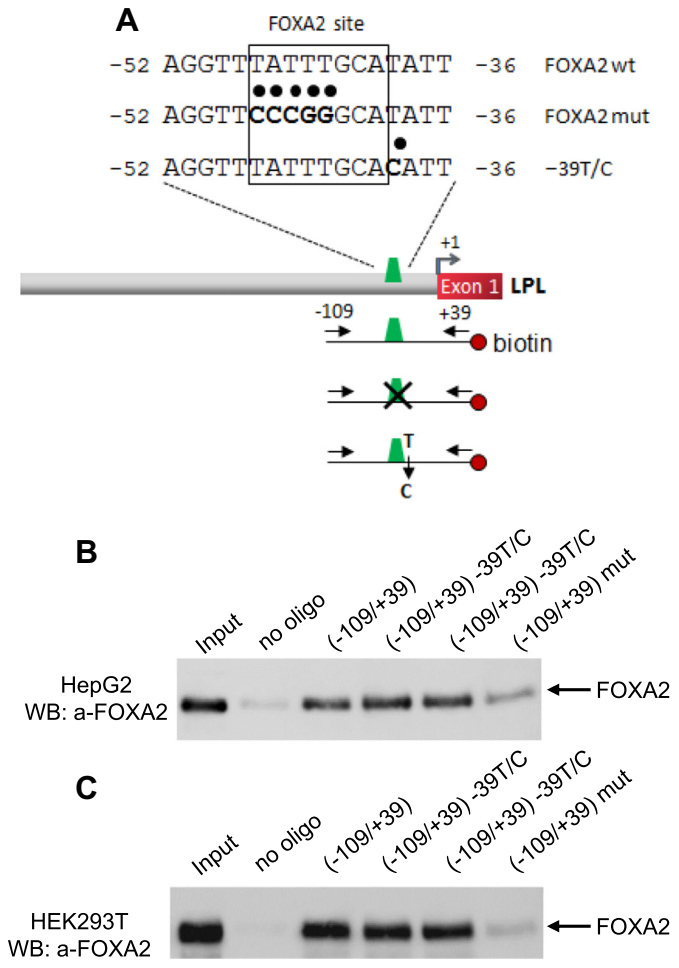

Fig. 6. A single nucleotide substitution downstream of the FOXA2 site does not affect the binding of FOXA2 to the LPL promoter. (A) Schematic representation of the human LPL promoter showing the biotinylated promoter fragments used for the experiments of panels B and C and the primer sets (arrows) used for the amplification of the fragments. Nucleotide mutations in the sequence of LPL promoter are indicated with black dots and in bold. (B) DNA-affinity precipitation using HepG2 nuclear extracts and biotinylated PCR fragments corresponding to the −109/+39 region (wild type or mutated) of the human LPL promoter. FOXA2 binding to the probes was detected by Western blotting using the anti-FOXA2 antibody. (C) DNA-affinity precipitation using whole cell extracts from HEK293T cells expressing FOXA2 and biotinylated probes corresponding to the region −109/+39 (wild type or mutated) of the human LPL promoter. DNA-bound FOXA2 was detected by Western blotting using the anti-FOXA2 antibody. The experiments in B and C were performed two times and representative images are presented.

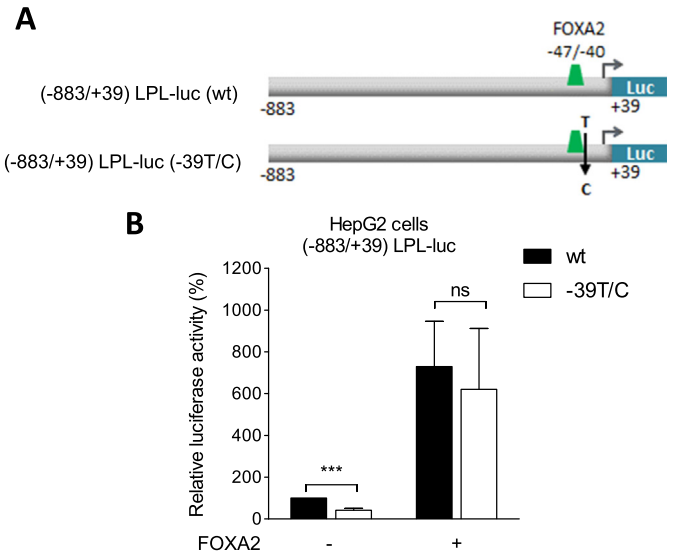

Fig. 7. A single nucleotide substitution downstream of the FOXA2 site does not affect FOXA2 mediated transactivation of LPL promoter. (A) Schematic representation of the wild type LPL promoter construct and the corresponding construct bearing a single T/C substitution (at nucleotide −39) after the FOXA2 site that is shown in Fig. 6A. (B) HepG2 cells were transiently transfected with the (−883/+39) LPL-luc (wt) or (−883/+39) LPL-luc (−39T/C) reporter plasmids (1 μg) in the presence or in the absence of the FOXA2 expression vector (0.25 μg). The normalized, relative luciferase activity (±SD) calculated from six independent experiments performed in duplicate is presented. ***, $p < 0.001$; ns, not significant.

[57]. Recently Liu et al. generated a mouse with the LPL gene specifically ablated in hepatocytes [34]. The unexpected finding of this study was that deletion of hepatic LPL resulted in a significant decrease in plasma LPL content and activity and as a result, the postprandial TG clearance was markedly impaired, and plasma TG and cholesterol levels were significantly elevated. These findings suggested that despite the low levels of expression in the adult liver, hepatic LPL has a physiologically significant role in lipoprotein metabolism that needs to be explored further under pathological or non-pathological conditions.

4.2. FOXA2 as a central regulator of lipid and lipoprotein metabolism in the liver

In the present study we show that the human lipoprotein lipase gene is a direct target of the transcription factor FOXA2 in hepatic cells. The activation of the LPL gene by FOXA2 is mediated via a novel FOXA2 responsive element that is localized in the proximal LPL promoter. Mutations in this FOXA2 site abolished binding of FOXA2 and the FOXA2-mediated transactivation of the LPL promoter in hepatic cells whereas silencing of FOXA2 was associated with a reduction in the mRNA and protein levels of LPL. Importantly, we show that insulin inhibits the expression of LPL in HepG2 cells via a mechanism that involves the activation of AKT kinase and the subsequent translocation of FOXA2 from the nucleus to the cytoplasm.

FOXA2 (also called Hepatocyte Nuclear Factor 3β) is expressed mainly in the liver and also in pancreas, stomach, intestine and lung [38]. In the liver, FOXA2 has been shown to stimulate the oxidation of fatty acids, to increase the production of ketone bodies and to increase the secretion of lipoproteins (VLDL, HDL) during fasting [44,47]. Using adenovirus-mediated gene transfer combined with gene expression profiling it was shown that a constitutively active form of FOXA2 (that cannot be inhibited by AKT) increased the expression of genes involved in HDL metabolism, β-oxidation, ketogenesis, glycolysis and TG degradation including the genes for the lipases LPL and LIPC [44]. In another study, it was found that almost half of the genes expressed in the adult liver including the LPL gene contain at least one FOXA2 binding site [53]. Although FOXA2 is a nuclear factor that activates gene transcription when bound to DNA due to the presence of two transactivation domains [38], FOXA2 may also inhibit gene expression. In a previous study we showed that FOXA2 binds to three sites on the proximal promoter of the human ABCA1 gene, one of which is the TATA box and compromises the upregulation of ABCA1 gene expression by oxysterol-activated LXRs [50]. In the liver, excess cholesterol is converted to bile acids for excretion through the bile [58–60]. Importantly, inactivation of FOXA2 in the liver inhibited the expression of bile acid transporters resulting in intrahepatic cholestasis [48]. It was also shown that patients with cholestatic syndromes have lower FOXA2 levels in the liver [48]. Thus, FOXA2 emerges as a key regulator of lipid and lipoprotein metabolism in the liver.

Interestingly, the expression of the LPL gene in the adult mouse liver is also induced strongly by oxysterols, either synthetic or endogenous following a cholesterol-rich diet [33]. It was shown that LXRs induce LPL gene expression in the liver by acting on a distal LXRE present in the first intron of the LPL gene [33]. In preliminary experiments we found that FOXA2 cooperates with the LXRs to synergistically induce the transcription of the LPL gene in hepatic cells and that silencing of FOXA2

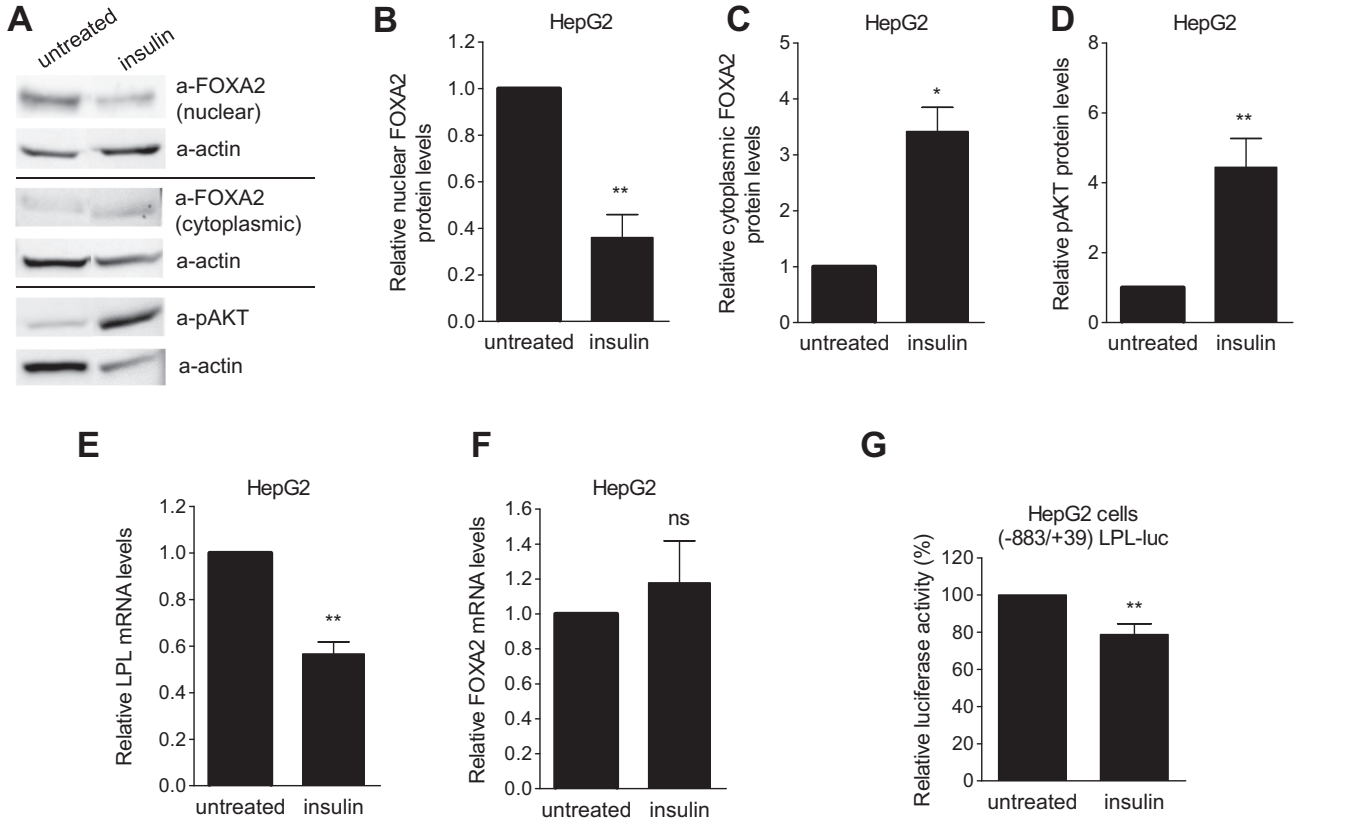

Fig. 8. Nuclear exclusion of FOXA2 by insulin results to downregulation of LPL gene expression. (A) HepG2 cells were treated with insulin (500 nM) for 24 h or left untreated. Nuclear and cytoplasmic protein extracts were isolated and subcellular localization of FOXA2 was determined by immunoblotting using the anti-FOXA2 antibody. The protein levels of actin (loading control) and pAKT (positive control) were determined by immunoblotting using the corresponding antibodies. The experiment was performed at least three times and representative images are presented. (B–D) Levels of nuclear FOXA2 (panel B), cytoplasmic FOXA2 (panel C), pAKT (panel D) and actin were quantified by densitometry and the normalized relative protein levels are shown as histographs. Results are expressed as mean (±SD) from at least three independent experiments. (E and F) HepG2 cells were treated with insulin (500 nM) for 24 h or left untreated and total RNA was extracted. LPL (panel E) and FOXA2 (panel F) mRNA levels were determined by reverse transcription qPCR, normalized relative to the mRNA levels of the GUSB gene and shown as histographs. Results are expressed as mean (±SD) from three independent experiments. (G) HepG2 cells were transiently transfected with the (−883/+39) LPL-luc reporter plasmid (1 μg). Following transfection, the cells were treated with 500 nM insulin for 24 h or left untreated. Normalized relative luciferase activity values are shown. Each value represents the average (±SD) from two independent experiments performed in duplicate. *, $p < 0.05$; **, $p < 0.01$; ns, not significant.

abolishes LPL gene induction by oxysterols (Kanaki and Kardassis, unpublished). These observations indicate that FOXA2 may control the levels of LPL gene in response to intracellular or extracellular signals and facilitate the cross talk between the signaling pathways that are induced by these signals. For instance, inhibition of FOXA2 by insulin could prevent the overexpression of LPL by oxysterols under conditions of cholesterol overload such as a high fat diet which could lead to insulin resistance [57].

The regulation of the human LPL gene by FOXA2 could be a general regulatory mechanism that may operate in tissues other than the liver that express the LPL gene such as the adipocytes. To address this hypothesis, we transfected 3T3-L1 pre-adipocytes with different LPL promoter fragments fused with the luciferase report gene and found that deletions of the LPL promoter from position −883 to −109 did not affect the promoter activity but further deletion to position −28 abolished the activity of the LPL promoter in a similar fashion as in HepG2 cells (Fig. S2A). In agreement with this finding, mutagenesis of the FOXA2 element reduced the basal activity of the −109/+39 LPL promoter by 50%, indicating the importance of this element for the regulation of LPL in 3T3-L1 cells (Fig. S2B). However, differentiation of 3T3-L1 pre-adipocytes to mature adipocytes was associated with a severe reduction in FOXA2 mRNA levels (Fig. S2C) and nuclear protein levels (Fig. S2D) whereas the mRNA levels of LPL gene were increased during adipocyte differentiation (Fig. S2C). These data suggest that the LPL gene expression is not regulated by FOXA2 in adipocytes. However, the −47/−40 element of the LPL promoter may facilitate the involvement of other adipocyte transcription factors that regulate the LPL gene.

4.3. The proximal LPL promoter bears a dual specificity responsive element that binds Oct-1 and FOXA2 and is responsive to insulin

Mutations in the LPL promoter in humans are associated with reduced LPL expression levels and promoter activity [61]. In one of these cases, a compound heterozygote [−39T/C; −39T/G] was identified with familial combined hyperlipidemia and reduced post-heparin LPL levels. The −39T/C substitution is localized within a binding site for the transcription factor Oct-1 [54,55]. Oct-1 is a member of the POU domain of transcription factors that bind to a DNA sequence motif known as the octamer motif having the consensus sequence 5′ "ATGC(A/T)AAT" 3′ [62]. Oct-1 is ubiquitously expressed and serves as a sensor for both metabolic and stress signals [62–64]. In liver cells, Oct-1 binds to the promoter of the carbohydrate response element binding protein (ChREBP) gene and inhibits its expression [65]. Interestingly, insulin increases the activity of the ChREBP promoter in hepatic cells and stimulates ChREBP expression via the octamer motif [65,66] suggesting that insulin signaling regulates the activity of Oct-1 by an unknown mechanism. The precise role of Oct-1 in LPL gene regulation has not been elucidated but the decrease in the LPL promoter activity caused by the −39T/C substitution which destroys the octamer motif suggests that this factor plays a positive role in LPL gene transcription. The close proximity of the −39T/C substitution to the FOXA2 binding site identified in the present study (−47/−40) prompted us to functionally characterize this substitution in the context of the hepatic LPL regulation. Our data showed that the −39T/C substitution reduced

LPL promoter activity by 60% in HepG2 cells but had no effect on the binding of FOXA2 to the LPL promoter in vitro as well as on the FOXA2-mediated transactivation of the LPL promoter in HepG2 cells. Importantly, both FOXA2 and Oct-1 factors are inhibited by insulin in hepatic cells (Fig. 8 and ref. [66]). The combined data propose that the −47/−38 region of the human LPL promoter is a novel dual insulin-responsive element that can bind either Oct-1 or FOXA2 and could facilitate the inhibition of the human LPL gene expression by insulin and possibly by other factors that regulate the activity of the two nuclear proteins in LPL-expressing cells.

4.4. Significance of LPL regulation by FOXA2 in the liver

In a previous paper [50] we had shown that FOXA2 inhibits the expression of the human transporter ABCA1 thus revealing a novel role of this transcription factor in the biogenesis of HDL. With our new study we reveal a wider role of this transcription factor in the liver that is not restricted to HDL biogenesis but through an insulin-AKT-FOXA2-LPL signaling cascade may control the catabolism of TG-rich lipoproteins such as VLDL and chylomicrons. This pathway may prevent the accumulation of LPL in the liver under certain conditions such as cholesterol overload which strongly induces liver LPL thus protecting this tissue from the toxic effects of LPL overexpression as demonstrated recently in mouse studies [57]. Understanding the mechanisms by which FOXA2 regulates the expression of the LPL gene and other genes involved in lipid and glucose metabolism in the liver may open the way to novel therapeutic strategies for patients with metabolic disorders such as dyslipidemia, diabetes and the metabolic syndrome.

Supplementary data to this article can be found online at http://dx.doi.org/10.1016/j.bbagrm.2017.01.007.

Transparency document

The Transparency document associated with this article can be found, in the online version.

Acknowledgments

We would like to thank Paraskevi Papakosta for technical assistance and all members of the Kardassis lab for helpful suggestions, protocols, materials and discussions. This work was supported by grants from the Greek General Secretariat for Research and Technology (SYNERGASIA 09SYN-12-897 and ARISTEIA II 4220) to DK.

References

[1] G. Olivecrona, Role of lipoprotein lipase in lipid metabolism, Curr. Opin. Lipidol. 27 (2016) 233–241.
[2] L. Camps, M. Reina, M. Llobera, G. Bengtsson-Olivecrona, T. Olivecrona, S. Vilaro, Lipoprotein lipase in lungs, spleen, and liver: synthesis and distribution, J. Lipid Res. 32 (1991) 1877–1888.
[3] L. Camps, M. Reina, M. Llobera, S. Vilaro, T. Olivecrona, Lipoprotein lipase: cellular origin and functional distribution, Am. J. Phys. 258 (1990) C673–C681.
[4] I.J. Goldberg, D.R. Soprano, M.L. Wyatt, T.M. Vanni, T.G. Kirchgessner, M.C. Schotz, Localization of lipoprotein lipase mRNA in selected rat tissues, J. Lipid Res. 30 (1989) 1569–1577.
[5] T.G. Kirchgessner, R.C. LeBoeuf, C.A. Langner, S. Zollman, C.H. Chang, B.A. Taylor, M.C. Schotz, J.I. Gordon, A.J. Lusis, Genetic and developmental regulation of the lipoprotein lipase gene: loci both distal and proximal to the lipoprotein lipase structural gene control enzyme expression, J. Biol. Chem. 264 (1989) 1473–1482.
[6] B. Staels, J. Auwerx, Perturbation of developmental gene expression in rat liver by fibric acid derivatives: lipoprotein lipase and alpha-fetoprotein as models, Development 115 (1992) 1035–1043.
[7] I.J. Goldberg, Lipoprotein lipase and lipolysis: central roles in lipoprotein metabolism and atherogenesis, J. Lipid Res. 37 (1996) 693–707.
[8] J.R. Mead, D.P. Ramji, The pivotal role of lipoprotein lipase in atherosclerosis, Cardiovasc. Res. 55 (2002) 261–269.
[9] J.R. Mead, A. Cryer, D.P. Ramji, Lipoprotein lipase, a key role in atherosclerosis? FEBS Lett. 462 (1999) 1–6.
[10] T. Coleman, R.L. Seip, J.M. Gimble, D. Lee, N. Maeda, C.F. Semenkovich, COOH-terminal disruption of lipoprotein lipase in mice is lethal in homozygotes, but heterozygotes have elevated triglycerides and impaired enzyme activity, J. Biol. Chem. 270 (1995) 12518–12525.
[11] P.H. Weinstock, C.L. Bisgaier, K. Aalto-Setala, H. Radner, R. Ramakrishnan, S. Levak-Frank, A.D. Essenburg, R. Zechner, J.L. Breslow, Severe hypertriglyceridemia, reduced high density lipoprotein, and neonatal death in lipoprotein lipase knockout mice. Mild hypertriglyceridemia with impaired very low density lipoprotein clearance in heterozygotes, J. Clin. Invest. 96 (1995) 2555–2568.
[12] M. Shimada, S. Ishibashi, T. Inaba, H. Yagyu, K. Harada, J.I. Osuga, K. Ohashi, Y. Yazaki, N. Yamada, Suppression of diet-induced atherosclerosis in low density lipoprotein receptor knockout mice overexpressing lipoprotein lipase, Proc. Natl. Acad. Sci. U. S. A. 93 (1996) 7242–7246.
[13] H. Yagyu, S. Ishibashi, Z. Chen, J. Osuga, M. Okazaki, S. Perrey, T. Kitamine, M. Shimada, K. Ohashi, K. Harada, F. Shionoiri, N. Yahagi, T. Gotoda, Y. Yazaki, N. Yamada, Overexpressed lipoprotein lipase protects against atherosclerosis in apolipoprotein E knockout mice, J. Lipid Res. 40 (1999) 1677–1685.
[14] M. Shimada, H. Shimano, T. Gotoda, K. Yamamoto, M. Kawamura, T. Inaba, Y. Yazaki, N. Yamada, Overexpression of human lipoprotein lipase in transgenic mice. Resistance to diet-induced hypertriglyceridemia and hypercholesterolemia, J. Biol. Chem. 268 (1993) 17924–17929.
[15] P. Benlian, J.L. De Gennes, L. Foubert, H. Zhang, S.E. Gagne, M. Hayden, Premature atherosclerosis in patients with familial chylomicronemia caused by mutations in the lipoprotein lipase gene, N. Engl. J. Med. 335 (1996) 848–854.
[16] R.M. Fisher, S.E. Humphries, P.J. Talmud, Common variation in the lipoprotein lipase gene: effects on plasma lipids and risk of atherosclerosis, Atherosclerosis 135 (1997) 145–159.
[17] S.S. Fojo, H.B. Brewer, Hypertriglyceridaemia due to genetic defects in lipoprotein lipase and apolipoprotein C-II, J. Intern. Med. 231 (1992) 669–677.
[18] C.L. Parrott, N. Alsayed, R. Rebourcet, S. Santamarina-Fojo, ApoC-IIParis2: a premature termination mutation in the signal peptide of apoC-II resulting in the familial chylomicronemia syndrome, J. Lipid Res. 33 (1992) 361–367.
[19] P.W. Reymer, E. Gagne, B.E. Groenemeyer, H. Zhang, I. Forsyth, H. Jansen, J.C. Seidell, D. Kromhout, K.E. Lie, J. Kastelein, et al., A lipoprotein lipase mutation (Asn291Ser) is associated with reduced HDL cholesterol levels in premature atherosclerosis, Nat. Genet. 10 (1995) 28–34.
[20] J.D. Brunzell, Familial Lipoprotein Lipase Deficiency, in: R.A. Pagon, M.P. Adam, H.H. Ardinger, S.E. Wallace, A. Amemiya, L.J.H. Bean, T.D. Bird, C.T. Fong, H.C. Mefford, R.J.H. Smith, K. Stephens (Eds.), GeneReviews(R), University of Washington, Seattle, Seattle (WA), 1993.
[21] S. Santamarina-Fojo, H.B. Brewer Jr., The familial hyperchylomicronemia syndrome. New insights into underlying genetic defects, JAMA 265 (1991) 904–908.
[22] S. Santamarina-Fojo, The familial chylomicronemia syndrome, Endocrinol. Metab. Clin. N. Am. 27 (1998) 551–567 (viii).
[23] J.K. Otarod, I.J. Goldberg, Lipoprotein lipase and its role in regulation of plasma lipoproteins and cardiac risk, Curr. Atheroscler. Rep. 6 (2004) 335–342.
[24] B.G. Nordestgaard, S. Abildgaard, H.H. Wittrup, R. Steffensen, G. Jensen, A. Tybjaerg-Hansen, Heterozygous lipoprotein lipase deficiency: frequency in the general population, effect on plasma lipid levels, and risk of ischemic heart disease, Circulation 96 (1997) 1737–1744.
[25] I.J. Goldberg, M. Merkel, Lipoprotein lipase: physiology, biochemistry, and molecular biology, Front. Biosci. 6 (2001) D388–D405.
[26] J.D. Brunzell, P.H. Iverius, M.S. Scheibel, W.Y. Fujimoto, M.R. Hayden, R. McLeod, J. Frolich, Primary lipoprotein lipase deficiency, Adv. Exp. Med. Biol. 201 (1986) 227–239.
[27] K. Schoonjans, J. Peinado-Onsurbe, A.M. Lefebvre, R.A. Heyman, M. Briggs, S. Deeb, B. Staels, J. Auwerx, PPARalpha and PPARgamma activators direct a distinct tissue-specific transcriptional response via a PPRE in the lipoprotein lipase gene, EMBO J. 15 (1996) 5336–5348.
[28] S.E. Michaud, G. Renier, Direct regulatory effect of fatty acids on macrophage lipoprotein lipase: potential role of PPARs, Diabetes 50 (2001) 660–666.
[29] P.G. Blanchard, W.T. Festuccia, V.P. Houde, P. St-Pierre, S. Brule, V. Turcotte, M. Cote, K. Bellmann, A. Marette, Y. Deshaies, Major involvement of mTOR in the PPARgamma-induced stimulation of adipose tissue lipid uptake and fat accretion, J. Lipid Res. 53 (2012) 1117–1125.
[30] M. Laplante, H. Sell, K.L. MacNaul, D. Richard, J.P. Berger, Y. Deshaies, PPAR-gamma activation mediates adipose depot-specific effects on gene expression and lipoprotein lipase activity: mechanisms for modulation of postprandial lipemia and differential adipose accretion, Diabetes 52 (2003) 291–299.
[31] C.F. Semenkovich, M. Wims, L. Noe, J. Etienne, L. Chan, Insulin regulation of lipoprotein lipase activity in 3T3-L1 adipocytes is mediated at posttranscriptional and post-translational levels, J. Biol. Chem. 264 (1989) 9030–9038.
[32] A. Vidal-Puig, M. Jimenez-Linan, B.B. Lowell, A. Hamann, E. Hu, B. Spiegelman, J.S. Flier, D.E. Moller, Regulation of PPAR gamma gene expression by nutrition and obesity in rodents, J. Clin. Invest. 97 (1996) 2553–2561.
[33] Y. Zhang, J.J. Repa, K. Gauthier, D.J. Mangelsdorf, Regulation of lipoprotein lipase by the oxysterol receptors, LXRalpha and LXRbeta, J. Biol. Chem. 276 (2001) 43018–43024.
[34] G. Liu, J.N. Xu, D. Liu, Q. Ding, M.N. Liu, R. Chen, M. Fan, Y. Zhang, C. Zheng, D.J. Zou, J. Lyu, W.J. Zhang, Regulation of plasma lipid homeostasis by hepatic lipoprotein lipase in adult mice, J. Lipid Res. 57 (2016) 1155–1161.
[35] J.R. Friedman, K.H. Kaestner, The Foxa family of transcription factors in development and metabolism, Cell. Mol. Life Sci. 63 (2006) 2317–2328.
[36] D.G. Overdier, A. Porcella, R.H. Costa, The DNA-binding specificity of the hepatocyte nuclear factor 3/forkhead domain is influenced by amino-acid residues adjacent to the recognition helix, Mol. Cell. Biol. 14 (1994) 2755–2766.
[37] A. Rada-Iglesias, O. Wallerman, C. Koch, A. Ameur, S. Enroth, G. Clelland, K. Wester, S. Wilcox, O.M. Dovey, P.D. Ellis, V.L. Wraight, K. James, R. Andrews, C. Langford, P.

Dhami, N. Carter, D. Vetrie, F. Ponten, J. Komorowski, I. Dunham, C. Wadelius, Binding sites for metabolic disease related transcription factors inferred at base pair resolution by chromatin immunoprecipitation and genomic microarrays, Hum. Mol. Genet. 14 (2005) 3435–3447.
[38] K.H. Kaestner, H. Hiemisch, B. Luckow, G. Schutz, The HNF-3 gene family of transcription factors in mice: gene structure, cDNA sequence, and mRNA distribution, Genomics 20 (1994) 377–385.
[39] S.L. Ang, J. Rossant, HNF-3 beta is essential for node and notochord formation in mouse development, Cell 78 (1994) 561–574.
[40] D.C. Weinstein, A. Ruiz i Altaba, W.S. Chen, P. Hoodless, V.R. Prezioso, T.M. Jessell, J.E. Darnell Jr., The winged-helix transcription factor HNF-3 beta is required for notochord development in the mouse embryo, Cell 78 (1994) 575–588.
[41] R.M. O'Brien, E.L. Noisin, A. Suwanichkul, T. Yamasaki, P.C. Lucas, J.C. Wang, D.R. Powell, D.K. Granner, Hepatic nuclear factor 3- and hormone-regulated expression of the phosphoenolpyruvate carboxykinase and insulin-like growth factor-binding protein 1 genes, Mol. Cell. Biol. 15 (1995) 1747–1758.
[42] A.K. Pandey, V. Bhardwaj, M. Datta, Tumour necrosis factor-alpha attenuates insulin action on phosphoenolpyruvate carboxykinase gene expression and gluconeogenesis by altering the cellular localization of Foxa2 in HepG2 cells, FEBS J. 276 (2009) 3757–3769.
[43] J.C. Wang, J.M. Stafford, D.K. Scott, C. Sutherland, D.K. Granner, The molecular physiology of hepatic nuclear factor 3 in the regulation of gluconeogenesis, J. Biol. Chem. 275 (2000) 14717–14721.
[44] C. Wolfrum, E. Asilmaz, E. Luca, J.M. Friedman, M. Stoffel, Foxa2 regulates lipid metabolism and ketogenesis in the liver during fasting and in diabetes, Nature 432 (2004) 1027–1032.
[45] C. Wolfrum, J.J. Howell, E. Ndungo, M. Stoffel, Foxa2 activity increases plasma high density lipoprotein levels by regulating apolipoprotein M, J. Biol. Chem. 283 (2008) 16940–16949.
[46] C. Wolfrum, M. Stoffel, Coactivation of Foxa2 through Pgc-1beta promotes liver fatty acid oxidation and triglyceride/VLDL secretion, Cell Metab. 3 (2006) 99–110.
[47] L. Zhang, N.E. Rubins, R.S. Ahima, L.E. Greenbaum, K.H. Kaestner, Foxa2 integrates the transcriptional response of the hepatocyte to fasting, Cell Metab. 2 (2005) 141–148.
[48] I.M. Bochkis, N.E. Rubins, P. White, E.E. Furth, J.R. Friedman, K.H. Kaestner, Hepatocyte-specific ablation of Foxa2 alters bile acid homeostasis and results in endoplasmic reticulum stress, Nat. Med. 14 (2008) 828–836.
[49] N. Xu, P. Nilsson-Ehle, M. Hurtig, B. Ahren, Both leptin and leptin-receptor are essential for apolipoprotein M expression in vivo, Biochem. Biophys. Res. Commun. 321 (2004) 916–921.
[50] E. Thymiakou, D. Kardassis, Novel mechanism of transcriptional repression of the human ATP binding cassette transporter A1 gene in hepatic cells by the winged helix/forkhead box transcription factor A2, Biochim. Biophys. Acta 1839 (2014) 526–536.
[51] I.M. Bochkis, J. Schug, N.E. Rubins, A.R. Chopra, B.W. O'Malley, K.H. Kaestner, Foxa2-dependent hepatic gene regulatory networks depend on physiological state, Physiol. Genomics 38 (2009) 186–195.
[52] O. Wallerman, M. Motallebipour, S. Enroth, K. Patra, M.S. Bysani, J. Komorowski, C. Wadelius, Molecular interactions between HNF4a, FOXA2 and GABP identified at regulatory DNA elements through ChIP-sequencing, Nucleic Acids Res. 37 (2009) 7498–7508.
[53] E.D. Wederell, M. Bilenky, R. Cullum, N. Thiessen, M. Dagpinar, A. Delaney, R. Varhol, Y. Zhao, T. Zeng, B. Bernier, M. Ingham, M. Hirst, G. Robertson, M.A. Marra, S. Jones, P.A. Hoodless, Global analysis of in vivo Foxa2-binding sites in mouse adult liver using massively parallel sequencing, Nucleic Acids Res. 36 (2008) 4549–4564.
[54] W.S. Yang, D.N. Nevin, R. Peng, J.D. Brunzell, S.S. Deeb, A mutation in the promoter of the lipoprotein lipase (LPL) gene in a patient with familial combined hyperlipidemia and low LPL activity, Proc. Natl. Acad. Sci. U. S. A. 92 (1995) 4462–4466.
[55] L. Previato, C.L. Parrott, S. Santamarina-Fojo, H.B. Brewer Jr., Transcriptional regulation of the human lipoprotein lipase gene in 3T3-L1 adipocytes, J. Biol. Chem. 266 (1991) 18958–18963.
[56] M. Merkel, P.H. Weinstock, T. Chajek-Shaul, H. Radner, B. Yin, J.L. Breslow, I.J. Goldberg, Lipoprotein lipase expression exclusively in liver. A mouse model for metabolism in the neonatal period and during cachexia, J. Clin. Invest. 102 (1998) 893–901.
[57] J.K. Kim, J.J. Fillmore, Y. Chen, C. Yu, I.K. Moore, M. Pypaert, E.P. Lutz, Y. Kako, W. Velez-Carrasco, I.J. Goldberg, J.L. Breslow, G.I. Shulman, Tissue-specific overexpression of lipoprotein lipase causes tissue-specific insulin resistance, Proc. Natl. Acad. Sci. U. S. A. 98 (2001) 7522–7527.
[58] G.A. Kullak-Ublick, B. Stieger, P.J. Meier, Enterohepatic bile salt transporters in normal physiology and liver disease, Gastroenterology 126 (2004) 322–342.
[59] J.J. Eloranta, G.A. Kullak-Ublick, Coordinate transcriptional regulation of bile acid homeostasis and drug metabolism, Arch. Biochem. Biophys. 433 (2005) 397–412.
[60] A. Mennone, C.J. Soroka, S.Y. Cai, K. Harry, M. Adachi, L. Hagey, J.D. Schuetz, J.L. Boyer, Mrp4 −/− mice have an impaired cytoprotective response in obstructive cholestasis, Hepatology (Baltimore, MD) 43 (2006) 1013–1021.
[61] W.S. Yang, D.N. Nevin, L. Iwasaki, R. Peng, B.G. Brown, J.D. Brunzell, S.S. Deeb, Regulatory mutations in the human lipoprotein lipase gene in patients with familial combined hyperlipidemia and coronary artery disease, J. Lipid Res. 37 (1996) 2627–2637.
[62] P. Wang, T. Jin, Oct-1 functions as a sensor for metabolic and stress signals, Islets 2 (2010) 46–48.
[63] P. Wang, Q. Wang, J. Sun, J. Wu, H. Li, N. Zhang, Y. Huang, B. Su, R.K. Li, L. Liu, Y. Zhang, H.P. Elsholtz, J. Hu, H.Y. Gaisano, T. Jin, POU homeodomain protein Oct-1 functions as a sensor for cyclic AMP, J. Biol. Chem. 284 (2009) 26456–26465.
[64] J. Kang, M. Gemberling, M. Nakamura, F.G. Whitby, H. Handa, W.G. Fairbrother, D. Tantin, A general mechanism for transcription regulation by Oct1 and Oct4 in response to genotoxic and oxidative stress, Genes Dev. 23 (2009) 208–222.
[65] K. Uyeda, J.J. Repa, Carbohydrate response element binding protein, ChREBP, a transcription factor coupling hepatic glucose utilization and lipid synthesis, Cell Metab. 4 (2006) 107–110.
[66] A.S. Sirek, L. Liu, M. Naples, K. Adeli, D.S. Ng, T. Jin, Insulin stimulates the expression of carbohydrate response element binding protein (ChREBP) by attenuating the repressive effect of Pit-1, Oct-1/Oct-2, and Unc-86 homeodomain protein octamer transcription factor-1, Endocrinology 150 (2009) 3483–3492.